

# **INFLUENCE OF PHYSICAL AND CHEMICAL PROPERTIES OF SOLIDS ON HEAVY METAL ADSORPTION**

**Chandima Thanuja Kumari Gunawardana**

BSc. (Civil Engineering, Honours) (University of Peradeniya, Sri Lanka)

PG Diploma (Civil Engineering) (University of Peradeniya, Sri Lanka)

A THESIS SUBMITTED IN PARTIAL FULFILMENT OF THE  
REQUIREMENTS OF THE DEGREE OF DOCTOR OF PHILOSOPHY

FACULTY OF BUILT ENVIRONMENT AND ENGINEERING  
QUEENSLAND UNIVERSITY OF TECHNOLOGY

AUGUST 2011



# KEYWORDS

---

Adsorption, Heavy metals, Pollutant build-up, Stormwater pollution, Stormwater quality, Urban water quality



# Abstract

---

Partition of heavy metals between particulate and dissolve fraction of stormwater primarily depends on the adsorption characteristics of solids particles. Moreover, the bioavailability of heavy metals is also influenced by the adsorption behaviour of solids. However, due to the lack of fundamental knowledge in relation to the heavy metals adsorption processes of road deposited solids, the effectiveness of stormwater management strategies can be limited. The research study focused on the investigation of the physical and chemical parameters of solids on urban road surfaces and, more specifically, on heavy metal adsorption to solids.

Due to the complex nature of heavy metal interaction with solids, a substantial database was generated through a series of field investigations and laboratory experiments. The study sites for the build-up pollutant sample collection were selected from four urbanised suburbs located in a major river catchment. Sixteen road sites were selected from these suburbs and represented typical industrial, commercial and residential land uses. Build-up pollutants were collected using a wet and dry vacuum collection technique which was specially designed to improve fine particle collection. Roadside soil samples were also collected from each suburb for comparison with the road surface solids. The collected build-up solids samples were separated into four particle size ranges and tested for a range of physical and chemical parameters.

The solids build-up on road surfaces contained a high fraction (70%) of particles smaller than 150 $\mu$ m, which are favourable for heavy metal adsorption. These solids particles predominantly consist of soil derived minerals which included quartz, albite, microcline, muscovite and chlorite. Additionally, a high percentage of amorphous content was also identified in road deposited solids. In comparing the mineralogical data of surrounding soil and road deposited solids, it was found that about 30% of the solids consisted of particles generated from traffic related activities on road surfaces.

Significant difference in mineralogical composition was noted in different particle sizes of build-up solids. Fine solids particles ( $<150\mu\text{m}$ ) consisted of a clayey matrix and high amorphous content (in the region of 40%) while coarse particles ( $>150\mu\text{m}$ ) consisted of a sandy matrix at all study sites, with about 60% quartz content. Due to these differences in mineralogical components, particles larger than and smaller than  $150\mu\text{m}$  had significant differences in their specific surface area (SSA) and effective cation exchange capacity (ECEC). These parameters, in turn, exert a significant influence on heavy metal adsorption.

Consequently, heavy metal content in  $>150\mu\text{m}$  particles was lower than in the case of fine particles. The particle size range  $<75\mu\text{m}$  had the highest heavy metal content, corresponding with its high clay forming minerals, high organic matter and low quartz content which increased the SSA, ECEC and the presence of Fe, Al and Mn oxides. The clay forming minerals, high organic matter and Fe, Al and Mn oxides create distinct groups of charge sites on solids surfaces and exhibit different adsorption mechanisms and bond strength, between heavy metal elements and charge sites. Therefore, the predominance of these factors in different particle sizes leads to different heavy metal adsorption characteristics.

Heavy metals show preference for association with clay forming minerals in fine solids particles, whilst in coarse particles heavy metals preferentially associate with organic matter. Although heavy metal adsorption to amorphous material is very low, the heavy metals embedded in traffic related materials have a potential impact on stormwater quality. Adsorption of heavy metals is not confined to an individual type of charge site in solids, whereas specific heavy metal elements show preference for adsorption to several different types of charge sites in solids. This is attributed to the dearth of preferred binding sites and the inability to reach the preferred binding sites due to competition between different heavy metal species. This confirms that heavy metal adsorption is significantly influenced by the physical and chemical parameters of solids that lead to a heterogeneity of surface charge sites.

The research study highlighted the importance of removal of solids particles from stormwater runoff before they enter into receiving waters to reduce the potential risk posed by the bioavailability of heavy metals. The bioavailability of heavy metals not only results from the easily mobile fraction bound to the solids particles, but can also occur as a result of the dissolution of other forms of bonds by chemical changes in stormwater or microbial activity.

Due to the diversity in the composition of the different particle sizes of solids and the characteristics and amount of charge sites on the particle surfaces, investigations using bulk solids are not adequate to gain an understanding of the heavy metal adsorption processes of solids particles. Therefore, the investigation of different particle size ranges is recommended for enhancing stormwater quality management practices.





# List of Publications

---

## Peer Reviewed Journal Papers

- **Gunawardana, C.,** Goonetilleke, A., Egodawatta, P., Dawes, L. and Kokot, S. (2011). Role of solids in heavy metal pollution of receiving waters. *Journal of Environmental Engineering* (In Press).

## Conference Papers

- **Gunawardana, C.,** Goonetilleke, A., Egodawatta, P., Dawes, L. and Kokot, S. (2010). Role of suspended solids in heavy metal pollution of receiving waters. Paper presented at the Challenges in Environmental Science and Engineering, (CESE-2010), Cairns, Australia.
- **Gunawardana, C.,** Goonetilleke, A., Egodawatta, P. and Dawes, L. (2011). Composition and source identification of road deposited pollutants. Paper presented at the First International Postgraduate Conference on Engineering, Designing and Developing the Built Environment for Sustainable Wellbeing (eddBE2011), Brisbane, Australia.



# Table of Contents

---

Keywords .....	i
Abstract .....	iii
List of Publications .....	vii
Table of Contents .....	ix
List of Figures .....	xiii
List of Tables.....	xvii
List of Appendices .....	xxi
List of Abbreviations.....	xxiii
Statement of Original Authorship .....	xxv
Acknowledgments.....	xxvii
Dedication .....	xxix
<b>CHAPTER 1:INTRODUCTION.....</b>	<b>1</b>
1.1 Background.....	1
1.2 Research hypotheses .....	2
1.3 Aims and objective .....	3
1.4 Justification of the research .....	3
1.5 Contribution to knowledge .....	4
1.6 Scope.....	5
1.7 Outline of the thesis .....	6
<b>CHAPTER 2:LITERATURE REVIEW.....</b>	<b>7</b>
2.1 Introduction.....	7
2.2 Water quality impacts .....	8
2.2.1 Pollutant sources .....	9
2.2.2 Stormwater pollution processes .....	16

2.2.3	Primary stormwater pollutants in the urban environment.....	19
2.3	Role of solids in urban stormwater .....	26
2.3.1	Adsorption.....	27
2.3.2	Adsorption characteristics of solids .....	28
2.3.3	Mechanisms of heavy metal association to solids .....	32
2.4	Influential parameters .....	36
2.4.1	Physical properties of solids .....	37
2.4.2	Chemical properties of solids.....	45
2.4.3	Influence of the solution characteristics.....	49
2.5	Heavy metals as an adsorbate .....	50
2.6	Adsorption/desorption of heavy metals .....	52
2.7	Summary .....	53
<b>CHAPTER 3:RESEARCH DESIGN .....</b>		<b>57</b>
3.1	Background .....	57
3.2	Research methodology .....	57
3.2.1	Study site selection .....	58
3.2.2	Build-up sample collection .....	58
3.2.3	Sample testing and batch experiments .....	59
3.2.4	Data analysis .....	60
3.3	Study tools .....	60
3.3.1	Sample collection system.....	60
3.3.2	Selection of vacuum cleaner and sprayer.....	61
3.3.3	Sample collection efficiency .....	64
3.3.4	Data analysis techniques .....	66
3.4	Summary .....	76
<b>CHAPTER 4:STUDY SITE SELECTION AND DATA COLLECTION.....</b>		<b>77</b>
4.1	Background .....	77
4.2	Study area selection .....	78
4.2.1	Gold Coast .....	78
4.3	Study site selection .....	79

4.3.1	Characteristics of the study sites.....	80
4.4	Sample collection.....	89
4.4.1	Build-up sample collection .....	89
4.4.2	Dry and wet vacuuming.....	91
4.4.3	Transport and handling of samples.....	93
4.4.4	Surface texture depth .....	93
4.4.5	Soil samples collection .....	93
4.5	Laboratory experiments .....	94
4.5.1	Sub sampling the build-up .....	94
4.5.2	Laboratory testing .....	96
4.5.3	Analysis of physical and chemical parameters .....	98
4.6	Adsorption/desorption experiment design .....	111
4.6.1	Equilibrium time for heavy metal adsorption .....	113
4.6.2	Adsorption/desorption experiment .....	114
4.7	Summary .....	116
 <b>CHAPTER 5:PHYSICAL AND CHEMICAL CHARACTERISTICS OF</b>		
<b>SOLIDS..... 119</b>		
5.1	Background.....	119
5.2	Build-up solids load .....	119
5.3	Investigation of physical and chemical characteristics.....	122
5.3.1	Particle size distribution.....	122
5.3.2	Total organic carbon (TOC) .....	125
5.3.3	Mineralogy.....	126
5.3.4	Clay analysis .....	131
5.3.5	Specific surface area (SSA) .....	132
5.3.6	Effective cation exchange capacity (ECEC).....	137
5.4	Characterisation of the build-up sample composition and pollutant source identification.....	140
5.4.1	Mineralogy of surrounding soil .....	141
5.4.2	Analysis of pollutant characteristics .....	145

5.5	Understanding of physical and chemical characteristics .....	149
5.5.1	Analysis of physical and chemical characteristics for different particle sizes .....	151
5.6	Conclusions.....	167
<b>CHAPTER 6:INFLUENCE OF PHYSICAL AND CHEMICAL CHARACTERISTICS ON HEAVY METALS ADSORPTION.. 173</b>		
6.1	Background .....	173
6.2	Heavy metal adsorption in different particle size fractions .....	174
6.3	Heavy metal adsorption behaviour for different particle size ranges .	180
6.3.1	Selection of data for analysis .....	181
6.3.2	Data pre-processing .....	182
6.4	Analysis of heavy metals in bulk build-up samples.....	202
6.5	Conclusions.....	210
<b>CHAPTER 7:INTERACTION OF HEAVY METALS WITH SOLIDS ..... 215</b>		
7.1	Introduction.....	215
7.2	Adsorption/desorption experiments .....	216
7.2.1	Selection of metal elements (adsorbate) .....	216
7.2.2	Characteristics of the selected solid samples (adsorbent).....	217
7.2.3	Data processing .....	218
7.2.4	Determination of equilibrium time .....	219
7.3	Adsorption and desorption of heavy metals.....	220
7.3.1	Adsorption of heavy metals to road deposited solids .....	220
7.3.2	Desorption of heavy metals from road deposited solids.....	223
7.4	Heavy metal adsorption in relation to physical and chemical properties of solids .....	226
7.4.1	Cr adsorption and desorption .....	227
7.4.2	Zn adsorption and desorption.....	231
7.4.3	Cu adsorption and desorption .....	235
7.4.4	Pb adsorption and desorption.....	238
7.5	Conclusions.....	242

<b>CHAPTER 8:CONCLUSIONS AND RECOMMENDATIONS FOR FURTHER RESEARCH.....</b>	<b>245</b>
8.1 Conclusions.....	245
8.1.1 Identification of important physical and chemical parameters of solids for heavy metal adsorption .....	246
8.1.2 The influence of physical and chemical characteristics on heavy metal adsorption.....	247
8.1.3 Adsorption and desorption of heavy metals in solids .....	250
8.1.4 Practical application of research outcomes.....	251
8.2 Recommendations for further research.....	252
<b>CHAPTER 9:REFERENCES.....</b>	<b>255</b>





# List of Figures

---

Figure 2.1: Water cycle changes associated with urbanisation (Adapted from Arnold et al. 1996) .....	8
Figure 2.2: Hypothetical representations of surface pollutant load over time (Adapted from Vaze and Chiew 2002) .....	19
Figure 2.3: Adsorption on a surface (Adapted from McBride 1994).....	27
Figure 2.4: Electrical double layer of negatively charged particle: Guoy-Stern Colloidal Model (Adapted from Weber et al. 1991).....	29
Figure 2.5: A hydrated cation (adapted from Wulfsberg 1991) .....	30
Figure 2.6: Characteristic interactions associated with bonds (adapted from Weber et al. 1991).....	31
Figure 2.7: Building unit in primary silicates (Adapted from White 2006).....	42
Figure 2.8: pH dependent adsorption behaviour of heavy metal on soil (Adapted from Elliott et al. 1986).....	50
Figure 3.1: The design of the water filter system of the Delonghi Aqualand model .....	63
Figure 3.2: The Swift Compact water sprayer (60L) .....	64
Figure 4.1: Gold Coast soil information of (Adapted from GCCC 2004) .....	79
Figure 4.2: Location of the study sites .....	81
Figure 4.3: Study sites in Clearview Estate: (a) Merloo Drive (b) Yarrimbah Drive (c) Winchester Drive and (d) Carine Court .....	83
Figure 4.4: Study sites in Nerang: (a) Stevens Street (b) Lawrence DR (c) Hilldon Court and (d) Patrick Road.....	85
Figure 4.5: Study sites in Benowa: (a) Strathaird Road (b) Mediterranean Drive (c) De Haviland Avenue and (d) Village High Road .....	87

Figure 4.6: Study sites in Surfers Paradise: (a) Hobgen Street (b) St Paul's Pl (c) Thornton Street and (d) Via Roma Drive .....	89
Figure 4.7: Collection of build-up sample through dry vacuuming .....	90
Figure 4.8: Collection of build-up sample through wet vacuuming: (a) Spraying and (b) Wet sample vacuuming .....	92
Figure 4.9: Micronized samples filled in (a) Ring holder (b) Crystal slide.....	103
Figure 4.10: Solid sample analysis using BET instrument: (a) SmartPrep and (b) TriStar analyzer .....	107
Figure 5.1: Cumulative particle size distribution of solids build-up in each suburb.....	123
Figure 5.2: Cumulative particle size distribution of solids build-up on St Paul's Place in Surfers Paradise .....	124
Figure 5.3: Mineralogical variations in four suburbs: a) Clearview Estate b) Nerang c) Surfers Paradise and d) Benowa .....	127
Figure 5.4: Thin film X-ray diffraction patterns of <75 $\mu$ m solids collected from Lawrence Drive at Nerang .....	131
Figure 5.5: Mineralogical variations of solids and soil samples in four suburbs .....	142
Figure 5.6: Thin film X-ray di.ffraction patterns of soil collected at Nerang suburb.....	144
Figure 5.7: PC 1 vs PC 2 biplot obtained from PCA analysis for soil and weighted average road deposited solids samples.....	147
Figure 5.8: PC 1 vs PC 2 biplot obtained from PCA on the particle size range <75 $\mu$ m.....	152
Figure 5.9: PC 1 vs PC 2 biplot obtained from PCA on the particle size range 75-150 $\mu$ m.....	159
Figure 5.10: PC 1 vs PC 2 biplot obtained from PCA on the particle size range 150-300 $\mu$ m.....	162

Figure 5.11: PC 1 vs PC 2 biplot obtained from PCA on the particle size range 300-425 $\mu\text{m}$ .....	165
Figure 6.1: PC 1 vs PC 2 biplot obtained from PCA for particle size range <75 $\mu\text{m}$ .....	184
Figure 6.2: PC 1 vs PC 2 biplot obtained from PCA for particle size range 75- 150 $\mu\text{m}$ .....	192
Figure 6.3: PC 1 vs PC 2 biplot obtained from PCA for particle size range 150-425 $\mu\text{m}$ .....	198
Figure 6.4: PC 1 vs PC 2 biplot obtained from PCA on all the particle size ranges .....	203
Figure 6.5: PC 1 vs PC 3 biplot obtained from PCA on all the particle size ranges .....	204
Figure 7.1: Variation in metal solution concentrations with time.....	219
Figure 7.2: GAIA biplot of Cr adsorption and desorption (a) with physical and chemical properties (b) with physical and chemical properties and Fe, Al and Mn .....	228
Figure 7.3: GAIA biplot of Zn adsorption and desorption (a) with physical and chemical properties (b) with physical and chemical properties and Fe, Al and Mn .....	232
Figure 7.4: GAIA biplot of Cu adsorption and desorption (a) with physical and chemical properties (b) with physical and chemical properties and Fe, Al and Mn .....	236
Figure 7.5: GAIA biplot of Pb adsorption and desorption (a) with physical and chemical properties (b) with physical and chemical properties and Fe, Al and Mn .....	239



# List of Tables

---

Table 2.1: Typical road runoff contaminants and their sources (Adapted from Ball et al. 1998) .....	12
Table 2.2: Sources of heavy metals in the urban environment (Adapted from Sansalone et al. 1996; Walker et al. 1999).....	22
Table 2.3: Specific surface areas of soil minerals (Adapted from Sparks 2003) .....	40
Table 2.4: Cation exchange capacity (CEC) of soil minerals (Adapted from Sparks 2003).....	46
Table 2.5: Binding fractions of metal association in dust, sediment and soil (Adapted from Harrison et al. 1981) .....	51
Table 3.1: Sample collection data for the wet and dry vacuuming system .....	66
Table 3.2: List of preference functions.....	73
Table 4.1: Description of selected road sites in Clearview Estate .....	82
Table 4.2: Description of selected road sites in Nerang .....	84
Table 4.3: Description of selected road sites in Benowa.....	86
Table 4.4: Description of selected road sites in Surfers Paradise.....	88
Table 4.5: Number of antecedent dry days.....	91
Table 4.6: Parameters and test methods .....	97
Table 4.7: Parameters and test methods for soil sample analysis .....	98
Table 5.1: Average solid load in build-up samples in each suburb.....	120
Table 5.2: Average TOC in the different particle sizes of solids in each suburb (average $\pm$ standard deviation) .....	125
Table 5.3: Mineralogical variation as a percentage of total solids weight .....	130
Table 5.4: Average EGME SSA and BET SSA of different particle sizes of solids (average $\pm$ standard deviation).....	134

Table 5.5: Effective cation exchange capacity (ECEC) for the different particle sizes of solids in each suburb .....	138
Table 5.6: Basic data set for PROMETHEE II ranking for particle size <75µm...	156
Table 5.7: PROMETHEE II ranking for particle size <75µm.....	158
Table 5.8 Physical and chemical properties and influential factors for different particle sizes .....	169
Table 6.1: Average heavy metal load in different particle sizes per unit area of road surface (average ± standard deviation).....	175
Table 6.2: Average heavy metal concentration in different particle sizes (average ± standard deviation) .....	177
Table 6.3: Comparison of heavy metal concentrations of road deposited solids with typical guideline values used in contaminated land assessment ...	180
Table 6.4: Correlation matrix for the particle size range <75µm.....	186
Table 6.5: Correlation matrix for the particle size range 75-150µm.....	193
Table 6.6: Correlation matrix for the particle size range 150-425µm.....	199
Table 6.7: Correlation matrix for the PCA analysis of all the particle size ranges.....	205
Table 6.8: Heavy metal adsorption characteristics of different particle sizes .....	212
Table 7.1: Physical and chemical properties of the solids particles subject to batch adsorption/desorption experiments.....	218
Table 7.2: Adsorbed Cr, Cu, Zn and Pb concentration ( $q_{0-i}$ ) and adsorbed metals as a percentage of total adsorbed metal concentration ( $((q_{0-i} / q_T)\%$ ) .....	221
Table 7.3: The adsorption capacity ( $q_T$ ) of road deposited solids for 0.1mM concentration of Cr, Cu, Zn and Pb in three different particle sizes .....	223
Table 7.4: Desorbed Cr, Cu, Zn and Pb concentrations ( $q_{ex}$ ) and desorption as a percentage of total adsorbed metal concentration ( $((q_{ex} / q_T)\%$ ) .....	224
Table 7.5: PROMETHEE II ranking for Cr adsorption.....	229
Table 7.6: PROMETHEE II ranking for Zn adsorption .....	233

Table 7.7: PROMETHEE II ranking for Cu adsorption.....	237
Table 7.8: PROMETHEE II ranking for Cu adsorption.....	240





# List of Appendices

---

Appendix A	Analysis of physical and chemical parameters of solids.....	289
Appendix B	Analysis of heavy metal in solids .....	319
Appendix C	Interaction of heavy metals with solids .....	329



# List of Abbreviations

---

Al	-	Aluminium
BET	-	Brunauer-Emmett-Teller
C	-	Commercial
Ca	-	Calcium
Cd	-	Cadmium
CEC	-	Cation exchange capacity
Cr	-	Chromium
Cu	-	Copper
DOC	-	Dissolved organic carbon
EC	-	Exchangeable cations
ECEC	-	Effective cation exchange capacity
EGME	-	Ethylene glycol monoethyl ether
Fe	-	Iron
GAC	-	Granular activated carbon
HCl	-	Hydrochloric acid
Hg	-	Mercury
HNO <sub>3</sub>	-	Nitric acid
I	-	Industrial
K	-	Potassium
LFB	-	Laboratory fortified blanks
LRB	-	Laboratory reagent blanks
MB	-	Methylene blue
MCDM	-	Multi Criteria Decision Making Methods
Mg	-	Magnesium
Mn	-	Manganese
N	-	Nitrogen
Na	-	Sodium
Nd	-	Not detected
NH <sub>4</sub> Cl	-	Ammonium chloride
Ni	-	Nickel

OH <sup>-</sup>	- Hydroxyl
OM	- Oxygen
Pb	- Lead
PCA	- Principal component analysis
PCB	- Polychlorinated biphenyls
PCs	- Principal components
PSD	- Particle size distribution
R	- Residential
SSA	- Specific surface area
TOC	- Total organic carbon
TSS	- Total suspended solids
XRD	- X-ray diffraction
Zn	- Zinc
(-COOH)	- Carboxyl

# Statement of Original Authorship

---

The work contained in this thesis has not been previously submitted for a degree or diploma from any other higher education institution to the best of my knowledge and belief. The thesis contains no material previously published or written by another person except where due reference is made.

---

Chandima Gunawardana

---

Date



# Acknowledgments

---

It is a great pleasure for me to express my warm and sincere thanks to numerous people who helped me during this research study. I am extremely grateful to my principal supervisor Prof. Ashantha Goonetilleke for the invaluable support, professional guidance and continuous encouragement provided to me throughout this research. I wish to further extend my sincere appreciation to my associate supervisors Dr. Prasanna Egodawatta and Associate Prof. Les Dawes for their dedicated support and professional guidance throughout the research. Special thanks is also extended to Adjunct Prof. Serge Kokot for his advice and guidance during data analysis and batch experiment studies.

I am grateful to the Faculty of Built Environment and Engineering, Queensland University of Technology (QUT), for providing financial support for this research project. Appreciation is also extended to Adjunct Prof. Evan Thomas and Mr. Randall Scott at Gold Coast City Council (GCCC) for permitting me to conduct field investigations within Council property. My appreciation is also extended to the Queensland Police Service for providing permission to work at the study sites.

I wish to acknowledge the generous support provided by the QUT technical staff during my field investigations and laboratory experiments. In particular, I would like to convey my thanks to Mr. Jonathan James, Mr. Matthew Mackay, Mr. James Hazelman, Mr. David Venn, Mr. Scott Allbery, Mrs Ellainne Steele and Mrs Sonya Canham for their support in carrying out the field investigations. My appreciation is further extended to Mr. Tony Raferty, Mr. Bill Kwiecien, Ms. Leonora Newby, Mr. Nathaniel Raup, Mr. Shane Russell and Mr. Nick Ryan for providing the necessary technical support and for providing access to laboratory facilities. A very special thanks also goes to Dr. Wayde Martens for the free allocation of the TriStar analyser (BET) instrument and for technical support.

The support given by Mrs. Diane Kolomeitz, Mrs. Kerrie Petersen and Mrs. Karyn Gonano for improving my thesis writing skills is gratefully acknowledged. My acknowledgments are further extended to my fellow researchers Ms. An Liu, Mr. Damitha Peiris, Ms. Nandika Miguntanna, Ms. Nadeeka Miguntanna, Mr. Parvez Mahbub, Mr. Rajitha Nawarathna, Mrs. Rupika Bandara, Mr. Isri Mangangka and Mr. Ashley Locke for their support in this research. Finally, I would like to express my gratitude to all relatives and friends for the support and encouragement I received.



# Dedication

---

I wish to dedicate this thesis to my parents, Mr. W. Gunawardana and Mrs. Sujatha Gunawardana, and to my sister Champika for their love, unlimited support and encouragement throughout this doctoral research.



# Chapter 1: Introduction

---

## 1.1 BACKGROUND

Urbanisation leads to the conversion of rural pervious areas into urban land with a high percentage of impervious area. Urbanisation significantly influences the urban water environment by increasing the quantity of stormwater runoff and dramatically altering stormwater quality (Goonetilleke et al. 2005; Prakash 2005). Anthropogenic activities inherent in urban land use generate a diversity of pollutants in the urban environment (Goonetilleke et al. 2005; Hengren et al. 2006). A significant portion of these pollutants accumulate on impervious surfaces and are transported to receiving water bodies by stormwater runoff. Therefore, urban stormwater runoff has been identified as a primary source of pollutants in receiving water bodies. Furthermore, the distributed nature of stormwater inlets to receiving water bodies increases the complexity of stormwater management strategies.

Due to the growing concern about stormwater runoff pollution, the development of effective stormwater management strategies to reduce the amount of pollutants entering stormwater is gaining increasing attention. In this context, accurate assessment of stormwater quality is very important. Stormwater runoff delivers a range of accumulated pollutants to urban receiving waters. Among them, solids play a key role by acting as a mobile substrate in the transport of potentially toxic pollutants such as heavy metals (Sartor and Boyd 1972).

The various anthropogenic activities common to the urban environment contribute a diversity of toxic heavy metals to stormwater runoff. Heavy metals in urban stormwater are transported primarily attached to solids (Sartor and Boyd 1972; Hengren et al. 2006; Zhao et al. 2010). As a result, certain heavy metals concentration is much higher in solids compared to the soluble concentration (Liebens 2001; Lau and Stenstrom 2005). The toxicity and bioavailability characteristics of heavy metals that could be discharged into natural water bodies are a challenging issue in stormwater management (Morrison et al. 1988). While

stormwater treatment facilities are often designed to remove solids from stormwater, the effectiveness of such management strategies can be limited by the complexities resulting from the association of stormwater pollutants with solids.

Although previous researchers confirm that the finer particles adsorb a relatively higher heavy metals load, in-depth studies explaining the reasons for such behaviour are limited (Vinklander 1998; Lau et al. 2005; Herngren et al. 2006). In order to investigate the association heavy metals with solids, it is necessary to identify the primary parameters which influence pollutant accumulation on solids and the process of pollutant adsorption to solids. Due to the dynamic nature of solids accumulation on road surfaces, the properties of these solids are complex. Consequently, the degree of influence exerted by the various parameters is highly variable. Therefore, an in-depth understanding and fundamental knowledge of the parameters which influence toxic heavy metal retention and release from the solids particles and the process of heavy metal interaction with solids particles is crucial for the development of effective stormwater management strategies.

## **1.2 RESEARCH HYPOTHESES**

This research is driven by the following hypotheses:

- Adsorption of heavy metals to solids is strongly influenced by the physical and chemical characteristics of solids and the selectivity of heavy metals to adsorption processes.
- The important physical and chemical characteristics of solids are influenced by location specific characteristics such as the geographic area and land use, resulting in differences in solids composition.

### **1.3 AIMS AND OBJECTIVE**

#### **Aims**

The project aims were:

- To identify the physical and chemical characteristics of solids that influence heavy metals adsorption
- To identify the variations in physical and chemical characteristics of different particle sizes of road deposited solids in relation to heavy metals adsorption
- To understand the different adsorption processes influenced by the physical and chemical characteristics of solids.

#### **Objective**

The primary objective of this research study was to understand the adsorption process of solids and to identify the critical characteristics which influence heavy metals adsorption.

### **1.4 JUSTIFICATION OF THE RESEARCH**

It is well recognised that pollutants originating from urban surfaces dramatically alter receiving water quality. To eliminate impacts on receiving waters due to stormwater runoff pollution, it is essential to have appropriate stormwater management strategies and efficient treatment designs. However, the effectiveness of such stormwater management strategies is strongly dependent on accurate assessment of stormwater quality characteristics.

Pollutants such as heavy metals attached to particulates can cause significant degradation of the urban receiving water environment. The bioavailability of particulate heavy metals during wash-off by stormwater runoff and the processes associated with stormwater management practices can increase the soluble metal content transfer to receiving water (Morrison et al. 1988). In natural systems, there is equilibrium between dissolved complexes and adsorbed metal elements. However,

the characteristics of urban stormwater runoff will lead to the destabilisation of the natural system equilibrium and the enrichment of heavy metal loads. A comprehensive understanding of adsorption processes will provide essential information on the mobility and bioavailability of heavy metals and, subsequently, enhance the mitigation of heavy metal pollution of urban receiving water environments (Morrison et al. 1988).

## **1.5 CONTRIBUTION TO KNOWLEDGE**

Research studies have shown that heavy metals are present in urban stormwater in dissolved and particulate phases (for example, Liebens 2001; Vinklander 1998). However, detailed studies explaining how heavy metals are attached to particles are limited (Lau et al. 2005; Murakami et al. 2008).

The current research study provides an in-depth understanding of the influence of specific physical and chemical characteristics that govern the heavy metal adsorption to different particle sizes of solids. Additionally, the research study has created fundamental knowledge in relation to the different mechanisms of heavy metals adsorption to solids particles, the parameters which help to establish stable bonds with heavy metals, and the processes that contribute to the bioavailability of heavy metals in urban stormwater runoff.

The influence of common substances associated with road surface solids such as organic matter, minerals and amorphous material which contribute to altering their surface properties in relation to adsorption processes have been clearly articulated in this research study. These important phenomena have not been subject to in-depth investigations in the past, although their influence has been explicitly acknowledged in research literature. The study outcomes identify the crucial role played by the different solids components present in the road surface environment on heavy metal adsorption to solids particles.

The knowledge created in relation to the adsorption processes of road deposited solids has extended the understanding of the fate of heavy metals in urban stormwater runoff. Additionally, the knowledge created regarding influential parameters in heavy metal adsorption can be extended to investigate the adsorption of other chemical pollutants to solids particles. Finally, this knowledge can contribute to the design of effective stormwater management strategies.

## **1.6 SCOPE**

The research focused on the physical and chemical characteristics of solids which influence pollutant adsorption and the key processes in relation to urban stormwater pollution. The research project investigated the particulate pollutant build-up on urban impervious surfaces. The following points outline the specific scope of the research study.

- The study sites were confined to the Gold Coast area. However, the knowledge created regarding the adsorption processes of solids is also applicable to other geographic areas, as the study was based on the hypothesis that adsorption processes are generic.
- The research was confined to road surface pollutants. Road surfaces are the major contributor of pollutants to urban stormwater. Once again, this was based on the hypothesis that adsorption processes are generic.
- Field investigations were carried out in three different land uses, namely, residential, industrial and commercial, to enable the evaluation of the different characteristics of solids. The different land uses were selected from four different suburbs. However, land use was not considered as a variable in this research.
- Four road sites per suburb were chosen, based on the hypothesis that each road represents the relative diversity of the pollutant load in the area.
- In each land use, roadside soils were investigated to identify the influence of surrounding soil input to the build-up of pollutants on road surfaces.

- Influence of seasonal variation of pollutant build-up was not taken into account. The investigations were based on the hypothesis that the adsorption processes are independent of seasonal variation.
- The research study focused only on heavy metals adsorption to solids. Other pollutants were not investigated.
- The research focused only on the physical and chemical parameters. Organic matter decay and microbiological parameters were not investigated.

## **1.7 OUTLINE OF THE THESIS**

The thesis consists of eight chapters. Chapter 1 introduces the research problem, and presents the aims, objectives and overview of the research study. A state-of-the-art literature review is presented in Chapter 2. The research methods and design – including the study tools, the field investigation apparatus, and the concepts and application of the various data analysis techniques—are described in Chapter 3. Chapter 4 discusses the selection of study sites, field sample collection procedures and laboratory testing procedures.

Chapters 5, 6 and 7 discuss the outcomes of the data analysis. The physical and chemical characteristics of solids and correlations among these parameters are discussed in Chapter 5. Chapter 6 discusses the influence of the physical and chemical characteristics of solids on heavy metal adsorption. Chapter 7 discusses the outcomes of the batch adsorption experiments undertaken to validate the knowledge created, based on the field samples collected.

Conclusions and recommendations for further research are provided in Chapter 8. The final chapter provides the references used throughout the thesis.



# Chapter 2: Literature Review

---

## 2.1 INTRODUCTION

The movement of population to urban areas is continuing in most parts of the world. Improved living standards resulting from the availability of transportation systems, services, and employment opportunities attract increased population to urban areas. However, population growth and an increase in anthropogenic activities in urban areas lead to the expansion of the urban footprint (Hall and Ellis 1985). Thus, even though urbanisation is an important indicator of economic growth, it gives rise to a number of adverse impacts on natural systems, such as water pollution, resulting from various anthropogenic activities.

Urbanisation in a catchment results in an increased percentage of impervious surfaces. As much as 35-40% of the surfaces in an urban area are covered by roads, car parks, roof surfaces and other hard surfaces (Angino et al. 1972). These impervious surfaces allow only a relatively small portion of stormwater to infiltrate the soil. The effects of the changes to pervious surfaces on stormwater can be discussed under two categories: water quantity changes and water quality changes (Fulcher 1994; Goonetilleke et al. 2005; Gnecco et al. 2005).

The primary quantitative impacts of urbanisation are increased runoff volume, increased peak discharge, reduction of lag time and reduction of base flow. Quantitative impacts can be primarily attributed to the increase in catchment imperviousness, hydraulic conveyance through channels, other drainage structures and the removal of vegetation (Arnold and Gibbons 1996; Farahmand et al. 2007). As urbanisation increases, a series of changes occur in the natural water cycle (Arnold and Gibbons 1996). These, in turn, closely correlate with the impacts on hydrologic processes. Figure 2.1 illustrates the changes in runoff and infiltration due to the increase in surface imperviousness that comes with urbanisation. These changes lead to the production of high surface runoff volumes. The high surface

runoff volumes, in turn, lead to an increase in runoff velocities and peak flow rates. Reduction in lag time occurs due to enhanced conveyance of stormwater runoff due to reduced roughness and uniform slopes (Hall and Ellis 1985; Espey et al. 1969; Zoppou 2001). Impervious surfaces and modified drainage systems contribute a greater proportion of runoff to receiving water bodies (Hall and Ellis 1985). This increased runoff results in floods, erosion and degradation of stream habitats, and the deterioration of water quality.

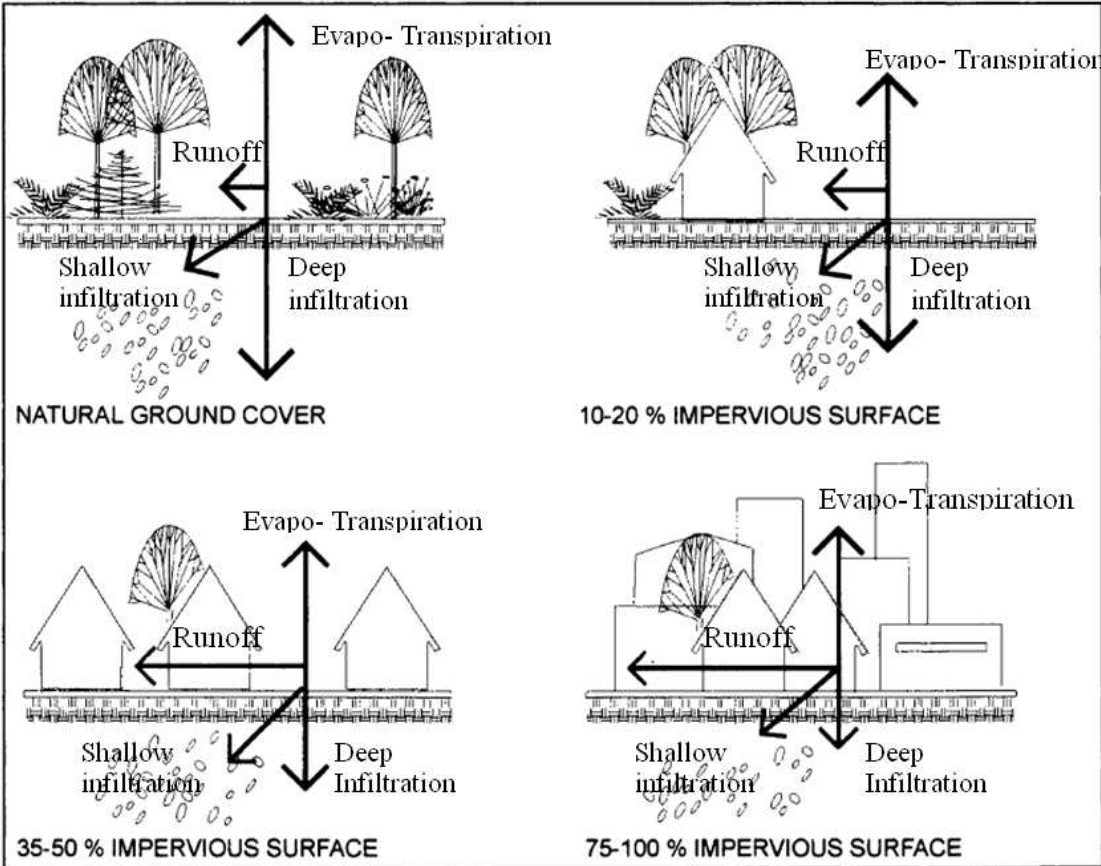


**Figure 2.1: Water cycle changes associated with urbanisation (Adapted from Arnold et al. 1996)**

**2.2 WATER QUALITY IMPACTS**

The changes in impervious cover due to urban land use not only influence water quantity impacts, but also impact on the quality of receiving water bodies. Increased anthropogenic activities in urban areas increase pollutant generation and deposition on impervious surfaces. These pollutants are washed off during storm events,

resulting in high pollutant loads to receiving water bodies. As noted by Hoffman et al. (1984), 50% of total river pollutants originate from stormwater.

The diverse nature of pollutants in urban stormwater runoff creates significant water quality impacts in receiving water bodies (Brabec et al. 2002). These impacts include sedimentation, salinity, temperature changes and degradation of aquatic habitats. These pollutants can alter the physical, chemical and biological processes in receiving water bodies. This alteration, in turn, can lead to adverse impacts on recreational activities and on the aesthetic quality of receiving waters (Settacharnwit et al. 2003).

The severity of the impacts of stormwater runoff pollutants on the quality of receiving waters depends on pollutant concentrations, the type of pollutant and the pollutant load. As noted by past researchers, the pollutant concentration and total load associated with stormwater runoff can be higher than that of secondary treated domestic sewage effluent (Sartor and Boyd 1972; Cordery 1977; Novotny and Chester 1981). The loads and types of pollutants incorporated into stormwater are dependent on the activities associated with the surrounding land use (Goonetilleke et al. 2005). Runoff from road surfaces, for example, has received considerable attention due to the abundance of harmful pollutants generated by traffic activities (Ellis et al. 1997; Herngren et al. 2006).

### **2.2.1 POLLUTANT SOURCES**

Pollutants in the urban environment result from complex and diverse sources (Adachi and Tainosho 2004). The identification of such sources and an understanding of their characteristics is important in urban water quality research (Brinkmann 1985; Charbonneau and Kondolf 1993; Pitt et al. 1995). The primary sources responsible for the accumulation of pollutants in urban surfaces are:

- Transportation activities
- Industrial, commercial and residential activities
- Construction and demolition activities
- Corrosion

- Vegetation inputs
- Soil erosion
- Atmospheric fallout.

(Sartor and Boyd 1972; Brinkmann 1985; Pitt et al. 1995)

### **A. Transportation activities**

Transportation activities contribute large amounts of pollutant to stormwater through vehicle traffic and road surface wear (Sartor and Boyd 1972; Bannerman et al. 1993; Fulcher 1994). The rapid growth of transportation activities increases pollutant generation and the consequent pollutant load on road surfaces. According to estimates by the Department of Transport and Regional Services, Australia (2007), a substantial growth in commercial vehicles (3.5% per annum) and private cars (1.7% per annum) is expected between 2005 and 2020.

Transportation activities are the major source of sediments, metals and hydrocarbons in receiving waters (Walker et al. 1999; Wik and Dave 2009). Pollutants generated from vehicular traffic can be in solid, liquid or gaseous forms. These pollutants are mainly generated from:

- Combustion exhaust
- Lubricant leakages
- Abrasion products (tyre wear, brake lining)
- Load losses from vehicles
- Road surface wear

(Brinkmann 1985; Bannerman et al. 1993; Adachi and Tainosho 2005).

The accumulation and generation of pollutants on road surfaces is very rapid. For example, Muschack (1990) estimated that particles from tyre abrasion on urban roads in Germany range between 55 to 657kg/km/year, and Adachi and Tainosho (2004) estimated that the annual tyre dust emitted to the Japanese environment was 2.1x10<sup>8</sup>kg in 2001. According to Dannis (1974), during the lifetime of a tyre (which

can be 40 000km) an average of 37% of original tread rubber is subject to wear. These facts indicate the significance of transportation activities for pollutant generation on road surfaces. Furthermore, particles on road surfaces are subject to the complex mixing processes that occur during transport and other on-road activities. These processes continue to alter the composition of particles due to their interactions with the road through heat and friction (Beckwith et al. 1986).

These particles contain a wide range of toxic compounds that can leach to water and create toxicity in the environment (Evans 1997). For example, the main components of brake lining are fibres for mechanical strength, abrasives for increasing friction, lubricants for stabilising the frictional properties, binders for maintaining structural integrity and fillers for adjusting the proportions of the various constituents (Stanford and Jain 2001). These materials typically contain zinc, magnesium and antimony. Similarly, other traffic related material, such as tyre dust and particles resulting from pavement wear, contain high levels of heavy metals (McKenie et al. 2009). Furthermore, the particle composition can vary considerably due to differences in manufacture. The impact associated with different particles may also differ due to the various shapes and sizes of the particles. For example, the particles generated by traffic contain a rough morphology and porous structure. Particles originating from vehicle movement, on the other hand, can be very fine, ranging from 5µm to 300µm and primarily containing metallic elements which exert a toxic effect (Cadle and Williams 1978). Based on a detailed investigation of road surface pollutants, Ball et al. (1998) summarised the pollutants present on road surfaces and their sources, as listed in Table 2.1.

The majority of pollutants generated by traffic and road surface wear predominantly accumulate on road surfaces (Brinkmann 1985). The relatively higher amount of pollutant accumulation resulting from transportation activities leads to high pollutant loads from road surfaces, compared to other impervious surfaces (Sartor and Boyd 1972; Shaheen 1975; Ellis and Revitt 1982; Fulcher 1994; Ball et al. 1998). The generation of pollutants on road surfaces varies widely depending on road surface characteristics, traffic density, maintenance practices (such as road sweeping) and land use (Sartor and Boyd 1972).

Even though pollutants present on road surfaces are mainly traffic related, other factors such as atmospheric deposition and erosion from surrounding land can also provide a significant contribution to pollutant loads. However, since road surfaces represent a significant proportion of impervious surfaces in a catchment, they are considered as the most significant pollutant source in urban areas.

**Table 2.1: Typical road runoff contaminants and their sources (Adapted from Ball et al. 1998)**

<b>Contaminant</b>	<b>Primary source</b>
Particulates	Pavement wear, vehicles, maintenance activities
Nitrogen/Phosphorous	Roadside fertiliser applications, atmosphere
Lead	Auto exhaust, tyre wear, lubricating oil and grease, bearing wear
Zinc	Tyre wear, motor oil, grease
Iron	Auto rust, steel highway structures (e.g. guard rails), moving engine parts
Copper	Metal plating, bearing and brush wear, moving engine parts, brake lining wear, fungicides, insecticides
Cadmium	Tyre wear, insecticide application
Chromium	Metal plating, moving parts, brake lining wear
Nickel	Diesel fuel and petrol exhaust, lubricating oil, metal plating, brush wear, brake lining wear, asphalt paving
Manganese	Moving engine parts, auto exhaust
Sulfate	Roadways surfaces, fuels, deicing salts
Petroleum hydrocarbons	Spills, leakages of motor lubricants, hydraulic fluids, asphalt surface leachate
Polychlorinated biphenyls (PCB)	Background atmospheric deposition, PCB catalyst in synthetic tyres, spraying of rights-of-way
PAH	Asphalt surface leachate

## **B. Industrial, commercial and residential activities**

Industrial, commercial and residential activities contribute a range of pollutants to urban runoff. As noted by Bannerman et al. (1993), parking lots and road surfaces are the most critical source areas for pollutant accumulation in industrial and commercial land uses. Pollutant type and concentration varies with various land uses and their associated activities (Arnold and Gibbons 1996).

The most common pollutants that are emitted to the urban environment from industrial activities are heavy metals, hydrocarbons and nutrients (Sartor and Boyd 1972). Past researchers have noted that industrial sites generate relatively higher pollutant loads than commercial and residential land uses (for example, Sartor and Boyd 1972; Bannerman et al. 1993; Bian and Zhu 2008). However, the pollutant load can vary according to the nature of the industry and its operational practices. Commercial activities such as vehicle maintenance, liquid storage, and equipment storage and maintenance can also introduce similar pollutants to urban runoff (Pitt et al. 2004).

In residential areas, activities such as lawn and garden maintenance and household cleaning contribute pollutants to urban surfaces (US EPA 2005). As noted by Bannerman et al. (1993), lawns and driveways contribute high phosphorous load in residential land uses due to the use of detergents. Fertilisers used in garden maintenance can contribute high nitrogen and phosphorus loadings to urban runoff. Furthermore, the addition of pesticides contributes to hydrocarbon loading to urban runoff. Activities such as yard trimming and maintenance of lawns contribute weeds, and branches. Disposal of wash water with detergents from household activities, such as car washing and household cleaning, and roof runoff can pollute the receiving water; this can result in high loads of nutrients, heavy metals, and hydrocarbons (US EPA 2005).

### **C. Construction and demolition activities**

Construction and demolition activities contribute considerable amounts of pollutants to urban runoff. Solids particles, litter and chemicals (heavy metals, nutrients and pesticides) are the most significant pollutants present at construction sites (US EPA 1993). However, the total amount of pollutants generated can vary considerably depending on the type of construction activity and the management of the site. Potentially, solids from construction sites are the major pollutant in stormwater runoff. Brinkmann (1985) has noted that, in most cases during the wash-off, solids distribute according to their grain size. A high solids load can result in sedimentation in receiving waters (US EPA 1993).

### **D. Corrosion**

Corrosion of metallic surfaces initially occurs due to atmospheric moisture and oxygen. Acid rain increases the corrosion of the rusted surfaces. Rain water is naturally acidic due to the reaction of water vapour, carbon dioxide and nitrogen in the atmosphere. In the urban environment, metallic surfaces and structures such as roofs, gutters and fences are corroded as they are exposed directly to rainfall and to the atmosphere. In the study carried out by Brinkmann (1985), it was found that the rate of corrosion depends on the availability of corrodible materials, the frequency and the intensity of exposure to an aggressive environment, the frequency of drying and wetting of the surface, maintenance practices and the surface material. Wash-off processes on metallic surfaces (common roofing and gutter materials) can contribute high loads of heavy metals to stormwater as a corrosion by-product which is easily removed by rainfall (Pitt et al. 1995; Gnecco et al. 2005).

### **E. Vegetation inputs**

Vegetation matter commonly found in urban areas includes plant materials such as leaves, grass, pollen and bark. These can clog pipes and drainage channels. According to Novotny et al. (1985), a mature tree can produce between 15 to 25kg of leaf residue during the fall season. Vegetation input to stormwater runoff can vary depending on catchment characteristics, land use pattern and seasonal variations. Vegetation matter is a significant source of nutrients and organic pollutants to urban



stormwater (Cordery 1977; Allison et al. 1998). According to the findings of Allison et al. (1998), nutrient contribution by leaf litter is relatively low compared to the total nutrient load in stormwater runoff.

#### **F. Soil erosion**

Erosion is considered as a natural source of solids to stormwater. Erosion of stormwater drains due to increased peak flow and high flow velocities, contribute soil particles to stormwater runoff. Unpaved surfaces in urban areas, agricultural lands and construction and demolition sites are highly prone to erosion (Brinkmann 1985; Novotny et al. 1985). Loss of vegetation cover increases soil erosion. The severity of erosion varies depending on factors such as the soil type, land cover, climatic conditions, topography and intensity of rainfall (hydrological processes) (Farahmand et al. 2007). Furthermore, hydrologic change such as high peak flows has a significant influence on erosion.

#### **G. Atmospheric fallout**

Atmospheric fallout originates as air pollution. Industries, vehicle exhausts and wind blowing over unprotected pavements introduce pollutants to the atmosphere (James et al. 1985). Vehicle exhausts emit dust particles to the air, and as the dust particles are small, they can remain in the atmosphere for a considerable time (Pitt et al. 2004). Therefore, emissions from these activities initially pollute the atmosphere and will eventually return to the ground surface as atmospheric fallout and then contribute to stormwater runoff pollution (Brinkmann 1985). These particles are clearly a significant source of heavy metals and hydrocarbons (Rogge et al. 1993). James et al. (1985) noted that significant amounts of solids and nutrients contribute to stormwater runoff from the atmosphere. Furthermore, they noted that meteorological conditions such as rainfall, wind direction and wind velocity are influential parameters for dust fall.

### 2.2.2 STORMWATER POLLUTION PROCESSES

Pollutant processes on urban impervious surfaces are complex and are generally separated into build-up and wash-off (Vaze and Chiew 2002). Pollutant build-up describes the accumulation of pollutants on impervious surfaces over a dry period. Pollutant wash-off describes the removal of accumulated pollutants from the impervious surfaces during stormwater runoff events.

#### A. Build-up

As described by Duncan (1995), build-up is a dynamic process, in equilibrium between pollutant deposition and removal, and between pollutant sources and sinks at a given time. Researchers have identified that the pollutant accumulation on a surface depends on the following primary factors:

- Land use
- Antecedent dry period
- Time elapsed since roads were last cleaned
- Local traffic volume and characteristics
- Fraction of impervious area
- Pavement type and condition
- Road cleaning practices
- Meteorological conditions

(Sartor and Boyd 1972; Bradford 1977; Pitt 1979).

These factors directly influence the pollutant build-up load, available pollutants and the pollutant distribution on surfaces (Sartor and Boyd 1972; Deletic and Maksimovic 1998; Vaze and Chiew 2002). Road surfaces have a high pollutant build-up load compared to other impervious surfaces in urban areas (Ball et al. 1998; Brodie and Porter 2006; Sabin et al. 2006).

Pollutant build-up load in different land uses has been studied widely (for example Sartor and Boyd 1972; Novotny et al. 1985; Ball et al. 1998; Deletic et al. 2005). Due to differences in anthropogenic activities and pollutant sources, the pollutant load and pollutant types tend to vary (Sartor and Boyd 1972; Goonetilleke et al. 2005; Bian and Zhu 2008). Furthermore, pollutant distribution and concentration can vary considerably, even in similar land uses (Gobel et al. 2006). This is due to differences in population density, building density and anthropogenic activities in the area.

Sartor and Boyd (1972) found that road surface particles are not uniformly distributed across the surface. Study outcomes found that 95% of pollutants are accumulated closer to the kerb and lie in the first one meter strip of the road. They further noted that vehicle-induced wind turbulence tends to blow particles towards the kerb line. This observation was confirmed by Deletic and Orr (2005) who reported that 66% of total road pollutant load lies within a 0.5m strip next to the kerb. However, substances such as oil, grease and lubricants spilled on the surface are concentrated along the centre of the traffic lane.

Particle size distribution of build-up pollutants is important as it can significantly influence the pollutant composition. Past researchers have found that build-up on road surfaces has a significant fraction of fine particulates (Walker and Wong 1999; Hengren et al. 2006; Bian and Zhu 2008). Deletic and Orr (2005) noted that the particle size distribution of solids varies across a roadway. They found that the median diameter of particles in the middle of the road is smaller than the particles near the kerb due to dispersion. However, Patra et al. (2008) found that the majority of the large sand size particles disperse across the road due to vehicular induced turbulence and the movement of these particles are more rapid than that of the fine particles. The particle dispersion is primarily influenced by particle size, shape, vehicle speed, traffic density, vehicle types, antecedent dry days and road surface conditions (Namdeo et al. 1999; Patra et al. 2008).

The antecedent dry period in relation to pollutant build-up is an important parameter (Yamada et al. 1993; Egodawatta and Goonetilleke 2006). Ball et al. (1998), Deletic and Maksimovic (1998) and Vaze et al. (2000) have noted that the pollutant build-up increases with the antecedent dry period. Sartor and Boyd (1972) suggested that the rate of pollutant build-up is high for several days immediately after road sweeping or a rainfall event. The rate then reduces and, ultimately, the total build-up approaches a near constant value. Similarly, Egodawatta and Goonetilleke (2006) noted that the build-up load asymptote to a constant value as antecedent dry days increase. In mathematical modelling of the build-up process, it has been treated as a linear, exponential, power, log-normal or stochastic function (Tai 1991; Haiping and Yamada 1998; Vaze and Chiew 2002).

## **B. Wash-off**

Pollutant wash-off removes the accumulated pollutants on catchment surfaces during rainfall events. After the surface gets wet during a rainfall event, the pollutants on the surface are either dissolved or loosened. Then, both dissolved and particulate pollutants are washed off due to the energy of the rain drops and the energy in flow. The amount of pollutant washed-off by a rainfall event depends on the amount of pollutants accumulated during the preceding dry period, the energy of rain drops available to loosen the particles, slope of the surface and the rainfall intensity (Pitt et al. 2004; Egodawatta and Goonetilleke 2008).

However, rainfall may remove only a portion of the pollutants accumulated on the surface (Vaze and Chiew 2002). Based on field studies, Vaze and Chiew (2002) proposed two alternative views of the wash-off processes: source limiting or transport limiting. These two possible wash-off concepts are illustrated in Figure 2.2. Source limiting refers to the situation where the pollutant build-up accumulates from zero over the antecedent dry days [Figure 2.2(a)] and most of the available pollutant load is then washed off during a storm event. On the other hand, the transport limiting process assumes that a storm event removes only a fraction of the surface pollutant load and the build-up occurs relatively quickly to return the surface pollutant load back to the previous level within several days [Figure 2.2(b)]. Vaze

and Chiew (2002) further suggested that wash-off disintegrates and dissolves most of the available surface pollutants.

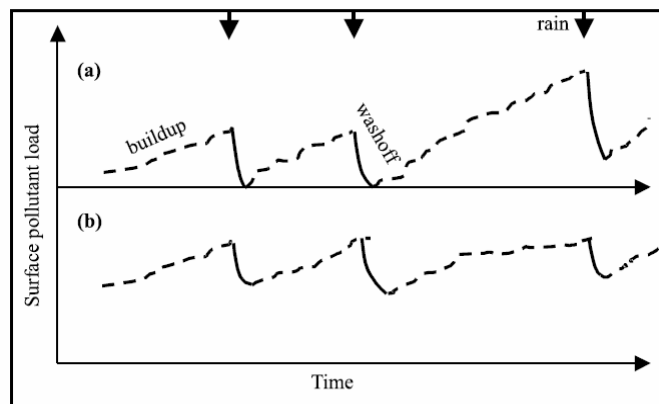


**Figure 2.2: Hypothetical representations of surface pollutant load over time (Adapted from Vaze and Chiew 2002)**

The initial period of stormwater runoff is defined as the ‘first flush’. The first flush contains a high pollutant concentration and is substantially higher than the later part of the runoff (Gupta and Saul 1996; Lee et al. 2002). First flush is influenced by parameters such as catchment area, rainfall intensity, impervious area and antecedent dry period (Wanielista and Yousef 1993; Gupta and Saul 1996). However, Lee et al. (2002) found that there is no correlation between the first flush and the antecedent dry period.

### 2.2.3 PRIMARY STORMWATER POLLUTANTS IN THE URBAN ENVIRONMENT

It is widely recognised that stormwater runoff exerts a significant influence on the degradation of receiving water quality by transporting a variety of pollutants. Therefore, it is important to identify the types of pollutants in urban stormwater. In the following section, the most common types of urban stormwater pollutants built up on urban surfaces, and their sources and significant characteristics are discussed. Primary stormwater pollutants common to urban catchments are:

- Solids
- Heavy metals
- Organic matter

- Nutrients
- Hydrocarbons
- Litter.

### **A. Solids**

Solids deposited on a road surface are heterogeneous and are the result of atmospheric deposition, inputs from surrounding soil and pollutants originating from traffic related activities (Fergusson and Kim 1991). Traffic related pollutants originate from tyre and brake abrasion products, combustion exhaust and pavement wear (Rogge et al. 1993; Adachi and Tainosho 2004; Kreider et al. 2010). Solids originating from natural sources are erosion, residue from vegetation and deposition of atmospheric dust. It has been found that the anthropogenic sources contribute a higher amount of fine particles to the urban environments than natural sources (Fergusson and Ryan 1984). A study carried out by Rogge et al. (1993) on particle composition found that the dominant source of solid particles on urban roads is vehicles.

As noted by Beckwith et al. (1986) solids particles on road surfaces are subjected to complex mixing processes which occur during transport and other on-road processes and which continue to alter their chemical composition. Such changes in chemical composition are also common for the natural soil inputs found on road surfaces. Furthermore, due to frequent traffic activities, traffic related particles can combine with soil mineral components and produce unique mixtures (Kreider et al. 2010).

Solids in the dry state are referred to as ‘clay’ (<2 $\mu\text{m}$ ), ‘silt’ (2-75 $\mu\text{m}$ ) and ‘sand’ (>75 $\mu\text{m}$ ), depending on the particle size. Once fine solids particles (<100 $\mu\text{m}$ ) enter stormwater runoff, they are referred to as ‘suspended solids’ which remain in suspension in water as a colloid or due to the motion of the water (Sawyer et al. 1994; Andral et al. 1999). The physical impacts of solids present in receiving water bodies include increased turbidity and reduction of light penetration through water, thus retarding photosynthesis and increasing the temperature of the surface layer.

However, the chemical impacts of solids are the most significant. Past researchers have identified solids as the primary carriers of chemical pollutants such as heavy metals, hydrocarbons, organic compounds and nutrients to the receiving water bodies as adsorbents (Sartor and Boyd 1972; Ellis 1976; Vinklander 1998; Weltens et al. 2000; Vaze and Chiew 2004; Lau et al 2005).

Goonetilleke and Thomas (2003) highlighted the importance of the removal of smaller particles from stormwater runoff, as this ensures the removal of heavy metals and hydrocarbons. Similarly, Li et al. (2005) noted the importance of the removal of particles less than 35µm from stormwater runoff as these represented 97% of road generated particles. Kang et al. (2007) investigated methods to optimise the removal of particles and concluded that smaller particles require some type of destabilization treatment to be removed by settling. In a study carried out by Kang et al. (2007), alum ( $\text{Al}_2(\text{SO}_4)_3 \cdot 18\text{H}_2\text{O}$ ), ferric chloride ( $\text{FeCl}_3 \cdot 6\text{H}_2\text{O}$ ) and cationic polymer were used to destabilise the finer particles. These chemicals are used to reduce the negative charge of finer (clay-size) particles. As the negative charge is reduced due to the added chemical agents, particles can easily coagulate and settle (Sansalone and Kim 2008).

## **B. Heavy metals**

Stormwater runoff contains significant amounts of heavy metals (Viklander 1998; Walker et al. 1999; Davis et al. 2001). Common heavy metals found in urban stormwater are zinc (Zn), lead (Pb), copper (Cu), cadmium (Cd), chromium (Cr), iron (Fe), mercury (Hg) and manganese (Mn) (Viklander 1998; Walker et al. 1999; Hengren et al. 2006). Heavy metals are present in both dissolved and particulate-bound phases in stormwater runoff (Sansalone et al. 1996). Sansalone et al. (1997) found that Zn, Cd and Cu are mainly in dissolved form, while Pb, Fe, Al and Cr are mainly particulate bound.

Heavy metals in urban stormwater have received considerable attention in recent years due to their toxicity and non-degradable quality. Heavy metals can exert an ecological risk by persisting in the environment and biogeochemical recycling (Liu et

al. 2009). Heavy metals are also of concern in relation to human health because of their toxicity and their potential to cause harmful effects even at low concentrations. Specifically, exposure to heavy metals adversely affects red blood cells and the nervous system, and causes various cancers and kidney damage. Most heavy metals in urban stormwater originate from industrial and commercial land uses (Sartor et al. 1974). The significant sources of heavy metals in urban runoff are vehicular traffic, pavement surfaces, industrial activities and corrosion of metal surfaces (Sansalone et al. 1997; Viklander 1998; Walker et al. 1999). Table 2.2 below lists the common sources of heavy metals.

**Table 2.2: Sources of heavy metals in the urban environment (Adapted from Sansalone et al. 1996; Walker et al. 1999)**

Source	Fe	Al	Pb	Zn	Cd	Cr	Mn	Cu	Ni
Fuel leakages and exhaust		■				■		■	■
Tyres				■	■				
Brakes			■	■		■	■	■	
Engine wear		■				■		■	■
Vehicular component wear	■	■		■		■			
Pavement wear								■	
Corrosion of metal surfaces				■					

The majority of heavy metals originating from traffic are in particulate form and these particulate bound heavy metals can be leached or become bio-available at a later time as a result of various processes. As noted by Davis and Upadhyaya (1996), particles generated from vehicles in the urban environment are subject to chemical changes once those particles are exposed to air. Ter Haar and Bayard (1971) showed that about 75% of the Pb in vehicle exhaust particles that are in different forms—such as PbBr, PbBrCl and Pb(OH)Br—changed to Pb oxides and carbonates within 18 hour of emission. Similarly, Wik et al. (2009) found that 70% of the Zn in tyre wear



particles which was originally in ZnO form had leached from the particles in a 24 hour to 11 day period. Wik et al. (2009) carried out their study at a neutral pH (pH 6-7) level of runoff water in an urban environment. Likewise, several past studies have demonstrated the bioavailability of toxic compounds from vehicle exhaust, tyre wear particles and lubricants after exposure to the environment (Olson and Skogerboe 1975; Stone et al. 1975; Harrison 1981; Post and Buseck 1985). These bio-available metal elements can then adsorb to other solids particles.

### **C. Organic carbon**

Organic carbon is an oxygen demanding material. Presence of organic carbon in receiving water bodies reduces the dissolved oxygen in water due to oxidation by microorganisms. Additionally, the presence of organic carbon in water leads to undesirable odours and decreases its recreational value (Ellis 1989). On the other hand, the presence of dissolved organic carbon (DOC) leads to impacts such as increased solubility of heavy metals and PAHs in receiving waters (Warren et al. 2003).

Road deposited solids can contain organic carbon of both natural and anthropogenic origin (Rogge et al. 1993; Xie et al. 1999). The primary sources of natural organic carbon in urban road deposited solids are vegetation inputs, litter, and animal waste (Xie et al. 1999; Goonetilleke et al. 2005). Organic carbon of anthropogenic origin from sources such as tyre wear and vehicle emissions is also dominant in road deposited solids (Rogge et al. 1993). Rogge et al. (1993) found that organic particulates of anthropogenic origin dominate the finer particles fraction, whilst the natural organic carbon is dominant in the coarser fraction. However, the finer particles can contain more organic matter than the coarser particles (Gromaire-Mertz et al. 1999; Hengren et al. 2006). Sartor and Boyd (1972) found that the amount of organic carbon in road surfaces varies depending on the characteristics of land use and the frequency of road sweeping.

Road surfaces contribute significant amounts of organic carbon to urban stormwater runoff (Sartor and Boyd 1972). The organic carbon can be present as dissolved

(DOC) and particulate organic carbon. The dissolved organic carbon which is of colloidal size plays an important role in receiving waters as it leads to the enhancement of the heavy metals and hydrocarbons bioavailability due to complexation reactions (Hamilton et al. 1984; Parks and Baker 1997). Organic carbon adsorbed to solid particles increases their adsorption capacity for hydrophobic chemicals (Warren and Zimmerman 1994; Parks and Baker 1997; Wang et al. 2008). Characteristics of organic matter in road deposited solids are discussed in greater detail in Section 2.4.

#### **D. Nutrients**

Runoff from urban areas contains nutrients such as nitrogen and phosphorus compounds. Additionally, carbon, calcium, potassium, iron and manganese are also considered as nutrients. In stormwater runoff, nitrogen and phosphorus are the most significant nutrient compounds that deteriorate receiving water bodies. Nutrients enter stormwater runoff due to fertiliser application, plant matter, detergent usage, soil leaching and animal waste (Ellis 1989). Nutrient compounds are essential for plant growth. They are considered as a pollutant when excess nutrient concentrations are present in stormwater runoff. The presence of excess nutrients in receiving waters increases the growth of algae and other aquatic plants. The decomposition of these dead plants depletes the dissolved oxygen in water which, in turn, leads to the degradation of the aquatic ecosystem (Brick and Moore 1996). Furthermore, excessive growth of algae reduces light penetration through water and interferes with fishing, swimming and boating activities.

Nutrients in stormwater can be present either in particulate form or in dissolved form. Nutrients are more common in runoff from residential land uses compared to industrial and commercial land uses due to the use of fertilisers in lawns.

#### **E. Hydrocarbons**

The two main types of hydrocarbons present as urban pollutants are Total Petroleum Hydrocarbons (TPH) and Polycyclic Aromatic Hydrocarbons (PAHs). Due to their

carcinogenic and mutagenic properties these hydrocarbons may affect a variety of biological processes and are toxic to the environment. Therefore, hydrocarbons are a major concern in relation to public and ecosystem health (ATSDR 1995). The growing high levels of hydrocarbons in urban runoff (Van Metre et al. 2000) are attributed to the increase in traffic activities with population growth.

Urban stormwater contains a range of hydrocarbon compounds such as oils, phenols, and grease. Both natural and anthropogenic sources contribute hydrocarbons to the urban environment (Guo et al. 2004; Hwang and Foster 2006). PAHs mainly originate from the incomplete combustion of fossil fuels, anaerobic degradation of organic materials and forest fires (NRC 1983; Hwang and Foster 2006). Crankcase oils are the main source of TPH (Latimer et al. 2004; Brown and Peake 2006). Hydrocarbons are generally found in road surfaces, vehicle service stations and parking lots due to fuel and lubrication leaks from poor vehicle maintenance and vehicular activities (Hoffman et al. 1984; Wallker et al. 1998; Brown and Peake 2006). Additionally, manufacturing industries, power plants, petrochemical plants, oil refineries and chemical plants release hydrocarbons due to incomplete combustion of fossil fuels and organic materials (Arya 1999; Walker et al. 1999; Gobel et al. 2006). Most of these hydrocarbons accumulate on urban surfaces through atmospheric deposition (Yang and Baumann 1995). Generally, petroleum products release a broad spectrum of hydrocarbon classes to the environment (Neff 1990; Rogge et al. 1993).

Past researchers have noted that significant quantities of hydrocarbons in stormwater runoff are associated with fine particles (Rogge et al. 1993; Ellis et al. 1997; Hengren 2005; Hwang and Foster 2006). For example, Ellis et al. (1997) found that 70-75% of the total hydrocarbons present in stormwater are associated with solids. This was further confirmed by Hwang and Foster (2006) who found that high molecular weight PAHs were mainly generated from vehicle emissions. Rogge et al. (1993) noted that a significant amount of PAH can also be present in tyre particles. As noted by Warren et al. (2003), hydrocarbons can also be present in dissolved or colloidal form in stormwater runoff.

## **F. Litter**

Litter in stormwater consists of materials such as food containers, packaging materials and vegetative materials such as plant debris. Litter is a highly visible material that leads to clogging of the drainage systems and reduces the aesthetic value of water when discharged into a receiving water body. Although the accumulation of litter on road surfaces and other urban surfaces is not a major source of water pollution, it attracts significant maintenance efforts due to its high visibility (Goonetilleke and Thomas 2003). Litter on road surfaces can be effectively removed by road sweeping (Sartor and Boyd 1972).

### **2.3 ROLE OF SOLIDS IN URBAN STORMWATER**

Solids particles are considered as one of the most important pollutants in stormwater due to their capacity to adsorb toxic pollutants such as heavy metals and hydrocarbons (Morrison et al. 1988; Hengren et al. 2005; Lau et al. 2005; Dong et al. 2000; Van Metre 2000). Fine solids particles are more significant in this context. Due to their fine nature and low density (in most instances), solids easily remain suspended and are transported with stormwater runoff. Together with pollutants attached to surfaces, solids in stormwater can do significant damage to receiving water quality (Hoffman et al. 1985). Therefore, the investigation of the role of solids in stormwater runoff is important.

It is widely recognised that the adsorption characteristic of solids is the major factor that influences pollutant accumulation on the surface. Adsorption is a surface phenomenon and is a result of intermolecular interactions between the solids and pollutants (e.g. heavy metal cations) (Sposito 1984). Such interaction occurs due to surface charges on clay minerals, organic matter and metal oxides (Greenland and Hayes 1981; Zhuang and Yu 2002). The charge sites on the solids are influenced by physical and chemical properties of the solids particles and the surrounding solution characteristics (Roger et al. 1998; Wang et al. 1998). Researchers have shown that the surrounding solution characteristics influence the adsorption process. Additionally, competitive adsorption of heavy metals is influenced by the valency, ionic radius and concentration of heavy metal cations (Young et al. 1987; Kaoser et

al. 2005; Liu et al. 2009). Due to the physical and chemical variability among solids, heavy metals and surrounding solution chemistry, adsorption is considered to be a system specific process. As concluded by Covelo et al. (2007a), among these parameters, particle properties have the most significant influence on adsorption compared to the other parameters.

Important physical properties of solids which may influence adsorption include particle size, specific surface area and mineralogy (Ellis 1976; Sansalone et al. 1998; Viklander 1998; Charlesworth and Lees 1999; Jartun et al. 2008). Cation exchange capacity and organic matter content have been identified as the important chemical properties which influence adsorption (Zhuang and Yu 2002). pH and electrical conductivity are the most influential solution characteristics of stormwater in the adsorption process (Jain and Ram 1997; Arnepalli et al. 2008).

### 2.3.1 ADSORPTION

Adsorption can be defined as the accumulation of substances or materials at the interface between the solid surface and solution (Sparks 2003). The adsorbing surface is the ‘adsorbent’, and the material concentrated or adsorbed at the surface is the ‘adsorbate’ (Weber and Smith 1988; Stumm 1992; Sparks 2003). On this basis, the solid particles are generally referred to as ‘the adsorbent’ (See Figure 2.3).

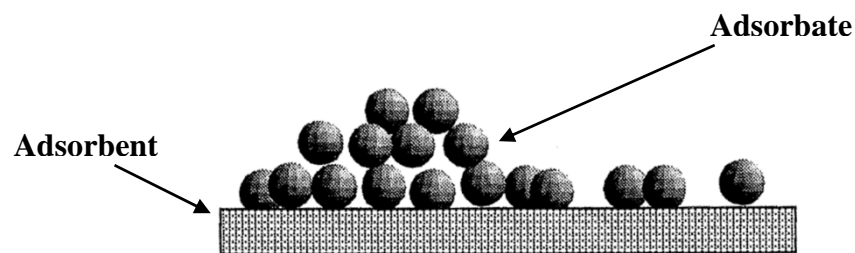


**Figure 2.3: Adsorption on a surface (Adapted from McBride 1994)**

The adsorption capacity of a material is defined as ‘the quantity of adsorbate adsorbed per unit mass of adsorbent’ (Bernardin 1985; Filep1999). Adsorption capacity is also referred to as ‘the specific adsorbed amount’. It can be defined in two

ways (Filep 1999). Where the total adsorbed amount is calculated by the mass of adsorbent, the relative specific amount (q) is commonly expressed in the form of Equation 1:

$$q = \frac{\bar{x}}{\bar{m}}, \text{mol} / \text{g} \quad \text{Equation 1}$$

Where,

$\bar{x}$  = Total adsorbed amount (mol); and

$\bar{m}$  = Mass of the adsorbent (g).

When the total adsorbed amount is related to the unit surface area ( $A^*$ ,  $\text{cm}^2$ ), the relative specific amount is referred to as ‘the absolute specific amount ( $\bar{q}$ )’, defined in the form of Equation 2:

$$\bar{q} = \frac{\bar{x}}{A^*}, \text{mol} / \text{cm}^2 \quad \text{Equation 2}$$

For the pollutant adsorption system (adsorbent, adsorbate and the surrounding solution) investigated in this research study, the relative specific amount (q) is used, because in stormwater runoff, the pollutant adsorbed to solids is commonly estimated on the basis of mass rather than the particle surface area.

### 2.3.2 ADSORPTION CHARACTERISTICS OF SOLIDS

Adsorption mainly occurs due to the electrical charge on the particle surface (Sawyer et al. 1994). The ionic environment discussed below explains how the charged particle behaves in a solution.

Soil minerals contain a variety of charge sites (binding phases) that exhibit electrical charge characteristics that influence the attraction of ionic compounds. When the negatively charged particles are in suspension in water, the positively charged ions in the solution will initially accumulate on the charged particles to maintain the electro

neutrality. This will form a firm layer around the surface of the particle, which is known as the ‘Stern Layer’ (Olphen 1963; Sawyer et al. 1994; EPA 1999; Filep1999). The ions are attracted electrostatically to the surface of a particle. Attraction of positively charged ions occurs only up to an equilibrium limit. Additional positively charged ions to the negative particle are repulsed by the positively charged Stern Layer.

This constant competing process of attraction and repulsion surrounding the particle results in the formation of a Diffuse Layer, with a mixture of charged ions surrounding the particles and the Stern Layer. The attached positively charged ions in the Stern Layer and the charged interface in the Diffuse Layer is referred to as ‘the electrical double layer, as illustrated in Figure 2.4. The charged ions will not be uniformly distributed throughout the liquid phase, but will be concentrated near the charged surface. The presence of charged ions is at a maximum level at the particle surface and decreases with distance from the surface. The thickness of the Diffuse Layer depends on the type and concentration of ions in the water interface (Sawyer et al. 1994; EPA 1999).

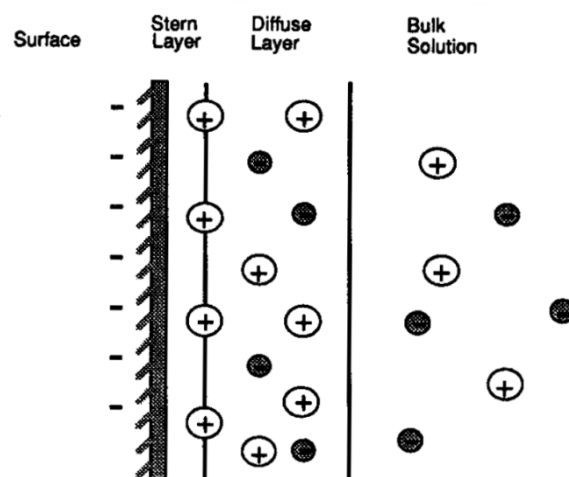


**Figure 2.4: Electrical double layer of negatively charged particle: Guoy-Stern Colloidal Model (Adapted from Weber et al. 1991)**

When two particles with a similar primary charge (as described above) approach each other, their Diffuse Layers begin to interact. The similar primary charges they

possess result in repulsive forces. The repulsive forces are neutralised to some extent by an attraction force known as ‘Van der Waal’s attraction’. Van der Waal’s attraction occurs due to short range interactions. This force decreases rapidly with increasing distance between particles. When particles with the same charge come closer, the repulsive force increases and keep the particles separated. Therefore, the motion of the particles continuously changes direction as a result of impact with other particles in the solution. Thus, each particle has an irregular path, which is known as ‘Brownian motion’ (Shaw 1992; Sawyer et al. 1994; EPA 1999). When two particles approach each other in suspension due to the Brownian motion, their Diffuse Layer begins to interfere. This interference leads to changes to the distribution of ions in the double layer of both particles.

Similarly, when the heavy metal cations are exposed to the environment, they undergo a variety of reactions. When heavy metal cations make contact with water or moisture, the metal cations become hydrated. This is due to the polarisation of water molecules. The O-H bond of the water molecule is polarised due to the higher electro negativity of the oxygen atom compared to the hydrogen atom. Therefore, a partial negative charge on the oxygen atom and a partial positive charge on the hydrogen atom arise. These polarised water molecules are then attracted to a positively charged metal cation and the metal cation is surrounded by water molecules (See Figure 2.5). This cation is then referred to as ‘a hydrated ion’ and denoted as Aq (Wulfsberg 1991).



**Figure 2.5: A hydrated cation (adapted from Wulfsberg 1991)**



The adsorption of cations at a surface or interface occurs as a result of binding forces created between the adsorbate and the adsorbent (Weber et al. 1991). A variety of different types of binding forces could be attributed to the bonding between individual atoms, ions, or molecules of adsorbate and molecules of adsorbent (Israelachvili 1985; Weber et al. 1991). The driving forces arising between the adsorbent and adsorbate are a result of the chemical equilibrium of the system (Israelachvili 1985). The free energy of the system influences the forces arising between the adsorbent and adsorbate (Weber et al. 1991). Broadly, these bonds are categorised into three types, namely, physical, chemical and electrostatic bonds. The significant features of these forces, as described by Israelachvili (1985), are illustrated in Figure 2.6.

Category and Characteristic Interaction	Representation of Interaction	Interaction Range
<b>CHEMICAL</b> Covalent		Short Range
Hydrogen Bond		Short Range
<b>ELECTROSTATIC</b>		
Ion-Ion		1/r
Ion-Dipole		1/r^2
<b>PHYSICAL</b>		
Dipole-Dipole (Coulombic)		1/r^3
(Keesom energy)		1/r^6
Dipole-Induced Dipole (Debye energy)		1/r^6
Instantaneous Dipole-Induced Dipole (London dispersion energy)		1/r^6

**Figure 2.6: Characteristic interactions associated with bonds (adapted from Weber et al. 1991)**

The nature and extent of the bonds that occur between heavy metals (adsorbate) and solids (adsorbent) lead to various mechanisms of adsorption which are influenced by the characteristics of the system (adsorbent, adsorbate and the surrounding solution) (Weber et al. 1991; Bradl 2004).

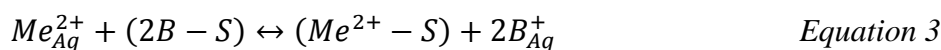
### 2.3.3 MECHANISMS OF HEAVY METAL ASSOCIATION TO SOLIDS

The different mechanisms by which heavy metals associate with solids particles include adsorption, cation exchange and precipitation. Adsorption comprises of inner-sphere and outer-sphere complexation (Weber et al. 1991; McBride 1994; Bradl 2004). These two methods are also referred to in the literature as ‘specific adsorption’ (inner-sphere complexation) and ‘non-specific adsorption’ (outer-sphere complexation) (Polcaro et al. 2003). Some researchers contend that cation exchange on particles that occurs by ion exchange is a different mechanism to adsorption (Farquhar et al. 1997). However, cation exchange is commonly referred to as ‘outer-sphere complexation’ in the research literature, as ion exchange is an electrostatic phenomenon associated with outer-sphere complexation (McBride 1994; Polcaro et al. 2003; Bradl 2004; Mozgawa and Bajda 2005). Therefore, cation exchange will be referred to as an adsorption mechanism in the current study.

#### A. Ion exchange

Electrostatic forces at the permanent charge sites of the minerals and cations result in ion exchange interaction (Weber et al. 1991). The permanent charge sites in minerals result from isomorphic substitution of ions in the lattice structure of the minerals, where charges are not subject to change due to the changes in the surrounding solution. Ion exchange is an outer-sphere complexation arising from nonspecific bonding mechanism. Therefore, exchanged cations are weakly bound to the particle surface. These cations can be easily replaced (reversed) by other cations. Thus, ion exchange may be considered the most reliable method for the transport of positively charged ions through water.

The ion exchange process involves adsorption of high charge ions from solution and the simultaneous release of low charge ions to solution. This process is influenced by energy and entropy (McBride 1994). The exchange of heavy metal cations ( $Me^{2+}$ ), dissolved in solution, for an exchangeable cation ( $B^+$ ) associated with the solid surface ( $S$ ) can be described as:



where Aq refers to the aqueous phase (Weber et al. 1991).

Ion exchange reactions are extremely fast at the surface (Sparks 2003). The affinity or preference of one heavy metal element over the other is known as 'selectivity' (Harter 1992). Exchange affinities (order of selectivity) of cations are generally related to the ion radii ( $r$ ), valency (ion charge -  $q$ ), susceptibility to hydration, and mineral type (Elliott et al. 1986; McBride 1989; Weber et al. 1991; Alloway 1995; Sparks 2003). Selectivity is an important indicator in ion exchange mechanism. The affinity of cations for soils increases with increasing charge and decreasing hydrated radius. Selectivity is influenced by the charge density of the ion ( $C=q/r$ ). Generally, the cations with the largest ionic radii and lowest hydration energies form strong bonds with clay exchange sites (McBride 1994).

In ion exchange of different valency cations, higher valency ions are preferred over the lower valency ions. For metal elements with equal valency, ionic radii become an important parameter for selectivity. Since metal ions are hydrated in the road environment, as explained in Section 2.3.2, ions with small hydrated radius are preferred for ion exchange. The smaller ions have higher charge densities than the larger ions with the same valency and attract more water molecules, resulting in a larger hydrated radius. Therefore, the ions with a higher hydrated radius exert weaker forces of attraction and, physically, it is difficult to bring these metal elements to adsorption sites (Yong et al. 1992). For example, the selectivity of elements with ionic radii  $\text{Cu}^{2+}$  (0.072nm),  $\text{Zn}^{2+}$  (0.074nm),  $\text{Cd}^{2+}$  (0.097nm), and  $\text{Pb}^{2+}$  (0.12 nm) is in the order of  $\text{Pb} > \text{Zn} > \text{Cu} > \text{Cd}$ , which is opposite to the ionic radii (Elliott et al. 1986; Morera et al. 2001; Gomes et al. 2001; Kaoser et al. 2005). This is attributed to the larger hydrated radii of  $\text{Pb}$  (0.187nm),  $\text{Zn}$  (0.216),  $\text{Cu}$  (0.206nm) and  $\text{Cd}$  (0.23nm), respectively (Liu et al. 2009; Kaoser et al. 2005).

The amount of exchangeable heavy metals in solids depends on the CEC of solids, metal concentration and different metal cations in surrounding solution. The cation exchange capacity (CEC) of solids is an indication of the ability of solids to hold exchangeable cations. Other than the permanent charge sites in clay minerals, variable charge sites of metal oxides and organic matter also possess CEC values (McBride 1994; Sparks 1996). However, this depends largely on the pH of the surrounding solution (McBride 1994).

Ion exchange mechanism is the most common mechanism for metal adsorption to solids particles. Fine particles in road deposited solids contain clay minerals, which contain permanent charge sites. In clay minerals, ion exchange can occur in surface exchange sites and interlayer exchange sites. Different selectivity can be displayed by the external and interlayer sites towards divalent and monovalent cations. For example, McBride (1994) confirmed that the interlayer surface of smectite provides favourable sites for exchange of divalent and multivalent cations rather than monovalent cations. The exchange of  $Zn^{2+}$  by replacing  $Na^+$  creates more packets of clay palettes.

## **B. Chemisorption**

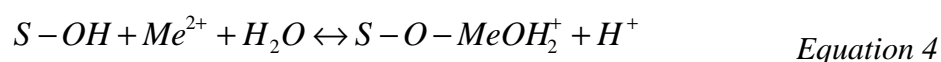
Chemisorption is also known as ‘inner-sphere complexation’ or ‘specific adsorption’ which forms strong covalent bonds between heavy metal elements and solids particles. As a result, the chemical form of the metal will change and a chemical compound is formed (Gregg and Sing 1967; Weber and Smith 1988).

Chemisorption occurs due to reactions between surface functional groups in solids and ions in the surrounding solution (Bradl 2004). Surface functional group is a chemically reactive molecular unit bound to the structure of a solid (Sposito 1984). Soil contains a variety of surface functional groups for chemisorption, such as: mineral oxides and hydroxides of Fe, Al and Mn ( $Al_2O_3$ ,  $FeOOH$ ,  $TiO_2$ ,  $SiO_2$ ); edge sites of layered silicate minerals; and organic matter. The charges on these surfaces are highly pH dependent and occur through protonation and deprotonation reactions (Weber et al. 1992). Most common surface functional groups in soils organic matter are carboxyl ( $-COOH$ ), carbonyl and phenolic groups (Bradl 2004). The most predominant surface functional groups on oxide surfaces and clay minerals are the hydroxyl groups (Sposito 1984).

Crystalline minerals which contain plate like surfaces adsorb very little metal elements through chemisorption. Bonds probably occur at the edge sites which contain OH groups. In contrast to the crystalline minerals, non-crystalline metal oxides contain a large number of surface functional groups due to their structural

disorder. Therefore, these metal oxides adsorb a relatively greater amount of heavy metals through complexation reactions (McBride 1994).

The metal elements react with the OH<sup>-</sup> or O<sup>2-</sup> groups at the mineral surfaces and edges that are negatively charged at high pH values (Weber et al. 1991; McBride 1994). The adsorbing metal ion directly bonds to atoms at the surface by chemisorption mechanism with the adsorbing cation. Thus, the properties of the particle surface and the nature of the metal element influence the tendency for adsorption. These reactions depend largely on the pH of the surrounding solution. Heavy metal ion hydrolysis can be described as given below:



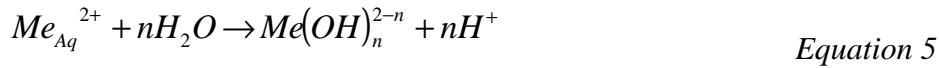
where Me is the metal cation and S is a surface.

Chemisorption is largely a non-exchangeable form of metal adsorption mechanism where extraction of these metals requires extreme treatment at high pH and temperature (McBride 1994).

Electro negativity is an important factor in the preference for metal elements for chemisorption (McBride 1994). When the atomic radius of a cation decreases, the ionisation energy tends to increase and, thereby, the electro negativity of the cation increases. Strong covalent bonds are formed by the higher electro negativity metal elements. Trivalent metal ions such as Cr<sup>3+</sup> and Fe<sup>3+</sup> are preferred over the divalent metal ions for chemisorption. Selectivity for chemisorption is also explained by the Lewis Hard Soft Acid Base (HSAB) principle (Hancock and Martell 1989; Inglezakis and Grigoropoulou 2004). Metal cations in solution are Lewis Acids, and functional groups are Lewis Bases. Based on the electro negativity, three categories of these acids and bases have been identified: hard, intermediate and soft acids. According to the HSAB principle, hard acids prefer (Cr<sup>3+</sup>, Fe<sup>3+</sup>, Al<sup>3+</sup>, Mn<sup>2+</sup>), hard bases (metal oxides, carboxyl COO<sup>-</sup> and hydroxyl OH<sup>-</sup>), and soft acids (Cd<sup>2+</sup>) prefer soft bases (edge sites of clay minerals, NH<sub>2</sub><sup>-</sup>) (Wulfsberg 1991; Alloway 1995). Ni<sup>2+</sup>, Cu<sup>2+</sup>, Zn<sup>2+</sup> and Pb<sup>2+</sup> are categorised as intermediate acids.

### C. Precipitation

Precipitation is mainly a function of pH and relative quantities of metal ions present in solution. Metals may precipitate on the surface of solids particles as oxides, hydroxides, carbonates, sulphides or phosphates. As shown by Elliot et al. (1986), hydrolysis of divalent cations reaction can be written as follows:



Likewise, metal hydroxides precipitate on the soil particle surface. These cannot be easily distinguished. In general, precipitated solids phases occur when metal concentrations in solution become very high (heavily loaded). It is a slow process compared to other mechanisms. In soils, for most of the metal elements, precipitation is less likely than the other two mechanisms, due to low metal concentrations (Sparks 2003). The precipitation of more abundant metal elements of Al, Fe, Mn, Ca and Mg is common.

Surface precipitation may occur as oxides, hydroxides or carbonates of positively charged ions. Metal precipitation as a carbonate form occurs in high alkaline (high pH >9) solutions. Since road deposited solids' pH is in the range of 6-7.5, metal precipitation as hydroxides is more common than as carbonates. Metal hydroxide precipitates have very low solubility; hence, their mobility can be monitored by pH control. Metal precipitation is higher in carbonate and sulphate dominant soils.

### 2.4 INFLUENTIAL PARAMETERS

Literature explaining the adsorption behaviour of road deposited solids is comparatively limited. Several studies on soil chemistry have demonstrated the ability of soil clays to adsorb metal cations (Ongley et al. 1982; Elliott et al. 1986; Sanchez et al. 1999). While such studies have been undertaken for materials other than road deposited solids, the knowledge created is useful in identifying the possible influential parameters in the adsorption behaviour of solids.

Past researchers have commonly used specific surface area, cation exchange capacity, mineralogy, and particle size to describe the adsorption process (Sanchez et al. 1999). For example, studies by Elliott et al. (1986) and Zhuang and Yu (2002), examined the metal adsorption behaviour of soils and clay minerals respectively, in relation to soil mineralogy, cation exchange capacity and pH. The findings of both studies suggest that all these parameters have significant influence on adsorption. In addition to these parameters, Polocaro et al. (2003) used exchangeable cations to study heavy metal adsorption by soils.

In reviewing the available information from the literature, probable influential parameters of solids for heavy metals adsorption can be discussed under three categories: physical properties of the particle, chemical properties of the particle and surrounding solution characteristics. Physical properties include particle size, specific surface area (SSA) and solids mineralogical composition (Dong et al. 1984; Johnston 1996; Jain and Ram 1997; White 2006). Cation exchange capacity (CEC), exchangeable cations (EC) and organic matter content (OM) are the chemical properties that primarily influence adsorption (Rengasamy and Churchman 1999; Cerato and Lutenecker 2002). Surrounding solution properties such as pH, electrical conductivity (EC), ionic strength and dissolved organic carbon in stormwater can also influence adsorption (Elliott et al. 1986; Weber and Smith 1988; Sansalone et al. 1997; Filep 1999). Each of these factors has a unique influence on metals adsorption to solids.

#### **2.4.1 PHYSICAL PROPERTIES OF SOLIDS**

Solids of different sizes and shapes which have different mineral composition exhibit a wide range of properties. The following discussion evaluates the importance of each parameter in the adsorption process.

##### **A. Particle size**

Urban stormwater runoff transports a wide gradation of solids particles. Particle size can range up to >10000 $\mu$ m (Sansalone et al. 1998). Among these, particles smaller

than 100 $\mu\text{m}$  in diameter remain in suspension during wash-off, while particles larger than 100 $\mu\text{m}$  are easily settled due to gravity (Andral et al. 1999; Azema et al. 2002). The settling velocity of finer particles is low and often influenced by the shape and size of particles. Similarly, fine particles can be transported a greater distance by urban runoff (Dong et al. 1984). Therefore, clay-sized particles are the most important because of their mobility (Dong et al. 1984).

Difference in metal adsorption due to particle size has been noted by past researchers (Sartor and Boyd 1972; Dong et al. 1984; Roger et al. 1998). For example, in a study carried out by Roger et al. (1998) on road runoff, it was found that 90% of the particles had a diameter less than 100 $\mu\text{m}$ , and 78% had a diameter less than 50 $\mu\text{m}$ . Additionally, researchers have confirmed that the finest particles in urban stormwater have the highest concentration of pollutants, especially metals (Sansalone and Buchberger 1997; Roger et al. 1998; Hengren et al. 2006). Hengren et al. (2006) carried out a study on heavy metals concentration in five different particle size ranges in urban stormwater runoff. They found that most of the heavy metals are adsorbed to particles below 150 $\mu\text{m}$ , and maximum concentration was found in the 0.45 - 75 $\mu\text{m}$  size range. Similar behaviour was reported by Birch and Scollen (2003), who showed that the highest metals concentration is in the fraction smaller than 62 $\mu\text{m}$ .

Most importantly, the particle size determines the mobility of the associated pollutants (Deletic and Orr 2005). Li et al. (2006) summarised the data in the literature on metal concentrations as a function of different particle sizes, and showed that the concentration increases with decreasing particle size. Similarly, based on a detailed study of the adsorption of metal ions on sediments, Jain and Ram (1997) found that there is a decrease in adsorption with the increase in particle size. The above findings confirm that the finest particles have the highest adsorption capacity.

## **B. Specific surface area**

Specific surface area (SSA) is measured as the surface area per unit mass, assuming a constant particle density, and expressed as  $\text{m}^2/\text{g}$  (Filep 1999; White 2006). The



increase in SSA increases the adsorption ability of particles by providing a large interface to metal elements to interact with the particle surface (White 2006). Researchers have noted that the SSA increases with decreasing particle size (Sansalone et al. 1997). As noted by Bolt et al. (1976), the SSA of a particle is related to the solids composition.

SSA varies in solids based on mineralogy, organic matter content and particle size distribution (Cerato and Luttenegger 2002). A large variety of minerals are present in the clay fraction of particles. Clay minerals, oxides and hydroxides of Fe and Al, (inorganic components) have high SSA. For example, clays such as montmorillonites have a specific surface area up to  $810\text{m}^2/\text{g}$ , and kaolinites have a specific surface area typically in the range of  $10 - 40\text{m}^2/\text{g}$  (Bell 1993). Thus, the type of minerals and their proportions play an important role in determining the SSA of particles (Yukselen and Kaya 2006). Specific surface area is considered as a constant related to the particle composition, and particle size is not affected by external variables such as the water content. Specific surface area of common soil minerals are tabulated in Table 2.3.

The presence of swelling clays in solids contributes two different surface area values, namely, external surface area and internal surface area (Gregg and Sing 1967; Sparks 2003). Swelling clays are clays with an expanding layer lattice, such as montmorillonite and smectite (Sparks 2003). As the term implies, the external surface area takes into account the outer surface area. Minerals such as kaolinite, illite, metal hydroxides and oxides contain external surface area only. The internal surface area comprises of the interlayer surface areas of swelling clays. A wide range of solids have a larger internal surface area than external surface area, which is about 80-90% of the total surface area (Filep 1999). In general, the presence of metal oxides of Fe, Al and Mn and organic matter (humus) content in soils increases the SSA of particles. However, it has been found that in swelling clays, coatings of these metal oxides and organic matter cause a decrease in SSA, since these oxides can occupy the interlayer surface and/or block the interlayer surface (Sakurai et al. 1990; Zhuang and Yu 2002). For example, Sakurai et al. (1990) found that for montmorillonite (swelling 2:1 clay mineral), Al oxide coatings cause a decrease in SSA. However, for kaolinite (non-swelling clay), they found that the Fe oxide coating leads to an

increase in SSA. Similar influence of organic matter coatings have been discussed by Warren and Zimmerman (1994). Therefore, the above findings indicate that the influence of coatings of metal oxides and organic matter on the surface properties of solids is entirely dependent on the material coated and the type of coating material (Sakurai et al. 1990).

**Table 2.3: Specific surface areas of soil minerals (Adapted from Sparks 2003)**

Mineral	Specific surface area ( $\text{m}^2 \text{g}^{-1}$ )
Kaolinite	7 – 30
Halloysite	10 – 45
Pyrophyllite	65 – 80
Talc	65 – 80
Montmorillonite	600 – 800
Diocahedral vermiculite	50 – 800
Triocahedral vermiculite	600 – 800
Muscovite	60 – 100
Biotite	40 – 100
Chlorite	25 – 150
Allophane	100 – 800
Aluminum oxide	100 – 220
Iron oxide	70 – 250
Manganese oxide	5 - 360

Several methods are available to measure SSA (Cerato and Lutenegeerl 2002; Yukselen and Kaya 2006). Comparing the available methods, Yukselen and Kaya (2006) concluded that the Brunauer-Emmett-Teller (BET)  $\text{N}_2$  adsorption method measures only external surfaces, and that polar liquid methods measure both internal and external surface areas.

### C. Mineralogy

Roger et al. (1998) found that road deposited solids contain high mineral content resulting from the surrounding land. Minerals in solids could exert a significant influence on metal adsorption to particles. Different types of minerals with different characteristics occur in the environment. These differences occur due to the mineral structure. Two types of minerals are mainly present in soils, namely, primary minerals (primary silicates) and secondary minerals. These exert different influences on the chemical characteristics of soils. Secondary minerals can be categorised into two groups: secondary silicates (clay minerals) and non-silicates (oxides and hydroxides of Fe, Al and Mn; carbonates; sulphates; chlorides and phosphates). Secondary minerals are formed by the weathering of primary minerals (Nesbitt 1992). These secondary minerals are the most important constituents in soil.

The most important building unit in primary silicates is  $[\text{SiO}_4]^{4-}$  tetrahedral. In this case, four oxygen ions are located around  $\text{Si}^{4+}$  and possess four negative charges (See Figure 2.7). The silicates tetrahedral can be present in three different forms: separate structural units; two dimensional sheets (mica, muscovite), more often linked together and sharing oxygen ions; and three dimensional frameworks (feldspar, quartz). The central ion of the basic unit can often be replaced by another ion with similar size, which results in the formation of different forms of silicates. This is called an isomorphous substitution (Bell 1993; Sparks 2003). When the substitution of Si occurs by a lesser valency ion ( $\text{Si}^{4+}$  by  $\text{Al}^{3+}$ ), permanent negative charge results in the lattice structure.  $\text{Al}^{3+}$  is partly substituted for  $\text{Si}^{4+}$  as a central ion, and  $\text{Al}^{3+}$ ,  $\text{Mg}^{2+}$ ,  $\text{Fe}^{2+}$  and  $\text{Fe}^{3+}$  substitution is also possible.  $\text{Ca}^{2+}$ ,  $\text{Na}^+$  and  $\text{K}^+$  ions do not occupy a central position due to the large size of the ion (Brikeland 1999). They are present as an attachment to the negative charge sites of the lattice structure.

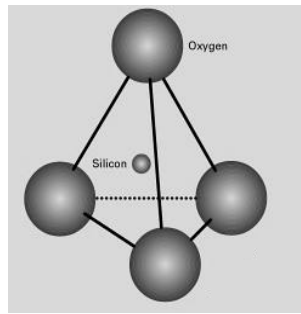


**Figure 2.7: Building unit in primary silicates (Adapted from White 2006)**

The common primary silicate minerals in soils are quartz, feldspar and mica. These minerals have a regular structure and open space (not close packed) which can be filled with ionic impurities (McBride 1989). Quartz ( $\text{SiO}_2$ ), which is a three dimensional framework silicate mineral, is the most common mineral in soils. The quartz structure (crystal lattice) is electrically neutral (Sparks 2003). Therefore, it is highly resistant to chemical and physical processes in soil.

Albite and microcline belong to feldspar framework silicates. In feldspars, one of the four  $\text{Si}^{4+}$  is replaced by  $\text{Al}^{3+}$  and possesses a negative charge (isomorphous substitution) in the framework. The charge can be balanced by the  $\text{K}^+$ ,  $\text{Na}^+$  or  $\text{Ca}^{2+}$ . If the framework charge is balanced by the  $\text{K}^+$ , microcline ( $\text{KAlSi}_3\text{O}_8$  - potassium feldspar) is formed. If the charge is balanced by the  $\text{Na}^+$ , albite ( $\text{NaAlSi}_3\text{O}_8$  - sodium feldspar) is formed. The geometry of feldspar consists of cages (cavities) which are sufficiently large to accommodate large cations, such as  $\text{Ba}^{2+}$  (McBride 1989).

Muscovite is a form of mica which is a two dimensional silicate (sheet silicate). Different forms of mica are present by substitution of Si with Al, Mg or Fe. In muscovite, one of the four  $\text{Si}^{4+}$  ions is substituted by  $\text{Al}^{3+}$  and generates a negative charge in the silica sheets. In muscovite, the negative charge is balanced by  $\text{K}^+$  present between layers. Muscovite contains a high negative charge. Therefore,  $\text{K}^+$  ions in the interlayer are strongly bound to the structure and prevent the replacement of  $\text{K}^+$  ion by the cation exchange process (Filep 1999). Therefore, some portions of

the mineral charge sites may not be exchangeable, and most of the CEC in muscovite could occur at the edge sites of the mineral. The majority of the layer silicate minerals (swelling clays) common in soil, such as smectite and vermiculite, are formed by the weathering of mica.

Clay minerals are secondary minerals which are formed by the transformation of primary minerals. Most clay minerals are layer silicates which consist of a silicon tetrahedral sheet and aluminium octahedral sheets, combined either in 1:1 or 2:1 ratio. In the 1:1 minerals such as kaolinite, most of the interlayer charges are balanced (interlayer is neutralised). Small portions of isomorphous substitutions could occur in such minerals (McBride 1994). Therefore, edge sites play an important role in the chemical behaviour of 1:1 minerals (Filep 1999). These minerals do not swell in water and have low surface area and cation exchange capacity. The 2:1 layer silicates are formed based on the mica structure (smectite, vermiculite, illite and chlorite). These clay minerals can swell in water. Therefore, they have high surface area and cation exchange capacity due to the interlayer area. However, in chlorites, the interlayer surfaces do not expand in water due to the hydroxyl sheets in the interlayer space. Therefore, these minerals have low cation exchange capacity and low specific surface area compared to other clay minerals. Charge sites in these minerals occur only on the external surface and in the edge sites (McBride 1994).

Edge sites occur at the edges and breaking points in minerals. At edge sites, -SiOH and -AlOH groups are present; these can release protons and negative charges can be formed (Filep 1994). These edge sites have pH dependent charges that are negative at high pH (alkaline) and positive at low pH (acidic) (Helling et al. 1964; Johnston 1996). Dissociation of these edge sites (silanol group) at typical pH value of soils (pH <7) can be described as:



(McBride 1994).

Other than the above minerals, soil contains nonsilicate minerals of Fe, Al and Mn oxides, hydroxides and oxyhydroxides. Although these oxides are found in small quantities in soil, they play an important role in soil chemical processes (Sparks 1996). This is attributed to their high surface area resulting from their disorganised structure and reactivity (Taylor et al. 1983). These metal oxides (Al - gibbsite, Fe - goethite and hematite, Mn - manganite) could be present in crystalline form or non-crystalline form in soil (Filep 1999). However, Fe, Al and Mn oxides in soils are very fine grain, poorly crystalline compounds that exist in amorphous oxide form (Sparks 1994). These metal oxides can be present as separate particles, as coatings on clay (silicate minerals), and sand particles and fillings in cracked faces (gels) (Taylor et al. 1983). The metal oxides can also be present in organic matter as coating on humic substances or by forming complexations with organic matter in the soil (Taylor et al. 1983).

Fe and Al oxides are more commonly found in the soil environment than Mn oxides (McBride 1994). While Al oxides are present in soils in smaller quantities than Fe oxides, they have an important role in soil properties since Al exists in these minerals in a trivalent state, whereas  $\text{Fe}^{2+}$  is more generally dominant in the weathering process (Taylor et al. 1983). Metal oxides do not contain a permanent charge and have low CEC values. The Fe, Al and Mn metal oxides which are non-crystalline aluminosilicates possess a pH dependent charge. Therefore, the most important binding sites for these metal oxides are edge sites (McBride 1994). In general, these oxides are negative in alkaline solution and positive in acidic solution. Metal oxides adsorb heavy metals, forming covalent bonds, which is an inner-sphere complexation, as the metal ions bond directly to the surface group without any intervening water molecules.

The clay fraction is comprised of minerals of diameter smaller than  $2\mu\text{m}$  (Dawes 2006). Due to the combination of high surface charge and the small size of clay particles ( $<2\mu\text{m}$ ), this results in high surface charge density (Zhuang and Yu 2002) which provides an active surface for cation adsorption. Surface reactions of charged particles are important in the adsorption of heavy metals. Adsorption of other pollutants is directly or indirectly influenced by the nature and amount of surface

charge. The type and amount of clay present in solids influences the cation exchange capacity (CEC) of the particle (Sparks 2003; Dawes 2006). Furthermore, the different minerals present in the particle can affect the level of CEC available. Khalil (2005) found that soils with low clay content have low CEC. The quartz, feldspar, mica and metal oxides noted above can also be found in road deposited solids. Consequently, it is important to identify the load and type of clay present in particles as these are important parameters that influence adsorption (Dawes 2006).

#### **2.4.2 CHEMICAL PROPERTIES OF SOLIDS**

##### **A. Cation exchange capacity (CEC)**

Cation exchange capacity (CEC) is the measure of the total capacity of the particle to hold exchangeable cations (Hartmann et al. 1998; Rengasamy and Churchman 1999; Sposito 2000). It therefore represents the negative charge that is present per unit mass of solid particles (Rengasamy and Churchman 1999). The negative charges on the solids particles are counterbalanced by the positive charge ions of  $\text{Na}^+$ ,  $\text{Ca}^{2+}$ ,  $\text{Mg}^{2+}$  and  $\text{K}^+$  (Ming and Dixon 1987). Thus, most commonly, CEC is expressed as centimoles of positive charge per kilogram of soil ( $\text{cmol}(+)/\text{kg}$ ).

The ions attached to negative charges can be replaced by the other ions, such as heavy metals. Thus, CEC is an important property of solids in assessing the ability of particles to hold heavy metal cations on their surface. Solids with high CEC represent a high ability to adsorb heavy metals. Generally, clay minerals have high CEC which ranges from 3 to  $750\text{cmol}(+)/\text{kg}$  (Rengasamy and Churchman 1999; Sparks 2003). Different clay minerals have differing CEC values arising from the crystal structure. CEC values of common soil mineral components are tabulated in Table 2.4. Therefore, if the clay type is known, its CEC value can be determined.

Solids particles can exhibit two types of negative charges: permanent and variable (pH dependent) charge (Sparks 2003; Bortoluzzi et al. 2006). These different forms of charges are present in solids due to the different permanent charges present on clay minerals. Variable charges occur in organic matter, metal oxides and edge sites

of clay minerals. Cations and anions are adsorbed to solids based on the charges on their surface. Filep (1999) noted that when the surrounding solution pH value decreases below pH 5.5, the negative charges in kaolinite disappear and the positive charges begin to appear. However, most clay particle surfaces are usually negatively charged between pH 5 and pH 8 (White 2006).

**Table 2.4: Cation exchange capacity (CEC) of soil minerals (Adapted from Sparks 2003)**

<b>Mineral</b>	<b>Cation Exchange capacity (CEC) (cmol kg<sup>-1</sup>)</b>
Allophane	5 - 350
Trioctahedral vermiculite	100 - 200
Montmorillonite	80 - 150
Dioctahedral vermiculite	10 - 150
Halloysite	10 - 40
Muscovite	10 - 40
Biotite	10 - 40
Chlorite	10 - 40
Kaolinite	2 - 15
Talc	<1

The CEC of solids is a reflection of their mineralogy and organic matter content (Bell 1993). Particles with high CEC tend to have a significant amount of clay minerals and organic matter (Bridge et al. 1993). Clay size particles generally have greater adsorption ability due to the small particle size, and high and more active surface area. Rengasamy and Churchman (1999) found that the behaviour of solids is governed by the surface area and charge. Yukselen and Kaya (2006) found that the total SSA and CEC of soils are highly correlated.



## **B. Exchangeable cations**

In most particles,  $\text{Ca}^{2+}$ ,  $\text{Mg}^{2+}$ ,  $\text{K}^+$  and  $\text{Na}^+$  are present in exchangeable form (Rengasamy and Churchman 1999). Usually, exchangeable cations are held in clay particles, organic matter and metal oxides (Tucker 1983). The occupancy of available exchangeable sites depends on the size of the available exchangeable cations (ionic radii).

The sum of the exchangeable cations  $\text{Ca}^{2+}$ ,  $\text{Mg}^{2+}$ ,  $\text{K}^+$  and  $\text{Na}^+$  ( $\sum\text{Exch. (Ca+Mg+K+Na)}$ ) is often similar in value to the CEC (Rengasamy and Churchman 1999). However, in acidic soils ( $\text{pH} < 5.5$ ), a certain fraction of exchange charge sites in solids is occupied by aluminium (Fenton et al. 1996; Evans and Scott 2007). Similarly, based on a study on charge characteristics of tropical soils in Queensland, Gillman and Sumpter (1986) stated the necessity of measuring exchangeable Al to estimate the charge characteristics of solids. Therefore, effective cation exchange capacity (ECEC) is often used instead of CEC for acidic soil. This is defined as:

$$\begin{aligned}\text{ECEC} &= \text{Exchangeable cations} + \text{Exchangeable acidity} \\ &= \text{Exchangeable (Ca+Mg+K+Na+Al)}\end{aligned}$$

(Baker and Eldershaw 1993; Rengasamy and Churchman 1999; Dawes and Goonetilleke 2003).

## **C. Organic matter (OM)**

Road deposited solids could contain natural organic matter and organic matter of anthropogenic origin. Natural organic matter, rather than the organic matter of anthropogenic origin, is the most important for metal adsorption due to its surface charge (Lin and Chen 1998). The main constituents of natural organic matter are: carbon (C) (52-58%), oxygen (O) (34-39%), hydrogen (H) (3.3-4.8%) and nitrogen (N) (3.7-4.1%). Other elements in OM are phosphorus (P) and sulphur (S). Organic matter has a high specific surface area (as high as  $800\text{-}900\text{m}^2/\text{g}$ ) and a CEC that ranges from 150 to  $300\text{cmol}/\text{kg}$  (Sparks 2003). Because of the high specific surface area and CEC, organic matter is an important adsorbent of heavy metals.

Natural organic matter in solids is mainly derived from plants and animals and consists of compounds of various products in different stages of decomposition, such as organic residue and humic (humus) and non-humic compounds (Filep 1999; Covelo et al. 2008). The organic residue includes un-decayed plant and animal tissues and their partially decomposed by-products. The non-humic compounds include waxes, oils and fats. The physical and chemical properties of these non-humic compounds are still recognisable (Stevenson 1965; Filep 1999). These compounds are rapidly subject to microbial attack and are unstable in the environment. In contrast, the humic compounds which are relatively stable are formed during the decomposition of organic residues, and are relatively resistant to decomposition. Humic compounds in soils include fluvic acid, humic acid and humin.

The humic compounds are very important in heavy metal distribution in solids due to the dominant surface functional groups and charge surfaces (Hart 1982; Lin and Chen 1998). As noted by Ross (1993), about one third of the organic matter represents the cation exchange sites in soils, and the remaining portion form surface complexations. During decomposition, organic matter is oxidised and organic acids containing functional groups are formed (Hofstede 1994).

The most common surface functional groups in organic matter are -COOH (carboxyl), -OH (hydroxyl), -C<sub>6</sub>H<sub>4</sub>-OH (phenolic), -NH<sub>2</sub> (amino) and -NH (imino) compounds, which are capable of binding cations (Stevenson 1976; Filep 1999). Among these, metals are mainly bound to the -COOH and -OH groups due to the ionization of these groups. Thus, these groups can form stable complexations with positively charged heavy metal cations. Different humic compounds exhibit different behaviour and capacity for metal adsorption due to the different concentrations of -COOH and -OH groups (Stevenson 1976). Humic compounds with low molecular weight are more effective in metal adsorption than the higher molecular weight compounds, due to high surface functional groups.

Soil organic compounds, including humic acids, are complex. They are often present as particulate matter, colloidal, or are associated with solids (McBride 1994). Particulate organic matter mainly consists of organic residue. The humic and non-humic compounds are adsorbed to the mineral surface (Covelo et al. 2008; Liu et al. 2009). OM-clay mineral interaction can be caused by physical adsorption via Van der Waal forces, electrostatic attractions (cation exchange) and the ligand exchange process (Hart 1982; Schnitzer and Khan 1989). The type of interaction depends on the type of organic compound, the nature of the exchangeable ion on the mineral surface, and the surface acidity (Schnitzer and Khan 1989).

These organic compounds can also be adsorbed to metal oxides. However, adsorption of organic matter on oxide surfaces is at a maximum at about pH 5 and decreases with the increase of pH (at pH>7.5) (Hart 1982; Tipping 1986). Warren and Zimmerman (1994) found that organic adsorption to oxide surfaces and oxide adsorption to organic matter surfaces can occur in a natural environment. A similar conclusion was reached by several researchers (Hart 1982; Lin and Benjamin 1992). These organic coatings on solids surfaces increase the negative surface charge of the solid particles and thereby enhance the adsorption of positively charged cations to solids surfaces (Hunter and Liss 1982; Hart 1982; Warren and Zimmerman 1994).

#### **2.4.3 INFLUENCE OF THE SOLUTION CHARACTERISTICS**

Adsorption occurs due to a physical, chemical or electrostatic bond between the adsorbent and adsorbate. This bond can be affected by changes in the surrounding solution characteristics and by the influence of the adsorption process. pH, dissolved organic carbon and ionic strength can have an influence on adsorption. Among these influences, pH is the most important parameter for heavy metal adsorption to solids (Sparks 2003).

pH is a measure of the acidity or alkalinity of a solution. Both solids and heavy metals have chemical characteristics that are affected by the concentration of hydrogen ions ( $H^+$ ) in the solution. For example, surface functional groups in solids are directly influenced by the  $H^+$  or  $OH^-$  ions (solution pH) in the surrounding

solution (Bernardin 1985). At low pH values, these sites develop positive charges due to the adsorption of protons. As pH increases, these sites develop a neutral charge and, ultimately, reach a negative charge. Therefore, the extent of adsorption at a given pH varies among the metal elements. Elliott et al. (1986) carried out a study on the pH dependent adsorption behaviour of heavy metals, and concluded that the adsorption capacity varied directly with solution pH, as illustrated in Figure 2.8.

Other than the adsorption capacity, pH also influences the adsorption mechanism. Metal precipitation is most sensitive to the pH of the solution (Bradl 2004). Different metal elements have different pH values for precipitation (Adriano 2001). However, in stormwater runoff, expected pH variation is within the range of 6 to 7.5 (Yaziz et al. 1989; Huang et al. 2007). Due to the low pH variation in stormwater runoff and road deposited solids, the effect of pH variation on the metal adsorption process would be relatively low.

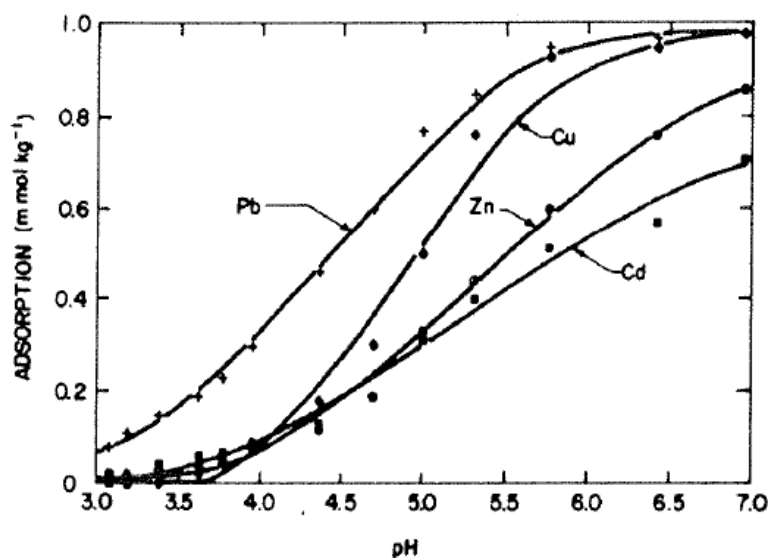


**Figure 2.8: pH dependent adsorption behaviour of heavy metal on soil (Adapted from Elliott et al. 1986)**

## 2.5 HEAVY METALS AS AN ADSORBATE

Heavy metals are bound to different binding sites on solids particles. These metals are exchangeable metals, bound to carbonates, Fe and Mn oxides, organic matter and

residual metals (Harrison et al. 1981; Dong et al. 2000; Guo et al. 2006; Li et al. 2006). Exchangeable metals are bound to particles by weak bonds. Thus, changes in water ionic composition can easily affect sorption-desorption processes of exchangeable metals. Significant metal concentrations can be associated with sediment carbonates and these metals would be influenced by changes of pH. Fe and Mn oxides exist as a coating on particles and are excellent binding sites for heavy metals.

A significant portion of heavy metals can be bound to various forms of organic matter (coatings on mineral particles and natural organic matter). Furthermore, metal elements are present in primary and secondary mineral structures. These may hold trace metals within their crystal structure; these metals are known as ‘residual metals’. These metals are not released in solution under natural conditions (Tessier et al. 1979; Harrison et al. 1981; Al-Chalabi and Hawker 1996). Table 2.5 provides the form of association of heavy metal with these binding sites (Harrison et al. 1981). Additionally, heavy metals can be adsorbed to traffic related particles on the road surface, such as particles resulting from tyre wear, brake pad wear and road surface wear.

**Table 2.5: Binding fractions of metal association in dust, sediment and soil (Adapted from Harrison et al. 1981)**

<b>Binding sites</b>	<b>Form of adsorption</b>
Soluble	Metal precipitate
Exchangeable	Ion exchangeable
Carbonate	Precipitate or Co-precipitate
Fe-Mn oxides	Specifically adsorbed
Organic matter	Complex, adsorbed (Specific)
Residual	In mineral lattices

The extent of metal adsorption is influenced by the concentration of heavy metal cations in the solution. This concentration determines the competition by other cations for bonding sites, which are influenced by the type of metal cation that have

different valency and ionic radii. Competition and interference between metal cations can have a significant effect on cation adsorption by soils (Elliott et al. 1986). In general, the selectivity of the metal cations has been explained by the ionic radius, valency, susceptibility to hydration, and the Lewis Hard Soft Acid Base (HSAB) principle (Weber et al. 1991; Elliott et al. 1986; McBride 1989; Hancock and Martell 1989; Inglezakis and Grigoropoulou 2004). However, as noted by past researchers, a consistent rule in relation to metal selectivity for solids cannot be always defined as it depends on a number of factors, such as the nature of the surface functional groups, and the concentration of metal elements and pH (Schnitzer and Khan 1989; Buffle and Stumm 1994; Sparks 2003; Bradl 2004).

## **2.6 ADSORPTION/DESORPTION OF HEAVY METALS**

Extensive research studies have been carried out to identify the different adsorption mechanisms of metal elements through batch adsorption studies (Elliott et al. 1986; Young et al. 1987). However, the majority of these laboratory studies were performed on well-characterized, homogeneous material such as pure clay minerals (montmorillonite, kaolinite, vermiculite and mica) and metal oxides (Kraepiel et al. 1999; Abollino et al. 2003; Pitcher et al. 2004; Covelo et al. 2007a). The studies on road deposited solids are comparatively limited. Unlike well-characterized material, natural solids contain varying proportions of clay minerals; primary silicate minerals; organic matter; oxides of Fe, Al, and Mn; and anthropogenic particles that have a range of surface properties (Covelo et al. 2007a).

Although studies have been carried out on the adsorption behaviour of soils, the conclusions drawn are not always consistent. This is attributed to the complex nature of different binding sites involved in metal adsorption. Furthermore, due to the dynamic nature of solids accumulation on road surfaces, properties of these solids are relatively different to soils. Therefore, there is great potential to exhibit a wide range of surface properties and, consequently, differences in heavy metal adsorption behaviour.

It is difficult to distinguish the heavy metal adsorption process of solids. This is due to the complexity in adsorbent properties and the behaviour of heavy metal ions in aqueous media. Adsorption-desorption experiments have been a common approach adopted to study adsorption behaviour (Young et al. 1987; Liu and Gonzalez 1999; Plassard et al. 2000; Polcaro et al. 2003; Castaldi et al. 2008), comparison of different adsorption isotherms (Elliott et al. 1986; Abollino et al. 2003; Covelos et al. 2004) and sequential extraction procedures (Al-Chalabi and Hawker 1996; Banerjee 2003; Sutherland et al. 2004) to identify the metal adsorption characteristics on different material. Amongst these methods, adsorption-desorption experiments are more successful than the latter methods, since it simultaneously provides mobility and bio-availability of metal elements (Davis and Upadhyaya 1996; Plassard et al. 2000; Delmas et al. 2002; Polcaro et al. 2003; Castaldi et al. 2008;).

## **2.7 SUMMARY**

Urbanisation increases impervious surfaces and increases the pollutant load carried by the stormwater runoff, which ultimately leads to deterioration of the receiving waters. A diversity of pollutants is typically generated due to a range of anthropogenic activities common to different urban land uses. The pollutant build-up on road surfaces has been identified as the most significant pollutant contributor in urban areas. The main pollutant processes which affect water quality are pollutant build-up and wash-off.

The primary pollutants that deteriorate the quality of stormwater are solids, heavy metals, organic carbon, nutrients, hydrocarbons and litter. Solids, which are an important pollutant in stormwater runoff, can be present in high concentrations in runoff, and create physical and chemical impacts on receiving waters. Heavy metals, hydrocarbons and nutrients are mainly adsorbed to solids particles. Therefore, the chemical effect of solids on water quality is a major concern, and knowledge of the adsorption characteristics of solids is critical.

The adsorption of the heavy metal cations on solids surfaces occurs due to the interaction forces between the metal cation and the charge sites in these surfaces. The

nature and the strength of the bonds lead to different mechanisms of adsorption, namely, ion exchange, chemisorption and precipitation. The adsorption mechanisms and the extent of adsorption are affected by the type of metal cations, solids surface characteristics and surrounding solution characteristics. Heavy metal concentration, valency and ionic radius of the metal cation are the most significant characteristics which influence competitive metal adsorption. In road deposited solids, the preferred heavy metal interaction mechanisms cannot be reliably inferred from the surrounding pH, since pH in stormwater runoff mostly varies in a narrow range. However, it has been identified that the properties of solids have a significant influence on metal adsorption.

The possible influential parameters of solids in heavy metal adsorption are particle size, specific surface area, mineralogy, cation exchange capacity, exchangeable cations and organic matter content. Fine solids particles concentrate a high amount of heavy metal content than coarser particles due to their high SSA which exerts a significant influence on heavy metal adsorption. On the other hand, the existence of surface charge sites and surface functional groups are the most important parameters for the adsorption of heavy metal cations to solids. A variety of charge sites arise on mineral surfaces, metal oxides and organic matter of solids. The charges on these surfaces can be mainly categorised as permanent charge sites and pH dependent charges that arise on surface functional groups. The charge surfaces exchange cations ( $\text{Ca}^{2+}$ ,  $\text{Mg}^{2+}$ ,  $\text{K}^+$ ,  $\text{Na}^+$  and  $\text{Al}^{3+}$ ), and the exchangeable charge characteristics of solids are reflected by the CEC of solids.

Mineralogical components exhibit permanent charge sites that arise in the lattice structure of the minerals and the pH dependent charge sites on the edge sites or breaking points of the mineral structure. Consequently, charge characteristics of different minerals vary due to their lattice structural arrangement. The different proportions of these mineral components in solids significantly influence the charge characteristics of solids. Metal oxides of Fe, Al and Mn exhibit mainly pH dependent charge characteristics, while the permanent charge sites are limited on these surfaces. Similarly, surface functional groups of natural organic matter exhibit pH dependent charge characteristics, and natural organic matter has high CEC. The different



proportions of these charge components and the poorly understood matrix of road deposited solids make it difficult to understand the physical and chemical behaviour of solids and the heavy metal adsorption process.

Considerable knowledge has been developed in relation to heavy metal adsorption to well-characterised material and natural soils. However, it is unlikely that similar adsorption behaviour will apply to road deposited solids due to their complex and heterogeneous matrix. Adsorption-desorption experiments have been a common approach adopted to study the adsorption behaviour of road deposited solids. However, an in-depth understanding of the crucial role played by the physical and chemical parameters of solids particles is vital to obtain a clear understanding of the heavy metal adsorption process.



# Chapter 3: Research Design

---

## 3.1 BACKGROUND

As outlined in Chapter 2, fundamental knowledge of pollutant adsorption to solids particles is essential to provide robust solutions for stormwater treatment. In this regard, identifying solid particle properties is important. The research methodology was formulated after a comprehensive review of published research in the area. The research study was primarily based on build-up pollutant collection from urban road surfaces.

Road deposited particulates in the urban environment originate from complex and diverse sources and this results in high variability in particle properties. Therefore, a range of data is required for an in-depth understanding of particle properties. Thus, in order to generate such data, the research design entailed a series of field investigations to collect build-up pollutants. Various techniques such as dry vacuuming, brushing and sweeping, or a combination of these techniques, have been used by previous researchers for sampling build-up pollutants. As the present study aimed to collect solids that were very fine, it was important to select an efficient, reliable and convenient sampling technique.

This chapter discusses the research design, methodology and tools used in this study to achieve the aims and objectives stated in Section 1.2 of Chapter 1. Specifically, the study tools, the sample collection method, the apparatus and analytical tools and their appropriate selection criteria are discussed. The data analysis techniques and the justification of each technique are also discussed.

## 3.2 RESEARCH METHODOLOGY

Considerable attention is often directed to heavy metal pollution in urban stormwater runoff. It has been found that high heavy metal load is primarily in the solids phase rather than the dissolved phase. To facilitate the research study objectives, the

research methodology was formulated as a series of field investigations and laboratory experiments. The research methodology involved the following primary activities:

- Study site selection
- Build-up sample collection
- Sample testing and batch experiments
- Data analysis.

### **3.2.1 STUDY SITE SELECTION**

A high fraction of the solids in stormwater originate from paved surfaces (Sartor et al. 1974; Bannerman et al. 1993; Jartun et al. 2008). In urban areas, for example, roads have been recognised as a major contributor of solids to urban stormwater runoff (Bannerman et al. 1993; Egodawatta and Goonetilleke 2006; Zhao et al. 2010). Therefore, road surfaces were selected for the present investigation. As field investigations were designed to collect solids with different particle properties, study sites were selected from four different suburbs to represent a diversity of solids composition. Although it was hypothesised that the pollutant adsorption process is independent of land use, sites were selected based on three different land uses. This allowed the evaluation of the variability of heavy metal concentrations and behaviour, as well as an understanding of the various forms of metals and their interaction with solids particles.

### **3.2.2 BUILD-UP SAMPLE COLLECTION**

Solid particle accumulation on road surfaces is subject to change due to complex and continuous on-road processes. Therefore, sampling was carried out for two different antecedent dry periods. According to previous research findings, pollutant accumulation in the initial period is rapid and tends to reach equilibrium in around seven to nine dry days (Ball et al. 1998; Egodawatta and Goonetilleke 2006). Consequently, sampling times were selected such that the antecedent dry period for one sampling episode was less than eight days and the other greater than eight days. The sampling was carried out in two different seasons as it was anticipated that there

would be variations in the composition of build-up pollutants. However, the seasonal variations in build-up were not taken into account.

The field investigations focused on collecting pollutant build-up samples from urban road surfaces. The collection of build-up and wash-off samples is the common approach adopted in studying stormwater pollutants. However, researchers have found that the wash-off process removes only a portion of pollutants that are available on the surface (Sartor et al. 1974; Vaze and Chiew 2002; Egodawatta et al. 2007). Therefore, if wash-off was also considered in the present study, it would only result in identifying the influential parameters on pollutant adsorption to solids which have been subjected to wash-off due to particular rainfall intensity. Consequently, solely evaluating the build-up pollutants that represent all available pollutants was the most effective method to achieve the research project objectives.

To investigate the solids composition, roadside soil samples were collected in addition to build-up solids. Soils deposited on the road surfaces can be an important source of pollutants to road surfaces. Since soil is in a relatively stable compound compared to solids, only one sample was collected from each suburb in order to investigate the mineralogical characteristics for comparison with the build-up solids.

### **3.2.3 SAMPLE TESTING AND BATCH EXPERIMENTS**

The collected build-up solids samples were tested for heavy metals and a range of physical and chemical parameters that were identified as the governing parameters of metal adsorption to solids surface. The soil samples were analysed for selected physical and chemical parameters to enable the comparison of solids composition. In order to confirm the identified adsorption behaviour of solids particles, batch adsorption and desorption experiments were carried out. All the laboratory tests were conducted according to the appropriate standards methods (US EPA 1994, APHA 2005). Furthermore, in order to ensure the accuracy of the test data, appropriate standard quality control procedures were adopted.

### **3.2.4 DATA ANALYSIS**

Data analysis was carried out in four different steps. Initially, general variability of physical and chemical parameters of solids particles was analysed using loads and concentrations of each parameter. Secondly, the solid sample composition was compared to roadside soil sample composition to identify the possible pollutant sources. Thirdly, primary correlations of physical and chemical parameters were investigated and the influence of these parameters on metal adsorption was evaluated. Finally, the metal adsorption process of solids was identified through the analysis of batch adsorption data. In this context, both univariate and multivariate data analysis techniques were used. The data analysis techniques were selected according to the specific requirements of the analysis to be performed and the capability of the analytical technique.

## **3.3 STUDY TOOLS**

Field investigation techniques and the apparatus to accomplish the study objectives were selected after consideration of ease of handling the equipment and its portability to the study sites. Furthermore, appropriate data analysis techniques were selected with respect to specific analytical requirements.

### **3.3.1 SAMPLE COLLECTION SYSTEM**

Road deposited solids typically consist of a wide range of particle sizes. These particles can contain relatively high pollutant loads due to their direct interaction with traffic related activities (Shaheen 1975; Ellis and Revitt 1982; Ball et al. 1998). However, fine particles have been identified as the significant particle size range in terms of stormwater pollution due to their inherent high adsorption capacities resulting from their relatively high surface area to volume ratio (Roger et al. 1998; Charlesworth and Lees 1999; Zhao et al. 2010). Under these circumstances, studying fine solids particles from road surfaces was crucial in order to achieve the research study objectives. This made it necessary to select an appropriate technique for build-up sample collection to enhance the collection of fine particles, and this was selected after careful examination of the efficiency, advantages and disadvantages of the techniques used in previous research studies.

In the past, sampling road deposited particles has been conducted by sweeping, brushing or vacuuming (Ball et al. 1998; Bris et al. 1999; Deletic and Orr 2005; Lau and Stenstrom 2005; Shilton et al. 2005; Herngren 2005; Vaze and Chiew 2002; Egodawatta 2007). Brushing or sweeping is a more general technique that is used to collect particles when finer particles are not crucial for the study. Several researchers have used vacuuming to enhance the collection efficiency of fine particles (Ball et al. 1998; Herngren 2005; Egodawatta 2007). Vaze and Chiew (2002) collected samples combining vacuuming and brushing, to further enhance collection efficiency. However, Bris et al. (1999) conducted an experiment consisting of dry and wet vacuuming techniques and identified that wet vacuuming was efficient in collecting finer particles compared to conventional vacuuming, as wetting the finer particles improves their recovery. Deletic and Orr (2005) used the wet method for sample collection, which involved spraying deionised water and simultaneously vacuuming the accumulated material on the surface. They delivered sufficient pressure to dislodge finer particles without disturbing the surface. In the present investigation, an improved method of sample collection known as dry and wet vacuuming was conducted to collect pollutant build-up, thereby combining the two methods.

### **3.3.2 SELECTION OF VACUUM CLEANER AND SPRAYER**

#### **Selection of vacuum cleaner**

Selecting a suitable vacuum cleaner was an important consideration for field investigations. Both domestic and industrial vacuum cleaners have been used by past researchers for sampling build-up pollutants from urban impervious surfaces (Tai 1991; Ball et al. 1998; Deletic and Orr 2005). Vaze et al. (2000) used an industrial vacuum system for sample collection and found that it is more efficient in particle collection due to the high power generation. Nevertheless, domestic vacuum cleaners have been successfully used by several researchers for field sample collection (Tai 1991; Ball et al. 1998; Herngren 2005). Tai (1991) has shown that the retention efficiency of the conventional domestic cleaner he used was 96.4% for particles <75µm. He suggested that the filtration system used in a domestic cleaner increased the collection efficiency. Consequently, features considered in selecting a suitable

vacuum cleaner for the present study were the efficient filtration system and high power generation. Furthermore, due to the large number of field investigations involved in this research, additional consideration was given to portability, ease of handling and the power requirement of the apparatus.

Accordingly, the selected vacuum cleaner for the research study was a Delonghi Aqualand model which incorporates an efficient filtration system. According to the manufacturer's specifications, the HEPA filter provided has 99.97% efficiency in filtration. The same vacuum system was successfully used by Herngren (2005), Egodawatta (2007) and Miguntanna (2009a) to investigate pollutant build-up on road surfaces. As suggested by Herngren (2005), water filtration system used in this vacuum retains the dust and subsequently prevents its circulation back into air. The Delonghi Aqualand model consists of a highly compact 1500W suction power with adjustable suction control. The system is a simple and portable unit that can be easily packed when moving between sites. Power supply to the vacuum cleaner can be provided by a generator.

The vacuum cleaner consisted of a water filtration system with a High Efficient Particulate Air (HEPA) filter which ensured the minimal escape of finer particles from the exhaust system (See Figure 3.1). The filtration mechanism directs the air intake through a water column and the water in the vacuum cleaner compartment captures the dust particles. The hose of the vacuum cleaner is connected to small foot with a brush that concentrates airflow through a smaller area. Hence, it consumes power efficiently.



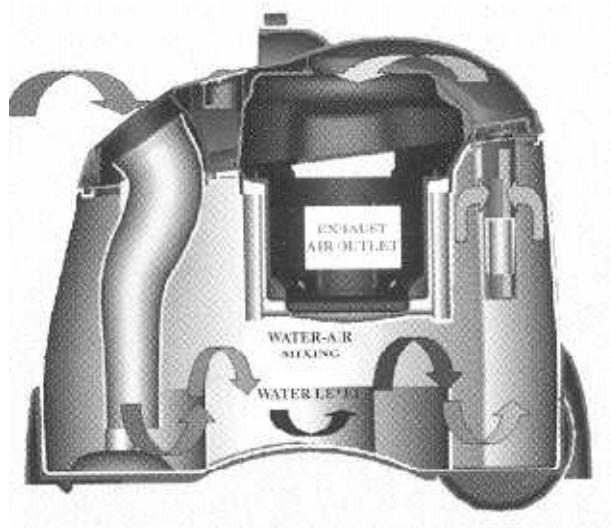


**Figure 3.1: The design of the water filter system of the Delonghi Aqualand model**

### **Selection of sprayer**

Most of the stormwater pollutants are attached to finer particles. A significant portion of these finer particles are embedded on the road surface (Bris et al. 1999). The collection of finer particles was an important consideration in this research study. The efficiency of finer particle collection by the vacuum cleaner was enhanced by wetting the surface with a water sprayer, which helped to dislodge the finer particles. Thus, selecting a suitable sprayer was an important consideration. Essentially, the sprayer needed to deliver sufficient pressure to dislodge the finer particles without destroying the surfaces. Deletic and Orr (2005) used commercially available sprayers to dampen the road surface. However, they did not mention the appropriate water pressure needed to dislodge the pollutants from road surfaces. It is essential to use an appropriate pressure, as high pressure would disturb the parent asphalt surface. Furthermore, the suitable pressure should be maintained to avoid blowing particles away during the spraying. Thus, it was important to select a sprayer with a pressure control unit. Additionally, portability and convenient use of the system in the field were also considered when choosing a sprayer.

In the present study, a portable 12 volt electric sprayer (Swift Compact Sprayer), as shown in Figure 3.2, was used for dampening the road surface. A pressure control

module and pressure gauge is attached to the sprayer. Thus, the pressure can be adjusted as required in the field for a calibrated value. Once the pressure was adjusted, the pressure control module monitored the water output pressure in the nozzle. Additional advantages of the Swift Compact Sprayer were: sufficient water storage capacity (60L) to be used in the field; a moulded water level indicator; a 6m long flexible delivery hose which makes it easier to use in the field while the sprayer is located in the vehicle itself; a lance with an adjustable nozzle; a locked out trigger and storage tank fitted with a drain; a sealed lid, and moulded handles for lifting.



**Figure 3.2: The Swift Compact water sprayer (60L)**

### **3.3.3 SAMPLE COLLECTION EFFICIENCY**

The sample collection efficiency of the vacuum cleaner and sprayer was tested on an actual road surface that was subject to daily traffic (Mahbub et al. 2009). In addition to the efficiency, the suitable water pressure to dislodge particles was decided through this experiment. Thus, three adjacent plots of 1m x 1m were selected for the experiment. One hundred grams of clean dry closely graded sand (150-600 $\mu$ m) and fine sand (<150 $\mu$ m) were used as the pollutants. The pollutant sample represented fine solids that are significant as stormwater pollutants and are largely expected to be present on road surfaces (Ball et al. 1998; Herngren 2005). The selected plot surfaces were cleaned thoroughly by repeated washing with deionised water prior to the test, and allowed to dry for one hour by applying airflow. Then, solid samples were carefully distributed without spilling particles over the edges. Furthermore, it was assumed that during the one-hour dry period, the same amount of pollutant had built-up on the three plots. After thorough cleaning of the vacuum system, the vacuum

cleaner compartment was filled with deionised water. Then, the sampling in the three plots was conducted as follows:

- On the first plot (Plot 1), 100g of sand was applied. Then, the vacuuming system was used to collect the dry samples. Deionised water was sprayed from the sprayer at 3 bar pressure for three minutes. Then, the wet sample was collected by the vacuum cleaner.
- On the second plot (Plot 2), 100g of fine sand was applied. Then, the vacuuming system was used to collect the dry samples. Deionised water was sprayed from the sprayer at 2 bar pressure for three minutes and the wet sample was vacuumed.
- On the third plot (Plot 3), without distributing sand, a dry sample was collected using the vacuuming system. Deionised water was sprayed from the sprayer at 1 bar pressure very close to the road surface for three minutes. Then, the wet sample was collected by the vacuum cleaner.

After vacuuming the sample, the hoses and foot were thoroughly cleaned using deionised water, and it was ensured that all particulates were collected. Then, the collected sample was oven dried and the recovered weight was measured. As illustrated in Table 3.1, the dry sample and wet sample from each plot were measured separately to determine the collection efficiency of wet sampling. ‘Dry samples’ refers to the samples collected by the vacuuming system before spraying, whilst ‘wet samples’ refers to the samples collected by the vacuuming system after spraying.

The efficiency of the dry and wet vacuuming system was calculated by the percentage of the total weight of the dry and wet samples collected at each plot. Furthermore, to obtain the optimum spraying pressure, the percentage collection efficiency of the wet samples at Plot 1 and Plot 2 was compared. According to Table 3.1, the total sample recovery efficiency was found to be in the 90% range (from 89.4% to 90.5%), which was considered satisfactory for the envisaged investigations. It was also found that the wet sample collection efficiency increased from 58.6% to 70.6% when the spraying pressure was reduced from 3 to 2 bars. Even though the

total collection efficiency was reduced slightly at the 2 bar pressure, considering the increase in the wet sample collection efficiency, it was decided to apply the 2 bar pressure for the field sample collection.

**Table 3.1: Sample collection data for the wet and dry vacuuming system**

	<b>Plot 1</b>	<b>Plot 2</b>	<b>Plot 3</b>
Applied sand weight(g)	100.0	100.0	0.00
Dry sample collected (g)	79.14	66.14	2.20
Wet sample collected (g)	14.16	26.11	0.65
Sprayer pressure (bar)	3	2	1
Efficiency of total collection (%)	90.5	89.4	-
Efficiency of wet sample collection (%)	58.6	70.6	-

Based on the above results, it was decided to use vacuuming and spraying to achieve an acceptable efficiency in the field sample collection process. Possible loss of particles would have occurred due to the entrapment of particles in the vacuum cleaner compartment and hoses, and minor losses would occur through particles being blown away during the spraying. This experiment was conducted on an actual bituminous surface. Thus, the results obtained would closely represent the actual sampling environment of the selected road sites.

### **3.3.4 DATA ANALYSIS TECHNIQUES**

The present study was undertaken in order to understand the adsorption process of solids and to investigate the relative importance of physical and chemical parameters on heavy metals adsorption. In this context, data analysis techniques needed to be identified by considering the nature of the data and the capability of the techniques to achieve the study objectives.

The present research generated a relatively large amount of data of a highly variable nature. It was hypothesised that the selected physical and chemical parameters are

influenced by site specific characteristics such as land use, geographical location and traffic characteristics. Consequently, univariate statistical data analysis techniques were not adequate to explore the collected data. Additionally, a method capable of quantitative assessment and comparison of variables needed to be applied to identify the relative significance of the individual physical and chemical parameters on pollutant adsorption. Consequently, multivariate data analysis techniques were also used, and Principal Component Analysis (PCA) for pattern recognition and Multi Criteria Decision Making (MCDM) methods for ranking objects and visually displaying the relationships between variables and objects were employed. The following sections describe the various data analysis techniques used in the study. The application of these techniques in data analysis and the results obtained are discussed in Chapters 5, 6 and 7.

#### **A. Univariate statistical data analysis techniques**

Univariate data analysis techniques were primarily used to explore the variability of data and can be used to identify the variation of two variables. Many pollutant parameters associated with urban solids occur in highly variable concentrations. Consequently, summary statistics such as mean and standard deviation (SD) are used to describe the characteristics of a single variable data set (Adams 1995). Mean is the ordinary arithmetic average of the data set, while standard deviation (SD) measures the dispersion of data with respect to the mean value. A tightly grouped data set gives a small standard deviation and widely scattered data gives a large standard deviation (Adams 1995).

#### **B. Principal Component Analysis (PCA)**

Principal Component Analysis (PCA) is the most common pattern recognition technique used for multivariate statistical data (Kokot et al. 1998; Vega et al. 1998). PCA has been successfully used in the area of water quality research studies to analyse multivariate statistical data (Qu and Keldertman 2001; Facchinelli et al. 2001; Adachi and Tainosho 2005; Goonetilleke et al. 2005; Hengren et al. 2005; Settle et al. 2007). For example, Settle et al. (2007) used PCA for the investigation of the physical and chemical behaviour of solids in urban stormwater runoff and

Goonetilleke et al. (2005) applied PCA to identify linkages between various pollutant parameters and correlations with land use.

Using PCA, Herngren et al. (2005) investigated relationships between heavy metals and solids in urban stormwater runoff. Furthermore, PCA has been used to identify the behaviour and sources of heavy metals (Facchinelli et al. 2001; Qu and Keldertman 2001) and to identify the sources of the road deposited solids (Adachi and Tainosho 2005). Covelo et al. (2007a) used PCA to identify the patterns in the metal retention behaviour of the sorbents, Abollino et al. (2003) to identify the significant metal binding phases in minerals, and Dawes and Goonetilleke (2006) to identify the soil attributes based on the soil properties. In this study, PCA was employed to investigate the relationships among the physical and chemical parameters that influence metal adsorption to solids and to characterise the adsorption behaviour of heavy metal to solids particles. Furthermore, solids particle composition was also characterised with the use of PCA.

PCA is a data reduction technique commonly employed to investigate relationships among objects and variables in a data matrix. It is a powerful technique that attempts to explain the variance of a large data set of inter-correlated variables by transforming them into the new orthogonal axes called 'principal components' (PCs). PCA reduces the dimensionality of the data set by explaining the correlation among the large set of variables in terms of a small number of underlying factors or principal components, without loss of much information in the data set (Vega et al. 1998). The first principal component axis describes the maximum variance of the data in one direction. Successively, the amount of variance of the original data set decreases from the first to the last significant principal component (Adams 1995; Kokot et al. 1998; Settle et al. 2007). PCA method mathematically transforms the original data into a covariance matrix. Therefore, the principal components can be defined by the eigenvectors of a variance-covariance matrix. Thus, the eigenvectors represent the loadings or coefficients used to transform the original data into principal components (Adams 1995). The Scree plot is the graphical variation of the eigenvalues in the descending order with corresponding principal components. Thus, the number of principal components that should be taken into account in the analysis

is determined by the weights of the eigenvector in the Scree plot, which coincides with the point that shows a pronounced change of slope (Jackson 1991; Adams 1995).

To apply PCA to a data set, the raw data must be arranged into a matrix representing variables by columns and objects by rows. Hence, in the present study, the build-up solids samples were taken as objects and the physical and chemical parameters and water quality data were taken as variables. Since these variables represent different units, to avoid different scale effects of these variables, the data was subjected to standard pre-treatment techniques. The most common pre-treatment techniques are standardisation, mean centering and auto scaling (Kokot and Yang 1995; Libarando et al. 1995; Tyler et al. 2007). Standardization is usually recommended when the variables measured are recorded in different units (Adams 1995). In standardisation, the individual value in each cell is divided by the standard deviation of that column. This ensures that each variable will have equal weighting with a standard deviation of 1 (Kokot et al. 1998). Mean centering is subtracting the mean value of each column (variable) from each element in their respective column. The combination of the above two methods is called 'auto scaling'. In this research, to reduce the data heterogeneity, the original data was subject to auto scaling by mean centering and standardisation (Purcell et al. 2005; Settle et al. 2007).

Once the data was pre-treated by any of the above methods, it was subjected to PCA analysis. However, PCA is sensitive in detecting outlier objects (Settle et al. 2007). Outliers represent the data that are unrepresentative of the majority of data. These objects lie outside the  $T^2$  Hotelling ellipse. After the initial observations of pre-treated data, it was pre-processed to eliminate the objects that were irrelevant to the current study.

Graphical interpretation of the outcomes is one of the advantages of PCA and is usually presented as scores and loadings plots. The important information about the objects derived from PCA is graphically presented in scores-scores plot. The relationships among variables are described in the loadings plot. Relationships

among variables and objects are best displayed in a PCA biplot, which is obtained when scores and loadings are displayed on the same plot. Also, a combination of the PC score and corresponding loadings plots provide information which is often unavailable through conventional data analysis (Carmody et al. 2006). A biplot represents the loading of each variable as a vector and the score of each object in the form of a data point, and scores and loadings give the interpretation of the correlation between them. The angle between variable vectors gives the degree of correlation between variables. An acute angle between two vectors indicates a strong correlation between the respective variables, whereas an obtuse angle indicates a weak correlation. Right-angled vectors indicate no correlation. The vector direction is indicative of the correlation between variables and objects. A grouping of objects is the indicator of similarities in objects.

Theoretical interpretation of PCA can be found in Adams (1995) and Massart et al. (1998). However, PCA biplots with low variance would not interpret the variation of total data matrix. In such instances, analytical techniques such as correlation matrix and PROMETHEE and GAIA analyses were carried out to interpret the validity of observed correlations through PCA biplot. In the present study, PCA was carried out by using StatistiXL and Sirius 7.0 software.

### **C. Multi Criteria Decision Making Methods (MCDM)**

Multi criteria decision making methods are used for decision making in multivariate problems to obtain an optimum decision. Decision is achieved via ranking procedures designed to rank objects by comparing the performance or preference of one object to another (Keller et al. 1991). There are many MCDM methods available in the literature, namely, ELECTRE, SMART, Preference Ranking Organization Method for Enrichment Evaluation (PROMETHEE) and Graphical Analysis for Interactive Assistance (GAIA) (Keller et al. 1991; Salminen et al. 1998; Lahdelma et al. 2003; Martin et al. 2007). In general, each method has its own characteristics. In comparison to the above methods, ELECTRE facilitates additional options for thresholds when defining criteria (Salminen et al. 1998). PROMETHEE is a more refined method than ELECTRE that quantifies the degree of preference of an object



as compared with another for each criterion (Massart et al. 1997). Furthermore, compared to the PCA method, the advantages of PROMETHEE is that it is a non-parametric method, and can even compare as few as two objects (Carmody et al. 2005).

Among these methods, the PROMETHEE ranking method coupled with GAIA methods are more suitable due to their simplicity and sophisticated technique (Brans et al. 1986; Keller et al. 1991). The combination of PROMETHEE ranking and GAIA visualisation techniques facilitates the identification of variables responsible for the ranking and often performs well compared to the other MCDM methods (Keller et al.1991; Khalil et al. 2004; Kokot et al. 2005; Ayoko et al. 2007). In general, PROMETHEE and GAIA have been successfully applied in a wide range of studies, and have been increasingly used in environmental research studies in recent years. For example, Khalil et al. (2004) successfully used these methods to rank different sites for sewage effluent disposal on the basis of their physico-chemical characteristics. Carroll et al. (2004) identified suitable soils for effluent renovation using these methods. Hengren et al. (2006) used PROMETHE ranking to classify particle sizes based on heavy metals adsorption. Furthermore, they used GAIA to determine the correlations between the heavy metals and particle size ranges and to assess correlations with physio-chemical parameters. PROMETHEE and GAIA have been quite successfully used to select suitable adsorbent, to characterise the chemical composition of adsorbent (Carmody et al. 2005), and to identify the adsorption characteristics of adsorbents (Frost et al. 2007). Thus, the combination of PROMETHE and GAIA MCDM methods was selected in the present study, as an appropriate technique to rank and to identify the correlations among variables.

In this study, PROMETHEE was employed to rank the objects on the basis of physical and chemical parameters of different land uses, and GAIA was applied to analyse the variation in physical and chemical parameters in order to provide additional information not readily available using the PCA technique. Furthermore, these methods were also employed in the batch adsorption experiment to investigate the heavy metal adsorption process due to the low number of samples used. Decision Lab (Visual Decision Inc. 2000) software was used for PROMETHEE II and GAIA

analysis. The results and outcomes of the PROMETHEE II and GAIA methods are described in Chapters 5 and 7. Theoretical interpretation of these methods has been discussed in detail in the literature (Keller et al. 1991; Khalil et al. 2004). The data processing using these methods requires the definition of a number of functions and these are briefly described below.

## **PROMETHEE**

PROMETHEE is a non-parametric method used to rank a number of actions (objects or samples) on the basis of performance criteria (variables) in the data matrix, according to preferences and weighting conditions (Keller et al.1991; Kokot et al. 1999).





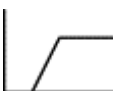

*Ranking order* – Each criterion is specified, either top-down (maximized) or bottom-up (minimized) rank order, according to the preference of the user (Keller et al. 1991; Carmody et al. 2005; Purcell et al. 2005).

*Weighting* - Each variable can be weighted based on the importance of one criterion over another: the larger the values that can be assigned, the more important the criterion. The criterion weight is a positive value, independent from the scale of the criterion. However, in general, most modelling initially uses the default weighting of 1 (Keller et al. 1991; Visual Decision Inc. 2000).

*Preference function* - The way one object is to be ranked relative to another is defined by a mathematical function known as the ‘preference function P’ (a, b). Furthermore, preference function translates the deviation between the evaluations of two actions (objects) on a single criterion (parameter) into a preference degree. The preference degree indicates an increasing function of the deviation. Thus, the smaller deviations will contribute weaker degrees of preference, while larger ones will contribute the stronger degrees of preference (Visual Decision Inc. 2000). In the Decision Lab software (Visual Decision Inc. 2000), six functions are available, as shown in Table 3.2.

*Threshold* - Each shape of the preference function depends on up to two thresholds which should be provided by the user. Indifference threshold  $q$  represents the largest deviation that the decision maker will consider negligible when comparing two actions on a single criterion. Preference threshold  $p$  represents the smallest deviation that is considered as decisive in comparison of two actions. Preference threshold  $p$  is usually greater than  $q$ . Gaussian threshold  $s$  is a middle value that is only used with the Gaussian preference function (Visual Decision Inc. 2000; Khalil et al. 2004).

**Table 3.2: List of preference functions**

Function	Threshold	Shape
Usual	No threshold	
U-shape	$q$ threshold	
V-shape	$p$ threshold	
Level	$q$ and $p$ thresholds	
Linear	$q$ and $p$ thresholds	
Gaussian	$s$ threshold	

In addition to these parameters, PROMETHEE allows the criteria to be modelled independently, as explained below.

### Step 1

This step involves transformation of the raw data matrix to a different (d) matrix. For each criterion, all entries in the data matrix are compared pair wise, and in all possible combinations by subtraction. This results in a different (d) matrix for each comparison.

## Step 2

In this step, for each criterion, a preference function  $P(a, b)$  is selected to describe how much one outcome (a) is preferred over another. One of six such preference functions available in the Decision Lab software may be chosen here (Visual Decision Inc. 2000). For each preference function ranking order, weighting and threshold values need to be allocated, as described above.

## Step 3

In Step 3, the sum of the preference values (weight \* preference function) of each criterion, result in a value known as a 'global preference index',  $\pi_i$ , which indicates the global preference of one object over another.

## Step 4

To compare how each object (action) outranks all the other objects, positive ( $\Phi^+$ ) and negative ( $\Phi^-$ ) outranking flows are computed from the  $\pi_i$  global preference index in this step. The  $\Phi^+$  outranking flow expresses how each object outranks all others, while the  $\Phi^-$  outranking flow indicates how each object is outranked by all the other objects. The higher  $\Phi^+$  and the lower  $\Phi^-$  indicate a high preference for an object. This procedure results in a partial pre-order—the 'PROMETHEE I' ranking.

## Step 5

In this step, a simple set of rules [described by Keller et al. (1991)] is applied to calculate the complete order or net outranking flow ( $\Phi$ ).

$$\Phi = \Phi^+ - \Phi^-$$

This procedure is known as 'PROMETHEE II'. The higher the value of  $\Phi$  for an object, the higher is its position in the rank order.

## GAIA

GAIA is a data visualisation method which displays PROMETHEE results. GAIA is linked to the PROMETHEE procedure. The GAIA matrix is constructed from a decomposition of the  $\Phi$  net outranking flows of PROMETHEE (Keller et al. 1991). The resulting data matrix is then processed by a Principal Component Analysis (PCA) algorithm, and displayed on a GAIA biplot. Interpretation of the GAIA biplot provides guidance for the PROMETHEE ranking of the objects. Similar to the PCA biplot, the GAIA biplot illustrates a distribution of objects and criteria vectors. Additionally, it shows the decision axis  $\pi_i$  which points to the approximate location of the preferred action and displays the degree of decision power. The significant advantage of GAIA over PCA is that the former facilitates model scenarios based on the choice of individual preference functions for each criterion, the choice of ranking sense and the criteria weights. Unlike PCA, most of the variance of the data matrix is explained by the two principal components in the GAIA biplot. The application of GAIA is detailed in the research literature (Keller et al. 1991; Ayoko et al. 2004; Khalil et al. 2004). The interpretation of GAIA biplot was carried out according to the guidelines provided by Keller et al. (1991) and Espinasse et al. (1997), as follows.

- i. More significant variables are represented by a long vector projected in GAIA biplot.
- ii. The independent variables are represented by orthogonal vectors.
- iii. The vectors oriented in the same direction represent equivalent information, while those oriented in the opposite direction represent conflicting information.
- iv. Objects projected in the same direction of a particular variable are strongly correlated to that variable.
- v. Dissimilar objects show different PC coordinates, while similar objects form a cluster.
- vi. The long decision vector,  $\pi_i$ , represents the strong decision power of the data. The best objects are the objects farthest from the origin in its direction.

### 3.4 SUMMARY

The research methodology formulated for the present study consisted of study site selection, build-up samples collection, sample testing and batch experiments, and data analysis. The research methodology primarily consisted of a series of field investigations and laboratory experiments. Field investigations were conducted to collect build-up pollutants on road surfaces. An innovative method of dry and wet vacuuming was used to collect build-up pollutants on impervious surfaces. The two pieces of apparatus used for field investigations in the research project were:

- Vacuum collection system
- Water sprayer.

Both pieces of apparatus were primarily selected as a result of considering their efficiency for the collection of fine particles from the road surface. The combined dry and wet vacuuming technique was tested for particle collection efficiency and was found to be satisfactory for use for sampling in the research project.

Analytical techniques were selected after considering their capability to undertake the data analysis to achieve the study objectives. Univariate and multivariate data analysis techniques were selected for the data analysis. Univariate data analysis techniques were used to explore the data set. Due to the complexity and large variance of data sets, the PCA multivariate analysis method was selected as a versatile technique for pattern recognition. Furthermore, the multi criteria decision making methods of PROMETHEE and GAIA were used for ranking objects and for identifying relationships among criteria.

# Chapter 4: Study Site Selection and Data Collection

---

## 4.1 BACKGROUND

A field investigation methodology was formulated to develop an appropriate database for the investigation of the adsorption processes of solids particles. Adsorption is influenced by the physical and chemical properties of solids particles. Therefore, for a comprehensive understanding of adsorption processes and to define relationships, it was important to analyse particles for a diversity of primary parameters that govern these processes. Consequently, suitable study sites were selected to collect a range of particles from diverse urban environments.

In evaluating the fundamental processes of build-up pollutants, the use of small test plots, rather than catchment scale studies, is recommended. This can help to overcome the constraints which may arise due to the heterogeneity of built-up areas (Herngren et al. 2005; Goonetilleke et al. 2009). Furthermore, the use of small plot areas reduces the influence of physical factors and the location specific nature of research study outcomes that commonly constrain their transferability to other, geographically different areas. Based on the above concept, pollutant build-up sample collection was confined to small plot areas for the development of knowledge on the adsorption processes of solids particles in pollutant build-up.

This chapter presents a detailed description of the study sites and the site selection criteria adopted. Additionally, it describes the collection procedures used for the sampling of build-up solids and soils. Considerable attention was given to the soil characteristics in the surrounding areas, as it was hypothesised that these would play an influential role in defining the characteristics of the build-up solids. The chapter also discusses the analytical laboratory procedures used and the design of the batch adsorption experiment undertaken for the validation of the research study outcomes.

## **4.2 STUDY AREA SELECTION**

### **4.2.1 GOLD COAST**

Study sites were selected from the Gold Coast region, located 100km south of Brisbane, the capital city of Queensland State and the sixth largest city in Australia. The Gold Coast, which is located just north of the Queensland and New South Wales border, is a city with surf beaches, waterways and canal systems, and is dominated by high-rise apartment buildings. It is famous for tourism and recreation. The population of the Gold Coast is approximately 515 000, and up to 120 000 visitors are added during peak periods (ABS 2009; GCCC 2009). Continuing population growth close to waterways has increased the urban development of the area.

The Gold Coast is typical of a subtropical environment, with average annual rainfall of 1500mm. The area has a relatively dry winter and most rainfall occurs in the spring and summer months; much of this is the result of storms. Consequently, most stream flow occurs in spring and summer (GCCC 2009). The drainage network consists of five main rivers and numerous creeks which flow into the nearby Moreton Bay and Broadwater. Rapid development along the waterways has impacted on water quality. Consequently, numerous water management practices are currently being implemented in the area.

A diversity of soil types can be found on the Gold Coast due to the presence of varied terrain. The most common soils in the Gold Coast (Moreton Bay region) are Dermosols (known as Red and Yellow Podzolic) and Kurosols which are mainly derived from the Neranleigh–Fernvale meta sediments and clayey sub-soils (Noble 1996; Isbell et al. 1997). Dermosols are B2 horizon clayey soils with relatively high salt content (Isbell 1996). Kurosols are B horizon soils with relatively acidic (pH 5.5) behaviour. Kurosols have unusual subsoil chemical features due to the presence of high exchangeable magnesium, sodium and aluminium (Isbell 1996). The inland of the Gold Coast contains the Dermosols and Kurosols clay rich soils. The coastal area has a sandy matrix which contains Anthrosols (man-made soils) and Dermosols (Noble 1996). Figure 4.1 presents the soil information for the Gold Coast (Noble 1996).



### 4.3 STUDY SITE SELECTION

The main criteria considered in study site selection were determined by the anticipated variation in physical and chemical properties of solids. Particle composition, especially the particle mineralogy, reflects the physical and chemical properties of solids. Thus, the study sites were selected to obtain solids samples with variations in mineralogical properties. Accordingly, four urbanised suburbs from the Gold Coast were selected for this study. In these suburbs, road surfaces were selected as study sites, since the research literature has identified roads as a primary pollutant source in urban areas.

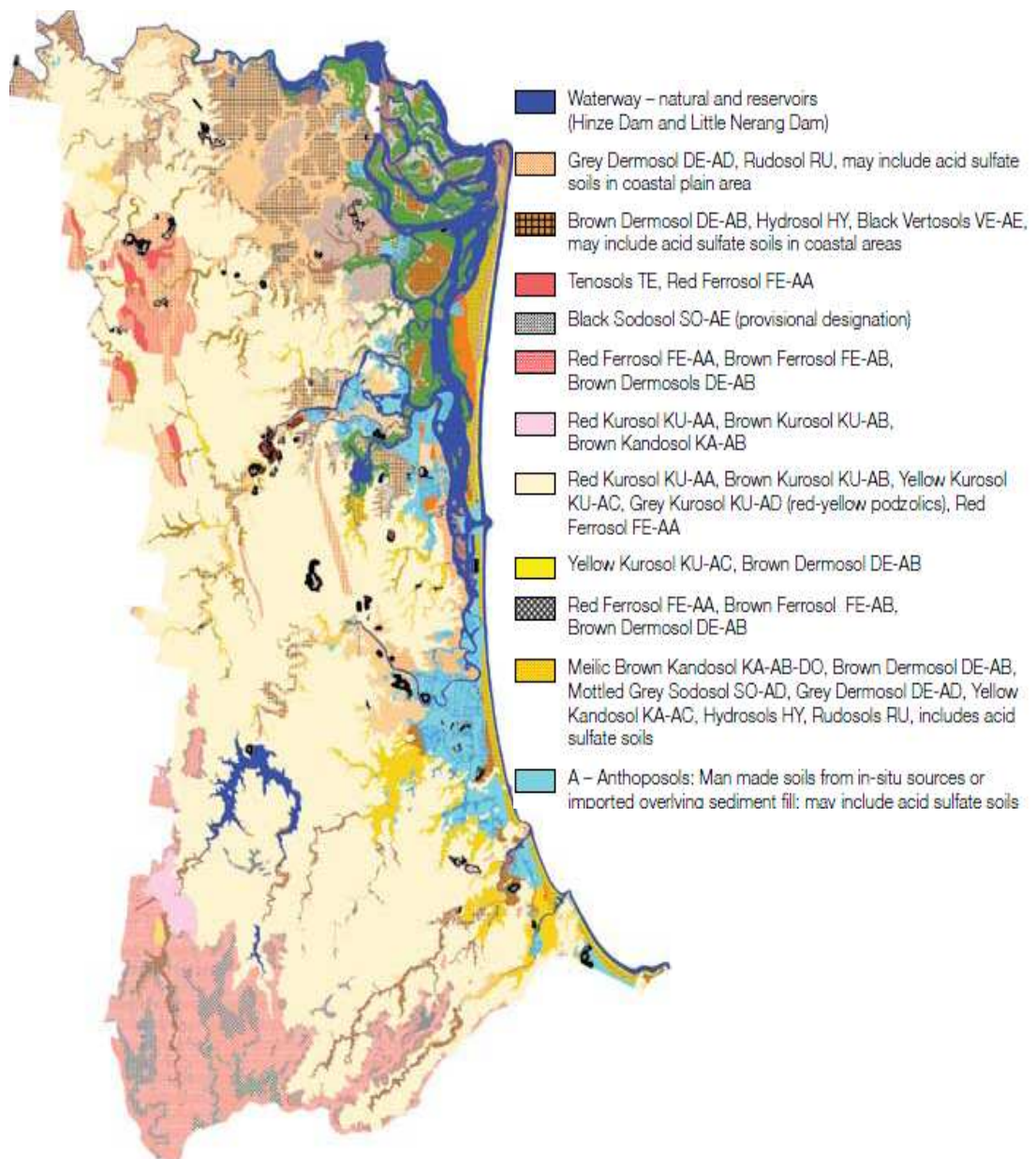


**Figure 4.1: Gold Coast soil information of (Adapted from GCCC 2004)**

A number of factors influence the characteristics of pollutant build-up in urban areas. For example, researchers have pointed out the influence of land use and traffic characteristics on pollutant accumulation, including heavy metals (Sartor and Boyd 1972; Hergren et al. 2006). Since traffic density in different land uses is not uniform, a considerable variation in the build-up of heavy metal content could be expected in different locations. Consequently, road surfaces were selected from different land uses such as light industrial, commercial and residential areas, to investigate the effect of different land uses. However, land use pattern was not considered as a variable in this research, as the adsorption process is independent of the land use. Additional consideration was given to the following primary characteristics of roads during site selection:

- Sufficient width of road section to minimise disturbance to traffic and residents during the sample collection
- Convenient accessibility to the site
- Relatively good surface texture
- Consistence longitudinal slope to obtain homogeneous samples.

#### **4.3.1 CHARACTERISTICS OF THE STUDY SITES**

Suburbs along the Nerang River were selected to capture the variation of soil properties inland and towards the coastline. The Nerang River is one of the major waterways within the Gold Coast and comprises a number of other creeks which flow into the Broadwater through Surfers Paradise. Figure 4.2 shows the selected suburbs, namely: Clearview Estate, Nerang, Benowa, and Surfers Paradise. Benowa and Surfers Paradise are much closer to the coast and consist of sandy soils and silt. Inland study sites such as Nerang and Clearview Estate contain clay-rich soils. From each suburb, four road surfaces with varying levels of traffic density were selected. It was assumed that the traffic density reflected the surrounding building density. Therefore, four road surfaces with different building density were selected from each suburb. This enabled evaluation of the spatial variation of pollutant build-up within the same suburb. A total of sixteen road surfaces were selected from the four suburbs.

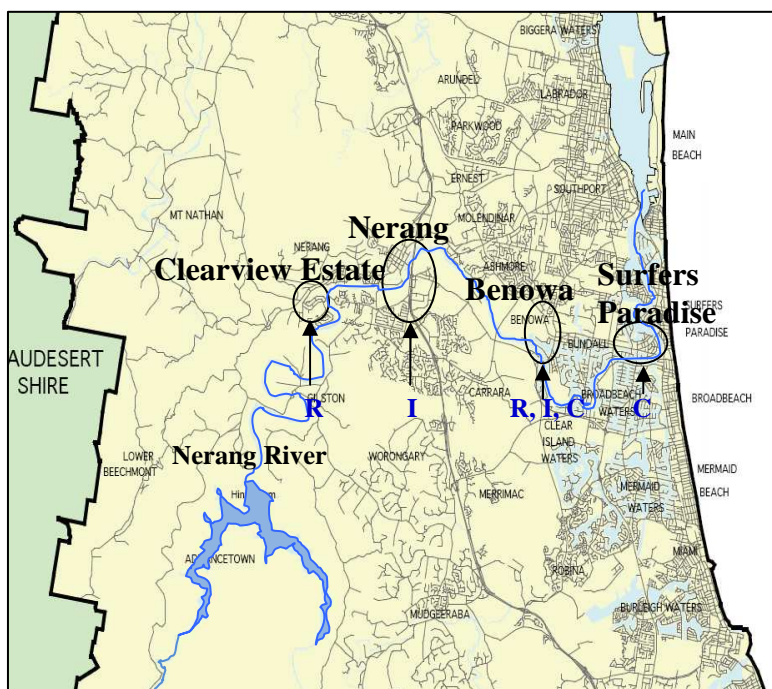


**Figure 4.2: Location of the study sites**

Note: R- Residential, C- Commercial, I- Industrial

Numerous road sites were considered prior to identifying the specific study sites from each suburb. After careful investigations, the sites were narrowed down to sixteen, according to the criteria described in Section 4.2. All selected roads were kerb protected, with two traffic lanes and a car parking lane. The selected sites have a dense-graded asphalt pavement surface, the common pavement material that is used for major roads in the region (Drapper et al. 2000).

The road surface condition was considered as an important factor in pollutant build-up. The texture depths of the road sites were measured, using the sand patch experiment (FHWA 2005; ASTM 2006). Additionally, location coordinates of sampling locations were recorded using a GPS (Garmin GPS 60, Trip and Waypoint Manager). Field investigations were carried out on one side of the road. The following is a description of the selected study sites in each suburb.

## A. Clearview Estate

Clearview Estate is the most upstream suburb along the Nerang River. It is located about 15km from Surfers Paradise. The suburb surrounds a central park with numerous sports grounds and recreational areas. It is a typical urbanised residential area located adjacent to a natural vegetation area with a population density of 1227 residents/km<sup>2</sup> (GCCC 2009). However, variability in urbanisation can be found within the suburb. The four selected roads, and their respective characteristics and location coordinates are listed in Table 4.1, and Figure 4.3 provides photos of the selected sites.

**Table 4.1: Description of selected road sites in Clearview Estate**

Site name	Characteristics	Location coordinates	Texture depth (mm)
Merloo Drive	Access road; medium size blocks; mild slope; good surface condition	28° 00.167'(S)	0.76
		153° 18.236'(E)	
Yarrimbah Drive	Close to highway, wide road; fair vegetation; large blocks; frequent traffic flow; fair slope and surface	28° 00.011'(S)	0.84
		153° 18.130'(E)	
Winchester Drive	Access road; mild slope; surface fair to rough; well maintained lawns	28° 00.072'(S)	0.87
		153° 18.766'(E)	
Carine Court	Access road; medium size blocks; fair slope; good surface condition; well maintained lawns	28° 00.018'(S)	0.92
		153° 18.829'(E)	

As shown in Figure 4.3, all of the above road sites are surrounded by detached family houses with well-maintained gardens. Housing density is different in each road. Other than Yarrimbah Drive, which is the primary access road to the suburb used by the residents, most of these roads serve as access roads. Yarrimbah Drive is a much busier road compared to the other three roads and subject to relatively high traffic

flow. The width of the roads was sufficient to close one lane for field investigations, so they were carried out with minimum disturbance to local traffic. Due to the relatively higher vegetation along Yarrimbah Drive, high organic matter was expected among the road surface pollutants. The other three road sites have relatively low traffic.



**Figure 4.3: Study sites in Clearview Estate: (a) Merloo Drive (b) Yarrimbah Drive (c) Winchester Drive and (d) Carine Court**

## **B. Nerang**

Nerang was the next suburb selected along the Nerang River, downstream of Clearview Estate. A considerable amount of light industrial and commercial services are present in the vicinity. Due to the high density of industries, the area has a relatively low population compared to the other suburbs, with an estimated 2009 population density of 429.4 residents/km<sup>2</sup> (GCCC 2009). After careful investigation of several possible road sites, four roads were selected (Figure 4.4). Geographical location, characteristics and surface texture of the selected roads are listed in Table 4.2.

Selected road sites in Nerang are used as access roads to the industrial and commercial services in the area. As outlined in Table 4.2, all the selected roads have a diversity of industrial enterprises. Thus, different types and high concentrations of heavy metal elements were expected in the collected samples. The selected roads are subjected to high traffic flow and heavy vehicle movement. Thus, the road surfaces are relatively coarser compared to the roads in Clearview Estate, and texture depths range between 0.93-1.14mm. Furthermore, due to regular movement of heavy vehicles and material transport, roads are subjected to spillages and oil leakages.

**Table 4.2: Description of selected road sites in Nerang**

Site name	Characteristics	Location coordinates	Texture depth (mm)
Stevens Street	Sheet metal, paint, furniture, welding, cement mixing industries; steep slope; large road width; coarse texture	27° 59.183'(S)	1.10
		153° 20.034'(E)	
Lawrence Drive	Vehicle service station; carpet, steel industries; busy road; car parking area wide road; good surface condition	27° 59.843'(S)	1.06
		153° 20.755'(E)	
Hilldon Court	Plumbing, metal work industries; vehicle service station; boat builder	28° 00.011'(S)	0.93
		153° 20.455'(E)	
Patrick Road	Boat builder; plumbing and furniture industries; wide road; minimum disturbance	27° 59.957'(S)	1.14
		153° 20.474'(E)	

Other than Stevens Street, all road sites have a flat or mild slope. Stevens Street has a steep slope and it is in a poorer condition when compared to the other roads. It was selected because straight sections of about 30m could be found and investigated with minimum disturbance to the businesses located along the road. With the exception of Stevens Street, all sites were located close to the Pacific Motorway. Hence, pollutants generated from high vehicular activities were expected to significantly contribute to the pollutant build-up at these sites, in addition to the pollutants

generated from adjacent industries. Lawrence Drive is a relatively busy road compared to the others, as it is an arterial road. Due to the relatively high traffic at the site, build-up sample collection was carried out in the roadside car parking area. Hilldon Court is also a busy road as it is also an arterial road with a large number of industries. Patrick Road provides access to a few industries only. Thus, it has light traffic and easy access for sample collection.



**Figure 4.4: Study sites in Nerang: (a) Stevens Street (b) Lawrence DR (c) Hilldon Court and (d) Patrick Road**

### **C. Benowa**

Benowa is a suburb located three kilometres west of Surfers Paradise. A major portion of the area is close to the coastal strip and was originally a wetlands drained by the Nerang River, which has now been converted into artificial islands. At present, the canal estate is a highly urbanised suburb with a population density of 1582.6 residents/km<sup>2</sup> (GCCC 2009). The diversity of properties available in the area ranges from medium size blocks, duplexes and townhouses to waterfront properties on lake, canal or Nerang River frontages. As for the selection of sites in Clearview

Estate and Nerang, several possible study sites were considered and refined down to four sites after a pilot investigation (Figure 4.5). The selected sites in Benowa, their characteristics and coordinate locations are listed in Table 4.3.

**Table 4.3: Description of selected road sites in Benowa**

Site name	Characteristics	Location coordinates	Texture depth (mm)
Strathaird Road	Warehouses, food stores, mechanical workshops, service station; coarse surface condition; fair slope; high traffic flow	28° 00.473'(S)	0.80
		153° 24.071'(E)	
Mediterranean Drive	School, playgrounds; medium size blocks; mild slope; high traffic flow at specific times	28° 00.269'(S)	0.82
		153° 23.275'(E)	
De Haviland Avenue	Residential access road; medium sized blocks; light traffic; good surface condition	28° 00.680'(S)	0.90
		153° 23.537'(E)	
Village High Road	Access road; medium size blocks; mild slope; good surface condition; well maintained lawns	28° 00.802'(S)	0.91
		153° 23.822'(E)	

Selected road sites in Benowa belonged to different land uses. Strathaird Road is used as an access road to a commercial area with various types of commercial activities. The road is quite busy and has roadside car parking lots. Thus, it was expected that high vehicular pollutant loads could be present at the site. Furthermore, high atmospheric pollutant deposition was expected as this road is in close proximity to a major road (Ashmore Road) and directly connected to a busway. The road surface was in a poorer condition compared to the other roads in this suburb.



Mediterranean Drive is an access road for Benowa High School and medium sized detached family houses. The particles eroded from local soils and vegetation input could be accumulated on the road surface due to its mild slope. Mediterranean Drive connects directly to Benowa Road. De Haviland Avenue and Village High Road are residential access roads. The residences along these roads are detached family houses and townhouses and waterfront properties on canal frontages. The roads are located close to waterways and the Nerang River. Thus, the build-up pollutants at these sites could contain particles eroded from local soils and could have different properties compared to the pollutants from the other sites.



**Figure 4.5: Study sites in Benowa: (a) Strathaird Road (b) Mediterranean Drive (c) De Haviland Avenue and (d) Village High Road**

#### **D. Surfers Paradise**

Surfers Paradise is a heavily developed suburb, with a population density of 3696.1 residents/km<sup>2</sup>, which is the second largest population density in the region (GCCC 2009). Surfers Paradise is located at the downstream end of the Nerang River, close to the beach. Hence, the area consists of sandy soils. The suburb has many high-rise

apartment buildings and a wide beach. These buildings reflect the density of development. The suburb is a commercial area, and the traffic flow in Surfers Paradise is comparatively high due to the visitors to the area. Photos of the selected four road sites are shown in Figure 4.6, and the nature and characteristics of these roads are given in Table 4.4.

**Table 4.4: Description of selected road sites in Surfers Paradise**

<b>Site name</b>	<b>Characteristics</b>	<b>Location coordinates</b>	<b>Texture depth (mm)</b>
Hobgen Street	Close to a primary school, playgrounds; medium size blocks; high traffic flow at specific times; good surface condition	28° 00.802'(S)	0.90
		153° 23.537'(E)	
St Paul's Place	Residential access road; large sized blocks; light traffic; good surface condition	28° 00.702'(S)	0.63
		153° 25.350'(E)	
Via Roma Drive	Main road, wide road section; medium size blocks; good surface condition; well maintained lawns;	28° 00.724'(S)	0.85
		153° 25.413'(E)	
Thornton Street	High rise apartments, grocery stores, beach front resorts; coarse surface condition; fair slope; high traffic flow	28° 00.618'(S)	1.11
		153° 25.883'(E)	

Via Roma Drive, close to the Via Roma Bridge, is at the end of Ashmore Road which is an arterial road in Surfers Paradise with a wide cross section. Thus, the sample collection was carried out with minimum disturbance to local traffic. Both Hobgen Street and St Paul's Place are connected to Via Roma Drive. Hobgen Street is surrounded by a primary school and a playground, and has car parking lots along the road. Hence, it is subjected to a high traffic flow. St Paul's Place is a residential access road. Thornton Street is located close to the Surfers Paradise beach and is directly connected to an arterial road. Since it is a busy road, sampling was carried out in the roadside parking area. It is a fairly flat road with coarse texture, having a

texture depth of 1.11mm. Since all of the roads in Surfers Paradise are located in close vicinity to arterial roads, a significant contribution of atmospheric deposition was expected at these sites.



**Figure 4.6: Study sites in Surfers Paradise: (a) Hobgen Street (b) St Paul's Pl (c) Via Roma Drive and (d) Thornton Street**

#### **4.4 SAMPLE COLLECTION**

##### **4.4.1 BUILD-UP SAMPLE COLLECTION**

Build-up sampling from sixteen road sites was carried out over the period from January 2009 to July 2009, thus covering two different climatic seasons. Build-up pollutant samples were collected from small plot surfaces demarcated in one traffic lane of the selected road sites. Previous researchers have noted that the particle size distribution and build-up pollutant load can vary across the road surface (Sartor et al. 1974; Deletic and Orr 2005). Deletic and Orr (2005) observed high fine particle load and heavy metal concentrations in the middle of the traffic lane. Accordingly, the

plot area was always demarcated in the middle of the traffic lane to obtain representative samples for the study and to maintain consistency in the sampling.

For the laboratory experiments undertaken, the required minimum amount of solids was approximately 19 to 48g. Based on a detailed study of pollutant build-up on road surfaces, Egodawatta and Goonetilleke (2006) noted that the maximum build-up that can be collected from road surfaces is  $6\text{g/m}^2$ . However, they noted that it varied from site to site. Furthermore, they identified that the build-up rate in the initial period after rainfall is in the range of 1 to  $2\text{g/m}^2/\text{day}$ . Therefore, a  $12\text{m}^2$  road surface area was vacuumed to collect the required amount of solids particles. This consisted of four plots, with each plot having an area of  $3\text{m}^2$ . Spacing between each plot was kept constant at each of the study sites. Thus, an approximately 30m long straight road section was reserved for the sample collection at each site. Plot boundaries were demarcated by a  $2\text{m} \times 1.5\text{m}$  frame along the traffic lane, as shown in Figure 4.7.



**Figure 4.7: Collection of build-up sample through dry vacuuming**

The pollutant build-up is a dynamic process which is influenced by various factors including land use, traffic density, road surface characteristics and antecedent dry days (Vaze and Chiew 2002; Deletic and Orr 2005; Hengren et al. 2006; Egodawatta 2007). An antecedent dry period influences the particle size of build-up solids and pollutant concentrations (Vaze and Chiew 2002; Kim et al. 2006;

Egodawatta and Goonetilleke 2006). According to past researchers, the build-up load approaches a near constant value in around seven to nine dry days (Ball et al. 1998; Egodawatta and Goonetilleke 2006). As noted in Section 3.2, in the present study, two different samples were collected from each road with dry days fewer than eight days (Days <8) and more than eight days (Days >8). Bureau of Meteorology observations were continuously monitored to determine the antecedent dry period for the selected sites. Antecedent dry days for each study site and for each sampling episode are tabulated in Table 4.5.

**Table 4.5: Number of antecedent dry days**

Study Site	Number of antecedent dry days	
	First field investigation	Second filed investigation
Clearview Estate	8	17
Benowa	14	8
Nerang	5	9
Surfers Paradise	10	4

#### 4.4.2 DRY AND WET VACUUMING

The vacuum cleaner described in Section 3.2 was used for the build-up sample collection. The vacuum cleaner was thoroughly cleaned with deionised water prior to sample collection. Three litres of deionised water was used as the filtration medium in the vacuum compartment. A sample of deionised water was collected into an acid washed polyethylene bottle as a blank. At the same time, the storage tank of the sprayer was cleaned thoroughly with deionised water and initially filled with 40L of deionised water. The minimum water level in the storage tank of the sprayer was maintained at 30L.

The demarcated first plot was vacuumed twice in a perpendicular direction to ensure the collection of finer particles present on the road surface. Following the dry vacuuming, the plot was dampened by spraying deionised water under a pressure of 2 bar for 3 min. from a standing position, while keeping the nozzle horizontal. This

was to optimise the build-up sample collection. The spraying nozzle was held about 0.5m above the road surface to ensure that the spraying did not disturb the embedded particles on the road surface [Figure 4.8 (a)]. Spraying was done in a sequential manner starting from one edge and progressing to the other parallel to the kerb line, and ensuring that the water did not flow out of the plot boundary. Immediately after spraying, the wet sample was vacuumed using the same vacuum cleaner. Vacuuming was done starting from the same edge and following the same order as the spraying [Figure 4.8 (b)].



**Figure 4.8: Collection of build-up sample through wet vacuuming: (a) Spraying and (b) Wet sample vacuuming**

Build-up sample in the vacuum compartment was then transferred to a clean 25L polyethylene container. Every component of the vacuum cleaner was washed thoroughly with deionised water and added to the container. Similar to the above procedure, the other three plots were vacuumed and collected into clean 25L polyethylene containers. Thus, duplicate build-up samples were collected from each

site. These duplicate build-up samples were used to recover dry solids particles to carry out the experiments on the physical and chemical parameters of solids.

#### **4.4.3 TRANSPORT AND HANDLING OF SAMPLES**

According to the protocol adopted, each build-up sample was labelled with the relevant information relating to the sample: collection date, location and sample number. Deionised water blanks and field water blanks were collected directly into acid washed 1L polyethylene containers at each site. These samples were labelled and preserved for testing as a standard quality control procedure, as specified in Australia / New Zealand Standards, Water Quality - Sampling (AS/NZS 5667.1: 1998). Collected samples were transported and stored in the laboratory on the same day. Sub sampling was done immediately after returning to the laboratory. pH and EC of the samples were measured as soon as possible. The samples were preserved by adding specified preservatives and refrigerated at 4°C, as specified in the US EPA Method 200.8 (US EPA 1994) and Standard Methods for the Examination of Water and Waste Water (APHA 2005).

#### **4.4.4 SURFACE TEXTURE DEPTH**

Texture depth is a descriptive measure of surface roughness and indicates the potential for pollutant build-up. Surface texture depth of each of the road surfaces was measured using the sand patch experiment (FHWA 2005; ASTM 2006). Initially, the road surface was cleaned using a brush to remove all loose material. Then, a known quantity of sand (600-850µm) was spread uniformly in a circular patch over the cleaned surface, using a rubber base. The diameter of the circle was measured along four directions to obtain the mean diameter of the circle. Then the surface texture depth was calculated, using an empirical equation (FHWA 2005; ASTM 2006).

#### **4.4.5 SOIL SAMPLES COLLECTION**

At each suburb, soil samples adjacent to road surfaces were collected to gather background information about the surrounding soil properties in the area, such as

mineralogy and pH. This data was used to interpret the influence of soil inputs to road surface pollutant build-up.

Soil samples were collected from transects parallel to the road at 3 to 4m from the kerb. Surface soils at a depth of 10-15cm were collected using a stainless steel shovel. Two soil samples were collected from each site at approximately 20m apart and mixed together. Collected samples were placed in self-sealing polyethylene bags and transported to the laboratory. The soil was oven dried at 40°C to maintain the consistency, stored in self-sealing polyethylene bags and kept in a cold dark place until further analysis. Soil sample collection and preservation were carried out according to the methods specified in the Australian Laboratory Handbook of Soil and Water Chemical Methods (Rayment and Higginson 1992).

## **4.5 LABORATORY EXPERIMENTS**

The potential influential parameters of pollutant adsorption were identified through a comprehensive literature review and a series of laboratory experiments conducted to measure these parameters. The following sections outline the analytical laboratory methods used.

### **4.5.1 SUB SAMPLING THE BUILD-UP**

The weight of the collected wet build-up samples was measured and, thereby, the collected liquid volume was calculated using the density of water. The collected liquid volume was required to calculate the pollutant load. The build-up samples were divided into three different portions: for total build-up load analysis, for separation into different particle sizes, and to extract dry solids particles for the physico-chemical analysis of solids.

Sub sampling of collected build-up was necessary to extract representative portions of total sample for the laboratory analysis. To obtain a homogeneous sample, the original build-up sample was thoroughly mixed, and 5L of sample was extracted. 3L of this collected sample was divided into three 1L bottles. These three representative



samples were needed, as different preservation methods were used for different chemical parameters. The obtained representative samples were for: aqueous heavy metals analysis; organic carbon analysis; and for pH, EC and particle size distribution analysis. The remaining 2L of sample was used to extract different particle sizes, as described in the following section. For analysis of mineralogy, specific surface area and exchangeable cations, the dry solids particles were separately extracted.

As noted by past researchers, variation in pollutant concentration can be found in different particle size ranges (Herngren et al. 2005; Lau and Stenstorm 2005). Consequently, to understand the pollutant adsorption behaviour of solids, it was important to study the physical and chemical properties of solids for different particle size ranges. In order to partition into different particle size ranges, the remaining 2L of representative build-up sample was passed through selected size ranges of sieves (425 $\mu$ m, 300 $\mu$ m, 150 $\mu$ m and 75 $\mu$ m). Selected particle size ranges were 300-425 $\mu$ m, 150-300 $\mu$ m, 75-150 $\mu$ m, and <75 $\mu$ m. The particles remaining on the 425 $\mu$ m sieve were discarded, and the retained particles on the other three sieves were washed with deionised water and diluted up to 2L using deionised water. This volume was divided into two equal representative portions for heavy metals and organic carbon analysis. One litre of the wet sieved sample passing through the 75 $\mu$ m sieve was passed through 1 $\mu$ m glass fibre filter paper to determine the dissolved fractions of heavy metals and organic carbon content. All samples were stored in acid washed polyethylene containers after adding preservatives appropriate for the analytical method to be used.

Immediately after the sub sampling, pH and EC were measured and all samples were preserved. Appropriate preservatives were selected according to the methods specified in the U.S. Environmental Protection Agency (US EPA 1994) and Standard Methods for the Examination Water and Waste Water (APHA 2005).

For the analysis of mineralogy, specific surface area and exchangeable cation analysis of solids, dry particles were required. As discussed in Section 4.4.1,

duplicate samples were collected from each road. The entire volume of duplicate build-up sample was passed through the sieve set, and the retained materials on the first three sieves were transferred to a desiccated ceramic petri dish. To separate the particles  $<75\mu\text{m}$ , the wet sieved sample passing through the  $75\mu\text{m}$  sieve was allowed to settle for 2 hours in the Imhoff Cone (Sansalone and Kim 2008). This allowed for the settling of the  $>1\mu\text{m}$  particle fraction, while the  $<1\mu\text{m}$  particle fraction was in suspension (Method 2540D, APHA 2005). The suspension water was carefully removed and the settled fraction was then carefully transferred to the desiccated ceramic dish. The samples in the ceramic dishes were allowed to air dry for 4 hours and were then oven dried at  $40^{\circ}\text{C}$  overnight, to separate dry solid particles. Finally, the separated particles were stored in an air-tight container (at  $4^{\circ}\text{C}$  temperature) for further analysis.

#### **4.5.2 LABORATORY TESTING**

The solids particles obtained were analysed for a range of physico-chemical parameters, as listed in Table 4.6. These parameters were chosen based on the understanding of their influence on pollutant adsorption to solids. Appropriate analytical methods and instruments were selected as a result of the findings of a detailed literature review (as described in Section 4.5.3).

**Table 4.6: Parameters and test methods**

Parameter	Method
pH	Method 4500H (APHA 2005), measured with combined pH/EC meter
Electrical conductivity (EC)	Method 2520B (APHA 2005), measured with combine pH/EC meter
Particle size distribution (PSD)	Used Malvern Mastersizer S
Solids	Method 2540 D (APHA 2005)
Total organic carbon (TOC) Dissolved organic carbon (DOC)	Method 5310C (APHA 2005), measured using Shimadzu TOC-5000A Total Organic Carbon analyser
Mineralogy	X-ray diffraction (Brindley and Brown 1984)
Specific surface area(SSA)	Ethylene glycol monoethyl ether (EGME) (Method adopted by Carter et al. 1986)
	Brunauer- Emmett- Teller
Exchangeable cations (Ca <sup>2+</sup> , Na <sup>+</sup> , Mg <sup>2+</sup> , K <sup>+</sup> and Al <sup>3+</sup> )	Method 15A1 (Rayment and Higginson 1992), Ammonium chloride at pH 7
Heavy metals	Method 200.8 (US EPA 1994), measured using Inductively Coupled Plasma – Mass Spectroscopy (ICP-MS)

Laboratory analysis was carried out for build-up samples, wet sieved particulate fractions, filtrates and dry solids samples. Additionally, soil samples were tested for selected parameters. Table 4.7 summarises the parameters analysed in soil samples and the test methods used.

**Table 4.7: Parameters and test methods for soil sample analysis**

<b>Parameter</b>	<b>Method</b>
pH	Method 4A1 (Rayment and Higginson 1992), pH of 1:5 soil/water suspension at 25°C
Electrical Conductivity (EC)	Method 3A1 (Rayment and Higginson 1992), EC of 1:5 soil/water suspension at 25°C
Organic matter (%OM) Soil	Loss on ignition method (Head 1980)
Mineralogy	X-ray diffraction (Brindley and Brown 1984)

Standard quality control procedures specified in the analytical method were followed throughout the laboratory studies to maintain accuracy and reliability. In addition to calibration blanks, field blanks and laboratory fortified sample matrix were tested for quality control purposes. Analytical grade chemicals were used for solution preparation and prepared according to standard procedure. All the glassware used for the analysis was thoroughly rinsed with deionised water and soaked for 24 hours in 50% HCl acid. The glassware was then soaked for 24 hours in 10% HCl acid, rinsed with deionised water and dried before use.

#### **4.5.3 ANALYSIS OF PHYSICAL AND CHEMICAL PARAMETERS**

This section discusses in detail the analytical methods (listed in Table 4.6) that were conducted for the solids and soil samples collected from the study sites. The selection of suitable apparatus and experimental methods is also discussed.

##### **A. pH and EC**

pH and EC are important parameters governing pollutant adsorption to solids. pH is a measure of the acidity or alkalinity of solids, while EC is a measure of the ionic concentration of solids. pH and EC give an important measure of the adsorption and desorption characteristics of solids, as changes in these parameters can increase adsorption or bio-availability of metal elements.

These parameters were determined immediately after return to the laboratory. A combined pH/EC meter was used to measure pH and EC of the total build-up samples. The pH/EC meter was calibrated using buffer solutions of pH and a standard salinity solution prior to use. For the soil samples, pH and EC were determined in 1:5 soil water suspension at room temperature.

## **B. Particle size distribution (PSD)**

The total build-up samples collected from each road surface were analysed for the particle size distribution (PSD) using a Malvern Mastersizer S instrument. This technique has been widely used to determine the PSD in water quality research studies as it is a convenient method to analyse a large number of samples with high accuracy (Herngren 2006; Egodawatta 2007; Goonetilleke et al. 2009).

The instrument consists of a particle dispersion unit connected with two flow cells to an optical measurement unit. This instrument uses a laser beam technique to record the scatter pattern from a flow of the particles. It then uses an analytical procedure to determine the size and distribution of particles. The manufacturer supplied software is used to analyse results obtained from the optical unit. The Malvern Mastersizer S instrument used in the present study consists of a Reverse Fourier lens of 300mm diameter which is capable of measuring 0.05 $\mu\text{m}$  to 900 $\mu\text{m}$  particles. The manufacturer recommends that the accuracy of the measuring process is  $\pm 2\%$  of the volume median diameter (Malvern- Instrument- Ltd 1997).

It is important to note that the PSD measured by the instrument is volume based. The instrument determines the PSD by the laser diffraction patterns, due to the scattering of the particles. Since the laser diffraction technique used in the instrument is sensitive to the volume of the particle, particle diameter is calculated from the measured volume of the particle by equating that volume to an equivalent sphere.

### **C. Solids**

Solids are the primary pollutant analysed in this study, and the concentration of solids in all build-up samples and wet sieved samples were analysed. Test method 2540D (APHA 2005) was used for measuring the solids load.

The solids were analysed by filtering a 150mL representative portion of sample through a 1µm glass fibre filter paper of known weight. The filter paper was oven dried at 1030C – 1050C. The solids load was determined by measuring the weight difference of the initial and final filter papers, which is the weight of residue retained. Filter papers were conditioned prior to analysis by pre washing with de-ionised water and oven drying.

### **D. Organic matter**

#### **Organic matter content in solid particulate fraction**

Organic carbon content in solids is an important parameter for the pollutant adsorption process (Ellis 1976). Past researchers have noted the increase in pollutant adsorption with the increase in organic matter (Roger et al. 1998; Wang et al. 2008).

Organic carbon content was determined using the Shimadzu TOC-VCSH Total Organic Carbon Analyzer. It is capable of detecting an extremely wide range of organic carbon from 4 µg/L to 25,000 mg/L. TOC determination in all build-up samples, wet sieved particle fractions and filtrate samples was carried out according to test method 5310C (APHA 2005). The instrument determined the inorganic carbon (IC), total carbon (TC) and total organic carbon (TOC). The TOC-VCSH unit is a completely automated instrument which uses an automatic sample injection system; it is programmed using manufacturer designed software. The results of the experiments are expressed as a concentration (mg/L). TC and IC standard solutions were prepared daily by diluting stock solutions. The precision of TOC measurement was maintained by using replicate measurement of samples.

## **Organic matter content in soil samples**

Typically, oxidation procedures are used to measure the organic matter content of soil samples. In these procedures, organic carbon in the sample is converted to CO<sub>2</sub> using an oxidant (Rayment and Higginson, 1992). Thus, these methods can only be used to determine the organic carbon (OC) content in the soils. Contents of other elements in organic matter—such as O, H, N, P and S— are not directly measured, but are derived from the organic carbon measurements. Total organic matter is determined by applying a conversion factor of 1.72 x 1.3 to the measured OC content (Baker and Eldershaw 1993; Baldock and Skjemstad 1999). In this study, the organic carbon content of soil was measured using the ‘loss on ignition’ method (Head 1980). A high temperature furnace (800°C) was used for the experiment, and the results were recorded as a percentage of organic matter to the initial weight of the sample.

## **E. Mineralogical analysis**

X-ray diffraction is the most widely used method for the identification of fine-grained soil minerals and for the study of the crystal structure. It is a powerful non-destructive technique for characterising crystalline materials. The mineralogy is determined by the X-ray diffractometer which consists of a high voltage generator, an X-ray source, an X-ray beam collimating system, and a detecting and recording system. In X-ray diffraction, a sample containing particles at all possible orientations is placed in a collimated beam of parallel X-rays. The diffracted beams of various intensities are scanned by the X-ray diffractometer and recorded automatically to produce charts. These charts give the intensity of a diffracted beam as a function of angle  $2\theta$  (where  $\theta$  is the reflection angle). All planes in a crystal produce refraction with an X-ray beam. Thus, each mineral produces a characteristic set of refractions. A complete X-ray diffraction pattern consists of a series of refractions of different values of  $2\theta$  (Sparks 2003).

## **Solid sample preparation**

Sample preparation and pre-treatment is the most important step in X-ray diffraction (XRD) analysis. Sample preparation techniques described by Brindley and Brown

(1984) were used in the present study. As described in Brindley and Brown (1984), samples used for the X-ray diffractometer should be ground to 1-5 $\mu$ m size.

The solids samples were homogenised by manual mixing, and representative solids samples of 300-425 $\mu$ m, 150-300 $\mu$ m, 75-150 $\mu$ m and <75 $\mu$ m size ranges were analysed for X-ray diffraction. Since the presence of humidity in the samples can influence the phase chemistry, solids samples were oven dried at 50°C overnight a day before preparation. A solids sample of 2.7g and 0.3g of aluminium oxide (Al<sub>2</sub>O<sub>3</sub> - corundum) was micronized with 10mL ethanol in the micronizing mill. A 10% weight of corundum was used as the internal standard. In order to disperse the sample and to prevent dust formation inside the jar during the milling, ethanol was used as a liquid medium. The micronizing process reduced the solid sample to close to a fine size of 1 $\mu$ m. The prepared 3g of sample was poured into a glass beaker and the jar was washed three times with ethanol to collect the remaining particles prior to drying overnight at 50°C. Due to the limited amount of solids in a few samples, micronized samples were prepared with 1g of particles with appropriate amounts of corundum at 10% weight. This pre-treatment technique removes the undesirable coatings in particles and promotes the dispersion of particles to improve the diffraction characteristics of the sample.

Two types of sample holders were used for XRD analysis to handle different types of samples: the ring holder (27mm diameter) and the crystal slide. These were selected based on the available sample weight. The ring holder [Figure 4.9 (a)] is the most common holder used in XRD analysis. However, when an adequate quantity of samples (3g) was not available to fill the ring holder, crystal slides [Figure 4.9 (b)] were used (1g). Sample holders were filled with micronized sample and lightly compacted to holder surface level to obtain a smooth and flat surface. This was an important step in the sample holder preparation process, as a tiny difference in loaded sample or compressed sample would have a major effect on phase identification.



The PANalytical X'Pert PRO Multi-purpose diffractometer was used in the present study to analyse the samples. This diffractometer is an automated computer controlled instrument where measurements operate on X'Pert Data Collector software. The X-ray diffraction patterns collected from the instrument facilitate the phase identification and quantitative analysis of the crystalline material. Once the sample analysis was completed, phase identification was carried out using a combination of X'Pert Data Viewer program and X'Pert HighScore Plus software. X'Pert HighScore Plus is a standard database for X-ray powder diffraction patterns, which enables quick phase identification of a variety of crystalline minerals. The quantitative analysis was assisted by the Siroquant V3 program which expresses the composition of the sample in percentage of dry weight of crystalline material. The percentage recoveries of corundum were within acceptable limits.

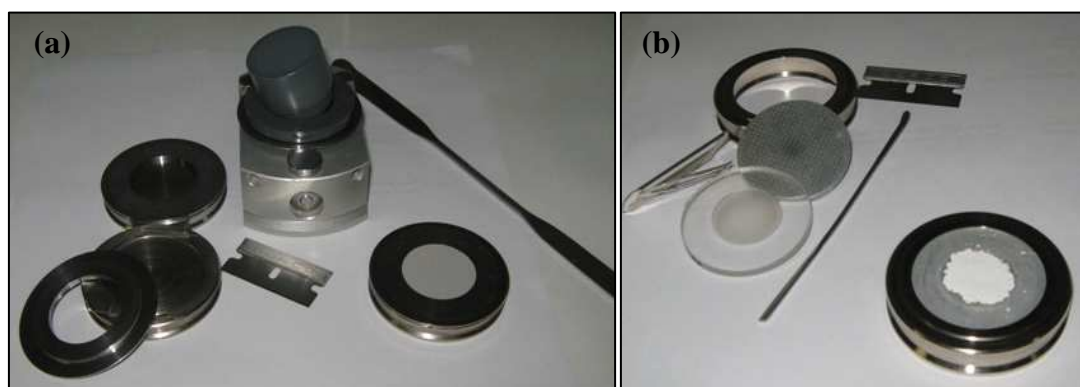


**Figure 4.9: Micronized samples filled in (a) Ring holder (b) Crystal slide**

### **Soil sample preparation**

Sample preparation techniques for soil and clay analysis have been described by Brindley and Brown (1984) and Bish (1993). The collected soil samples were disaggregated using a pestle and mortar, passed through a stainless steel sieve (2.36mm) and dried at 40°C overnight. A series of four sub samples (20-30g) of soil were taken from the bulk soil sample and homogenised by manual mixing. The sample needed to be ground into fine grain before being analysed by XRD, and this can be done either by hand or mechanical grinder. In the present study, grinding was done by a mechanical sample preparation mill which crushes the soil particles to a 1-5µm size. Grinding was done with care as excessive grinding can result in lattice

distortion (Cullity 1978). The sample was then pre-treated (as described above) prior to the X-ray diffraction analysis. The sample analysis was undertaken and results obtained using a method similar to that described for solids samples.

### **Clay analysis**

Clay minerals in build-up solids and soil samples were separately determined on oriented samples. In build-up solids, the analysis was carried out only for particles  $<75\mu\text{m}$  where the clay particles ( $<2\mu\text{m}$ ) were expected to be present. Use of oriented samples (thin films of clay) in XRD enhances the detection of clay minerals present in small quantities. Oriented sample analysis is a qualitative technique which provides only the representative sample peak intensities of each mineral.

Samples for analysis were prepared by suspension of solids particles in 20mL MilliQ-water, with the addition of HCl and  $\text{NH}_4\text{OH}$  to regulate the pH of the suspension. Initially, the pre-treated sample was well mixed by shaking for 30s. Then, to disaggregate the sample slurry, it was sonicated by using an ultrasonic probe (Branson Sonic Power Company). It was sonicated for approximately 45s by immersing the probe in the clay suspension sample and leaving it to settle for 5min. Within this time period, particles  $>5\mu\text{m}$  are settled, whilst  $<5\mu\text{m}$  particles suspend in the top 5mm of the slurry. Approximately 1.5mL of sample slurry was then removed using a Pasteur pipette. Afterwards, the slurry was applied to the silicon wafer plate ( $15\text{mm} \times 25\text{mm} \times 0.6\text{mm}$ ) and allowed to air dry at room temperature. Finally, the XRD patterns were obtained using the PANalytical X'Pert PRO XRD instrument. Measured data was collected using X'Pert Data Collector software, and clay identification was assisted by the TRACER program.

### **F. Specific surface area (SSA)**

Several methods are available to measure the specific surface area (SSA) of solids (Cerato and Lutenege 2002; Yukselen and Kaya 2006). The two most common methods used are:

- 1) Brunauer- Emmett- Teller (BET) N<sub>2</sub> adsorption - This method uses N<sub>2</sub> adsorption on the surface at low temperatures (at series of gas pressures). It determines the external surface area of particles.
- 2) The measurement of the total surface area by the adsorption of polar liquids such as ethylene glycol monoethyl ether (EGME), ethylene glycol (EG), methylene blue (MB), p-nitrophenol and polyvinylalcohol.

Numerous researchers have used the above two methods for the determination of SSA (Mulla et al. 1985; Tiller and Smith 1990; Sansalone et al. 1997; Cerato and Lutenegegerl 2002; Santamarina and Klein 2002; Yukselen and Kaya 2006). Both methods were initially employed in the present study to evaluate the most suitable technique for the SSA determination. The four particle size ranges of solids were analysed for SSA. Quality control was maintained through replicate measurements of granular activated carbon (GAC, 100 mesh) (Sansalone et al. 1998). Carbon activated at high temperature has a highly developed pore structure and possesses high SSA (Li et al. 2005).

### **Ethylene Glycol Monoethyl Ether (EGME) surface area**

Use of polar liquids such as ethylene glycol monoethyl ether (EGME) and ethylene glycol (EG) in total surface area measurement is common. However, EGME method appears to be far more common and has been used to determine the SSA by a number of investigators, for a wide range of soils (Carter et al. 1965; Heliman et al. 1965; Shaw 1992; Quirk et al. 1999; Sparks 2003; Wang et al. 2008) and for stormwater solids (Sansalone et al. 1998). It is a convenient and rapid method to determine SSA. The EGME SSA method adapted from Carter et al. (1986) was used in this study to measure SSA. Instrumentation used in this experiment included a vacuum desiccator to maintain high vacuum pressure, and a pressure pump and pressure control unit to maintain a constant pressure (635mmHg) inside the vacuum desiccator.

In the case of polar liquids, EGME forms monolayer coverage of the solid surface and interlayer spacing due to the high binding energy, and thereby helps to estimate the total surface area. One EGME molecule has a cross section coverage of  $0.52\text{nm}^2$ , and a molecular weight of  $90.12\text{g/mol}$ . Therefore, an EGME monolayer of  $1\text{m}^2$  requires  $0.000286\text{g}$  of EGME ( $\text{CH}_3\text{CH}_2\text{OCH}_2\text{CH}_2\text{OH}$ ). For quality control, a GAC sample was tested at each test run. GAC was exposed to the same conditions as the solids samples, including oven drying and equipment used. Consistent SSA values were obtained for all GAC test runs ( $1100\pm 11.9\text{m}^2/\text{g}$ ).

### **BET surface area**

The BET equation has been widely used by many researchers to determine SSA using nitrogen, ethane, water, ammonia and other gasses as adsorbates for soils and minerals. BET theory applies to the physical adsorption of gas molecules on a solid surface and serves as the basis for the analysis technique in the measurement of SSA of a material. In the nitrogen gas method,  $\text{N}_2$  is attracted to the particle surface by weak Van der Waals forces and forms multiple layers (Brunauer et al. 1938; Arnepalli et al. 2008). The BET- $\text{N}_2$  adsorption method has been widely used by researchers to determine the SSA (Elliott et al. 1986; Wang et al. 2008). The primary drawback of the BET method, as discussed by these researchers, is the weak capacity of  $\text{N}_2$  to adsorb to the interlayer surfaces of soils in a dry state (Cerato and Lutenecker 2002; Santamarina et al. 2002). Hence, the method only provides the external surface area of the particles.

The BET  $\text{N}_2$  gas adsorption experiment was carried out using the TriStar analyzer. The TriStar 3000 system consists of two units, the TriStar analyzer and a SmartPrep. The TriStar 3000 is an automated gas adsorption instrument with three ports which enables the simultaneous analysis of three samples. The SmartPrep unit is a flowing-gas, degassing unit for preparing samples. It contains six sample ports, each of which can be controlled independently. Additionally, the instrument has glass sample tubes ( $4.8608\text{ cm}^3$  volume tube with  $3/8$  inch diameter neck).

It is important to ensure that the samples for BET analysis are free of moisture. For this purpose, the samples were poured into glass tubes and degassed under  $N_2$  gas flow at  $110^\circ C$ , for a period of 24 hour before analysis. This process removes adsorbed contaminants from the surface and pores of the sample and, in turn, reduces the errors incurred due to the rise in vapour pressure while adsorption of  $N_2$  takes place. The degassing temperature was maintained at  $110^\circ C$  throughout the study to avoid mineralogical alteration (Zerwer and Santamarina 1994). Figure 4.10 (a) shows the degassing of samples in the SmartPrep.

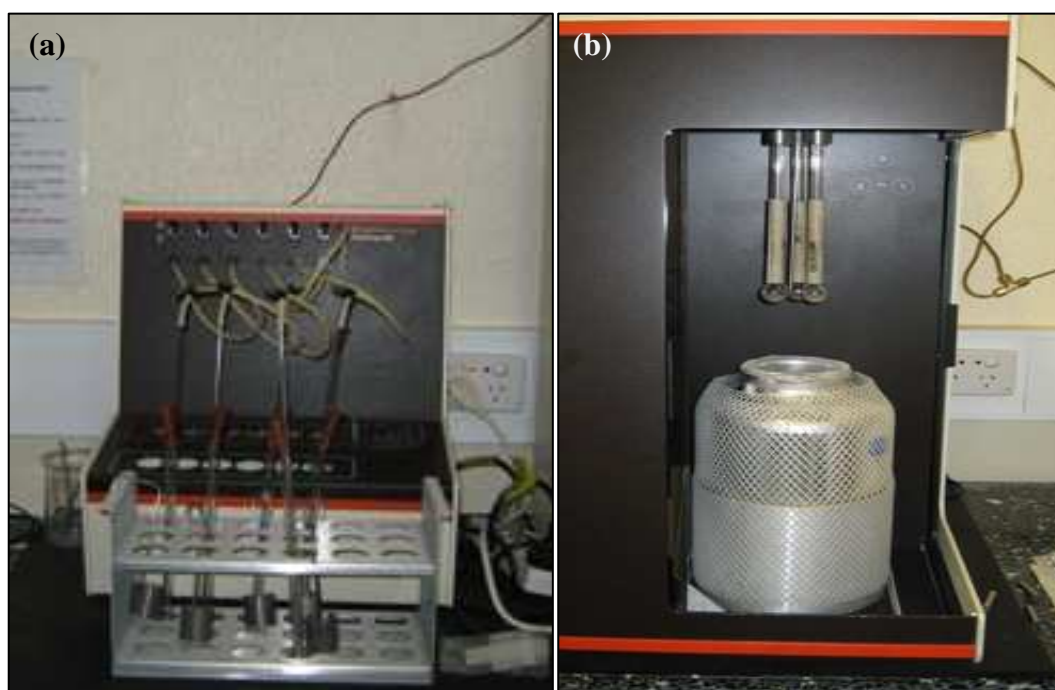


**Figure 4.10: Solid sample analysis using BET instrument: (a) SmartPrep and (b) TriStar analyzer**

Once the samples were dried and cooled, they were mounted on the TriStar analyzer on top of the Liquid  $N_2$  flask to maintain a low temperature (at  $77K$ ) while samples were being analysed. Figure 4.10 (b) shows three samples mounted on the TriStar analyzer. During the process, the samples were exposed to  $N_2$  at different relative pressures ( $P$ ) and saturation vapour pressures ( $P_0$ ). The TriStar computer program determined the surface area of the samples using adsorption isotherms, by relating the surface area to the volume of gas adsorbed on the sample as a monolayer coverage (Langmuir equation). More details on these instruments can be found in

instrument manuals (TriStar 3000 Operator's Manual, 2001). In the BET-N<sub>2</sub> gas method, for a batch of sixteen solids, one GAC sample was tested due to the limitation in the number of samples that can be tested at a time. Reported SSA of GAC was 1090±3.5m<sup>2</sup>/g.

#### **G. Exchangeable cations (Ca<sup>2+</sup>, Al<sup>3+</sup>, Mg<sup>2+</sup>, Na<sup>+</sup> and K<sup>+</sup>)**

The behavior of heavy metals adsorption to solids is governed by the surface charge of the particle. Charges develop in many components of the soils, particularly in clay minerals, organic matter and metal oxides. The measurement of surface charge estimates the ability of solids to retain ions on their surface. The actual exchange capacities are best estimated by the summation of exchangeable cations. This takes into account the exchangeable form of these cations in solids (Tucker 1983). Therefore, Ca, Al, Mg, Na and K cation concentrations were determined in the collected four particle sizes of solid samples. The exchangeable cations were determined by displacing them with a salt solution and analysing them in the solution. Different salts can be used to determine exchangeable cations. For natural soils, ammonium is usually used as this is only present as a minor fraction (if at all) in natural soils (Tucker 1983).

Inductively Coupled Plasma-Optical Emission Spectrometry (ICP-OES) or ICP-MS can be used to determine cations. ICP-OES is used where concentrations are relatively higher, whereas ICP-MS is used where concentrations are relatively lower. Since solids or soils have high exchangeable cation concentration, the use of an ICP-OES is recommended to determine exchangeable cations (US EPA Method 200.7, US EPA). ICP-OES uses Argon gas plasma to detect cations. It consists of a nebulizer to inject the sample. Once the sample is passed through the nebulizer, it atomises the sample and is directly introduced inside the plasma. The sample is broken down into charged ions while passing through the plasma, and the intensity of this ion emission is detected by the spectrometer and results are processed through a computer.

The instrument determines the dissolved cations in aqueous samples. Therefore, to analyse the exchangeable cations in dry solids samples, the cations need to be extracted from the particle. The extraction was carried out according to Method 15A1 in Rayment and Higginson (1992), using 1M ammonium chloride ( $\text{NH}_4\text{Cl}$ ) at pH 7.0 and without pretreatment for soluble salts. Solids particles were mechanically shaken to extract the exchangeable cations. Once the extraction was complete, the residual solution was analysed using an ICP-OES.

The elements analysed included Ca, Al, Mg, Na and K. Stock solutions of these metal elements were prepared in the same matrix, using corresponding metal chlorides at 1000mg/L. Different concentrations of standard solutions (multi-element) were prepared by diluting the stock solutions to calibrate the instrument. Individual element concentrations (mg/L) for the four particle size ranges of solids particles were measured and reported as positive charge per unit mass (meq(+)/100g). Effective cation exchange capacity was calculated by the summation of  $\text{Ca}^{2+}$ ,  $\text{Al}^{3+}$ ,  $\text{Mg}^{2+}$ ,  $\text{Na}^+$  and  $\text{K}^+$ , and presented in meq (+)/100g.

Quality control of the analysis was performed using calibrated standards (Rabb and Olesik 2008). Calibration standards were used with every batch of 10 samples to monitor instrument drift and the accuracy of results. Ten replicates per concentration of standard solutions were undertaken for each cation to determine the detection limit. Accuracy of the calibration curve was assessed against the known concentration of standard solutions.

## **H. Heavy metals**

Nine heavy metal species that originate primarily from anthropogenic activities such as vehicular traffic were selected for the study. These included: Iron (Fe), Aluminum (Al), Manganese (Mn), Copper (Cu), Lead (Pb), Zinc (Zn), Cadmium (Cd) and Chromium (Cr). These metal elements have been identified mostly in particulate form among urban road surface pollutants (Vinklander 1998; Deletic and Orr 2005; Dean et al. 2005; Herngren et al. 2006).

Metals adsorbed to solids particles are present in different binding sites. In order of mobility, the heavy metals in these binding sites are: exchangeable metals carbonate bound, Fe and Mn oxide bound, organic matter bound and residual (Tessier et al. 1979; Harrison et al. 1981). Typically, metals originating from anthropogenic activities tend to be adsorbed as per the first four mechanisms and metals in the residual fraction naturally occur within the crystal structure of silicate minerals (Ratusny et al. 2009). In this study, the adsorbed heavy metal elements (the total recoverable) were extracted using the acid extraction procedures explained in US EPA Method 200.8 (US EPA 1994) and Method 3030E (APHA 2005). Additionally, precipitated heavy metals (the easily soluble fraction) can be detected by examining the filtrate of the wet sieved fraction. The acid preserved total build-up, wet sieved particulate sizes and filtrates were analysed for the nine heavy metal elements. Sample preparation and heavy metals analyses were carried out according to US EPA Method 200.8 (US EPA 1994).

The total recoverable metal extraction from particulate matter in build-up and wet sieved particulate sizes was undertaken using nitric acid ( $\text{HNO}_3$ ) digestion according to US EPA Method 200.8 (US EPA 1994). In this regard, the SC154 (Environmental Express) hot block digester was used. Use of the hot block for digestion is recommended in both US EPA Method 200.8 (US EPA 1994) and Method 3030E (APHA 2005) for metal extraction. It is designed to digest samples using disposable polyethylene vials (SC475) which prevent silicon contamination in samples. The hot block consists of 54 heater wells to fit 50mL polyethylene vials. The temperature was initially set to reach the required temperature, and it ensured gentle heating of the samples whilst maintaining even temperature across the block while the digestion was in progress. Digested samples were then filtered to remove particulate matter, the volume made up to 50mL, and the samples refrigerated until analysis. For the analysis of dissolved heavy metals, the acidified portion of the filtrate was analysed directly.

The Inductively Couple Plasma – Mass spectrometer (ICP-MS), which is capable of detecting trace levels, was used for the multi-element metal concentration determination. The sample solutions were nebulized into Argon gas plasma and



subjected to ionization. The ions extracted from the plasma were passed through the mass spectrometer and separately detected by an electron multiplier detector on the basis of their mass-to-charge ratio.

The calibration of the ICP-MS instrument was done using high purity multi-element Accu Standards (ICP Multi-Element Standard QCS-03-1). Additionally, a number of quality control measures such as calibration blanks, internal standards, laboratory reagent blanks (LRB), laboratory fortified blanks (LFB) and field reagent blanks were used in the analysis. Single element metal solutions of Scandium, Bismuth, Indium, Terbium and Yttrium of 100g/mL (2% HNO<sub>3</sub>) prepared by AccuStandard were used to prepare the internal standards. The traceable certified reference material was prepared from multi-element standard solution from TraceCERT (Sigma-Aldrich). After each batch of 10 samples, a blank was analysed to ensure that no residue was carried over from the previous samples. Precision and accuracy of the heavy metals analysis and the digestion procedure were monitored using the LFB prepared by adding an aliquot of certified reference material; the percentage recovery was in the range of 85-115%.

#### **4.6 ADSORPTION/DESORPTION EXPERIMENT DESIGN**

The analysis of the physical and chemical parameters of solids and heavy metal concentrations (Chapters 5 and 6) allowed the identification of the probable metal adsorption mechanisms of solids. However, to confirm these preliminary conclusions, a batch adsorption experiment was performed. The experimental method was designed based on batch adsorption studies discussed in previous research literature (Elliott et al. 1986; Young et al. 1987; Polcaro et al. 2003). For this experiment, road deposited solids particles, which had been separated using wet sieving, were used. These solids particles already contained heavy metals and the metal concentrations (background metal concentration, mg/L) were known. The criteria considered for the selection of the primary constituents are discussed below, and a detailed discussion of the batch experiment is provided in Chapter 7.

### **A. Adsorbent (solids samples)**

The physical and chemical characteristics of the solids are the fundamental parameters which influence heavy metals adsorption. Therefore, these were considered as the primary criteria in the sample selection. As particle size has a significant effect on these parameters, the four different particle size ranges were separately subjected to the batch adsorption experiment. The selection of solids samples was carried out based on the preliminary interpretation of the physical and chemical properties of solids (as discussed in Chapter 5).

Since the purpose of the experiment was to validate the conclusions derived regarding the metal adsorption process of solids, only a selected number of samples were subjected to the experiment. It is important to note that the physico-chemical characteristics of solids vary widely due to the site specific nature of sampling. From each particle size, two samples were selected to represent those highly (H) favorable for metal adsorption and those less (L) favorable for metal adsorption sites. This was achieved by using an appropriate PROMETHEE model to select both the highly favourable and least favourable properties of solids for metal adsorption. PROMETHEE II ranking was then employed to select suitable samples. Consequently, two sets of samples from each particle size were selected to represent the physical and chemical variability of data.

### **B. Adsorbate (Metal elements)**

Among the nine metal species investigated, it was hypothesised that Al, Fe and Mn could mostly originate from soil sources as they are present as metal oxides in soil particles (Pierson and Brachaczek 1983; Polcaro et al. 2003). Zn, Cu, Pb, Ni, Cd and Cr were considered as the heavy metal elements which originate primarily from anthropogenic sources such as tyre and pavement wear and automobile emissions (Wang et al. 1998; Walker et al. 1999; Herngren 2005). Although potential occurrences of these metal elements are particularly high in the urban environment, a selected number of metal species were identified for the batch adsorption experiment based on the following selection criteria:

- Metal elements that show different adsorption behaviour (This would enable an in-depth understanding of the adsorption-desorption behaviour of solids)
- Metal elements that have high toxicity and high impact on the ecosystem health of urban receiving waters.

The metal elements selected according to these criteria are discussed in Section 7.2.

### **C. Concentrations of adsorbate (Metal ion concentrations)**

To reach equilibrium state there should be an excess concentration of metal ions in solution. Therefore, the selection of metal ion concentration for the batch adsorption experiments was always greater than the metal concentrations observed in build-up samples. Additionally, metal concentrations in stormwater runoff were also taken into account before selecting suitable concentrations. The maximum Zn, Cu, Pb, Cd and Cr concentrations observed by Herngren (2005) in wash-off samples were 3.6mg/L, 0.4mg/L, 0.03mg/L, 0.3mg/L and 0.02mg/L, respectively. The majority of metal concentrations in solids and stormwater runoff are <10mg/L. The concentration of each metal element was kept equal to maintain consistency with a fixed adsorbent weight. Therefore 0.1mM concentration was selected to achieve maximum adsorption capacity of road deposited solids (Polcaro et al. 2003).

#### **4.6.1 EQUILIBRIUM TIME FOR HEAVY METAL ADSORPTION**

To determine the time necessary to reach equilibrium state between metal solution and the solids (adsorbent), an equilibrium time batch experiment (Kinetic study) was carried out. The single metal element batch experiment was conducted using solids particles <425µm size. The research literature recommends an equilibrium time of 24 hours for soil (Elliott et al. 1986; Polcaro et al. 2003; Covelo et al. 2007b). Therefore, the equilibrium batch study was carried out over 3 days to identify the equilibrium time for road deposited solids.

Metal solutions were equilibrated with solids in 1L volumetric flasks. For each flask, a homogeneous mixture of 10g solids containing 2.5g from each particle size range

was added, followed by the addition of 0.1mmol/L metal solutions. pH was maintained at 6.5. The sample was stirred using a magnetic stirrer to obtain a homogeneous mixture. The experiment was carried out under controlled temperature (constant room temperature at  $20\pm 0.1^{\circ}\text{C}$ ). The flasks were covered with polyethylene wrap, to avoid contamination and to prevent evaporation of the solution. Samples were taken out at 2 hourly intervals in the initial 6 hours, then at 6 hourly intervals up to 1 ½ days and, finally, at 12 hourly intervals until the end of the 3 days. One at a time, 5mL of sample of each metal solution was collected and diluted with deionised water to 15mL (Hofstede 1994; Plassard et al. 2000). The samples were filtered using a  $0.45\mu\text{m}$  filter, and acidified samples were analysed according to US EPA Method 200.8 (US EPA 1994), using an ICP-MS. Based on the results, it was decided to maintain a 24 hour equilibrium time period in the metal adsorption experiment (See Section 7.2.4).

#### **4.6.2 ADSORPTION/DESORPTION EXPERIMENT**

##### **A. Adsorption experiment**

The equilibrium state batch adsorption study was carried out for single metal adsorption. A homogeneous 1g of solids sample (oven dried at  $50^{\circ}\text{C}$  for 24 hours) from each particle size was stirred in a polyethylene test tube for 24 hours, with 40mL of metal solutions and 0.1M  $\text{NaNO}_3$  as the supporting electrolyte to keep the ionic strength constant in the solution. The addition of  $\text{NaNO}_3$  avoided the colloid mobilization in the solution (Plassard et al. 2000). The metal solutions were prepared by dissolving metal nitrate in deionised water. Nitrates were used since these ions have no affinity with metals (Sillen 1971). The initial pH value of the suspension was taken after 30s and adjusted to pH 6.5, using dilute nitric acid ( $\text{HNO}_3$ ) and sodium hydroxide ( $\text{NaOH}$ ) to avoid metal precipitation at higher pH solutions. The pH value of the final equilibrium sample was determined before suspension of the sample and filtered through a  $0.45\mu\text{m}$  glass membrane filter. The filtrate was collected in a polyethylene test tube, acidified with  $\text{HNO}_3$ , and analysed according to US EPA Method 200.8 (US EPA 1994) for soluble metal ion concentration ( $C_i$ ) using ICP-MS. Control samples were simultaneously run to determine the migration of heavy metals from the solids surface to the solution during the stirring process (solids with deionised water with appropriate pH adjustment). Each analysis was repeated and

blanks were also tested at the same time in order to assess any possible errors (Young et al. 1987).

The amount of metal ions adsorbed (adsorption capacity) at equilibrium condition was obtained using the equation given below. Background metal load ( $q_b$ , mg/g) in the samples had been measured previously by using nitric acid digestion (US EPA Method 200.8, US EPA 1994).

$$q_T = q_b + \frac{V}{w} [C_o - C_i] \quad \text{Equation 7}$$

Where  $q_T$  - equilibrium adsorption capacity (mg/g);  $C_o$  - initial metal concentration (mg/L);  $C_i$  - equilibrium metal concentration (mg/L);  $V$  - volume (L); and  $w$  - weight of the adsorbent (g).

## **B. Desorption experiment (metal extraction)**

Extraction of metals from solids particles was carried out to study the ion-exchangeable metal adsorption process. To extract the metal solution for the adsorption experiment, samples were centrifuged for 15min at 1500rpm and the suspension was removed (Young et al. 1987). The solids were washed with ethanol to remove the metal solution trapped, and oven dried at 40°C to evaporate ethanol (Polcaro et al. 2003; So et al. 2006). The dried solids were treated with 40mL of 0.5M  $Mg(NO_3)_2$  and stirred until a new equilibrium state was achieved between  $Mg^{2+}$  ions and the heavy metal elements (24 hour), after adjusting the pH by the addition of NaOH or  $HNO_3$ . The final equilibrium pH value was determined to ensure the pH was kept constant over the reaction period. Equilibrium solution was filtered through a 0.45 $\mu$ m filter and analysed for the desorbed metal ion concentration ( $C_{ex}$  mg/L), using ICP-MS according to US EPA Method 200.8 (US EPA 1994). Final solids weight ( $w$ ) was also measured to determine if there were any losses during the experiment. The amount of heavy metals adsorbed by ion exchange to solids samples was determined by the amount of heavy metals released during the desorption experiment ( $q_{ex}$ ), using the following equation:

$$q_{ex} = \frac{C_{ex}}{w} \quad \text{Equation 8}$$

Where  $q_{ex}$  – heavy metals adsorbed by ion exchange (mg/g);  $C_{ex}$  - desorbed metal ion concentration (mg/L); and  $w$  - weight of the adsorbent after desorption experiment (g).

The metal concentrations (mg/g) determined from the above was converted to mmol/kg by dividing by the molecular weight of the relevant metal element.

### **C. Quality assurance**

For quality control purposes, in each batch adsorption/desorption experiment, control solids samples, blank metal solutions, laboratory fortified blanks (LFB) and laboratory reagent blanks (LRB) were subjected to the same procedures. The possible error sources in the experiment include heavy metals being adsorbed by the container wall, degradation with time and metals retained by the filters.

The ICP MS analysis was carried out according to US EPA Method 200.8 (US EPA 1994). Quality control of ICP MS analysis was monitored using internal standards, certified reference material and quality control blanks. Additionally, after each batch of 10 samples, a blank was analysed to ensure that no residue was carried over from the previous sample. All samples for metal analysis were kept at constant volume (35mL).

## **4.7 SUMMARY**

Field investigations were undertaken in the Gold Coast region. For these investigations, pollutant build-up samples were collected from sixteen road surfaces from four different suburbs along the Nerang River. In each suburb, soil samples adjacent to road surfaces were also collected. Build-up samples were collected using a dry and wet vacuuming system and were fractioned into four different particle size ranges.

Laboratory analysis was carried out for total build-up samples, particulate samples, dissolved samples and dry solids particles. Soil samples were analysed for selected physical and chemical parameters in order to compare build-up solids properties. The experimental methods and equipment used in the laboratory experiments have been described in detail, and the quality assurance and quality control procedures adopted have been outlined in this chapter.

A batch adsorption/desorption experiments was designed to validate the conclusions drawn from the detailed investigations undertaken regarding the adsorption of heavy metals to solids. The appropriate criteria considered in the selection of adsorbent (solids), adsorbate (heavy metals) and heavy metal concentrations have also been detailed in this chapter.





# Chapter 5: Physical and Chemical Characteristics of Solids

---

## 5.1 BACKGROUND

Physical and chemical characteristics of road deposited solids are primary factors that influence heavy metal adsorption to particulates (Sansalone et al. 1998; Bradl 2004). Therefore, understanding particulate characteristics is important for investigating the adsorption of heavy metals. The build-up samples collected from the road surfaces were tested for solids load, particle size distribution, total organic carbon, specific surface area, cation exchange capacity and mineralogy (as described in Section 4.4). Table A.1 in Appendix A gives the test results for the physico-chemical parameters measured in relation to the collected build-up samples. Since road deposited solids are very complex heterogeneous media, an understanding of the primary composition of solids and pollutant sources is also important in the characterisation of the solids properties.

This chapter focuses on defining the physical and chemical characteristics of particles that influence the pollution adsorption ability of solids particles. In this regard, the general variability of physical and chemical characteristics of build-up samples was initially investigated. This was followed by a comparison of the mineralogy of solids and surrounding soils in order to characterise the solids composition. Finally, fundamental co-relationships of the physical and chemical characteristics in each particle size range of solids were separately investigated.

## 5.2 BUILD-UP SOLIDS LOAD

The build-up solids load collected for each road surface in the four suburbs for two different sampling events and respective dry days is given in Table 5.1. The road surface texture, which is a primary indicator of surface condition, was measured. Road surfaces in the Nerang industrial land uses are relatively coarse compared to the other sites. It is hypothesised that the surface texture of these roads has been

influenced by heavy vehicle movement. All road surfaces in Nerang reported the highest solid loads compared to the other suburbs. For example, on average, build-up loads are 50% higher than on the Surfers Paradise road surfaces and 70% higher than

**Table 5.1: Average solid load in build-up samples in each suburb**

Suburb	Street name	Land use	Surfaces texture depth (mm)	Solids load (g/m <sup>2</sup> )	Dry days	Last rainfall event (mm)
Clearview Estate	Merloo Drive	Residential	0.76	0.36	8	1.4
				1.31	17	42.6
	Yarrimbah Drive	Residential	0.84	3.01	8	1.4
				0.66	17	42.6
	Winchester Drive	Residential	0.87	4.08	8	1.4
				1.50	17	42.6
Carine Court	Residential	0.92	2.65	8	1.4	
			3.00	17	42.6	
Nerang	Stevens Street	Industrial	1.10	6.65	5	3.8
				11.3	9	1.2
	Lawrence Drive	Industrial	1.06	5.20	5	3.8
				1.90	9	1.2
	Hilldon Court	Industrial	0.93	10.5	5	3.8
				8.11	9	1.2
Patrick Road	Industrial	1.14	7.83	5	3.8	
			28.8	9	1.2	
Benowa	Strathaird Road	Industrial	0.80	1.72	8	9
				5.89	14	1.4
	Mediterranean Drive	Commercial	0.82	6.61	8	9
				0.70	14	1.4
	De Haviland Avenue	Residential	0.90	2.13	8	9
				2.49	14	1.4
Village High Road	Residential	0.91	3.04	8	9	
			1.31	14	1.4	
Surfers Paradise	Hobgen Street	Commercial	0.90	2.35	4	2.2
				1.28	10	42.6
	St Paul's Place	Commercial	0.63	2.75	4	2.2
				2.65	10	42.6
	Via Roma Drive	Commercial	0.85	9.06	4	2.2
				4.00	10	42.6
Thornton Street	Commercial	1.11	7.74	4	2.2	
			5.42	10	42.6	

those at the other sites. Nevertheless, Nerang had the shortest antecedent dry period of all sites. Therefore, it is hypothesised that the road surface texture would have influenced the build-up solids load on the road surfaces.

Herngren et al. (2005) and Egodawatta (2007) also found that relatively coarse road surfaces accumulate higher solids loads. Other than Nerang, Surfers Paradise, which is a commercial area, also indicated a significantly high pollutant load. This is attributed to high traffic activity in the commercial land use (Bian and Zhu 2008). Additionally, the relatively coarse texture of the Surfers Paradise roads would enhance the retention of particulates and the generation of tyre wear particles. The lowest pollutant load was recorded at Clearview Estate which is a residential land use. Therefore, it can be concluded that land use characteristics significantly influence pollutant loads on urban road surfaces.

Furthermore, a significant variation in build-up solids loads can be observed within the same land use for the same antecedent dry period, even though these road surfaces were subjected to similar anthropogenic activities. Thus, the variation in build-up load is primarily attributed to differences in traffic characteristics. Therefore, it can be concluded that the nature of anthropogenic activities, traffic density, road surface condition and antecedent dry period would considerably influence build-up solids loads on urban road surfaces (Ball et al. 1998; Vaze and Chiew 2002; Egodawatta 2007).

A majority of the study sites showed a high build-up solids load on road surfaces with low antecedent dry period. The antecedent dry period was defined as 'the time period since the last rain event without considering the rainfall intensity'. At high antecedent dry period, some of these roads show relatively low solids load. For example, Clearview Estate had the highest antecedent dry period (17 days); however, a lower amount of solids was collected compared to the eight day antecedent dry period at the same site. Nerang sites, on the other hand, showed exceptional behaviour with high solids load with the increase in dry days. Further investigations revealed that the rainfall event prior to the shorter dry period was less significant in

both intensity and depth. Small events often fail to wash -off a significant portion of the build-up load and the subsequent build-up adds to a significant amount of pre-existing load (Egodawatta et al. 2007). Thus, the presence of pre-existing solids on the road surfaces would have influenced the collected build-up load (Egodawatta 2007).

### **5.3 INVESTIGATION OF PHYSICAL AND CHEMICAL CHARACTERISTICS**

According to the discussion in Section 5.2, there are significant differences in the build-up load in different suburbs. Similarly, differences can extend to the physical and chemical characteristics of the build-up load in different suburbs. The physical and chemical parameters considered for the analysis were particle size distribution, total organic carbon, specific surface area, cation exchange capacity and mineralogy. Individual characteristics of these parameters were separately investigated with respect to the particle size of solids.

#### **5.3.1 PARTICLE SIZE DISTRIBUTION**

The particle size distribution of solids is an important parameter due to the association of other pollutants with particulates (Lau and Stenstrom 2005). For this study, where solids were considered as the primary pollutant, the particle sizes of build-up solids were important. Particle size was analysed as volumetric percentages for each build-up sample. It is understood that particle size distribution of solids in build-up can vary with factors such as type of land use, traffic density, antecedent dry period and road surface conditions (Li et al. 2005; Egodawatta and Goonetilleke 2006; Herngren et al. 2006; Bian and Zhu 2008).

As evident in Figure 5.1, in all of the sites, more than 50% of particles were finer than 75 $\mu$ m. Similar observations have been noted by Herngren et al. (2006) for commercial and residential sites. Particles below 150 $\mu$ m are considered to be a critical size range which defines the characteristics of stormwater quality (Andral et al. 1999; Herngren et al. 2006; Goonetilleke et al. 2009; Miguntanna 2009a). On average, 70% of the particles in build-up samples collected in this study were less

than  $150\mu\text{m}$ . These results suggest that fine particles account for the majority of road deposited solids at the study sites. Such a composition of particulate pollutants confirms the findings of Walker and Wong (1999) who noted that 70% of the particles found on Australian road surfaces are less than  $125\mu\text{m}$ . This observed characteristic is also in close agreement with the findings of Hengren et al. (2006), Egodawatta (2007) and Miguntanna (2009b) who carried out similar build-up investigations in the same region.

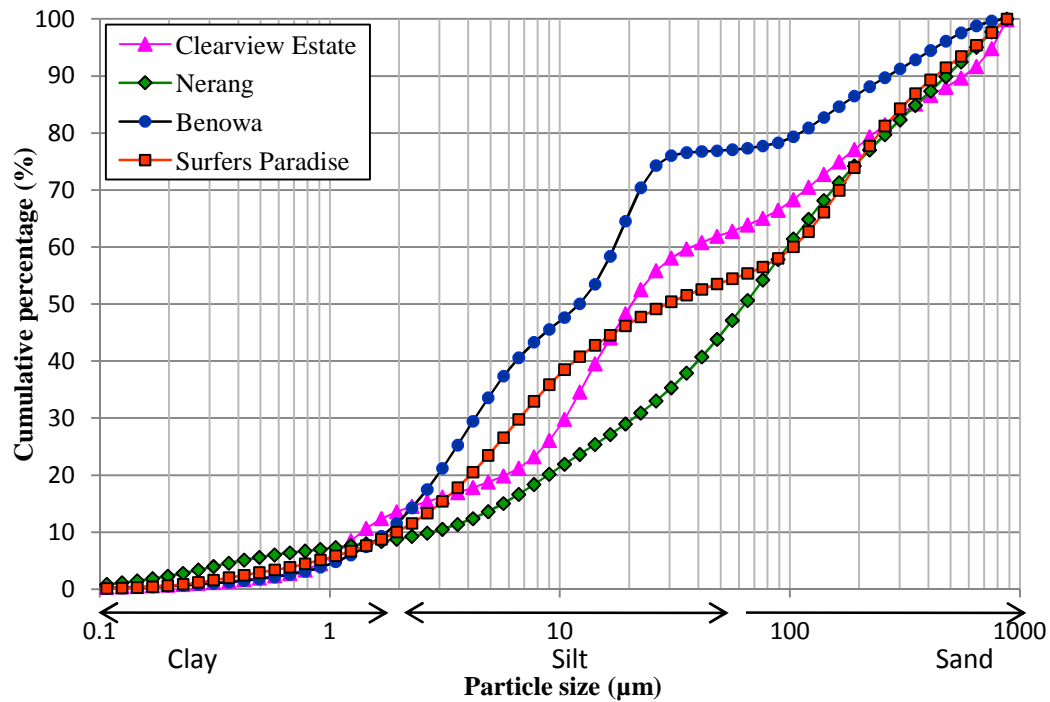


**Figure 5.1: Cumulative particle size distribution of solids build-up in each suburb**

Furthermore, the particle size distribution curves obtained for the four different suburbs indicate different characteristics. For example, the distribution for residential road surfaces at Clearview Estate and Benowa were relatively finer compared to the other two suburbs. Additionally, a higher percentage of large particle size content was evident in industrial road surfaces at Nerang. The distribution of fine particles in Nerang and Surfers Paradise is comparatively low compared to the other sites. Road surfaces in these suburbs were located in industrial and commercial areas, respectively. Due to high vehicle movements on these road surfaces, the accumulated finer particles would be easily resuspended by traffic induced wind (De Miguel et al. 1997; Lisiewicz et al. 2000). Even though the Nerang industrial road surfaces are

subjected to frequent heavy vehicle movement, the coarse road texture would have prevented the disintegration of soft particles such as organic matter trapped in surface voids. In addition, at Surfers Paradise, meteorological conditions such as wind would have removed some of the fine particles, and the relatively rough texture of the surface would have accumulated a large quantity of coarse particles ( $>150\mu\text{m}$ ). Benowa shows a relatively higher amount of finer particles ( $<150\mu\text{m}$ ) than other areas. The fine texture of road surfaces at these sites would have helped to accumulate fine particles. The particle size distribution analysis illustrated the variability in size distribution of build-up pollutants in different suburbs.

In order to investigate the influence of antecedent dry period on particle size variation of the build-up solids, the cumulative particle size distribution of build-up samples on each road for the two different antecedent dry periods were analysed. Figure 5.2 shows an example of the cumulative particle size distribution for two different antecedent dry periods ( $<8$  days and  $>8$  days) for a commercial area road surface at Surfers Paradise. Appendix A/Figure A.1 gives the variation of particle size distribution with dry days for the sixteen road surfaces investigated.

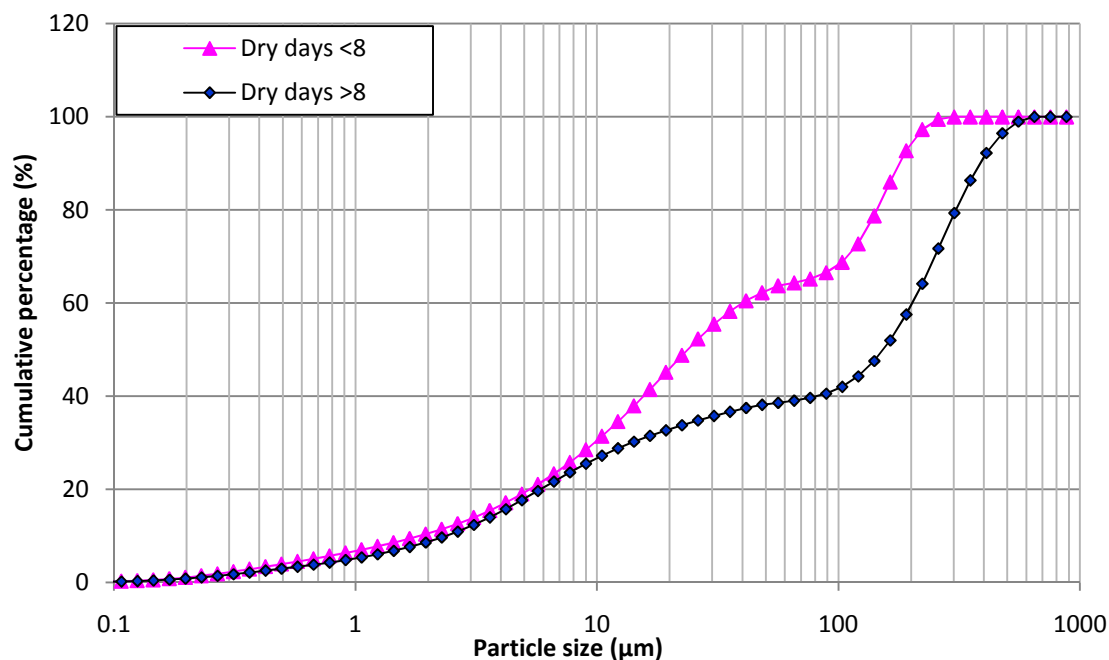


**Figure 5.2: Cumulative particle size distribution of solids build-up on St Paul's Place in Surfers Paradise**

As seen in Appendix A/Figure A.1, the fraction of fine particles on road surfaces reduces with the increase in dry period. This is common for a majority of the build-up samples (Appendix A/Figure A.1). This could be attributed to the re-suspension of fine particles on road surfaces over a number of dry days and eventual enrichment of coarse particles content on road surfaces (Sartor and Boyd 1972; Egodawatta and Goonetilleke 2006). However, there were a few roads (Appendix A/Figure A.1: A, F, I, J, N and O) which exhibited an increase in fine particles with the increase in dry days. It is suggested that due to the long time-gap between the two sampling events, particle composition would have changed. Therefore, it can be suggested that the dry period has a considerable influence on the particle size composition which in turn, can also influence other parameters.

### 5.3.2 TOTAL ORGANIC CARBON (TOC)

Organic carbon content is an important parameter as it has the ability to enhance the adsorption of other pollutants to particulates (Hart 1982). The organic carbon content in the build-up samples was measured as a concentration (mg/L) for each particle size range and was converted to load per unit weight of total solids (mg/g). This was to overcome any bias due to differences in build-up load. Average TOC load values and standard deviations for the different particle sizes of build-up samples from different suburbs are given in Table 5.2.

**Table 5.2: Average TOC in the different particle sizes of solids in each suburb (average  $\pm$  standard deviation)**

Suburb	Particle size range			
	<75 $\mu$ m	75-150 $\mu$ m	150-300 $\mu$ m	300-425 $\mu$ m
	mg/g			
Clearview Estate	1.74 $\pm$ 0.92	1.07 $\pm$ 0.66	0.72 $\pm$ 0.31	0.51 $\pm$ 0.35
Nerang	2.13 $\pm$ 1.50	0.14 $\pm$ 0.09	0.17 $\pm$ 0.10	0.14 $\pm$ 0.12
Benowa	6.97 $\pm$ 5.39	0.79 $\pm$ 0.38	0.77 $\pm$ 0.42	0.71 $\pm$ 0.45
Surfers Paradise	0.96 $\pm$ 1.20	0.65 $\pm$ 0.91	0.62 $\pm$ 0.62	0.42 $\pm$ 0.61

As evident in Table 5.2, organic carbon increases with the decrease in particle size. Confirming previous research findings, the smallest particle size range always shows significantly high organic carbon content, irrespective of location or land use (Roger et al. 1998; Herngren 2006). As noted by Sartor and Boyd (1972), this could be attributed to organic matter (such as leaf litter) on road surfaces having a relatively lower structural strength and being easily ground into fine particles by physical abrasion due to vehicular traffic. Furthermore, an appreciable fraction of organic matter in road deposited particles could be derived from organic particles released by vehicle tyre wear (Fergusson and Ryan 1984; Rogge et al. 1993). At the study sites, it was difficult to identify significant differences in organic matter content in particle sizes 150-300 $\mu\text{m}$  and 300-425 $\mu\text{m}$ .

Even though the majority of the study sites showed a similar range of organic matter content for each particle size, significantly higher TOC content was found in the smallest particle size ranges at Benowa. This could be attributed to the significant surrounding vegetation at these road sites. Other than Benowa, residential sites with significant vegetation at Clearview Estate also had high organic carbon content. This suggests that the higher percentage of organic carbon content in street deposited solids can be mainly attributed to plant debris. As Rogge et al. (1993) noted, vehicle exhaust, tyre wear, plant fragments and garden soil are the potential sources of organic materials in fine dust on roads. However, detailed analyses are needed to clarify the sources and characteristics of TOC. Characteristics of TOC are discussed in detail in Section 5.5.

### 5.3.3 MINERALOGY

As discussed in Section 2.6, mineralogical analysis of build-up pollutants can provide important information regarding the composition of build-up solids. The X-ray diffraction analysis carried out enabled the identification of the respective proportions of crystalline minerals as weight percentages of mineralogical component per solid load in each particle size range (unit sample weight). The resulting data is given in Table A.1 in Appendix A. Each of the solids samples had a unique mineralogy. The crystalline minerals detected included quartz ( $\text{SiO}_2$ ), albite



( $\text{NaAlSi}_3\text{O}_8$ ), microcline ( $\text{KAlSi}_3\text{O}_8$ ), chlorite ( $\text{H}_8\text{Mg}_6\text{O}_{18}\text{Si}_4$ ) and muscovite ( $\text{H}_2\text{KAl}_3(\text{SiO}_4)_3$ ). Additionally, minor proportions of orthoclase, kaolinite and riebeckite (which are clay minerals) were also detected in a few samples. Also, and most importantly, a significant proportion of amorphous content was detected in all samples, irrespective of particle size.

It was hypothesised that mineralogy can exert a significant influence on many physical and chemical characteristics of solids. Figure 5.3 illustrates the mineralogical variations of different particle sizes in the four suburbs. The proportions of mineral components for the different particle size ranges underline the variability of mineralogy.

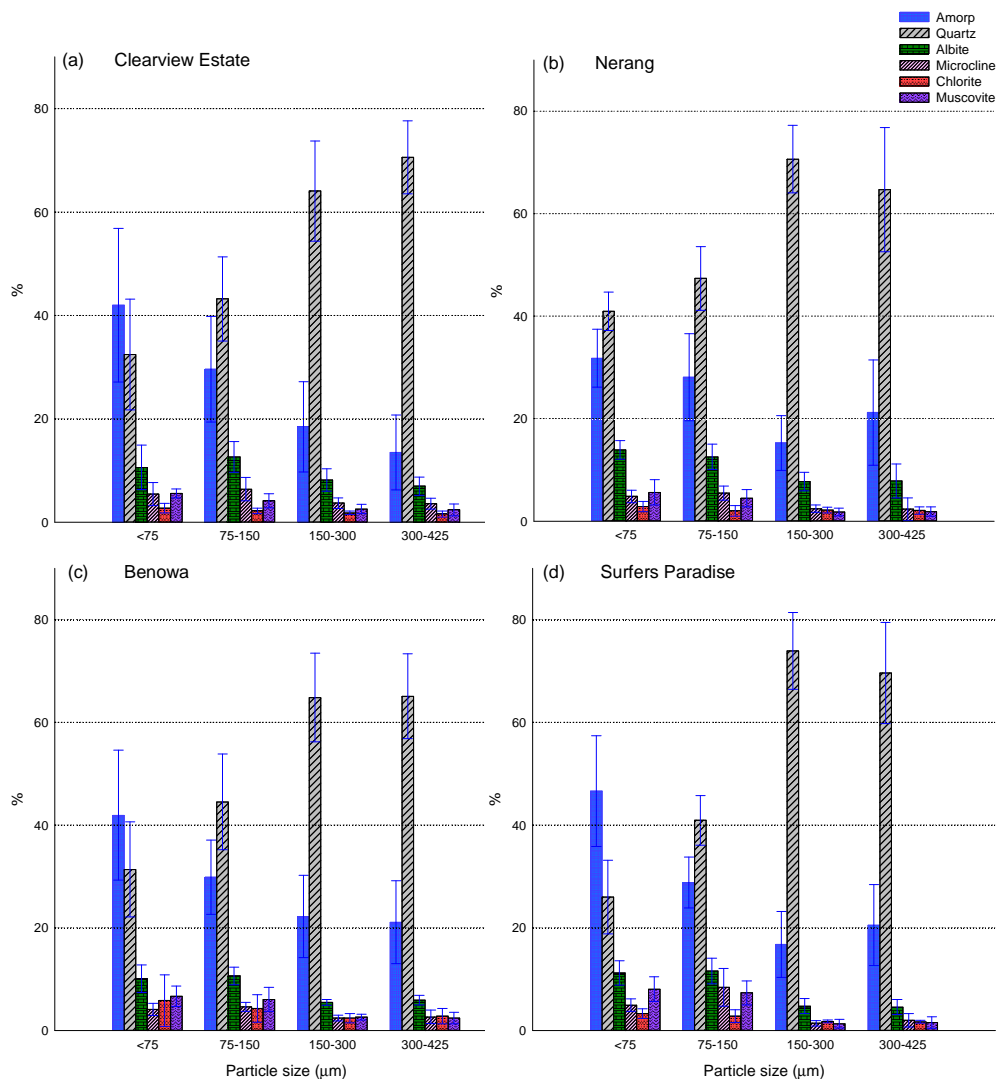


**Figure 5.3: Mineralogical variations in four suburbs: a) Clearview Estate b) Nerang c) Surfers Paradise and d) Benowa**

At all of the study sites, quartz was the dominant mineral, especially in larger particle size ranges. Unidentified amorphous content was the second largest component in all of the particle sizes. A certain amount of amorphous content could be attributed to organic matter content, smaller quantities of clay, and traffic related pollutants that have higher surface area and charge sites (Robertson et al. 2003; Khalil 2005; Bian and Zhu 2008). The amorphous content decreases with the increase in particle size. Interestingly, the reduction in amorphous content is proportional to the increase in quartz content. This indicates that the amorphous content is significant in influencing physical and chemical properties. Therefore, it was important to identify the constituents of the amorphous content, and these will be described later in this chapter. Clay forming minerals of albite, microcline, chlorite and muscovite are present in smaller fractions in all particle sizes. As expected, these clay forming minerals decrease with the increase in particle size. The feldspar minerals of albite and microcline were the most represented clay forming minerals. Another important component in clay forming minerals was muscovite. Chlorite was the least detected mineral in the road deposited solids.

The mineralogical percentages varied significantly for different particle sizes. Amorphous content was the dominant component in  $<75\mu\text{m}$  particles and ranged from 21-70% (Appendix A/Table A.1), whilst the quartz content was in the range of 12-47%. Clay forming minerals were well represented in  $<75\mu\text{m}$  size in all sites and ranged from 12-58%. Particle size 75-150 $\mu\text{m}$  also showed a similar range of clay forming minerals. The major difference between 75-150 $\mu\text{m}$  particles compared to  $<75\mu\text{m}$  particles was the increase in quartz and reduction in amorphous content. Particle size 75-150 $\mu\text{m}$  showed 14-50% amorphous content and 27-64% quartz. Due to the high proportions of clay forming minerals in 75-150 $\mu\text{m}$  and  $<75\mu\text{m}$  sizes, it could be expected that these two particle size ranges would exhibit physical and chemical parameters that are inherent to clay minerals and would be favourable for heavy metal adsorption.

As evident in Figure 5.3, based on the mean value of the eight samples in each suburb, road deposited solids consisted of quartz in more than 64% of their weight in particles larger than 150 $\mu\text{m}$ , whereas the remaining 36% consisted of amorphous

content, albite, microcline, chlorite and muscovite. According to the raw data matrix (Appendix A/Table A.1), quartz content in 150-300 $\mu\text{m}$  particles ranged from 47-83% and, in 300-425 $\mu\text{m}$  particles, it was in the range of 48-85%. Amorphous content ranged from 4-36% in 150-300 $\mu\text{m}$  particles, and 4-41% in 300-425 $\mu\text{m}$  particles. Similarly, proportions of other mineral components in 150-300 $\mu\text{m}$  particles and 300-425 $\mu\text{m}$  particles also lay in equal ranges in all of the study sites, independent of land use characteristics. This was attributed to the structural stability of quartz to resist the physical abrasion on road surfaces much better than the other mineral components and amorphous material. This leads to large particles (>150 $\mu\text{m}$ ) being dominated by quartz. Therefore, it could be expected that these two particle size ranges would exhibit similar physical and chemical parameters.

The mineral percentages shown in Figure 5.3 were calculated with respect to the solids loads in each particle size range. As observed in Section 5.2, the solids load in the four particle size ranges differed across the suburbs. Therefore, it was difficult to derive clear conclusions about the spatial variation and the influence of land use on sample composition. To understand the variability of the overall mineral composition of the collected samples, mineral percentages in each particle size with respect to the total solids load were analysed. Table 5.3 presents the mineralogical content as a percentage of build-up solids load.

As given in Table 5.3, the mineralogical variation of different land uses indicated that inland suburbs have higher clay forming mineral content than coastal suburbs. Highest amorphous content is found in Benowa and Clearview Estate suburbs. Nerang and Surfers Paradise suburbs, which are industrial and commercial land uses respectively, have the highest quartz content. These road surfaces had higher coarse particles than the other two suburbs (Figure 5.1). As noted in Section 5.2, the relatively coarse textured road surfaces in these suburbs would have influenced the accumulation of coarse particles. According to Table 5.3, the amorphous content in the total sample is the significant material in road deposited solids. This was attributed to particle size <75 $\mu\text{m}$ , which is the dominant particle size in road deposited solids, containing high amorphous content (Table 5.3). The mineralogical variations among suburbs were attributed to the different weight percentages of

particle sizes in road surface pollutants. Thus, this indicates that the road surface condition, traffic density, anthropogenic activities and soil type have an influence on the mineralogical composition of build-up solids.

**Table 5.3: Mineralogical variation as a percentage of total solids weight**

Suburb	Particle size (µm)	Amorp. (%)	Quartz (%)	Clay forming minerals (%)			
				Albite	Microcline	Chlorite	Muscovite
Clearview Estate	<75	20.7	15.8	5.28	2.67	1.37	2.68
	75-150	7.56	11.0	3.30	1.73	0.60	1.17
	150-300	3.15	11.5	1.38	0.66	0.32	0.43
	300-425	1.09	5.49	0.45	0.27	0.12	0.22
	Total	32.5	43.8	10.4	5.33	2.41	4.49
Nerang	<75	11.0	14.1	4.96	1.7	1.14	1.91
	75-150	9.36	13.7	3.59	1.62	0.55	1.32
	150-300	3.01	13.9	1.62	0.54	0.43	0.4
	300-425	4.15	6.65	1.21	0.45	0.26	0.52
	Total	27.6	48.4	11.4	4.31	2.38	4.15
Benowa	<75	21.9	15.9	5.24	2.15	3.17	3.37
	75-150	5.85	7.85	1.9	0.88	0.81	1.14
	150-300	4.70	14.5	1.24	0.58	0.56	0.57
	300-425	1.66	4.97	0.46	0.22	0.19	0.21
	Total	34.1	43.2	8.84	3.83	4.72	5.29
Surfers Paradise	<75	16.2	8.75	4.16	1.84	1.25	3.01
	75-150	6.12	8.37	2.44	1.52	0.65	1.78
	150-300	2.84	16.2	0.91	0.28	0.37	0.24
	300-425	4.15	17.0	0.93	0.29	0.41	0.26
	Total	29.3	50.34	8.44	3.93	2.67	5.29

### 5.3.4 CLAY ANALYSIS

It was observed that the amorphous content was quite high in all particle sizes of road deposited solids, especially in the  $<75\mu\text{m}$  particles. These fine particles could contain a fraction of clay minerals which contribute to the amorphous content, as observed in the X-ray diffraction analysis showing the low intensity reflections made by these minerals. Therefore, in order to identify the clay minerals, thin film clay analysis was carried out. Figure 5.4 shows the X-ray diffraction pattern obtained for the particle size  $<75\mu\text{m}$  collected from Lawrence Drive at Nerang. The results of thin film clay analysis for all road surfaces are given in Appendix A/Table A.2.

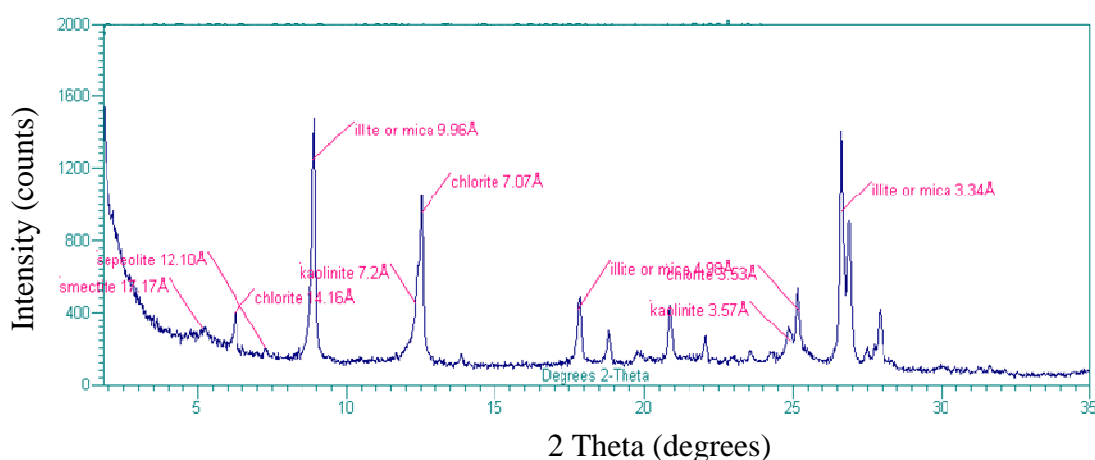


**Figure 5.4: Thin film X-ray diffraction patterns of  $<75\mu\text{m}$  solids collected from Lawrence Drive at Nerang**

In Figure 5.4, X-ray patterns of the thin film show the reflection patterns of illite, smectite, mica, kaolinite, chlorite and mixed layer illite-smectite. Illite, mica and chlorite minerals were present in all samples and kaolinite and sepiolite were present in a majority of the samples. Poorly defined reflections of smectite, amphibole, palygorsite and mixed layer illite-smectite were present in a few of the samples. The analysis indicated that the crystalline form of the above noted clay minerals were present in finer particles which were not detected in the powder diffraction patterns. Minor portions of these crystalline minerals in the solids would not have been detected in the amorphous content due to the limits of detection.

The qualitative measurements obtained from clay analysis indicated that clay minerals could account for a minor portion of the amorphous content in solids particles of  $<75\mu\text{m}$ . Furthermore, these clay minerals were not available in particles larger than  $75\mu\text{m}$  ( $75\text{-}425\mu\text{m}$ ), as the clay particles were generally smaller than  $2\mu\text{m}$  (Fitzpatrick et al. 1999). Nevertheless, high proportions of amorphous content were detected in the  $75\text{-}425\mu\text{m}$  particle size range. This indicated that materials other than clay minerals were present in the amorphous content throughout all particle size ranges of road deposited solids. There is a high possibility that these particles originated from traffic related sources. This hypothesis required detailed analysis of the amorphous content and comparison with the mineralogical composition of surrounding soil samples. Details of this analysis are given in Section 5.4.

### 5.3.5 SPECIFIC SURFACE AREA (SSA)

Specific surface area (SSA) of solids is a measure of a particle's ability to retain pollutants on its surfaces (Jain and Ram 1997; Polcaro et al. 2003). This parameter plays an important role in defining the adsorption of pollutants and for describing surface dependent adsorption behaviour, including ion exchange and surface precipitation. Specific surface area of air dried wet sieved solids samples was measured using two different techniques, namely: the ethylene glycol monoethyl ether (EGME) method and the Brunauer-Emmett-Teller (BET)  $\text{N}_2$  gas adsorption method that are widely employed in research for the measurement of SSA of soils.

These two different laboratory techniques have different capabilities in determining the total surface area (EGME) and external surface area (BET  $\text{N}_2$  gas) of particles (Brunauer et al. 1938; Yukselen et al. 2006; Arnepalli et al. 2008). Significantly high internal surface areas of soils and clay minerals have been widely discussed in the research literature (Santamarina et al. 2002; Yukselen et al. 2006; Arnepalli et al. 2008). However, the extent of internal surface area in build-up solids is not widely discussed. Therefore, to determine the most reliable method for SSA measurement of road deposited solids, both EGME and BET methods were employed and the results compared.

Both EGME and BET showed similar variation with respect to particle size, where SSA decreases with the increase in particle size (Appendix A/Table A.1). However, SSA measurements using the two methods showed significant differences. SSA values obtained by the EGME method were ten times higher than the BET SSA values. For example, average SSA of particle size  $<75\mu\text{m}$  was  $17.6\text{m}^2/\text{g}$  and  $1.78\text{m}^2/\text{g}$  using the EGME and BET methods, respectively (Appendix A/Table A.1). The average EGME SSA and BET SSA values and standard deviation for each particle size range for each suburb are given in Table 5.4. The SSA values were averaged for each suburb to identify the differences in SSA in different mineralogical locations. The EGME SSA values for the four particle size ranges varied from 0.27 to  $30.8\text{m}^2/\text{g}$ , while the BET SSA values varied from 0.11 to  $5.78\text{m}^2/\text{g}$  (Appendix A/Table A.1).

It can be seen from the data presented in Table 5.4 that the BET  $\text{N}_2$  gas adsorption method resulted in quite low SSA compared to the EGME method. The BET SSA measurement using the  $\text{N}_2$  gas adsorption method is based on the principle that solid materials will adsorb a monomolecular layer of the gas at a particular pressure (Brunauer et al. 1938). The  $\text{N}_2$  gas adsorption method measures the dry state of the sample, which may restrict the coverage of the interlayer surface area of the expansive-layer silicates or swelling clays that are tightly bound under dry conditions (Santamarina et al. 2002; Arnepalli et al. 2008). However, surface area measurement under wet conditions using the polar liquid EGME method is capable of measuring internal surface area, since EGME can reach the interlayer surfaces of swelling clays (Santamarina et al. 2002; Yukselen et al. 2006).

**Table 5.4: Average EGME SSA and BET SSA of different particle sizes of solids (average  $\pm$  standard deviation)**

Suburb	Particle size range				Particle size range			
	<75 $\mu$ m	75-150 $\mu$ m	150-300 $\mu$ m	300-425 $\mu$ m	<75 $\mu$ m	75-150 $\mu$ m	150-300 $\mu$ m	300-425 $\mu$ m
	EGME SSA (m <sup>2</sup> /g)				BET SSA (m <sup>2</sup> /g)			
Clearview Estate	14.3 $\pm$ 6.16	8.83 $\pm$ 3.95	4.22 $\pm$ 1.97	3.21 $\pm$ 1.52	2.73 $\pm$ 1.47	1.24 $\pm$ 0.97	0.68 $\pm$ 0.35	0.65 $\pm$ 0.20
Nerang	16.0 $\pm$ 5.41	7.50 $\pm$ 2.77	5.23 $\pm$ 1.93	2.31 $\pm$ 1.61	1.59 $\pm$ 0.73	0.63 $\pm$ 0.26	0.41 $\pm$ 0.16	0.47 $\pm$ 0.21
Benowa	17.6 $\pm$ 7.03	7.39 $\pm$ 5.80	3.52 $\pm$ 2.11	3.21 $\pm$ 1.23	1.37 $\pm$ 0.46	0.57 $\pm$ 0.23	0.31 $\pm$ 0.16	0.29 $\pm$ 0.09
Surfers Paradise	22.3 $\pm$ 3.41	13.6 $\pm$ 6.63	7.05 $\pm$ 4.55	2.70 $\pm$ 1.06	1.43 $\pm$ 0.47	0.50 $\pm$ 0.09	0.21 $\pm$ 0.05	0.20 $\pm$ 0.04

In fact, the clay analysis described in Section 5.3.3 revealed the presence of illite, mica, smectite and kaolinite in solids <75 $\mu$ m. Other than kaolinite, the interlayer surfaces present in these clay minerals would have contributed to the increase in the SSA measurement obtained by the EGME method which results in total surface area of particles. Furthermore, the presence of albite, microcline, muscovite and chlorite in four particle size ranges (See the mineralogical analysis in Section 5.3.3) would have influenced the higher EGME SSA values due to the presence of interlayers in these mineralogical components. Furthermore, the BET N<sub>2</sub> gas adsorption method may only measure the external surface area of these minerals (Tuul and Innes 1962; Allen 1990). Therefore, the presence of swelling clays in road deposited solids yields a higher SSA from the EGME method than from the BET method.

Particles with diameter <75 $\mu$ m had higher SSA than the other particle sizes for all sites (Table 5.4). Similar findings have been reported by past researchers (Horowitz 1991; Sansalone et al. 1997; Li et al. 2008). As identified in Section 5.3.3, high quartz content in >150 $\mu$ m particles would have influenced the difference in SSA in coarse and finer particles. Compared to the SSA of the four particle size ranges, it can be noted that the ratio of SSA of particles <75 $\mu$ m is four times larger than the particle size range 300-425 $\mu$ m. This is true for both EGME and BET SSA values. Similar observations have been noted by Vdovic et al. (1991) for EGME SSA. Additionally, it is evident that the average SSA of both EGME and BET decreases exponentially with the increase in particle size (See Appendix A/Figure A.2). Theoretical SSA values calculated for spherical particles, using the average diameter



of the particle size ranges and assuming a specific gravity of 2.65 (the same as for sand), also showed consistent variation with respect to particle size, although the variation followed a hyperbolic function (Appendix A/Figure A.2).

However, the SSA of spherical particles is approximately three orders of magnitude smaller than EGME SSA measurements obtained in this study. Vdovic et al. (1991) and Sansalone et al. (1997) also noted similar differences in measured and calculated SSA values. This means that particle properties other than size have influenced SSA to record considerably higher values. This may occur if the density of the solid particles is not constant and/or if there are surface irregularities. In fact, density variation of road deposited solid particles can be expected due to the different mineral proportions in the solids particles (See Section 5.3.3 Mineralogy). Also, in an on-road scenario, as a vehicle tyre passes over the road, particles on the road (such as dust and minerals) are subject to rolling shear against the surface, which may result in changes in surface morphology (Rogge et al. 1993). Thus, the variation between calculated and measured values can be attributed to the heterogeneous nature of the road deposited particles.

Increase in both EGME and BET SSA with the reduction in particle size could be attributed to the mineral components, organic matter content and traffic related material. As evident in Figure 5.3, clay forming minerals such as albite, microcline, chlorite and muscovite increase with the reduction in particle size, with particles smaller than 150 $\mu\text{m}$  recording 20-30% of the mineral content. The fineness and structural characteristics of these minerals could have increased the surface area of solids. For example, these minerals have high SSA, with muscovite 60-100 $\text{m}^2/\text{g}$  and chlorite 25-150 $\text{m}^2/\text{g}$  (Sparks 2003). Additionally, the amorphous content in road deposited solids also increases with the reduction in particle size. Hence, the amorphous content would have influenced the increase in SSA in the smallest particle size range. Although organic matter content has been identified as one of the important parameters influencing SSA, the variation in EGME and BET SSA for different particle sizes is not proportional to the variation in organic matter. For example, <75 $\mu\text{m}$  particles at Benowa had high TOC. The SSA for this particle size range is not proportionately high in keeping with the TOC content. Past researchers

have also noted the uncertainty regarding the influence exerted by organic matter on SSA (Eisma 1981). Vdovic et al. (1991) concluded that mineral composition is the significant parameter which influences SSA.

Furthermore, the highest EGME SSA was reported in respect of all particle sizes from Surfers Paradise samples which had low organic matter content. Road surfaces in Surfers Paradise are located in a highly urbanised area with high traffic density. In fact, these road surfaces had the highest amorphous content (Figure 5.3 and Appendix A/Table A.1). This suggests that solids samples could contain material other than organic matter which exerts a significant influence on SSA. These include clay minerals and traffic related material such as tyre and brake pad wear, and pavement wear. Tyre wear particles have complex shapes and morphologies and high porosity (Milani et al. 2004). Therefore, the significant presence of traffic related particles could have resulted in high EGME SSA. In contrast, Clearview Estate showed high BET SSA for all of the particle sizes. These particles had a significant content of clay minerals such as albite, microcline, chlorite and muscovite in all of the particle size ranges. Even though SSA of particles is nominally independent of the sampling location or land use characteristics, different land uses could have influenced SSA due to the mixed nature of pollutants in road deposited solids. Since the correlation of SSA with the amorphous content and organic matter was not very clear, detailed investigations were needed.

Analysis of EGME SSA values for the two different antecedent dry periods showed an increase in SSA for long dry periods for all particle size ranges on a majority of the road surfaces. However, the antecedent dry day period did not have a significant influence on BET SSA. A majority of the study sites showed similar values or reduction in BET SSA for the longer antecedent dry period. This suggests that, though BET SSA is not influenced by the antecedent dry period, EGME SSA or total surface area of particles would increase as a result of any internal cracks generated within the particle and morphological changes of particle surface by the prevailing traffic activities.

As a result of the above analysis, it was concluded that EGME SSA would give a more accurate estimation of solid particle surface area. Since the EGME method results in total specific-surface area of solids, it would govern the adsorption behaviour of road deposited solids. Therefore, for further investigations of solids properties, SSA values obtained using the EGME method were used to interpret the surface characteristics of solids particles.

### **5.3.6 EFFECTIVE CATION EXCHANGE CAPACITY (ECEC)**

Effective cation exchange capacity (ECEC) is an important parameter of solids as it determines the cation retention by particles and, hence, solids' pollutant adsorption. The ECEC of solids can be primarily attributed to the clay mineral component and organic matter content (Bortoluzzi et al. 2006).

The sum of the major exchangeable cations ( $\text{Ca}^{2+}$ ,  $\text{Mg}^{2+}$ ,  $\text{K}^+$  and  $\text{Na}^+$ ) is referred to as 'total exchangeable bases'. This is similar to the value of ECEC of the sample (Rengasamy and Churchman 1999). However, in acidic soils, in addition to  $\text{Ca}^{2+}$ ,  $\text{Mg}^{2+}$ ,  $\text{K}^+$  and  $\text{Na}^+$  ions, ECEC can, to a great extent, be accounted for by  $\text{Al}^{3+}$ ,  $\text{Fe}^{3+}$  and  $\text{H}^+$  ions (exchange acidity) (Blakemore et al. 1987). Therefore, pH values of the collected build-up samples were determined to assess whether these were acidic. The pH values for all samples ranged from 6 to 8.5. The differences in pH could be attributed to the prevailing soil conditions in the study area. Appendix A/ Table A.3 gives the pH values measured in the build-up samples collected. As noted in previous research, the acidic behaviour of solids (soils) activates below pH 5.5 (Rayment 2004; Evans and Scott 2007). According to the pH values obtained, the collected solids did not show acidic behaviour. Therefore, the ECEC was considered as the summation of  $\text{Ca}^{2+}$ ,  $\text{Mg}^{2+}$ ,  $\text{K}^+$ ,  $\text{Na}^+$  and  $\text{Al}^{3+}$  cations (Gillman and Sumpter 1986; Evans and Scott 2007).

ECEC of the different particle sizes varied between 0.44 and 25.5meq/100g (Appendix A/Table A.1). To understand the variation of ECEC among the different suburbs, mean values were separately analysed. Table 5.5 gives the mean values and data range for the different suburbs.

**Table 5.5: Effective cation exchange capacity (ECEC) for the different particle sizes of solids in each suburb**

Particle size range	ECEC (meq/100g)							
	<75µm		75-150µm		150-300µm		300-425µm	
Suburb	Mean	Range	Mean	Range	Mean	Range	Mean	Range
Clearview Estate	6.30	2.30-11.4	6.70	0.60-13.0	7.00	0.40-25.5	6.40	0.60-24.3
Nerang	13.8	2.30-22.7	9.20	2.80-16.1	6.00	1.70-10.2	5.50	2.00-9.00
Benowa	5.20	1.00-12.8	6.10	0.80-13.9	4.40	0.70-12.6	3.10	0.80-6.70
Surfers Paradise	12.5	2.00-23.3	7.90	2.00-24.3	3.80	2.00-7.00	4.50	2.00-10.4

According to Table 5.5, ECEC of the solids decreased with the increase in particle size. This suggests that the chemical parameters of road deposited solids can vary considerably with the particle size. Similar findings have also been reported by previous researchers (Dawes and Goonetilleke 2005; Khalil 2005; Dawes and Goonetilleke 2006). Thus, it appears that the ECEC variation with respect to particle size is compatible with the variation in TOC content, clay forming minerals and SSA. ECEC variation among suburbs does not show a consistent trend. This indicates that ECEC is influenced by several factors. Particle mineralogy and the organic matter are two essential factors (Lin and Chen 1998).

The highest ECEC in particles <150µm was recorded in the Nerang and Surfers Paradise samples despite the fact that these samples had a predominantly sandy matrix (dominated by quartz) (Table 5.3 and Figure 5.3). A primary reason could be that the clay fraction of these samples is essentially made up of illite, illite-mica and smectite, which are minerals with high to medium exchange capacities. The CEC of common clay minerals in solids samples is as follows: smectite (45-160cmol (+)/kg), illite, muscovite and chlorite (10-40cmol (+)/kg), and kaolinite (0-15cmol (+)/kg) (Shaw 1992; Sparks 2003).

The presence of even relatively small portions of these clay minerals increases the ECEC (Morras 1995). For example, smectite was present in all of the solids samples from Nerang (Appendix A/Table A.2). The organic matter content in these samples

would have also contributed to the ECEC. Surfers Paradise samples contained illite, mica and kaolinite. Also, these samples had the highest EGME SSA, which is a measure of the total surface area. Interlayer surface areas of clay minerals would have contributed to high exchangeable cations. Thus, internal surface area and interlayer minerals would contribute to high exchange sites. In the 75-150 $\mu\text{m}$  particle size range, muscovite and chlorite content was relatively high (>1.8%) in the Nerang and Surfers Paradise suburbs (See Table 5.3). Combination of relatively high organic matter content, clay forming minerals and SSA would be partially responsible for the high ECEC at these sites.

Particles >150 $\mu\text{m}$  from Clearview Estate and Nerang samples had higher ECEC. The Nerang samples contained high muscovite and chlorite content compared to the other suburbs (Table 5.3). Furthermore, the high organic matter in Clearview Estate samples in these particle sizes would have appreciably influenced the ECEC. Although Surfers Paradise samples showed higher EGME SSA, clay forming mineral content and organic matter in this particle size range was comparatively low. This would have influenced the lower ECEC in the Surfers Paradise samples.

The contribution of SSA, TOC and mineralogical components to ECEC could be different, however. For example, the highest ECEC reported in Nerang and Surfers Paradise implied that the highest contribution to ECEC would be from mineral components, amorphous content and SSA. TOC content in these study sites were comparatively low. Benowa which had the highest TOC content showed low ECEC. Furthermore, SSA observed using the EGME method showed high SSA in these study sites. This suggests that the availability of mineralogical components has a relatively higher influence on ECEC than the organic matter content, even though previous studies have indicated that TOC has a significant influence on cation exchange.

Carroll et al. (2004) reported that ECEC is dependent on the CEC/clay ratio and the amount of clay present in the sample. As indicated in Section 5.3.3, in terms of particle mineralogy (Figure 5.3), up to 20-30% of fine particles are made up of albite,

microcline, muscovite and chlorite. Similarly, Ruellan and Deletang (1967) noted that hydrated feldspar could be a possible source of high ECEC. However, the literature shows that even sand may have high ECEC values (Joffe and Kunin 1943; Karim and Islam 1956; Sanchez 1969). Thus, a high combination of all these minerals in fine particles would have contributed to the increase in ECEC. However, the influence of each parameter cannot be adequately explained from the present analysis alone due to the site specific differences. Knowledge of the correlations of each component would allow an understanding of the factors favourable for pollutant adsorption to solids and of correlations between different parameters.

According to the analysis in Section 5.3, 150-300 $\mu$ m and 300-425 $\mu$ m particles did not show significant variation in organic carbon content, mineralogy, SSA and ECEC compared to the other two particle sizes. Therefore, it can be expected that there was consistency in the physical and chemical characteristic of particles >150 $\mu$ m diameter compared to the smaller particles. Therefore, it is possible to hypothesise that particle composition, especially the mineralogical composition could be influenced by the physical and chemical behaviour of road deposited solids. However, a more detailed understanding is required for final clarification.

#### **5.4 CHARACTERISATION OF THE BUILD-UP SAMPLE COMPOSITION AND POLLUTANT SOURCE IDENTIFICATION**

Overall analysis in Section 5.3 indicated that physical and chemical parameters such as TOC, SSA and ECEC are correlated with mineralogy. However, it is difficult to conclusively understand the nature of correlations between these parameters without deriving an overall interpretation of the datasets. As described in Section 5.3.3, considerably high amorphous content was detected in road deposited solids samples. An in-depth understanding of this material was needed; in particular, an understanding of the constituents of the unidentified amorphous content. Generally, amorphous content represents the unsatisfactory reflections produced in X-ray diffraction (XRD) analysis which are caused by unidentified or non-crystalline material and low intensity reflections. These reflections could account for the organic matter content, minor portions of clay minerals and the particles generated due to

anthropogenic activities on road surfaces (Robertson et al. 2003; Khalil 2005; Bian and Zhu 2008).

Solids deposited on a road surface are heterogeneous. The dynamic nature of anthropogenic activities in the urban environment often results in the generation of pollutants from a wide variety of sources, with correspondingly diverse physical and chemical properties (Hopke et al. 1980; Fergusson and Kim 1991; Hollis 1991; Spassov et al. 2004). Road deposited solids consist of inputs from surrounding soil, atmospheric deposition and anthropogenic particles such as tyre and brake abrasion products, fuel leakages, combustion exhausts and pavement wear (Tai 1991; Rogge et al. 1993; Vinklander 1998; Adachi and Tainosho 2004; Wik and Dave 2009; Kreider et al. 2010). This indicates that a significant portion of amorphous content in solids may consist of anthropogenic pollutants originating from road surfaces.

Since the particle composition of road deposited particulates is also closely related to the background soil from the adjacent land, the composition of amorphous content can be confirmed by comparing the mineralogical analysis of surrounding soil samples (Xie et al. 2000; Jullien and Francois 2006). Consequently, the mineralogical data from 32 build-up solids samples and four soil samples from each suburb were compared. However, due to limitations in univariate data analysis, the nature of the relationships between different physico-chemical parameters was difficult to obtain. Therefore, in order to determine whether the amorphous content found in samples originated from soil input or anthropogenic sources, analysis was further refined using multivariate data analysis techniques.

#### **5.4.1 MINERALOGY OF SURROUNDING SOIL**

The mineralogical composition of soil samples collected from each suburb was evaluated (Section 4.5). Minerals detected included, quartz, albite, microcline, chlorite, muscovite and kaolinite (Appendix A/Table A.4). With the exception of kaolinite, minerals identified in soil samples were identical to those found in solids samples. Since kaolinite represented <2% of the soil composition, it was not included in this data analysis.

Comparison of mineralogical data of solids with background soil samples can provide valuable insight into the signature characteristics of soil inputs to road surface depositions. Consequently, the mineral composition of soils was compared with build-up solids from the two sampling events from each suburb, as given in Figure 5.5. Mineralogical data generated for the solids are in the form of percentage of mineral components for each particle size fraction.

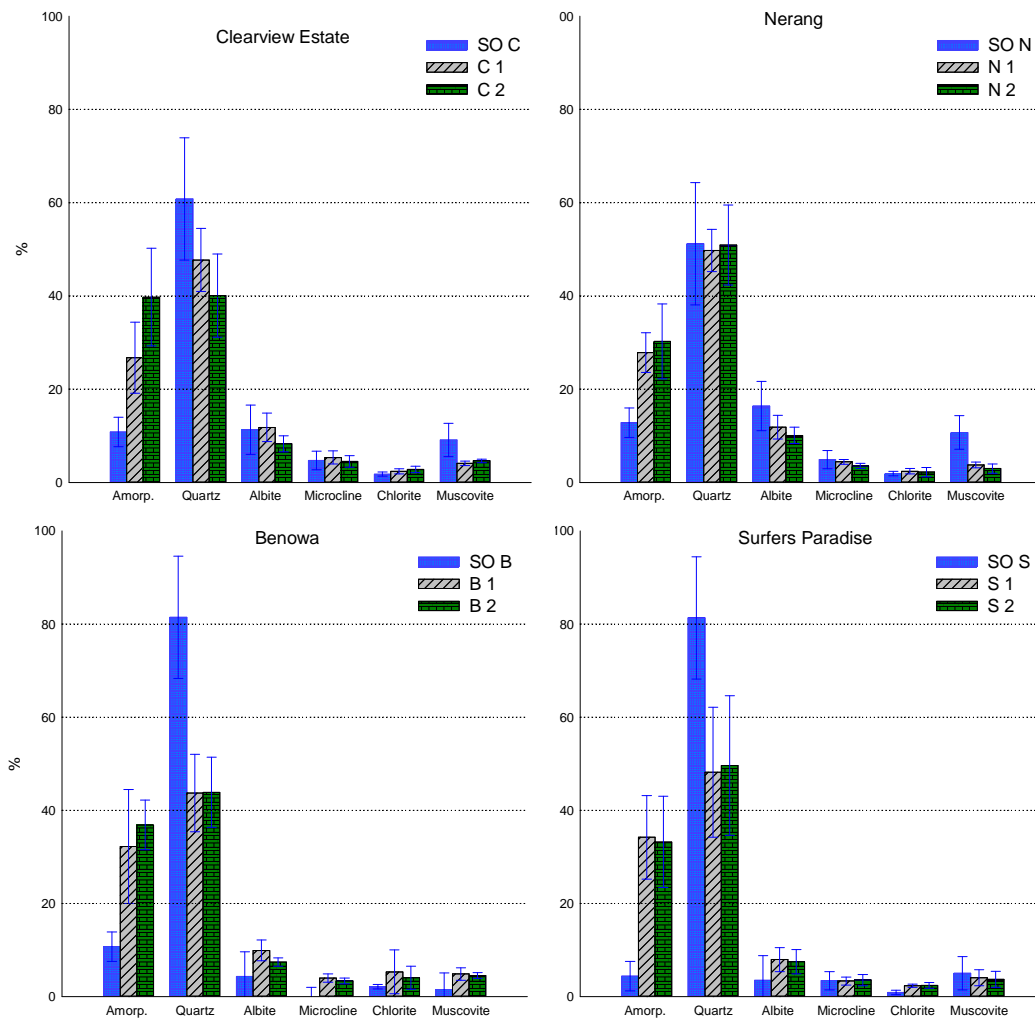


**Figure 5.5: Mineralogical variations of solids and soil samples in four suburbs**

Note: SO- soil, C- Clearview Estate, N- Nerang, B- Benowa, S- Surfers Paradise, 1 and 2- first and second sampling event

As seen in Figure 5.5, road deposited solids and soil samples had identical mineral components, with soil inputs dominating the road surface pollutants. This is in agreement with the findings of Xie et al. (2000) who noted that surface soils are a



significant component of street dust. The results showed that the road deposited solids consisted primarily of mineral matter, which accounted for about 60% of the sample. Among these minerals, quartz was the dominant mineral and ranged between 40-50%. In addition, amorphous content (unidentified material) of about 40% was detected in all the samples, irrespective of the study site.

The effect of geographical location on mineralogical composition is clearly evident in Figure 5.5. For example, in the soil samples, the quartz content in the coastal suburbs of Surfers Paradise and Benowa was around 80%, and in the inland suburbs such as Nerang and Clearview Estate, it was in the range of 50-60%. In contrast, clay forming minerals such as albite, microcline, muscovite and chlorite in solids samples in inland suburbs were always higher compared to coastal suburbs. This confirms the influence of geographical location on pollutant build-up.

According to Figure 5.5, un-diffracted amorphous material in soil samples range from 4.4% to 12.8%. The amorphous content in soils was in a similar range, as reported by Khalil (2005) and Dawes (2006). However, the amorphous content in road deposited solids was 10-40% higher compared to soil samples. This suggested that the road deposited solids contained on average of about 30% of material that can be classified as amorphous, albeit different to the amorphous material commonly present in soil samples. As noted by Bish and Post (1989), amorphous content in soils could be due to partially weathered minerals (non-crystalline mineral), low content of certain clay minerals that do not contribute to diffractograms due to the limit of detection, amorphous silicate (non-crystalline quartz) and organic matter.

Organic matter content detected in soil samples is given in Appendix A/Table A.4. Detected organic matter content of soil samples ranged between 4.4-6.1%. Thus, clay minerals in soils could account for the remaining portion of amorphous content. Therefore, in order to identify potential components of clay minerals in soil particles, thin film clay analysis, which can detect the presence of small fractions of clay minerals, was carried out.

A sample thin film X-ray diffraction pattern for a soil sample from Nerang is shown in Figure 5.6. Accordingly, clay minerals detected in soil samples were smectite, illite-mica, kaolinite, chlorite and a mixed layer of illite-smectite. Results of thin film clay analysis for the other sites are tabulated in Appendix A/ Table A.5. Qualitative measurements obtained from clay analysis of solids and soil samples indicated that minor portions of clay minerals could account for a portion of the amorphous content present in solids. The clay minerals detected in soil and solids samples did not show significant differences. However, high proportions of amorphous content were detected in the solids. This indicated that materials other than clay minerals were present in the road deposited solids.

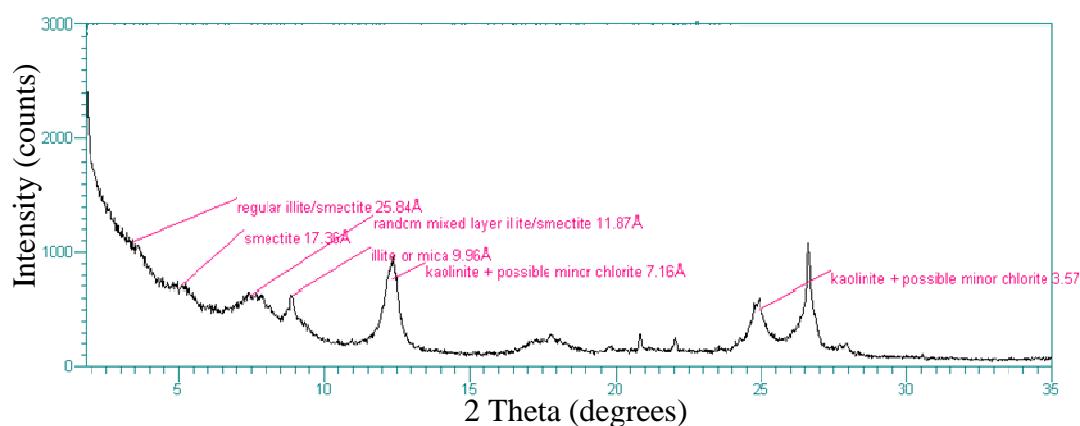


**Figure 5.6: Thin film X-ray diffraction patterns of soil collected at Nerang suburb**

Therefore, it can be postulated that the high percentage of amorphous content in solids samples was generated from traffic related sources. This can be confirmed by the variability of the amorphous content in solids, with traffic parameters. As noted by Kreider et al. (2010), traffic related pollutants on road surfaces are subject to change with a variety of driving conditions; for example, vehicle speed, load, acceleration, braking and steering. The influence of the above mentioned traffic parameters was also clearly evident in the present study, which indicated an approximately 5-10% high amorphous content in the Surfers Paradise and Benowa suburbs compared to Clearview Estate, which has a low traffic density.

In addition to the driving parameters, surface texture is an important parameter in relation to traffic related pollutant generation as it influences tyre wear or the frictional force between the tyre and pavement (Dahl et al. 2006). Therefore, the surface texture would have influenced the higher amorphous content of solids in the Nerang and Surfers Paradise suburbs compared to Clearview Estate (See Table 5.1 and Figure 5.5). Additionally, the increase in the amorphous content with different antecedent dry days could be noted in the solids from the two different sampling events. This suggests that, during the antecedent dry period, mineralogical composition was subject to change. This, in turn, indicates that the physical and chemical characteristics of the road deposited solids were influenced by the antecedent dry period. Thus, the road deposited solids composition showed dynamic behaviour in particulate accumulation and this confirms that amorphous material was of anthropogenic origin, primarily originating from traffic related sources.

Similarly, Robertson et al. (2003), employing geochemical and mineralogical analysis, identified that urban road deposited solids are predominantly composed of non-soil derived material containing high levels of heavy metals. As noted by Rogge et al. (1993), 7.6% of the fine particulate road dust in street surfaces in Los Angeles area is vehicular exhaust particles. Furthermore, there could be particles derived from pavement surface wear which account for non-mineral particles. Thus, mineralogical data provides valuable insights into the signature characteristics of road deposited solids and the role of surrounding soil on road surfaces.

#### **5.4.2 ANALYSIS OF POLLUTANT CHARACTERISTICS**

In order to identify the solids sample composition and the pollutant sources, detailed analysis was carried out. Due to the involvement of a large number of environmental factors such as land use and traffic characteristics at the study sites, it was difficult to identify the correlations among soils and solids using conventional univariate analysis. In these circumstances, the application of multivariate data analytical techniques has been found to be the most appropriate approach (for example, in Vega et al. 1998; Petersen et al. 2001; De Bartolomeo et al. 2004; Hengren et al. 2005; Settle et al. 2007). In this study, Principal Component Analysis (PCA), an analytical

tool frequently applied in the analysis of environmental data, was used. More details on the theory and application of PCA can be found in Section 3.3.4.

### **Data selection and pre-treatment**

Mineralogical data on solids and soil samples were subjected to PCA analysis. Mineralogical data was in the form of percentages. Data used for PCA was subjected to pre-treatment (Einax et al. 1998). Initially, all the data was mean centered and standardised (auto scaled) in order to ensure that all the variables had equal weights in the analysis (Settle et al. 2007). Finally, outlying objects of the data were identified, using the Hotelling  $T^2$  test (Details of this test are described in Section 3.3.4). The identified objects were removed from the data matrices in order to improve the variance of the PCA analysis. A detailed description of the interpretation of a principal component biplot is described in Section 3.3.4. A strong correlation between the respective variables indicates an acute angle between two vectors and a weak correlation indicates an obtuse angle between two vectors. Vectors at right angle are not correlated.

Objects represented the soil and road deposited solids samples from the four suburbs: Clearview Estate (C), Nerang (N), Benowa (B) and Surfers Paradise (S). Notations used for the objects are as follows: The first character represents the initial letter of the corresponding suburb name (accordingly, C, N, B and S represent Clearview Estate, Nerang, Benowa and Surfers Paradise, respectively); the second character represents the sampling event 1 or 2; the third character is a number representing the sampling road site; soil samples are denoted by SO; and the four soil samples are denoted by the initial letter of the suburb (C, N, B or S) to represent Clearview Estate, Nerang, Benowa and Surfers Paradise, respectively. In each suburb, samples were collected from four road sites. Names of these sites in each suburb are given in Appendix A/Table A.6 and Table A.7.

The pre-treated data matrix of (36 x 6), including objects of total build-up and soil, was subjected to PCA. The number of principal components to be used in analysis is decided by the Scree plot method, as discussed in Section 3.3.4. The Scree plot for

the present analysis is shown in Appendix A/Figure A.3. As seen in Figure A.3, the pronounced change of slope in the Scree plot occurs at the 3<sup>rd</sup> principal component. Accordingly, the first three PCs were selected for the analysis (Jackson 1991).

Figure 5.7 presents the PC 1 vs PC 2 biplot, and Appendix A/Figure A.4 shows the PC 1 vs PC 3 biplot. However, as seen in Appendix A/Figure A.4, the third principal component does not provide any further information than what is provided in the PC 1 vs PC 2 biplot. Therefore, only the first two principal components were selected for the analysis (Figure 5.7). PC 1 and PC 2 account for a total data variance of about 67%.

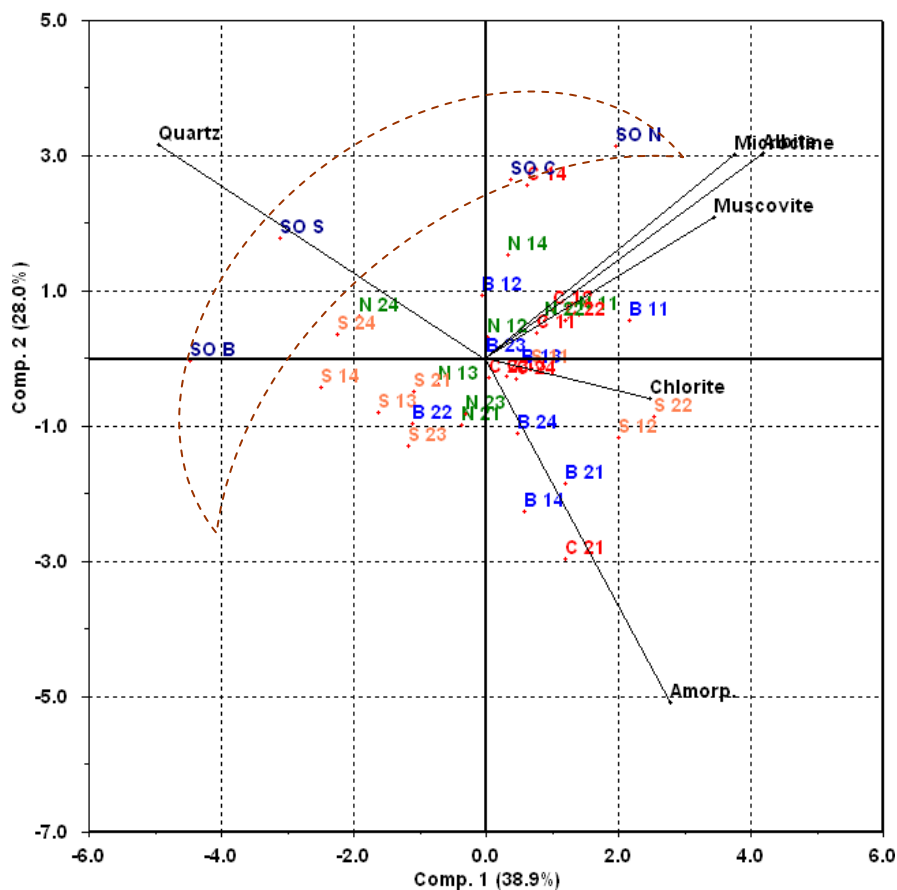


**Figure 5.7: PC 1 vs PC 2 biplot obtained from PCA analysis for soil and weighted average road deposited solids samples**

Note: SO- soil, C- Clearview Estate, N- Nerang, B- Benowa, S- Surfers Paradise, 1 and 2- first and second sampling event

As seen in Figure 5.7, PC 1 primarily explains the mineralogical variation of particles which are associated with quartz located on the negative axis and other mineral components located on the positive axis. This indicates that the characteristics of quartz are independent of all other mineral components and the variation of mineralogical components of solids. Thus, particles with high quartz content would exhibit different physical and chemical characteristics. PC 2 explains the pollutant source variability which is associated with amorphous material located along the negative axis, and all of the other mineral components along the positive axis. In Figure 5.7, all soil samples show positive scores on PC 2. This reflects the pollutant source variability of solids due to soil input and traffic related pollutants.

Objects scores for soil and a majority of solids from the inland sites of Nerang and Clearview Estate have the highest variance in the direction of minerals such as microcline, muscovite and albite. The majority of Clearview Estate and Nerang objects have positive scores on PC 1, while microcline, muscovite and albite minerals are located along the positive PC 1 axis. At the same time, the majority of objects belonging to the Surfers Paradise coastal sites show negative scores on PC 1. This indicates the variation in mineralogical components between inland and coastal sites. Clearview Estate and Nerang are rich in clay type minerals such as chlorite and muscovite. As in Section 5.3.3, this further validates the criteria considered in site selection, as discussed in Section 4.2.1. Therefore, inland and coastal objects would exhibit differences in physical and chemical characteristics related to mineralogical parameters.

All of the soil samples show positive scores on PC 2 and are clustered orthogonal to the direction of amorphous and quartz vectors. This is primarily due to the low content of amorphous material generally present in these soils. In the biplot, soil samples develop a cluster in the perimeter of the road deposited solids cluster (represented by the dotted line in Figure 5.7). However, soil samples are not entirely separated from the solids sample cluster. This indicates that road deposited solids have close correlation with soil, but there are differences due to the amorphous content. Therefore, it can be postulated that the amorphous content is the primary reason for the separation of soils from road deposited solids. Furthermore, the

analysis indicated that soils originating from the adjoining area (as a result of erosion or atmospheric deposition) are the major source of the mineral components in the road deposited solids.

In the PCA biplot, the amorphous content has a negative correlation with quartz and no correlation with albite, microcline and muscovite minerals. This indicates that the amorphous material contains relatively low mineral content. Therefore, it can be postulated that the major portion of the amorphous content in the solids could be material other than clay or non-crystalline mineral components. This further confirms that a high proportion of amorphous content in road deposited solids is derived from traffic related abrasion products such as tyre wear, brake pad wear and corrosion by-products. The mineralogical analysis of road deposited solids and the background soils allowed the assessment of the fraction of soil in pollutant build-up and the identification of the composition of the amorphous content.

## **5.5 UNDERSTANDING OF PHYSICAL AND CHEMICAL CHARACTERISTICS**

The initial analysis of physical and chemical parameters such as TOC, mineralogy, SSA and ECEC in relation to particle sizes of solids showed the possible relationships among different parameters (See Section 5.3). However, it was difficult to investigate these relationships on a one-on-one basis due to the involvement of a number of factors such as different land use characteristics, soil profiles and traffic characteristics. Therefore, a detailed analysis of the physico-chemical parameters was needed to understand the relationships between physical and chemical parameters. In this context, each particle size range was separately investigated. This was based on the hypothesis that the underlying physico-chemical parameters of solids would have similarity based on the particle size.

Physical and chemical parameters considered in the analysis were total organic carbon (TOC), specific surface area (SSA), effective cation exchange capacity (ECEC) and six mineralogical components: quartz, albite, microcline, muscovite, chlorite and amorphous mineral. A total of 128 representative objects–32 objects for

each particle size—were analysed. Due to the large number of parameters associated with particle characteristics, multivariate data analysis (PCA) and multi criteria decision making methods (PROMETHEE and GAIA) were carried out to identify the relationships in relation to physical and chemical parameters for each size range. Additionally, the raw data matrix was also explored. It is recommended that the raw data matrix should be consulted to confirm the observations from a PCA biplot.

Due to the relatively low data variance explained by the PCA analysis, it became clear that further data analysis was needed to further help in the interpretation of the observations derived from the PCA biplot. For this purpose, PROMETHEE analysis, a non-parametric method, was also carried out. The raw data matrix was also explored.

As discussed in Section 3.3.4, to set up a model for PROMETHEE analysis, a specific preference function, threshold value and weighting must be defined for each criterion. To facilitate the ranking order of the objects from best to worst performance, the parameters were maximised. In the present study, quartz was minimised, as a lesser quartz content would enhance the physical and chemical parameters such as SSA and ECEC. This indicates that the best performing samples would be low in quartz content. In this study, the V-shaped preference function was selected for all variables, and preference threshold  $p$  was set to the maximum load for each criterion (variable) other than quartz (Herngren et al. 2005; Ayoko et al. 2007). All parameters were given the same weighting, and hence, no variable was favoured over others. Therefore, the ranking was undertaken from the top down (maximised) selection so that the higher values of variables were ranked first. Furthermore, the PROMETHEE II ranking carried out was used to select suitable samples for the batch adsorption experiment described in Section 4.6. Details of the sample selection for the batch experiment are described in Section 7.2.

### **Data pre-processing**

Data pre-processing is carried out prior to submission to PCA and PROMETHEE analysis to avoid biased outcomes. All variables measured as concentrations were



converted into load per unit weight of build-up load (mg/g). This eliminated any bias due to different build-up loads at different sites (Section 5.2). Parameters measured in dry condition were converted per unit weight of solids. For example, SSA ( $\text{m}^2/\text{g}$ ), ECEC (meq/100g) and mineralogy was considered as a percentage of unit weight of solids. Furthermore, to extract data variance effectively, it was important to reduce noise in the raw data matrix and all the variables needed to have equal weight in the analysis (Purcell et al. 2005; Settle et al. 2007). Hence, the data matrix was auto scaled prior to the PCA analysis. Outlying objects of the data were identified using the Hotelling T2 test (See Section 3.3.2 and Section 5.4.2). After removing the outlying objects, the data matrices were subjected to PCA. Notations used for the objects (road deposited solids) were similar to those used in the analysis discussed in Section 5.4.2.

#### **5.5.1 ANALYSIS OF PHYSICAL AND CHEMICAL CHARACTERISTICS FOR DIFFERENT PARTICLE SIZES**

Particle properties were separately investigated for the different particle size ranges of solids. The particle size ranges were:  $<75\mu\text{m}$ ,  $75\text{-}150\mu\text{m}$ ,  $150\text{-}300\mu\text{m}$  and  $300\text{-}425\mu\text{m}$ . The following section describes the outcomes of the analysis in each particle size range.

##### **Particle size $<75\mu\text{m}$**

Preliminary data analysis indicated that this particle size range accounted for 50% of the build-up pollutants. The particle size contained about 40% amorphous material, 33% quartz, 11.5% albite, 5% microcline, 3.5% chlorite, and 6.5% muscovite. Average particle properties were: 9.5 meq(+)/100g ECEC, 3mg/g TOC (nearly 60%) and  $18\text{m}^2/\text{g}$  of SSA. This size range was responsible for the highest physical and chemical parameter values of build-up pollutants.

PCA analysis was carried out on the pre-treated data matrix of  $32 \times 9$ . The number of PCs used for the analysis was determined according to the Scree plot method. Consequently, two PCs for the analysis were selected based on the pronounced change of slope shown in the Scree plot (Appendix A/Figure A.5). The resulting

biplot of PC 1 vs PC 2 is shown in Figure 5.8. As can be seen in Figure 5.8, the first two PCs accounted for 31.8% and 16.9% of the total variance respectively; this is a total variance of 48.7%. The total variance accounted for by the first two principal components is comparatively low. Due to the low variance, the observations derived from Figure 5.8 required further analysis for confirmation.

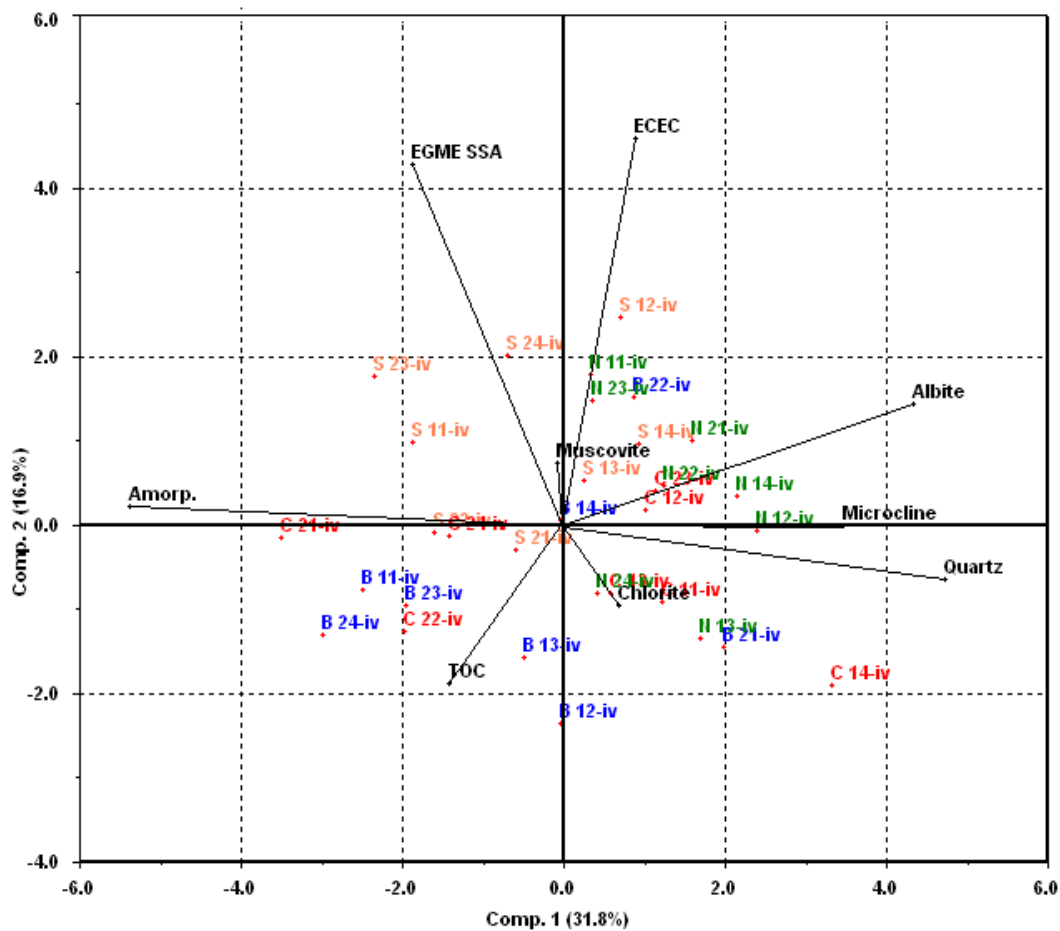


**Figure 5.8: PC 1 vs PC 2 biplot obtained from PCA on the particle size range <75 $\mu$ m**

Note: C– Clearview Estate, N- Nerang, B- Benowa, S- Surfers Paradise, 1 and 2- first and second sampling event, iv– particle size <75 $\mu$ m

As seen in Figure 5.8, PC 1 describes the variation of solids composition where mineralogical components of albite, microcline and quartz are in the direction of positive PC 1, while the amorphous content is in the direction of the negative PC 1 axis. PC 2 describes the variation of particle properties where SSA and ECEC are in the direction of the positive PC 2 axis, whilst TOC is in the direction of the negative

PC 2 axis. Objects which are in the positive PC 2 domain are highly correlated to ECEC and SSA. Similarly, the objects in the negative PC 2 domain, which are the Benowa and Clearview Estate samples, are highly correlated to organic matter content. As discussed in Section 5.3, this is due to the fact that residential sites in Benowa and Clearview Estate contribute high organic matter content to road surfaces.

As seen in Figure 5.8, high variance associated with ECEC and SSA indicates that these physical and chemical parameters are significantly high in the  $<75\mu\text{m}$  particle size range. SSA shows strong correlation to ECEC. This suggests that the high SSA of  $<75\mu\text{m}$  particles is associated with high exchangeable sites. The particles with high SSA would exhibit higher ECEC. High values of both parameters confirm the favourable influence of this particle size on heavy metal adsorption. ECEC is strongly correlated with clay forming minerals of muscovite and albite, and weakly correlated with microcline. As noted by past researchers, both albite and microcline (feldspar) minerals contain permanent negative charges due to the isomorphous substitution in their lattice structure (Filep 1999; Sparks 2003). Thus, high clay forming mineral content in this particle size range has contributed to high ECEC.

ECEC shows a negative correlation with TOC. As a principle, organic matter content which is in the form of humus (decomposed fraction) should contain higher cation exchange capacity than the clay minerals (Sparks 2003). However, according to Figure 5.8, it appears that the contribution of TOC content to ECEC in this particle size range is insignificant. Therefore, it can be concluded that the nature or source of organic matter in road deposited solids is influenced by the low contribution of TOC to the ECEC of solids. TOC in this particle size range is  $<0.5\%$  of the total sample weight (Table 5.2). Therefore, the elevated level of clay forming minerals in solids is partly responsible for this behaviour of TOC. Consequently, it is suggested that ECEC in this particle size range is mostly derived from mineralogy rather than organic matter content, and ECEC depends on the CEC/clay ratio (Carroll et al. 2004). Thus, road deposited solids samples with high clay forming minerals would exhibit high adsorption ability due to the correspondingly high ion exchange capacity.

As seen in Figure 5.8, quartz is negatively correlated to amorphous content. This indicates that the reduction in quartz content in solids samples would influence the increase in amorphous content. However, correlation of quartz with the feldspar mineral group (albite and microcline) and chlorite is opposite to the behaviour shown by the build-up samples discussed in Section 5.4. This could be attributed to the low percentage of quartz in the  $<75\mu\text{m}$  particles, since the amorphous content is the dominant component in this particle size range in a majority of the samples (See Section 5.3.2). Therefore, the properties and composition of amorphous material can have a significant influence on the physical and chemical parameters of  $<75\mu\text{m}$  solids particles.

Amorphous content shows strong negative correlation or no correlation to other mineralogical components of the solids. Thus, it suggests that a significant portion of amorphous content is derived from material other than un-diffracted mineral components. Furthermore, the amorphous content is associated with highly urbanised road sites in Surfers Paradise and Benowa (Figure 5.8). Therefore, it can be argued that the majority of the amorphous content in the road deposited solids could originate from traffic related sources. This confirms the outcomes derived in Section 5.4. Amorphous content has a weak correlation with ECEC and TOC. As identified in Section 3.5.2, amorphous content in this particle size range contains minor fractions of clay minerals which have high cation exchange capacity. Therefore, amorphous content in this particle size range would involve metal adsorption to particles.

Even though the samples for this study were selected from four different suburbs, distinct groups of objects cannot be observed in the PCA biplot (Figure 5.8). However, objects belonging to different suburbs form groups that intersect. Clusters with common characteristics are attributed, as the physical and chemical parameters of road deposited solids could be unique for a specific particle size which is mainly influenced by the solids composition. As observed in Section 5.3.3, this particle size range is dominated by traffic generated pollutants and these pollutants could have similar characteristics independent of geographical location or land use.

Furthermore, due to the low data variance explained by the PCA biplot, PROMETHEE II ranking and GAIA analysis was carried out to classify the objects and to confirm the observation derived by the PCA. Initially, PROMETHEE and GAIA analyses were carried out for the same data matrix (32 x 9) which was subjected to PCA. It was difficult to discriminate object groups on the basis of sites in the resulting ranking, due to the number of variables influencing the physical and chemical parameters of solids. Therefore, in order to explore this data set, sequential PROMETHEE analysis was carried out, starting from a small 16 x 9 matrix (Ni et al. 2010). Then, by eliminating randomly distributed objects in the ranking, two separate groups of objects were initially identified (refined data set). Gradually, more sets of objects were sequentially added to the refined data set, and by eliminating random objects, four separated object groups (basic data set) were identified in the ranking. Ultimately, the data analysis encompassed the entire data matrix; this enabled conclusions to be drawn based on the behaviour of the basic data set.

Initially, Surfers Paradise and Clearview Estate objects were selected since they represented the study sites which were the furthest apart. This matrix (16 x 9) was analysed using the PROMETHEE model described in Section 5.5, and the resulting PROMETHEE II net ranking order,  $\Phi$ , is given in Appendix A/Table A.8. According to the ranking, sites from the coastal suburb ranked first, confirming that these objects are enriched with high physico-chemical parameters that preferred pollutant adsorption, whilst objects of inland sites consisted of poorly favourable adsorbent properties.

The refined data set (13 x 9) was then derived by excluding the objects that were ranked in random order. The PROMETHEE II net ranking order for the refined data set showed two clearly separated object groups (Appendix A/Table A.9). Then, eight Nerang objects were added to this refined data set and submitted for the PROMETHEE II ranking, applying the same modelling condition as for the initial data set. The addition of Nerang objects influenced the preferred order, and these objects were spread between the extreme ends of the refined data set. The randomly ranked objects were again excluded from the data matrix. Next, the Benowa objects were added to the previous data matrix and refined by excluding randomly oriented

objects. Finally, the basic data set was identified. This data set consisted of 17 objects out of 32 original objects. In the resulting GAIA biplot of 17 x 9 matrix (Appendix A/Figure A.6), four suburbs are clearly distinguished from each other. The PROMETHEE II net ranking of this basic data set (Table 5.6) shows the objects are ranked in the order of geographical location, where Surfers Paradise objects are ranked at the top. It indicates a similar phenomenon to that explained above: that pollutant association to solids in coastal suburbs would be high in this particle size range.

**Table 5.6: Basic data set for PROMETHEE II ranking for particle size <75 $\mu$ m**

Sample	Net $\Phi$	Ranking order	Sample	Net $\Phi$	Ranking order
S 22-iv	0.255	1	N 23-iv	-0.033	10
S 14-iv	0.123	2	N 22-iv	-0.063	11
S 13-iv	0.120	3	N 21-iv	-0.071	12
S 21-iv	0.106	4	N 14-iv	-0.072	13
B 13-iv	0.072	5	N 13-iv	-0.107	14
B 11-iv	0.038	6	C 13-iv	-0.113	15
B 23-iv	0.033	7	C 11-iv	-0.124	16
B 21-iv	0.025	8	C 14-iv	-0.179	17
B 12-iv	-0.011	9			

Note: C– Clearview Estate, N- Nerang, B- Benowa, S- Surfers Paradise

With this basic understanding, the whole data set (32 x 9) was subjected to PROMETHEE and GAIA analysis and the resulting PROMETHEE II net ranking is shown in Table 5.7. Objects of Benowa are randomly scattered in the ranking given in Table 5.7, which indicates the wide variability of physical and chemical properties of these objects. However, according to the  $\Phi$  values in Table 5.7, it is evident that the six groups of objects are clearly separated. In the top cluster, the rank number from 2 to 5 has practically the same  $\Phi$  value. Similarly, groupings can be identified in rankings of 6 to 9, 10 to 13, 14 to 20, 21 to 26 and 27 to 32. This practically explains that even when the objects are ranked in a scattered manner, they have the

same properties. For example, Group 6 to 9 have objects from the four suburbs of Nerang, Clearview Estate, Benowa and Surfers Paradise and have less than 10% variance in their  $\Phi$  values.

Additionally, the raw data indicated that these objects have similar clay forming mineral content, amorphous content and specific surface area. This indicates that, although these objects lie in a random manner, they have similarity in solids composition and physical and chemical parameters to the cluster to which they belonged. Thus, it can be concluded that the solids composition is the most important indicator in the variation of physical and chemical properties of solids. However, physical and chemical properties of solids are not independent of land use and geographical location, since these site specific characteristics influence the sample composition. This is also in agreement with the conclusions drawn from the PCA biplot.

The GAIA biplot (Appendix A/Figure A.7) obtained for the above matrix accounts for 70.04% of the data variance and shows similar correlations to those observed in the PCA biplot (Figure 5.8). The GAIA biplot supports the initial PCA observation (Figure 5.8) in terms of correlations of criteria vectors. As can be seen in Appendix A/Figure A.7, ECEC strongly correlates with SSA. In addition, the negative correlation between TOC and ECEC observed in Figure 5.8 can also be seen in the GAIA biplot. Quartz shows strong correlation to amorphous content in the GAIA biplot, which is contrary to the observation from the PCA analysis. Minimisation of quartz criteria in the PROMETHEE model leads to this observation. The decision axis,  $\pi$ , is relatively long and oriented in the direction of EGME SSA and ECEC, indicating the high degree of significance of these parameters in this particle size. Additionally, the GAIA biplot shows that amorphous content has a weak correlation with SSA, and no correlation to ECEC. Hence, it indicates that even though amorphous material has high surface area, it does not behave as a binding site for pollutants. Therefore, pollutants in amorphous content would be present as residual fraction or as surface precipitation. The GAIA biplot obtained from the non-parametric method reflects similar correlations obtained using the PCA biplot; this confirms the validity of the correlations made through the PCA.

**Table 5.7: PROMETHEE II ranking for particle size <75µm**

Sample	Net $\Phi$	Ranking order	Sample	Net $\Phi$	Ranking order
S 22-iv	0.253	1	B 12-iv	-0.013	17
B 14-iv	0.163	2	S 24-iv	-0.014	18
S 13-iv	0.126	3	N 12-iv	-0.014	19
S 14-iv	0.125	4	C 12-iv	-0.016	20
S 21-iv	0.112	5	N 23-iv	-0.034	21
N 11-iv	0.093	6	B 24-iv	-0.058	22
C 23-iv	0.077	7	C 22-iv	-0.062	23
B 13-iv	0.073	8	N 22-iv	-0.063	24
C 21-iv	0.052	9	N 21-iv	-0.070	25
S 12-iv	0.036	10	N 14-iv	-0.072	26
B 23-iv	0.036	11	N 13-iv	-0.106	27
B 11-iv	0.035	12	C 13-iv	-0.111	28
B 21-iv	0.033	13	C 11-iv	-0.122	29
S 11-iv	0.015	14	B 22-iv	-0.152	30
C 24-iv	0.014	15	N 24-iv	-0.167	31
S 23-iv	0.004	16	C 14-iv	-0.172	32

Note: C– Clearview Estate, N- Nerang, B- Benowa, S- Surfers Paradise

### **Particle size 75-150µm**

This particle size accounts for 24% of the build-up pollutants. On average, these solids particles contain 30% of amorphous, 45% of quartz, and the rest accounts for clay forming minerals. The organic matter content in this particle size range is relatively low compared to the <75µm particles. The particle size exhibits relatively high SSA and high ECEC. With this understanding, PCA analysis was carried out to identify the correlations of physical and chemical parameters. The biplot obtained for the pre-treated data matrix of 32 x 9 is shown in Figure 5.9. Two principal components were suggested by the Scree plot shown in Appendix A/Figure A.8. As can be seen in Figure 5.9, the first two PCs account for 29.4% and 15.9% variance, which represents a total variance of 45.3%. The low variances explained by the two principal components suggested the necessity of another qualitative analysis to confirm the conclusions derived from the PCA biplot. Consequently, similar to the particle size <75µm, PROMETHEE II ranking and GAIA were used in this particle size range to classify the objects and to confirm the conclusions derived.



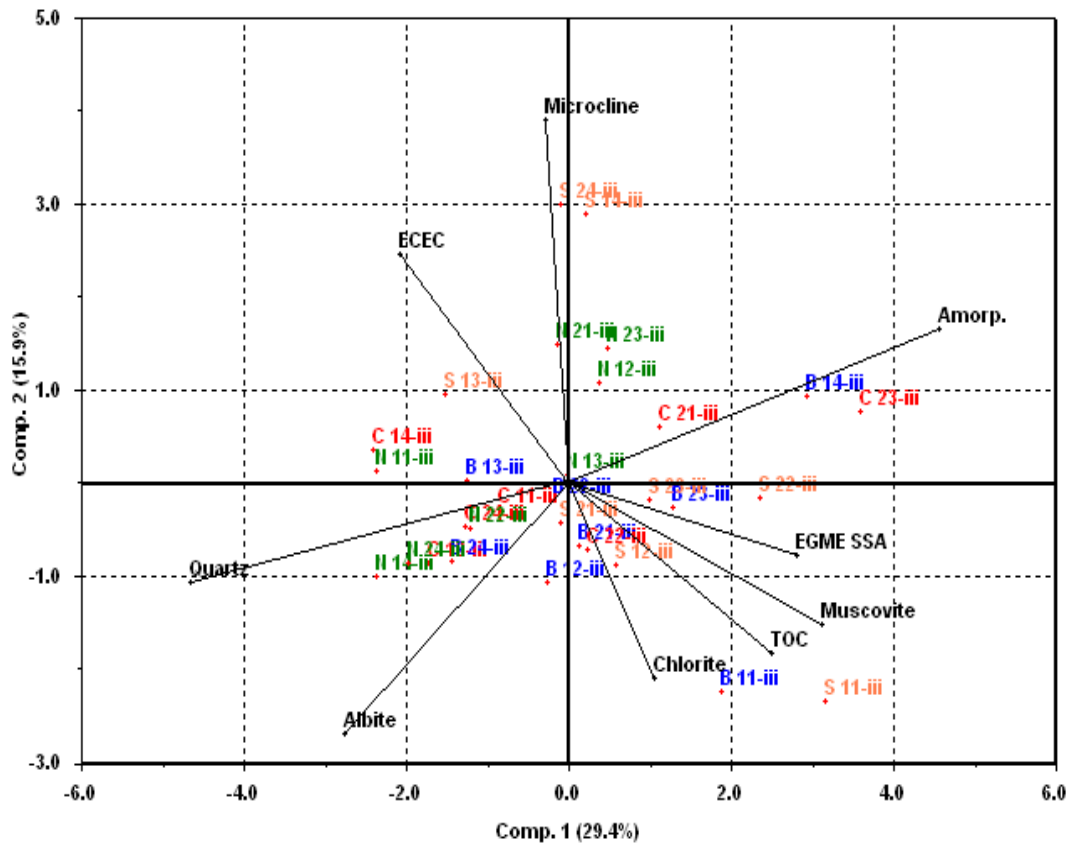


**Figure 5.9: PC 1 vs PC 2 biplot obtained from PCA on the particle size range 75-150µm**

Note: C– Clearview Estate, N- Nerang, B- Benowa, S- Surfers Paradise, 1 and 2- first and second sampling event, iii- particle size 75-150µm

As seen in Figure 5.9, PC 1 describes the variation of solids composition. Amorphous, muscovite and TOC are located along the positive PC 1 axis, and albite, quartz and ECEC along the negative PC 1 axis. PC 2 describes the variation of parameters responsible for the pollutant adsorption to particles. It is positively associated with ECEC and negatively associated with the clay forming minerals, EGME SSA and TOC. The majority of the objects in the PCA biplot are scattered, while most of the objects from the Nerang suburb form a cluster.

According to Figure 5.9, ECEC is located on the positive PC 2 axis and negative PC 1 quadrant, indicating the significance of ECEC in this particle size range. Thus, this implies that considerable amounts of pollutants could be attached to solids by ion

exchange mechanism in this particle size range. Similar to the  $<75\mu\text{m}$  particles, ECEC has strong correlation with microcline (feldspar) mineral and has negative correlation with organic matter. Hence, it suggests that the contribution of organic matter content to ECEC is very low in this particle size range also. Once again, this indicates that the CEC/clay ratio is the predominant parameter for ECEC compared to the organic matter content.

As evident in the PCA biplot, SSA is strongly correlated to muscovite, chlorite and TOC. Hence, it can be suggested that the surface area of particles would be mainly defined by the clay forming minerals and organic matter. However, these parameters do not correlate with ECEC. Therefore, it can be suggested that clay forming minerals and organic matter have high SSA which favours the high adsorption of metal elements to particles; however, the association could be occurring through a mechanism such as chemisorption (surface complexation) or precipitation.

Once again, amorphous content shows high variance along PC 1; this suggests that it is a significant component in the solids composition. Similar to the relationships observed in the particle size  $<75\mu\text{m}$ , amorphous content shows strong correlation with SSA and is weakly correlated to TOC. Thus, the amorphous content is a material with high SSA and organic matter content which could act as a carrier for high pollutant load. However, it can be suggested that the amorphous material would not associate with pollutants via ion exchangeable mechanism due to the low ECEC characteristics of this material. As identified in the  $<75\mu\text{m}$  particles, the amorphous content could account for material other than mineral components that typically result from traffic related activities.

PROMETHEE and GAIA analysis was carried out to identify the variation of physical and chemical parameters in this particle size range and to classify the objects. The data matrix of  $32 \times 9$  was analysed by applying the same model conditions used for the particle size  $<75\mu\text{m}$ . The PROMETHEE II net ranking order resulted in scattered distribution of objects, as given in Appendix A/Table A.10. Therefore, similar to the procedure for particle size  $<75\mu\text{m}$ , sequential

PROMETHEE analysis was carried out by eliminating randomly oriented objects and obtaining the basic data set. Consequently, the understanding gained from the basic data set was used to classify the objects in the PROMETHEE II net ranking of the whole matrix (Appendix A/Table A.10). Accordingly, it was found that Surfers Paradise objects are ranked at the top and the Nerang objects are ranked at the bottom, whilst the Benowa and Clearview Estate objects are scattered in between. This indicates that the samples in Surfers Paradise would contain characteristics favourable for pollutant adsorption in this particle size range. As in the case of the  $<75\mu\text{m}$  particles, this suggests that the physical and chemical properties of solids are governed by the particle composition, rather than by the sampling location or land use characteristics.

The GAIA biplot (Appendix A/Figure A.9) obtained for the above matrix accounts for 50% of the data variance, and it shows a similar distribution of objects to that found in the PCA biplot shown in Figure 5.9. In both figures, with the exception of the Quartz vector, all the variable vectors are oriented roughly in the same direction. In the PROMETHEE model, quartz was minimised, while all the other criteria were maximised. This has influenced the opposite orientation of the quartz vector in the GAIA biplot. Therefore, the GAIA biplot also shows the same correlations as the PCA biplot. Hence, the comparisons made with the aid of the MCDM methods, PROMETHEE and GAIA indicated the validity of the conclusions made through PCA analysis.

### **Particle size 150-300 $\mu\text{m}$**

This particle size represents less than 17% of the build-up pollutants. This size exhibited a sandy matrix with 67% quartz content. Amorphous content in this particle size was relatively low compared to the  $<150\mu\text{m}$  particle sizes. ECEC and TOC for this particle size range lie in the medium range compared to other particle sizes. PCA analysis was carried out based on pre-treated data matrix of 32 x 9. Figure 5.10 shows the principal component biplot for the first two PCs for this particle size range. The first two principal components were selected for analysis based on the Scree plot (Appendix A/Figure A.10). Accordingly, the selected first

two principal components account for 32.5% and 15.8% of the total data variance. Due to the relatively low data variance explained by the first two principal components (48.3%), it was necessary to use a different qualitative analysis to confirm the conclusions derived, as in the case of particle sizes <75µm and 75-150µm. For this purpose, PROMETHEE II ranking and GAIA analysis was carried out.

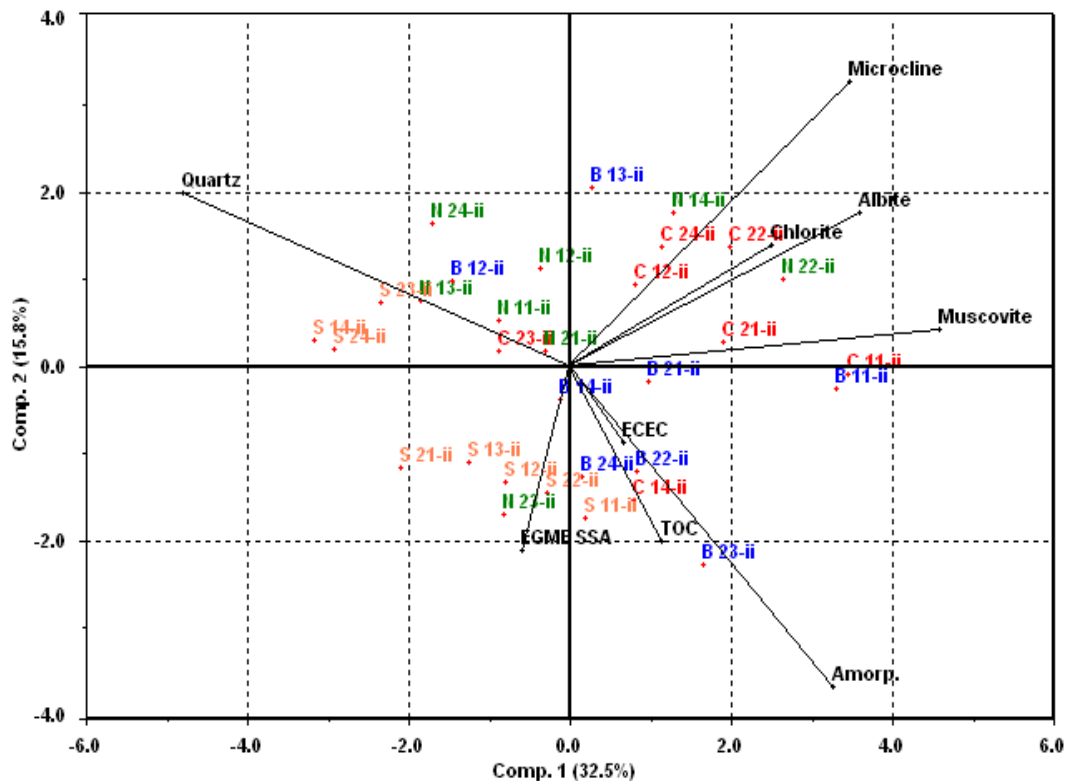


**Figure 5.10: PC 1 vs PC 2 biplot obtained from PCA on the particle size range 150-300µm**

Note: C– Clearview Estate, N- Nerang, B- Benowa, S- Surfers Paradise, 1 and 2- first and second sampling event, ii- particle size 150-300µm

As seen in Figure 5.10, particle mineralogical variation is along PC 1. Other than quartz, all of the mineral components are located on the positive PC 1 axis, whilst quartz is located on the negative PC 1 axis. PC 2 describes the variation of physical and chemical properties where all mineral components are in the direction of positive PC 2, while ECEC, TOC and SSA are in the direction of the negative PC 2 axis. Other than amorphous material, all of the mineralogical components (muscovite,

chlorite, microcline, albite and quartz) are positively associated with PC 2. Thus, source variability of pollutants can also be clearly observed in the PCA biplot.

Separation of objects from different road surfaces can be seen in Figure 5.10. Similar to the observations for finer particles, this is attributed to the differences in particle composition and the physical and chemical parameters. For example, Surfers Paradise objects are distributed with quartz and amorphous variables. Benowa objects are distributed with amorphous and clay forming minerals. Nerang and Clearview Estate objects are distributed with clay forming minerals and quartz content. As identified in the fine particle sizes, the distribution of objects in the PCA biplot is principally due to the variation in mineralogical composition of the samples.

As evident in Figure 5.10, variance associated with ECEC is very low compared to particle sizes 75-150 $\mu\text{m}$  and <75 $\mu\text{m}$ . This indicates that the 150-300 $\mu\text{m}$  particle size would contain low cation exchange capacity. Strong negative correlation of ECEC and quartz indicates that the increase in quartz content in this particle size has influenced the reduction of ECEC of solids. Therefore, pollutant adsorption by ion exchange in this particle size would be very low. Interestingly, SSA, TOC and ECEC are strongly correlated with each other in this particle size range, while ECEC is weakly correlated with clay forming minerals. This implies that ECEC in this particle size is influenced more by the organic matter content than by the mineral components. Therefore, heavy metals adsorbed to organic matter would be high and adsorption could mainly occur by ion-exchange. Furthermore, SSA leads to the increase in pollutant adsorption to particles by providing a large surface area for the interaction of cations with the particle surface.

Amorphous content shows strong correlation with ECEC, TOC, and EGME SSA. Correlation with ECEC implies that a significant quantity of surface active substances could be contained in amorphous material. These could be organic matter, metal oxides or un-diffracted mineral components. Therefore, amorphous content in this particle size fraction would act as a binding site for heavy metal cations. Thus, amorphous content in larger particles would contain lower traffic related material when compared to the fine particles.

Albite, microcline, chlorite and muscovite show strong correlation to each other. Therefore, the influence of each of these mineral components on particle properties would be very similar in this particle size range. Therefore, similar contributions can be expected by clay forming minerals for heavy metal adsorption in this particle size range. As expected, quartz shows physical and chemical characteristics which are independent of other mineral components. This behaviour was not observed in the case of the finer particle sizes. As observed in Section 5.3.3, this could be attributed to the dominant quartz content in the particle size range. Therefore, the particle size range 150-300 $\mu\text{m}$  would exhibit physical and chemical parameters which are related to quartz and would also influence the associated pollutant concentration.

PROMETHEE analysis was carried out to characterise the variation in objects and resulted in a highly scattered distribution in the PROMETHEE II net ranking order (Appendix A/Table A.11). Therefore, similar to <75 $\mu\text{m}$  and 75-150 $\mu\text{m}$  particle sizes, the sequential PROMETHEE analysis was carried out excluding randomly ranked objects, as described previously. The basic data set obtained from the analysis (Appendix A/Table A.12) revealed that the Clearview Estate samples were ranked first and Surfers Paradise Samples were ranked last. Nerang and Benowa objects were ranked between these two suburbs. This indicates that in this particle size range, Clearview Estate samples are enriched with favourable physical and chemical parameters for adsorption. This is attributed to the high clay forming mineral content. Therefore, high pollutant adsorption characteristic can be expected in inland sites for larger particles.

The GAIA biplot for the above matrix (Appendix A/Figure A.11) accounts for 53% of the total data variance. Similar to the finer particles, all of the variables in the GAIA biplot, other than quartz, are oriented approximately in the same direction as in the PCA biplot. However, the TOC criteria vector is very long in the GAIA biplot; this indicates significant TOC content in this particle size range. The object distribution was also found to be similar to the PCA biplot. The correlations observed through the GAIA analysis are similar to the PCA analysis. This confirms the observations derived from PCA analysis, although the variance associated with PC 1 vs PC 2 is low.

### Particle size 300-425µm

Particle size 300-425µm represented nearly 9% of the total sample. Sample composition was predominantly a sandy matrix containing low amorphous content. Physical and chemical parameters such as ECEC, TOC and clay formed the mineral content and amorphous content was in a similar range to that of particle size 150-300µm. For the PCA analysis carried out, the resulting biplot is shown in Figure 5.11. The number of PCs for the analysis was determined by the Scree plot method (Appendix A/Figure A.12) and the first two PCs were selected to investigate the physical and chemical parameters. Variances explained by the two principal components are 33.8% and 18.9%, which amounts to 52.7%. As for the fine particle sizes, due to the relatively low data variance explained by the first two principal components, PROMETHEE II ranking and GAIA analysis were also carried out.

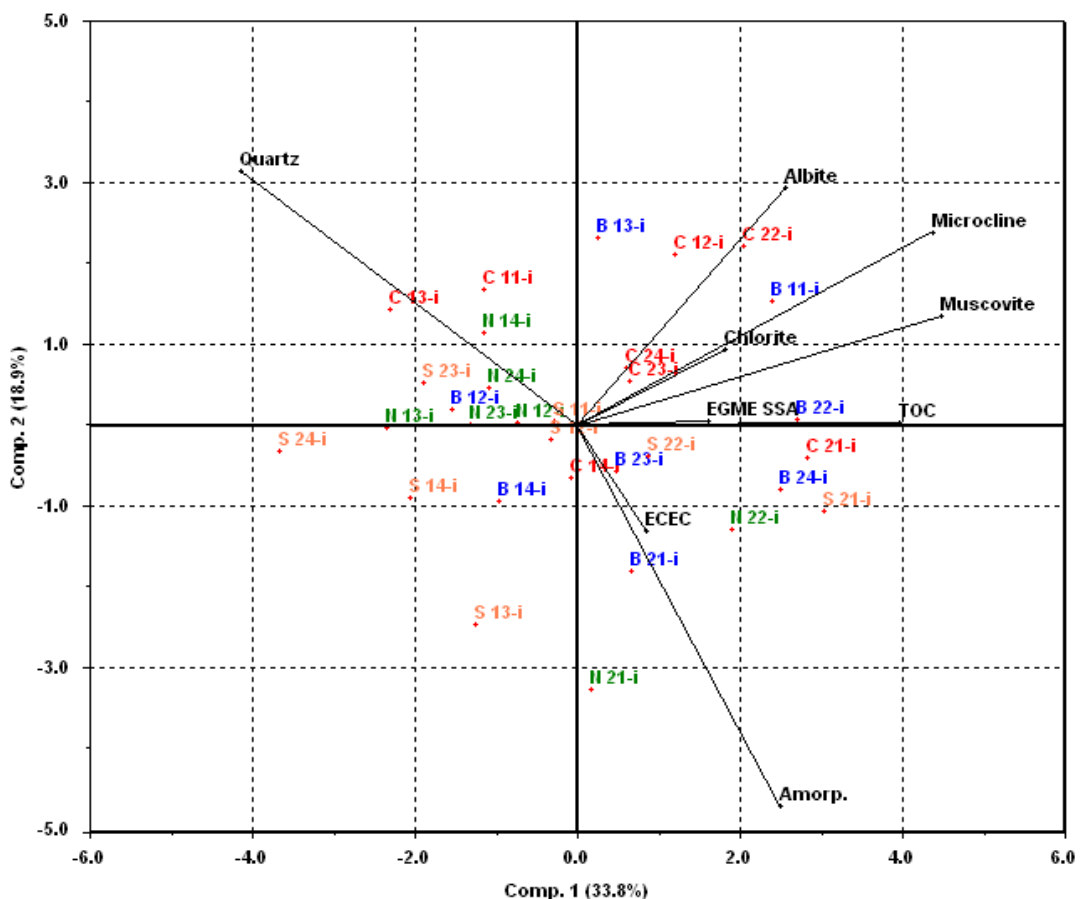


**Figure 5.11: PC 1 vs PC 2 biplot obtained from PCA on the particle size range 300-425µm**

Note: C– Clearview Estate, N- Nerang, B- Benowa, S- Surfers Paradise, 1 and 2- first and second sampling event, i- particle size 300-425µm

As evident in the PCA biplot (Figure 5.11), variability of particle properties is explained by PC 1, where SSA, TOC and ECEC are positively associated with this axis. Variation of solids composition is explained by PC 2, with mineralogical components of albite, microcline, muscovite and quartz located along the positive axis, while the amorphous content is located along the negative PC 2 axis.

Similar to the particle size 150-300 $\mu\text{m}$ , the variation associated with ECEC is relatively low; this indicates the low ion exchange capacity of this particle size range. This could be attributed to the high quartz content in the solids, which leads to the reduction in ECEC. However, ECEC strongly correlates with amorphous content. This suggests that the amorphous material in this particle size range would have the ability to adsorb cations. This could be attributed to the TOC content in amorphous material. Similarly, TOC and clay forming minerals such as albite, muscovite and chlorite content could also be responsible for ECEC of the samples. SSA and TOC are strongly correlated, whilst SSA is closely correlated to all of the clay forming minerals and amorphous content. This could be attributed to the structure and surface characteristics of organic matter and clay forming minerals.

Other than the quartz content, all of the physical and chemical parameters of solids are along the positive PC 1 axis; the quartz content in sample is along the negative PC 1 axis. Thus, quartz would possess physical and chemical characteristics independent of the other mineral components and also provide a relatively lower contribution to the physical and chemical parameters investigated. This is similar to the correlations found for the particle size 150-300 $\mu\text{m}$ . Correlations of amorphous content with other physical and chemical parameters also show similar behaviour to the 150-300 $\mu\text{m}$  particle size. Furthermore, all of the clay forming minerals (microcline, albite, muscovite and chlorite) show strong correlation. Thus, the variation of these clay forming minerals could be explained by a single variable. Variations observed in the majority of the variables are similar to those for particle size 150-300 $\mu\text{m}$ . The particle size 150-300 $\mu\text{m}$  and 300-425 $\mu\text{m}$  show similar mineralogical percentages, as described in Section 5.3 (Table 5.2). Hence, this implies that the majority of the physical and chemical parameters of solids are governed by the mineralogical composition of the sample. Additionally, Clearview



Estate samples are mostly associated with the clay forming mineral components. Therefore, it can be concluded that inland road sites would contain relatively higher clay forming minerals compared to other sites, even for the large particle size 300-425 $\mu\text{m}$ .

The PROMETHEE II ranking given in Appendix A/Table A.13 shows the widely scattered objects of the four suburbs. However, by sequentially excluding the objects as in the previous analysis, the basic data set was extracted. It revealed four clear clusters which ranked Benowa and Clearview Estate at the top and Surfers Paradise at the bottom. This indicates that Clearview Estate and Benowa are enriched with physical and chemical parameters favourable for heavy metal adsorption. According to the raw data matrix, this occurs primarily due to the clay content in the samples. PROMETHEE ranking of 300-425 $\mu\text{m}$  particles also showed a variation similar to the particle size 150-300 $\mu\text{m}$ .

The GAIA biplot obtained for the data matrix accounts for 58% of the total data variance (Appendix A/Figure A.13). PC 1 and PC 2 of the GAIA biplot were associated with the same criteria vectors as observed for the PCA biplot, and correlations found in the GAIA analysis are similar to those found in the PCA analysis. As in the case of the fine particle size ranges, GAIA analysis confirmed the correlations obtained from the PCA analysis.

## 5.6 CONCLUSIONS

The focus of this chapter was to investigate the variation of physical and chemical parameters of road deposited solids for different particle sizes. Accordingly, particle size distribution (PSD), solids load, total organic carbon (TOC), specific surface area (SSA), cation exchange capacity (ECEC) and mineralogy were investigated. Initially, univariate statistical analysis was carried out for each of the parameters to examine the differences in relation to particle size and sampling areas. Additionally, in order to identify the sources of particulate pollutants, a comparison of build-up samples with road side soil samples was undertaken. Finally, multivariate data analysis was

carried out to articulate the variations of all of the parameters for each particle size range. Univariate analysis indicated that physical and chemical parameters such as TOC, SSA, ECEC and clay forming minerals increase with the reduction in particle size. Table 5.8 provides a summary of the findings, and important outcomes from the analysis are then listed.

**Table 5.8 Physical and chemical properties and influential factors for different particle sizes**

<b>&lt;75µm</b>	<b>75-150µm</b>	<b>150-300µm</b>	<b>300-425µm</b>
Contains high organic carbon content  Benowa and Nerang show high TOC (R, C and I)	Contains relatively low organic matter content  Clearview Estate and Benowa show high TOC (R and C)	Contains low organic matter content  Clearview Estate and Benowa show high TOC (R and C)	Contains low organic matter content  Benowa and Clearview Estate show high TOC (R and C)
Clay rich minerals with high anthropogenic pollutants  Amorphous 40%, Quartz 32%, Clay forming minerals 26%	Clay rich minerals with medium anthropogenic pollutants  Amorphous 29%, Quartz 44%, Clay forming minerals 26%	Sandy matrix with low anthropogenic pollutants  Amorphous 18%, Quartz 68%, Clay forming minerals 13%	Sandy matrix with low anthropogenic pollutants  Amorphous 19%, Quartz 67%, Clay forming minerals 13%
High SSA which was mainly attributed to clay and amorphous content  Low influence of organic matter content	Medium SSA which was mainly attributed to clay forming minerals and amorphous content  Low influence of organic matter content	Negligible differences in SSA	Negligible differences in SSA
High ECEC mainly attributed to clay minerals  SSA has significant influence	Medium ECEC mainly attributed to clay forming minerals  SSA and organic matter have significant influence	Low ECEC mainly attributed to organic matter and clay forming minerals	Low ECEC mainly attributed to organic matter  Clay forming minerals have significant influence

Note: R– Residential, C– Commercial, I– Industrial

- Build-up pollutant load on the selected road surfaces is influenced by the road surface condition, traffic density, dry period and land use characteristics. More than 70% of the build-up pollutants on road surfaces are finer than 150 $\mu$ m particles.
- The particle size is the primary indicator of the physical and chemical properties of solids. SSA, TOC and ECEC decrease with the increase in particle size. Solid particle mineralogy also exerts an influence on the physical and chemical parameters.
- Residential land uses had the highest organic matter content. This suggests that the high percentage of organic carbon content in street deposited solids can be mainly attributed to plant debris.
- EGME SSA was identified as the most suitable method for determining SSA of road deposited solids.
- Antecedent dry period has an influence on the total surface area (EGME SSA) of the solids particles due to the internal cracks generated within the particle and morphological changes to the particle surface caused by traffic activities.
- The solids particles on road surfaces were predominantly composed of soil derived mineral components that originate from surrounding land uses. Quartz was the dominant mineral in larger particles and ranged between 40-50% of the sample, irrespective of the geographical location.
- Mineralogical analysis, together with clay analysis, indicated that traffic related sources contribute about 30% of the amorphous material to the build-up pollutant load. These particles contain traffic related abrasion products such as tyre wear, brake pad wear and corrosion products. The remaining portion of the amorphous content contained organic matter and minor fractions of non-crystalline minerals.
- Amorphous content is a material with high SSA which could be expected to carry high pollutant load. However, other than the pollutants in the residue of traffic related materials, pollutant adsorption to amorphous material through ion exchange is relatively low compared to the other minerals; this is due to the low influence of ECEC.

- ECEC in road deposited solids is mostly attributed to the clay forming minerals, rather than to the organic matter content. Therefore, pollutants associated by ion exchange would be mostly present in the clay forming minerals content of the road deposited solids.
- The physical and chemical parameters of road deposited solids are significantly influenced by the solids composition. The physical and chemical properties of solids are not independent of land use and geographical location, as site specific characteristics influences solids composition.
- Clear separation of physical and chemical characteristics of road deposited solids could be identified in particles larger than, and smaller than, 150 $\mu\text{m}$  due to the variation in the composition of mineralogical components and TOC content. Physical and chemical parameters of larger particles in the size range of 150-300 $\mu\text{m}$  and 300-425 $\mu\text{m}$  are less favourable to metal adsorption than the <150 $\mu\text{m}$  particles.
- Variations observed in the majority of the parameters in the particle size range 150-300 $\mu\text{m}$  are similar to the variations in the particle size range 300-425 $\mu\text{m}$ . Therefore, for analysis, these two particle sizes can be combined and considered as a single particle size of 150-425 $\mu\text{m}$ .
- In larger particles (150-300 $\mu\text{m}$  and 300-425 $\mu\text{m}$ ), muscovite is always correlated with SSA and chlorite content. Even though the correlation between chlorite and SSA is not always strong, muscovite has good correlation with both of these parameters. Similarly, microcline has close correlation with albite and chlorite. Therefore, chlorite and SSA can be considered as surrogates for muscovite and albite, and chlorite and ECEC as surrogates for microcline. Therefore, muscovite and microcline do not need to be included in the analysis.



# Chapter 6: Influence of Physical and Chemical Characteristics on Heavy Metals Adsorption

---

## 6.1 BACKGROUND

Numerous studies have shown that fine solids particles in stormwater runoff adsorb heavy metals to their surface (for example, Fergusson and Kim 1991; Smolders and Degryse 2002; Davis et al. 2001; Hengren et al. 2006). Heavy metal adsorption to road deposited solids is a complex process that can be influenced by a range of factors, such as available metal content and physical and chemical characteristics of the solids particles (Bachoc 1992; Morras 1995; Vignoles and Herremens 1995; Roger et al. 1998). However, in-depth studies explaining the role of different influential factors in heavy metal adsorption are limited (Liebens 2001; Lau et al. 2005).

In Chapter 5, variations of a range of influential physical and chemical characteristics of four different particle sizes of road deposited solids and correlations of these parameters were discussed. It was concluded that particle size and the composition of road deposited solids—which is primarily described by its mineral, amorphous and organic matter content—are the main factors that influence the physical and chemical characteristics. This chapter discusses the role of physical and chemical characteristics on heavy metal adsorption.

Initially, the primary characteristics of heavy metals associated with different particle sizes were investigated. This investigation was based on the hypothesis that particle size is the fundamental physical parameter which influences heavy metal adsorption. Variability of metal concentration with site specific characteristics was analysed, as available metal concentration is an important factor in further heavy metal adsorption to solids particles. The analysis was carried out individually for four different particle size ranges.

## 6.2 HEAVY METAL ADSORPTION IN DIFFERENT PARTICLE SIZE FRACTIONS

Data derived from field investigations were initially analysed to understand their general variability. In this regard, data relating to nine metal elements—including Iron (Fe), Aluminium (Al), Lead (Pb), Zinc (Zn), Cadmium (Cd), Chromium (Cr), Manganese (Mn), Nickel (Ni) and Copper (Cu)—adsorbed (total recoverable metal) in four particle size ranges (as identified in Chapter 5) were used. Heavy metal concentrations in each particle size range were measured using the acid extractable procedure described in Section 4.6.1. The dissolved metal (water-soluble metal) fraction was released during the wet sieving process (Table B.1 in Appendix B). Less than <24% of the total heavy metal content were present in dissolve form (Al, Mn, Fe, Ni, Cu and Pb) in build-up solids. The variability of heavy metals concentrations with catchment specific characteristics such as traffic and land use was investigated. The results obtained were compared with a range of published data to assess the consistency of the current data set.

Heavy metal weight per unit road surface area (metal loadings,  $\text{mg}/\text{m}^2$ ) obtained from the field investigations for each particle size fraction in each suburb were averaged for each suburb, as given in Table 6.1. The data relates to eight solids samples obtained from four road surfaces during two sampling episodes, for the calculation of average values. The results obtained for the four particle sizes ( $<75\mu\text{m}$ ,  $75\text{-}150\mu\text{m}$ ,  $150\text{-}300\mu\text{m}$ ,  $300\text{-}425\mu\text{m}$ ) investigated in the present study were compared with previously published data for similar particle size ranges of build-up. The present values are consistent with the metal loads in road deposited solids in industrial and commercial land uses reported by Lau and Stenstrom (2005). However, the metal loads observed in the present study are higher than the values reported by Hengren et al. (2006), but relatively lower than the values reported by Zhao et al. (2010). The differences in values with past studies is attributed to factors such as the variations in antecedent dry period at the time of sampling, the nature of anthropogenic activities, different sampling methods and the characteristics of the road surface texture (Sartor and Boyd 1972; Deletic and Orr 2005). Additionally, differences in traffic related heavy metals can be expected in different regions due to



**Table 6.1: Average heavy metal load in different particle sizes per unit area of road surface (average ± standard deviation)**

Suburb	Particle size (µm)	Al	Cr	Mn	Fe	Ni	Cu	Zn	Cd	Pb
		mg/m <sup>2</sup>								
Clearview Estate (R)	<75	12.4 ± 9.40	0.02 ± 0.01	0.47 ± 0.42	15.8 ± 16.5	0.01 ± 0.01	0.13 ± 0.11	0.40 ± 0.47	0.001 ± 0.001	0.06 ± 0.07
	75-150	10.6 ± 9.60	0.01 ± 0.01	0.42 ± 0.40	13.2 ± 11.6	0.02 ± 0.02	0.24 ± 0.10	0.73 ± 0.61	0.001 ± 0.001	0.07 ± 0.06
	150-300	5.30 ± 3.40	0.01 ± 0.01	0.22 ± 0.13	7.80 ± 4.70	0.01 ± 0.01	0.19 ± 0.10	0.37 ± 0.25	<0.001 ± 0.000	0.03 ± 0.02
	300-425	3.30 ± 1.20	0.02 ± 0.01	0.14 ± 0.15	6.40 ± 6.00	0.01 ± 0.01	0.12 ± 0.05	0.28 ± 0.26	<0.001 ± 0.000	0.05 ± 0.04
Nerang (I)	<75	24.8 ± 16.5	0.04 ± 0.02	1.01 ± 0.73	48.8 ± 28.6	0.06 ± 0.07	0.55 ± 0.37	1.90 ± 1.21	0.002 ± 0.002	0.29 ± 0.15
	75-150	7.40 ± 4.00	0.02 ± 0.02	0.48 ± 0.25	18.8 ± 9.50	0.04 ± 0.06	0.51 ± 0.37	1.14 ± 0.52	0.001 ± 0.001	0.19 ± 0.11
	150-300	8.10 ± 5.30	0.02 ± 0.02	0.51 ± 0.29	23.6 ± 17.6	0.05 ± 0.04	0.41 ± 0.30	1.15 ± 0.73	0.001 ± 0.001	0.16 ± 0.12
	300-425	8.30 ± 5.70	0.02 ± 0.01	0.26 ± 0.22	15.7 ± 13.5	0.01 ± 0.01	0.16 ± 0.08	0.55 ± 0.60	0.001 ± 0.001	0.05 ± 0.04
Benowa (R, I, C)	<75	30.1 ± 25.7	0.09 ± 0.06	0.79 ± 0.55	52.3 ± 48.5	0.06 ± 0.03	0.43 ± 0.42	1.72 ± 1.36	0.002 ± 0.002	0.46 ± 0.48
	75-150	14.9 ± 12.4	0.04 ± 0.03	0.47 ± 0.70	29.2 ± 27.7	0.04 ± 0.05	0.34 ± 0.33	1.43 ± 1.37	0.002 ± 0.002	0.26 ± 0.27
	150-300	5.20 ± 2.30	0.001 ± 0.001	0.18 ± 0.07	9.20 ± 4.10	0.01 ± 0.01	0.23 ± 0.11	0.72 ± 0.35	0.001 ± 0.001	0.12 ± 0.06
	300-425	4.60 ± 3.90	0.004 ± 0.002	0.15 ± 0.17	8.80 ± 8.20	0.01 ± 0.01	0.15 ± 0.17	0.54 ± 0.56	0.001 ± 0.001	0.09 ± 0.08
Surfers Paradise (C)	<75	7.30 ± 6.20	<0.001 ± 0.000	0.19 ± 0.13	12.8 ± 12.3	0.01 ± 0.01	0.20 ± 0.22	0.31 ± 0.38	0.004 ± 0.003	0.12 ± 0.15
	75-150	6.40 ± 3.50	0.02 ± 0.02	0.37 ± 0.25	14.7 ± 9.40	0.02 ± 0.02	0.64 ± 0.54	0.91 ± 0.63	0.004 ± 0.007	0.20 ± 0.17
	150-300	7.90 ± 6.80	0.01 ± 0.01	0.45 ± 0.37	20.4 ± 20.9	0.03 ± 0.03	0.66 ± 0.53	0.68 ± 0.43	0.008 ± 0.002	0.18 ± 0.13
	300-425	4.20 ± 3.60	0.02 ± 0.01	0.19 ± 0.14	10.9 ± 9.40	0.02 ± 0.03	0.12 ± 0.08	0.19 ± 0.14	0.001 ± 0.001	0.30 ± 0.29

Note: R– residential, I– industrial, C– commercial

the composition of vehicle parts and fuel characteristics (Westerlund 2001; Sanders et al. 2003).

As evident in Table 6.1, high variations in the heavy metal loads can be noted among the road surfaces in various urban land uses and among different particle sizes. The heavy metals load in each particle size range on Nerang industrial sites is approximately 50% higher than on Clearview Estate residential road surfaces. For example, the Zn load in the four particle size ranges in Nerang was between 0.55-1.90mg/m<sup>2</sup>, whereas in Clearview Estate it ranged between 0.28-0.73mg/m<sup>2</sup>. Metal loadings at Surfers Paradise commercial sites were intermediate to Clearview Estate and Nerang, whilst the highest Cd and Cu loadings were found at Surfers Paradise in four particle sizes (other than a few exceptions of Cu loading). In Benowa, Fe, Al, Cr and Pb loads were high in the <150µm particle size range compared to Nerang. This could be attributed to the presence of anthropogenic activities such as boat manufacturing and metal based industries. Higher metal loading in industrial and commercial road surfaces is attributed to factors such as the prevailing traffic conditions and land use characteristics. The variation of metal loadings with respect to land use and particle size is similar to the findings of Hengren et al. (2006) and Zhao et al. (2010).

The weight of heavy metals per unit weight of total solids load (metal concentration in solids particles, mg/g) was calculated for each site. Table 6.2 shows the mean and standard deviation of heavy metal concentration in solids for each particle size range. Table B.1 in Appendix B gives the heavy metals concentrations in the collected build-up samples. The relatively higher standard deviation values indicate the highly variable nature of heavy metal concentrations in different particle size ranges. This provides an indication of the variability of metal concentrations at different study sites within the same suburb. As evident in Table 6.2, the normalised metal concentrations in solids particles decreases with the increase in particle size. For example, the total metal concentration in Benowa reduces from 24.1mg/g to 6.1mg/g in the particle size range from <75µm to 300-425µm. Furthermore, the data reveals that the heavy metal concentrations in solids associated with the particle size range

**Table 6.2: Average heavy metal concentration in different particle sizes (average ± standard deviation)**

Suburb	Particle size (µm)	Al mg/g	Mn mg/g	Fe mg/g	Ni mg/g	Cu mg/g	Zn mg/g	Pb mg/g	Cd µg/g	Cr µg/g
Clearview Estate	<75	6.59±3.08	0.18±0.16	7.65±6.20	0.00±0.00	0.09±0.16	0.19±0.17	0.03±0.02	0.45±0.50	14.9±31.1
	75-150	5.47±3.40	0.22±0.16	6.92±3.17	0.01±0.01	0.16±0.12	0.43±0.29	0.04±0.01	0.65±0.80	9.81±12.2
	150-300	3.30±1.87	0.14±0.08	4.75±2.51	0.01±0.00	0.14±0.10	0.25±0.19	0.02±0.01	0.44±0.54	8.26±11.7
	300-425	1.56±0.72	0.07±0.03	2.85±2.13	0.01±0.01	0.08±0.05	0.15±0.09	0.04±0.04	0.45±0.62	13.6±18.5
	<b>Total</b>	<b>16.9</b>	<b>0.60</b>	<b>22.2</b>	<b>0.03</b>	<b>0.47</b>	<b>1.02</b>	<b>0.12</b>	<b>1.99</b>	<b>46.5</b>
	<b>Range</b>	0.45-11.7	<0.001-0.58	0.36-16.6	<0.001-0.034	<0.001-0.50	<0.001-1.01	<0.001-0.13	<1-2.60	<1-95.8
Nerang	<75	3.56±2.23	0.14±0.10	6.73±3.50	0.01±0.01	0.09±0.06	0.28±0.19	0.04±0.03	0.30±0.22	7.66±8.70
	75-150	1.09±0.60	0.07±0.03	2.78±1.15	0.01±0.01	0.10±0.10	0.18±0.15	0.03±0.03	0.18±0.12	3.96±4.60
	150-300	1.18±0.60	0.08±0.04	3.34±1.70	0.01±0.01	0.08±0.08	0.18±0.20	0.03±0.02	0.18±0.12	3.59±4.40
	300-425	0.83±0.71	0.03±0.02	2.06±1.75	0.001±0.00	0.03±0.02	0.07±0.08	0.01±0.00	0.14±0.20	2.96±3.30
	<b>Total</b>	<b>6.65</b>	<b>0.32</b>	<b>14.9</b>	<b>0.02</b>	<b>0.30</b>	<b>0.71</b>	<b>0.11</b>	<b>0.82</b>	<b>18.2</b>
	<b>Range</b>	0.05-8.68	<0.001-0.35	0.78-14.6	<0.001-0.03	<0.001-0.31	<0.001-0.62	<0.001-0.10	<1-10.7	<123.7
Benowa	<75	8.71±7.70	0.21±0.27	14.4±14.2	0.02±0.02	0.15±0.15	0.47±0.60	0.13±0.14	0.62±0.50	23.6±33.9
	75-150	4.43±0.90	0.15±0.12	8.52±8.01	0.01±0.01	0.15±0.12	0.47±0.42	0.09±0.07	0.67±1.29	6.86±17.9
	150-300	2.48±1.60	0.09±0.05	4.54±3.00	0.01±0.00	0.13±0.10	0.35±0.22	0.06±0.04	0.29±0.35	0.23±0.61
	300-425	1.88±1.90	0.06±0.05	3.90±3.52	0.003±0.00	0.07±0.05	0.17±0.17	0.04±0.03	0.55±0.92	0.72±1.47
	<b>Total</b>	<b>17.5</b>	<b>0.50</b>	<b>31.4</b>	<b>0.04</b>	<b>0.49</b>	<b>1.46</b>	<b>0.31</b>	<b>2.13</b>	<b>31.4</b>
	<b>Range</b>	0.25-25.8	<0.001-0.82	0.48-48.3	<0.001-0.07	<0.001-0.39	<0.001-1.80	<0.001-0.40	<1-4.10	<1-106.8
Surfers Paradise	<75	1.85±1.30	0.04±0.04	3.13±2.08	0.00±0.00	0.04±0.04	0.07±0.10	0.02±0.02	0.77±1.15	0.21±0.54
	75-150	1.50±0.40	0.08±0.03	3.26±1.02	0.01±0.00	0.13±0.09	0.2±0.09	0.04±0.03	0.60±0.80	7.52±10.9
	150-300	1.56±0.90	0.09±0.05	4.08±2.60	0.01±0.01	0.16±0.13	0.15±0.08	0.04±0.02	0.94±1.90	2.64±4.70
	300-425	0.89±0.50	0.04±0.02	2.35±1.63	0.003±0.00	0.03±0.02	0.04±0.03	0.06±0.11	0.14±0.19	3.30±7.40
	<b>Total</b>	<b>5.80</b>	<b>0.26</b>	<b>12.8</b>	<b>0.02</b>	<b>0.36</b>	<b>0.46</b>	<b>0.15</b>	<b>2.44</b>	<b>13.7</b>
	<b>Range</b>	0.30-4.68	<0.001-0.16	<0.001-8.12	<0.001-0.024	<0.001-0.46	<0.001-0.38	<0.001-0.30	<1-6.00	<1-32.9

<75 $\mu\text{m}$  is about one third of the overall heavy metal concentrations, with the exception of Cu and Zn. This highlights the fact that particle size has a significant influence on heavy metal association with solids and that fine particles have high metal adsorption capacity compared to coarse particles. This is further supported by the findings of past researchers who noted relatively higher amounts of particulate heavy metals in the finer fraction of road deposited solids (for example, Drapper et al. 2000; Deletic and Orr 2005; Herngren et al. 2006). In the majority of the study sites, high Cu and Zn concentrations were associated with the particle size 75-150 $\mu\text{m}$ . However, the heavy metal concentration was lowest in the 150-425 $\mu\text{m}$  fraction at all sites, with the exception of Pb, which was highest in the 300-425 $\mu\text{m}$  fraction at the Surfers Paradise sites.

As found in previous studies, Fe is the most abundant metal element in solids particles (Hopke et al. 1980; Herngren et al. 2006). It is possible that Fe could originate from vehicle component rust, brake lining material and vehicle exhaust (Hopke et al. 1980; Hildemann et al. 1989; Weber et al. 1992; Adachi and Tainosho 2004). However, a significant amount of Fe could also originate from soil sources. Al is the second most common metal element. As indicated in Section 5.3.3, the road deposited solids particles contain natural minerals such as albite ( $\text{AlNaO}_8\text{Si}_3$ ), microcline ( $\text{AlKO}_8\text{Si}_3$ ), chlorite ( $\text{H}_8\text{Mg}_6\text{O}_{18}\text{Si}_4$ ) and muscovite ( $\text{Al}_3\text{H}_2\text{KO}_{12}\text{Si}_3$ ) which could be a possible source of Al. Previous researchers have also shown that soil dust present on road surfaces accounts for a high percentage of Al (Pierson and Brachaczek 1983; Adachi and Tainosho 2005).

Zn was the most abundant metal element other than Fe and Al in all of the particle sizes, regardless of the study site. As mentioned in the literature, sources of Zn on road deposited solids are mainly from tyre wear (Blok 2005; Adachi and Tainosho 2004). Zn in tyre particles is typically present in the form of ZnO, which is an additive used to activate vulcanization (Fauser et al. 1999). Furthermore, zinc is also used in brake plates as a substitute for Cd (McKenzie et al. 2009). Among the measured nine metal elements, Cd was the least detected in all of the study sites, followed by Cr and Ni. Cd is typically used as plating in brake pads to prevent

corrosion (McKenzie et al. 2009). Cr and Ni are traffic related pollutants that are generated from tyre wear and brake pad wear (Viklander 1998; McKenzie et al. 2009). Cr is also present in minerals such as mica and chlorites (McGrath 1994). However, Cr in these minerals is tightly attached to the alumino silicate layer in clay minerals in a residual form (Hseu et al. 2002). As the extraction procedure used in the present study does not recover the residual metal elements, the Cr content detected would be primarily from traffic related sources (McGrath and Smith 1990; Banerjee 2003; Hseu 2004).

Measured metal concentrations in the majority of the particle sizes decreased in the order of Fe>Al>Zn>Cu>Mn>Pb>Ni≥Cr and Cd, irrespective of the sampling site. The majority of these metal elements would have originated from traffic related sources, rather than from soil inputs. The metal elements originating from traffic sources have the potential to change their form when exposed to air and can associate with mineral components and solids particles (See Section 2.2.3) (Harrison et al. 1981; Post and Buseck 1985; Davis and Upadhyaya 1996; Wik et al. 2009).

In contrast to the metal loads presented in Table 6.1, the normalised metal content in solids particles (in Table 6.2) was high at the Clearview Estate site. However, compared to the other three suburbs, the samples for Surfers Paradise indicated high Cu, Cd and Ni content in the 75-150µm and 150-300µm particle size ranges. Since Surfers Paradise is a highly commercial area with high traffic activities (Section 5.4), it is considered reasonable to find high Cu, Ni and Cd content there compared to the other suburbs.

The data given in Table 6.2 and the maximum and minimum metal concentrations in all particle sizes were compared with the quality guidelines used in the assessment of contamination of sediments (Table 6.3). Ni, Cu, Zn Cr and Cd in the four particle sizes exceeded the values specified in the Australian and New Zealand Guidelines for the Assessment and Management of Contaminated sites (ANZECC 1992). Similarly, the values exceeded the Canadian Council of Ministers of the Environment (CCME 1995) and the Ontario Ministry of Environmental Screening

Level Guidelines (Persaud et al. 1990). These guidelines specify that the disposal of such sediments needs to be guided by environmental considerations. It confirms that road deposited solids particles are of significant environmental concern due to their high metals content and need appropriate management practices to reduce the contamination of receiving waters.

**Table 6.3: Comparison of heavy metal concentrations of road deposited solids with typical guideline values used in contaminated land assessment**

Road deposited solids	Ni	Cu	Zn	Pb	Cd	Cr
	mg/kg					
Minimum	0.10	1.00	1.00	0.90	0.00	0.20
Maximum	70.4	498.8	1774.0	423.4	6.00	106.8
<b>Guideline values</b>						
ANZECC (1992) <sup>a</sup>	2	1-190	2-180	NA	0.04-2	0.5
CCME (1995) - Fresh water <sup>b</sup>	NA	197	315	91.3	0.35	90
Screening Level Guidelines (Ontario) <sup>c</sup>	75	110	820	250	10	110

<sup>a</sup> Australian and New Zealand Guidelines for the Assessment and Management of Contaminated sites (1992)

<sup>b</sup> CCME (Canadian Council of Ministers of the Environment 1995).

<sup>c</sup> Ontario Ministry of Environment Screening Level Guidelines (Persaud et al. 1990)

NA - not available

### 6.3 HEAVY METAL ADSORPTION BEHAVIOUR FOR DIFFERENT PARTICLE SIZE RANGES

Adsorption of heavy metals to solids particles is primarily dependent on the physical and chemical characteristics of particles and the metal species (Section 2.4). As identified in Section 2.4, the most significant physical and chemical parameters in this regard are cation exchange capacity, specific surface area, organic matter content, mineralogy and particle size. As noted in Section 5.5, these parameters are linked and thereby provide a complex physico-chemical profile for heavy metals interaction with solids. However, the influence of individual parameters on metal adsorption processes is not conclusively understood.

Based on the predominance of these parameters in solids, the mechanisms and the nature of bonding between solids and heavy metals tend to vary. The mechanisms by which metals may be attached to particles include cation exchange (outer-sphere complexation), chemisorption (inner-sphere surface complexation) and precipitation (Section 2.3). These mechanisms are influenced by different physical and chemical parameters, which lead to different interactions between solids and heavy metals. Analysis presented in this section focused on identifying the role of influential physical and chemical parameters on heavy metals adsorption and on investigating the fundamental mechanisms involved in adsorption. Initially, analysis was carried out individually for the four different particle size ranges and later combined to develop an overall understanding based on the combined data set.

### 6.3.1 SELECTION OF DATA FOR ANALYSIS

The original data matrices were re-arranged for this analysis based on the understanding gained from the analysis undertaken in Chapter 5. Findings from Chapter 5 indicated similarities in the physical and chemical characteristics in the 150-300 $\mu\text{m}$  and 300-425 $\mu\text{m}$  sizes, independent of the location of sampling. Both particle sizes showed similarity in correlation with mineralogical components and variations in terms of SSA, TOC and ECEC. Therefore, it was decided to combine particle sizes 150-300 $\mu\text{m}$  and 300-425 $\mu\text{m}$  for further analysis. Consequently, the data matrices were prepared accordingly. This resulted in three particle size categories as given below:

- <75 $\mu\text{m}$  (data matrix of 32 x 16)
- 75-150 $\mu\text{m}$  (data matrix of 32 x 16)
- >150 $\mu\text{m}$  (which included both the 150-300 $\mu\text{m}$  and 300-425 $\mu\text{m}$  particle size ranges, data matrix of 64 x 18).

The variables in the three matrices consisted of the physical and chemical parameters of solids and heavy metals. The physical and chemical parameters used for the analysis were: total organic carbon content; specific surface area; effective cation exchange capacity; and mineralogical components, namely, albite, chlorite, quartz

and amorphous content. The nine heavy metal elements used for the analysis were Al, Fe, Cr, Mn, Ni, Cu, Zn, Cd and Pb. Muscovite and microcline were not included in the analysis since the surrogate parameters for muscovite and microcline were identified from the analysis detailed in Chapter 5. Chlorite and EGME SSA were surrogates for muscovite; chlorite and ECEC were surrogates for microcline. The initial analysis, which included muscovite and microcline, showed a distribution of variables which was very similar to a distribution without these two parameters. Therefore, it was decided to exclude these parameters from the data matrix to eliminate any bias arising from having a number of correlating variables with similar physical and chemical properties. Thus, the resulting data matrix consisted of 16 variables.

### 6.3.2 DATA PRE-PROCESSING

After selecting data sets for analysis, each set was subjected to pre-processing. The pre-processing undertaken was similar to the pre-processing techniques described in Chapter 5. Data was in unit weight of build-up load (mg/g). Therefore, any bias resulting from different build-up loads at different sites was eliminated. Data preprocessing was carried out according to the following steps:

- Concentrations below the lower detection limit of the analytical instrument were set to half the detection limit value (Herngren et al. 2005). This was to maintain the consistency of the data set.
- The data matrix was auto-scaled by subtracting the column mean from each element in the respective columns and dividing by the standard deviation of the corresponding column.
- Atypical objects were identified using the Hotelling  $T^2$  test. The identified objects were removed from the data matrices in order to improve the sensitivity of the analysis.

The three data matrices resulting from pre-processing were subjected to PCA and the outcomes derived are discussed in detail below. Notations adopted to identify each object in PCA biplots are similar to the notations used in Section 5.4.2. The first character of the notation denotes the initial letter of the corresponding suburb.



Accordingly, C, N, B and S represent Clearview Estate, Nerang, Benowa and Surfers Paradise, respectively. The second character is a number representing the sampling event 1 or 2. The third character is a number representing the sampling road site. Consequently, in each suburb, four road surface samples were numbered 1 to 4. Road names of each suburb are given in Appendix A/Table A.7. The final character is a Roman numeral i, ii, iii or iv which indicates the particle size ranges 300-425 $\mu\text{m}$ , 150-300 $\mu\text{m}$ , 75-150 $\mu\text{m}$  and <75 $\mu\text{m}$ , respectively.

### **Particle size range <75 $\mu\text{m}$**

This particle size range accounts for 50% of the solids load in build-up pollutants. Furthermore, the size range is responsible for more than 51.6% of heavy metal content, with the exception of Cu and Zn which correspond with the highest physical and chemical parameter values which are favourable for metal adsorption (Section 5.5.1). The highest ECEC in this particle size range is primarily derived from clay forming minerals, rather than from the TOC content. Clay forming minerals play an important role due to their high EGME SSA and ECEC values. Clay forming mineral content is relatively higher than for the other particle sizes. Amorphous content is the dominant component in this particle size range and is primarily composed of traffic related particles. Therefore, these materials would influence the heavy metal adsorption characteristics of the particles. The solid particle pH was in the range of 6-8.8.

With this background understanding, the pre-treated data matrix consisting of 32 objects and 16 variables were first subjected to PCA. The number of principal components to be used in the analysis was determined by the Scree plot method. Consequently, two PCs were selected for the analysis based on the pronounced change of slope shown in the Scree plot (Appendix B/Figure B.1) (Jackson 1991). The corresponding biplot for PC 1 vs PC 2 is shown in Figure 6.1. Data variance represented by PC 1 and PC 2 explains a total variance of 51.6%. As variance explained is relatively low, confirmation of the outcomes using a secondary analysis is important in water quality research (Purcell et al. 2007). Therefore, outcomes of the PCA biplot were confirmed using a correlation matrix (Table 6.4).

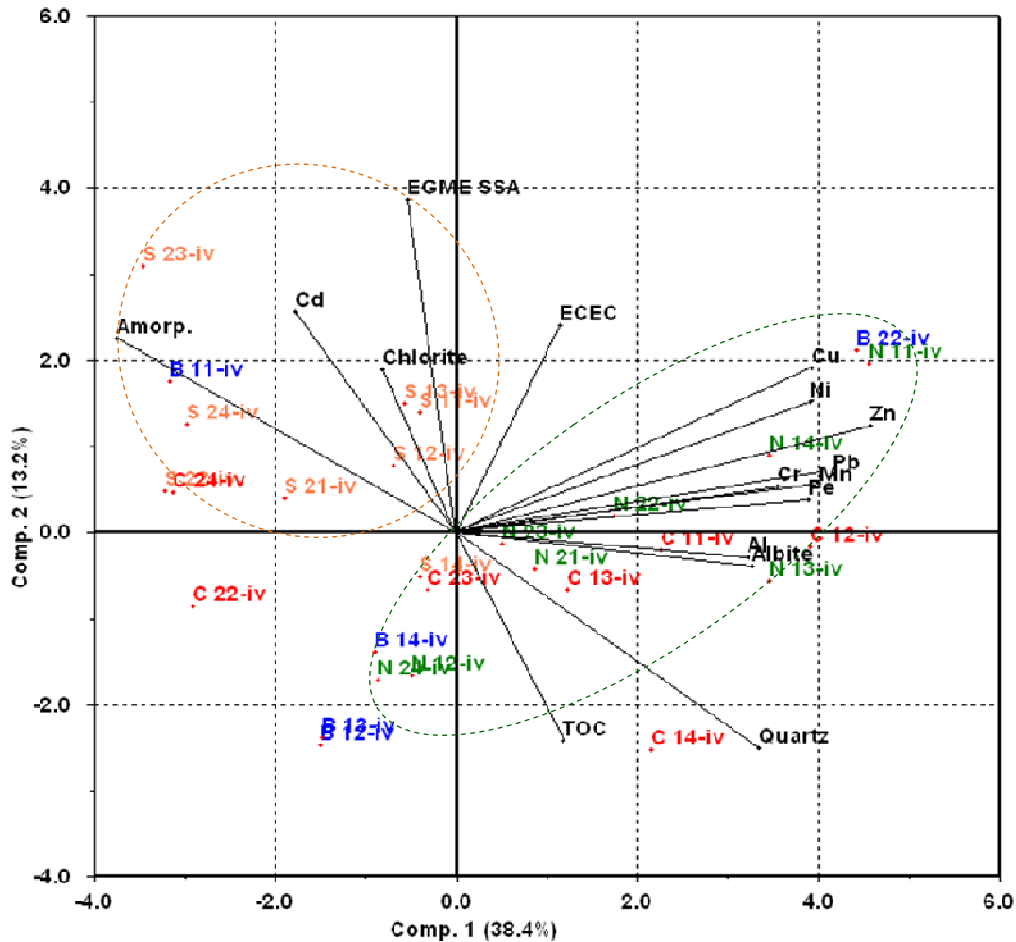


**Figure 6.1: PC 1 vs PC 2 biplot obtained from PCA for particle size range <75µm**

Note: C– Clearview Estate, N- Nerang, B- Benowa, S- Surfers Paradise, 1 and 2-first and second sampling event

The correlation matrix gives the extent of correlations of the overall principal component analysis (Farnham et al. 2003; Carroll and Goonetilleke 2005). It is important to note that in Table 6.4, heavy metals content in solids have low correlation coefficients with physical and chemical parameters such as TOC content and clay forming minerals content. Similar low correlation coefficients among variables have been noted in the research literature for the variables that are dependent on a range of parameters (Wu and Wang 2007). This is attributed to the nature of the road deposited solids that consist of several distinct groups of charge sites (Murakami et al. 2008; Covelo et al. 2007b). For example, solids organic matter could contain surface functional groups of carboxyl (-COOH), carbonyl and phenolic groups, and edge sites of layer silicate minerals (aluminol -Al-OH and silanol-Si-

OH), and metal oxides could contain different types of surface hydroxyls with different reactivities (reactivities depend on the coordination of the oxygen atom in the functional group) (Sposito 1984; McBride 1994; Cornell and Schwertmann 1996).

Additionally, mineral surfaces contain permanent charge sites (McBride 1994). Heavy metal elements could bind to any of these charge sites due to the competitive nature of heavy metal adsorption to solids and differences in heavy metal speciation (Benjamin and Leckie 1981; Spadini et al. 1994; Strawn et al. 1998; Zhuang and Yu 2002; Murakami et al. 2008). Consequently, the adsorption of a specific type of heavy metal would not be restricted to a particular charge site on solids while they can be selectively adsorbed to several types of charge sites. Therefore, correlation coefficients represent the influence of different physical and chemical characteristics for different adsorption mechanisms. This suggests that the physical and chemical characteristics of solids exert a significant influence on the types of adsorption mechanisms displayed by the heavy metals.

In Figure 6.1, most of the heavy metals are located on the positive PC 1 axis along with albite and quartz and, to a less extent, ECEC and TOC. Therefore, these variables are considered to be correlated. Amorphous content, Cd and EGME SSA are located along the negative PC 1 axis, indicating the influence of the amorphous content and EGME SSA on Cd association with solids particles. The EGME SSA, ECEC, amorphous content, Cd and chlorite are located on the positive PC 2 axis, while TOC, quartz and albite are located on the negative PC 2 axis. Thus, it can be concluded that PC 2 is primarily associated with the variability of the physical and chemical parameters of solids, whereas PC 1 is associated with the variability of the heavy metal concentrations.

**Table 6.4: Correlation matrix for the particle size range <75µm**

	EGME SSA	TOC	Al	Cr	Mn	Fe	Ni	Cu	Zn	Cd	Pb	ECEC	Amorp.	Quartz	Albite	Chlorite
EGME SSA	1															
TOC	-0.181	1														
Al	-0.191	0.178	1													
Cr	-0.049	0.124	<b>0.268</b>	1												
Mn	-0.112	0.056	<b>0.643</b>	0.293	1											
Fe	-0.154	0.133	<b>0.893</b>	<b>0.329</b>	<b>0.734</b>	1										
Ni	0.099	-0.047	<b>0.340</b>	<b>0.637</b>	<b>0.562</b>	<b>0.487</b>	1									
Cu	<b>0.239</b>	0.047	<b>0.230</b>	<b>0.737</b>	<b>0.419</b>	<b>0.36</b>	<b>0.757</b>	1								
Zn	-0.018	0.166	<b>0.565</b>	<b>0.577</b>	<b>0.781</b>	<b>0.701</b>	<b>0.623</b>	0.754	1							
Cd	0.157	-0.332	-0.14	-0.168	-0.166	-0.118	-0.109	-0.168	-0.153	1						
Pb	0.041	0.267	<b>0.333</b>	<b>0.497</b>	<b>0.563</b>	<b>0.490</b>	<b>0.560</b>	0.709	<b>0.795</b>	-0.121	1					
ECEC	<b>0.428</b>	-0.122	-0.012	0.008	0.217	0.132	0.097	0.218	0.324	0.017	0.229	1				
Amorp.	0.273	-0.234	-0.291	-0.466	-0.388	-0.391	-0.41	-0.419	-0.402	<b>0.419</b>	-0.531	-0.051	1			
Quartz	-0.375	0.202	<b>0.243</b>	<b>0.394</b>	<b>0.335</b>	<b>0.305</b>	0.374	0.385	0.393	-0.35	<b>0.478</b>	0.059	-0.878	1		
Albite	0.028	0.038	<b>0.246</b>	<b>0.385</b>	<b>0.459</b>	<b>0.437</b>	<b>0.42</b>	<b>0.329</b>	<b>0.416</b>	-0.417	<b>0.396</b>	<b>0.229</b>	-0.646	0.325	1	
Chlorite	0.197	-0.159	-0.056	0.036	-0.143	0.108	-0.027	0.007	-0.123	0.191	-0.154	-0.133	0.146	-0.275	-0.135	1

In Figure 6.1, clear groupings of objects with similar mineralogical composition and metal concentrations are evident. Objects from Surfers Paradise form a group (encompassed by the orange circle) possibly due to the high amorphous content (See Section 5.3 for details) and the corresponding highest Cd content (Section 6.1). These objects may also contain lower heavy metal concentrations other than Cd. Similarly, Nerang and Clearview Estate objects form a group (encompassed by the green circle) characterised by high clay forming minerals. Furthermore, Nerang objects are primarily associated with traffic related metal elements (Cu, Pb, Ni and Cr), and Clearview Estate objects are primarily associated with metal elements of geochemical origin such as Fe, Al and Mn (See Figure 6.2). Benowa objects are scattered in the biplot and do not form a clearly demarcated group. This could be attributed to the fact that Benowa objects belong to three different land uses, with the consequent variations in metal concentrations and mineralogical composition. Therefore, it can be concluded that object groups are formed based on their sources of origin and reflect differences in metal content which can be attributed to physical and chemical characteristics.

As evident in Figure 6.1, metals of geochemical origin (Fe, Al, Mn) are strongly correlated and form a cluster. These metals show strong correlation to albite and a weak correlation to chlorite content (See Table 6.4 for correlation coefficients). Fe, Al and Mn in soil are present as metal oxides or hydroxides which could be present either as coatings on clay minerals or complex with organic matter content (Taylor et al. 1983; Bradl 2004; Wang et al. 2008). As noted by Gillman and Bell (1976, 1978), highly weathered soils (including podzolic soil) in Queensland contain appreciable quantities of metal oxides and this results in variable charge (pH dependent) characteristics. Therefore, it can be argued that these metal oxides would be mostly present in amorphous oxide form in road deposited solids (Section 2.5.1). As evident in Figure 6.1, Fe, Al and Mn demonstrate a negative correlation with the amorphous content. This could be attributed primarily to the low proportions of metal oxides present compared to the other forms of amorphous content in the road deposited solids particles such as traffic related particles. As seen in Figure 6.1 and the correlation coefficients given in Table 6.4, the correlation coefficients for Fe, Al and Mn with clay forming minerals are stronger than the correlation with TOC. This

indicates that a significant proportion of Fe, Al and Mn oxides could be present as coatings on clay minerals in this particle size range.

It is known that the metal oxides of Fe, Al and Mn can absorb a significant proportion of other metal elements (McGrath 1998; Wang et al. 2008). As seen in Figure 6.1, Fe, Al and Mn metal elements show strong correlations with Zn, Cu, Pb, Ni and Cr. For example, Zn has high correlation coefficients with Mn (0.781), Fe (0.701) and Al (0.565) (Table 6.4). Similarly, Cu, Pb and Ni also show fairly good correlation with Mn, Fe and Al respectively. Thus, the correlation of Zn, Cu, Pb, Ni and Cr with Fe, Al and Mn indicates preferential association of these metal elements with the oxides of Fe, Al and Mn. Similar preferences have also been noted by previous researchers (Elliot et al. 1986; Bradl 2004).

Due to the low correlation coefficients observed for Fe, Al and Mn with ECEC (See Table 6.4), it can be suggested that heavy metals association with the oxides of Fe, Al and Mn would predominately occur due to mechanisms other than ion exchange. The possible reason for this behaviour is that the metal oxides mainly contain a variable charge, rather than a permanent charge. Therefore, heavy metals adsorption to metal oxides would mainly occur by chemisorption (Weber et al. 1991). The presence of Fe, Al and Mn in metal oxide form in solids particles would act as an adsorbent for the other metal elements.

Similarly, Zn, Cu, Pb and Ni content show a relatively good correlation with albite and ECEC. This is further supported by the correlation coefficients given in Table 6.4, having relatively high correlation coefficients for Zn (0.416), Cu (0.329), Pb (0.396) and Ni (0.420) with albite, compared to the other metal elements. This suggests that there is a significant portion of these metal elements associated with albite. However, in comparing the relatively low correlation coefficients to the correlation coefficients shown by the same metals with oxide forming metals, it could be postulated that adsorption to albite is a secondary form. Albite mineral possesses a high amount of permanent negative charges on its structure due to isomorphous substitution (See section 2.5.1). Therefore, the presence of permanent

charge sites is the primary reason for enhanced metal adsorption. Such adsorption would be primarily by ion exchange. This agrees with the findings of past researchers who have noted the cation exchangeable interaction of Zn, Cu, Pb and Ni elements in solids (Tiller and Hodgson 1962; Charlesworth et al. 2003).

According to the correlation matrix, Pb has a relatively high correlation coefficient (0.267) with TOC compared to all the other metal elements. This suggests the possibility of Pb adsorption to TOC. However, this is not a primary form of adsorption due to the low correlation shown, compared to correlations with metal oxides and albite. There is a strong possibility that Pb adsorption with organic matter is due to chemisorption mechanism (Pinheiro et al. 1999). This conclusion is based on the negative correlation observed between TOC and ECEC in Figure 6.1. ECEC reflects the charge sites on solids that can hold exchangeable cations (Filep 1999). Thus, the negative correlation of TOC and ECEC reflects the low influence of organic matter for the exchangeable cation bearing sites on organic matter. Therefore, it can be argued that the contribution of TOC to cation exchange in this particle size range is very low. This suggests that the adsorption of Pb to TOC occurs by a mechanism other than cation exchange.

As evident in Figure 6.1, TOC shows a very weak correlation with the rest of the metal elements. This suggests that a higher fraction of TOC in this particle size range is not in a form which is favourable for metal adsorption. Similar to the discussion in Section 5.5.1, it leads to the conclusion that, although the organic matter in these solids is mainly derived from plant debris (Section 5.3.2), the majority of TOC in this particle size range is present primarily in the form of organic residue (non-decayed portion). This confirms that the nature of the organic matter is very important in metal adsorption; much more so than its source, physical presence or amount.

Cd shows adsorption behaviour different to the rest of the heavy metals. According to Figure 6.1, Cd shows strong correlation to amorphous content. As discussed in Section 5.4, amorphous material predominantly originates from traffic related

sources. Therefore, Cd could be a highly traffic related metal element. Furthermore, the amorphous content shows weak or no correlation with the majority of the other metal elements. It was expected that traffic related substances in amorphous content would show strong correlation with heavy metal elements. However, the weak correlation with heavy metals other than Cd suggests that the majority of the metal elements in traffic related particles in this size fraction would leach out from particles and bond with mineralogical components or with organic matter in the solids. Therefore, Cd can be embedded in the traffic related particles of amorphous content.

As identified in Section 5.5, traffic related particles have high EGME SSA and this would lead to the removal of a large amount of heavy metals from the amorphous material. Although research studies show—for example—that tyre particles could adsorb heavy metal cations by displacing Zn (exchangeable form) when surrounded with high metal ion concentrations, present data show that amorphous content does not adsorb heavy metal cations by the ion exchange mechanism (Calisir et al. 2009; Rowley et al. 1984). This is possibly due to the low metal concentrations in the road surface environment.

As seen in Figure 6.1, Cd also correlates with chlorite, EGME SSA and ECEC. Therefore, the fraction of Cd released from traffic related particles would be adsorbed to chlorite clay minerals in this particle size range. It is postulated that this adsorption would occur by ion exchange mechanism. Due to the low concentration of Cd in the samples collected, it is difficult to derive definite conclusions regarding the form of Cd availability.

Quartz positively correlates with the majority of the metal elements, with the exception of Cd (See Figure 6.1 and Table 6.4). This result was unexpected, since binding phases in quartz is very low. As noted by Filep (1999), metal oxides and humic substances can be trapped in sand particles due to surface irregularities. However, a reason for the orientation of the quartz vector in Figure 6.1 could be that the low quartz content in this particle size range, which is about 32%, tends to reduce



its influence on metal adsorption behaviour. Due to the predominance of the amorphous content and clay forming minerals in this particle size range, the adsorption behaviour is primarily governed by these components.

### **Particle size range 75-150µm**

This size range contains relatively high heavy metal content in the total build-up, and Cu and Zn were predominant. Similar to the <75µm size range, the analysis of physical and chemical characteristics discussed in Section 5.5 indicated that permanent charge sites on clay minerals, especially on albite mineral, is responsible for ECEC in this particle size range, and the contribution of TOC to ECEC was very low. This is an indication of the low exchangeable sites (negative charge sites) in the organic matter. EGME SSA of this particle size range is mainly derived from organic matter content and chlorite (layer silicate) minerals. Quartz is the dominant mineralogical component, while the amorphous content is in a similar range to the quartz content.

The pre-treated data matrix with 32 objects and 16 variables was subjected to PCA. The first two principal components were selected for analysis based on the Scree plot method (Appendix B/Figure B.2). These components account for 46.4% of the total data variance. The resulting PCA biplot of PC 1 vs PC 2 is shown in Figure 6.2. The low variance explained by the PCA biplot is due to the involvement of a number of physical and chemical parameters in the adsorption of different heavy metal elements. Consequently, as in the case of the <75µm particle size range, a correlation matrix was also used to interpret the observations derived from the PCA biplot to compensate for its low variance (Table 6.5). As seen in Table 6.5, correlation coefficients for heavy metal elements with the clay forming minerals content, TOC content and ECEC are relatively low. This again suggests that a specific heavy metal cation can adsorb to several different types of charge sites in solids due to the competition among heavy metal elements (Spadini et al. 1994; Strawn et al. 1998; Christophi and Axe 2000). Therefore, as in the case of the <75µm particle size range, the low correlation coefficients reflect the degree of preference of each heavy metal element for different charge sites.

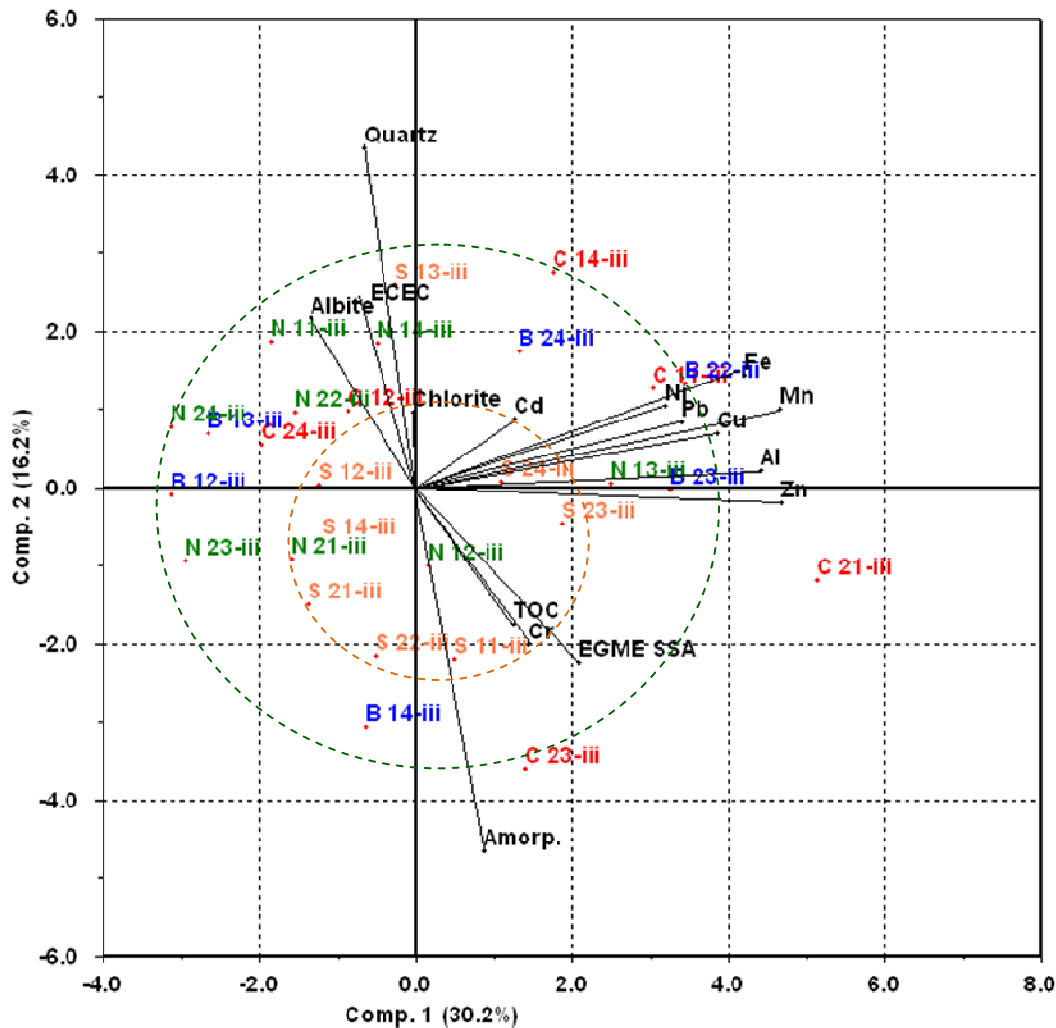


**Figure 6.2: PC 1 vs PC 2 biplot obtained from PCA for particle size range 75-150µm**

Note: C– Clearview Estate, N- Nerang, B- Benowa, S- Surfers Paradise, 1 and 2- first and second sampling event

As evident in Figure 6.2, all heavy metal elements are located on the positive PC 1 axis. This confirms the consistency in metal adsorption in this particle size range. Furthermore, TOC and EGME SSA are also located on the positive PC 1 axis, indicating the significant influence of these parameters on heavy metals adsorption to solids particles. Quartz, albite, ECEC and chlorite are located on the positive PC 2 axis and TOC, EGME SSA and amorphous content are located on the negative PC 2 axis. Therefore, it can be postulated that PC 2 interprets the physical and chemical characteristics of solids.

**Table 6.5: Correlation matrix for the particle size range 75-150µm**

	EGME SSA	TOC	Al	Cr	Mn	Fe	Ni	Cu	Zn	Cd	Pb	ECEC	Amorp.	Quartz	Albite	Chlorite
EGME SSA	1															
TOC	0.287	1														
Al	0.147	<b>0.439</b>	1													
Cr	<b>0.291</b>	0.040	0.198	1												
Mn	<b>0.239</b>	<b>0.256</b>	<b>0.886</b>	0.129	1											
Fe	0.134	<b>0.239</b>	<b>0.893</b>	-0.048	0.878	1										
Ni	<b>0.228</b>	-0.047	0.384	0.361	<b>0.502</b>	<b>0.350</b>	1									
Cu	<b>0.356</b>	-0.152	0.335	0.162	<b>0.541</b>	<b>0.378</b>	0.640	1								
Zn	<b>0.301</b>	0.049	<b>0.716</b>	0.342	<b>0.769</b>	<b>0.643</b>	0.505	0.728	1							
Cd	<b>0.229</b>	-0.139	0.172	0.093	0.300	0.271	-0.007	0.143	0.205	1						
Pb	0.112	-0.029	<b>0.377</b>	-0.106	<b>0.425</b>	<b>0.474</b>	0.369	0.753	0.589	-0.007	1					
ECEC	-0.194	-0.198	-0.102	-0.352	0.021	0.001	-0.087	0.008	-0.063	0.263	-0.048	1				
Amorp.	<b>0.333</b>	0.182	0.084	<b>0.202</b>	-0.009	-0.094	-0.113	0.044	0.211	-0.093	0.033	-0.235	1			
Quartz	-0.436	-0.112	-0.016	-0.231	0.007	0.090	0.154	-0.035	-0.191	-0.072	0.094	0.152	-0.869	1		
Albite	0.006	-0.352	-0.257	0.04	-0.11	-0.093	0.110	-0.111	-0.204	0.124	-0.367	0.025	-0.491	0.246	1	
Chlorite	<b>0.220</b>	0.145	-0.039	-0.312	0.079	0.033	-0.159	0.069	-0.039	0.099	-0.032	<b>0.286</b>	-0.194	0.040	-0.062	1

According to Figure 6.2, Surfers Paradise objects are distributed around the origin forming a cluster, while objects from the other suburbs overlap and spread beyond the Surfers Paradise objects group. The two clusters are clearly discriminated in the biplot and form two shells around the origin. These groupings reflect the fact that Surfers Paradise objects are much more consistent in their physical and chemical characteristics and heavy metal concentrations. Therefore, it can be postulated that they have similar adsorption characteristics. However, objects for other sites which lie in the outer shell may have differing adsorption characteristics and proportions of adsorbed metals under different mechanisms.

According to Figure 6.2, Fe, Al and Mn show strong correlation to all of the other metal elements. As noted in the discussion for the particle size  $<75\mu\text{m}$  range, this suggests that a significant proportion of Fe, Al and Mn in the samples would be present in oxide or hydroxide form, acting as a binder in solids. Similar to the  $<75\mu\text{m}$  size range, a majority of the other heavy metals are adsorbed to oxides of Fe, Al and Mn in this particle size range. However, Fe, Al and Mn show weak or no correlation with albite and chlorite (See Figure 6.2), while showing a strong correlation with TOC and EGME SSA (See Table 6.5). Therefore, it can be concluded that the oxide form of the metal elements is present primarily with organic matter rather than chlorite or albite, similar to the particle size range  $<75\mu\text{m}$ . This agrees with the findings of Farquhar et al. (1997), who noted that metal oxides are preferentially available with organic matter in most soils.

Similar to particle size range  $<75\mu\text{m}$ , Fe, Al and Mn show a strong correlation with Zn, Cu, Ni, Cd and Pb. However, instead of Cr, as in the case of the  $<75\mu\text{m}$  size range, Cd has a preference for metal oxides. It can be concluded that a significant proportion of the heavy metals would be adsorbed to metal oxides of Fe, Al and Mn. However, Fe, Al and Mn show very weak or no correlation with ECEC. Therefore, it can be suggested that heavy metals adsorption to metal oxides would not occur by ion exchange. Similar behaviour was observed in the case of  $<75\mu\text{m}$  particles, where heavy metal adsorption to metal oxides was found to take place by chemisorption.

This conclusion agrees with the observations of Barker et al. (1998), who noted that heavy metals adsorption to metal oxides is mainly by chemisorption.

However, it is a possibility that the organic matter itself contributes to adsorption, as it increases the surface area of a particle (Warren and Zimmerman 1994). As evident in Figure 6.2, both TOC and EGME SSA are strongly correlated, and these parameters are weakly correlated with Pb, Zn, Cu and Cr (See Table 6.5). Therefore, the direct adsorption of metal elements to organic matter in this particle size range could be higher than in the case of particles in the  $<75\mu\text{m}$  range. Strong correlation of EGME SSA with Pb, Zn, Cu and Cr, as shown in Figure 6.2, suggests that EGME SSA would play an important role in adsorbing these metal elements to organic matter. Similar to the  $<75\mu\text{m}$  particles, adsorption to TOC would occur by chemisorption. This hypothesis is based on the negative correlation of TOC with ECEC in Figure 6.2 and is supported by the correlation matrix given in Table 6.5.

Figure 6.2 shows that albite and chlorite are strongly correlated with ECEC. However, the majority of metal elements, with the exception of Ni and Cr, show a very weak correlation with albite and chlorite minerals. Therefore, it can be concluded that minor proportions of Ni and Cu would interact with albite and chlorite by cation exchange mechanism. All of the other heavy metal elements show very weak or no correlation to clay forming minerals. Even though clay minerals have high capacity for cation exchange in this particle size range, heavy metal elements adsorbed to clay minerals are considerably low. This suggests that the majority of the heavy metal elements in this particle size range show preference to chemisorption with other forms of charge sites. The possible reason for this behaviour would be the high preference for heavy metal elements to bind with the strongest charge sites (Zhuang and Yu 2002). Since the metals concentrations in 75-150 $\mu\text{m}$  particles are relatively low compared to the  $<75\mu\text{m}$  particles, competition of heavy metal elements for charge sites would be relatively low. This suggests that vacant charge sites would be present in clay forming minerals.

Cr shows significantly different adsorption characteristics compared to the other heavy metals. According to Figure 6.2, Cr strongly correlates with TOC, EGME SSA and amorphous material. However, according to Table 6.5, Cr is not correlated to TOC (0.04). Furthermore, Cr is negatively correlated to clay forming minerals and ECEC (Figure 6.2). This can also be confirmed by the correlation matrix which shows near zero or negative correlation coefficients for Cr with clay forming minerals and ECEC. This suggests that Cr is not adsorbed to organic matter or clay forming minerals in this particle size range. However, Cr is a trivalent cation with high electro negativity (hard base). Therefore, there is a high possibility for Cr to be adsorbed to solids particles by chemisorption or ion exchange mechanisms since it has high selectivity for charge sites. Since Cr is not correlated to organic matter, clay forming minerals or ECEC, it can be hypothesised that Cr could be present either as a precipitate or embedded to solid particles.

According to Figure 6.2, the amorphous content shows strong correlation with Cr and weak correlation with Zn, Al and Cu. Correlation coefficients given in Table 6.5 also confirm the positive correlations of Cr, Zn, Al and Cu with the amorphous content. Thus, a considerable amount of these metal elements would be present in traffic related particles. Compared to the <75 $\mu$ m particles, amorphous content in this particle size range shows a relatively higher metal content. The reduction in surface area with the increase in particle diameter would have possibly influenced this behaviour since it reduces the interaction with surrounding media and reduces metal leaching from the particles. As noted by the Gualtieri et al. (2005), morphological changes in traffic related particles have a strong influence on heavy metals leaching from the particles. Therefore, it can be hypothesised that metal leaching (migrate) from the amorphous content in this particle size range would be low compared to the finer particle size range.

### **Particle size 150-425 $\mu$ m**

Particle sizes 150-300 $\mu$ m and 300-425 $\mu$ m were combined in the analysis, as noted in Section 6.3.1. Metal content in the combined particle size range is low compared to the <150 $\mu$ m particles. Similarly, amorphous material, clay forming minerals and

organic matter content are considerably low compared to the finer particle sizes. The effect of ECEC on metal adsorption would be very low compared to the finer particles, and organic matter is the parameter most responsible for ECEC in this particle size range. Analysis of the physical and chemical characteristics carried out in Section 5.5 indicated that quartz is the dominant mineral, comprising of more than 60% of the sample. Due to the low proportions of clay forming minerals compared to the quartz content, the influence of albite, microcline, chlorite and muscovite in heavy metals adsorption would be low.

The pre-treated data matrix (64 x 18) was subjected to PCA. Since the variation of physical and chemical parameters for the combined size range of 150-300 $\mu\text{m}$  and 300-425 $\mu\text{m}$  was not analysed previously, muscovite and microcline minerals were also included in the analysis. The number of PCs needed for the analysis was determined based on the Scree plot method (Appendix B/Figure B.3). Accordingly, two principal components were selected for the interpretation of outcomes. According to Figure 6.3, the two PCs account for a total variance of 42%. The inclusion of a high number of physical and chemical parameters would be the reason for the low data variance explained by the PCA biplot. Consequently, a correlation matrix was also employed to confirm the outcomes from the PCA biplot (Table 6.6). Correlation coefficients of heavy metal elements with physical and chemical parameters are relatively low. As noted in relation to <75 $\mu\text{m}$  and 75-150 $\mu\text{m}$  particle size ranges, this indicated that the heavy metal elements are adsorbed on different surface charge sites on solids particles.

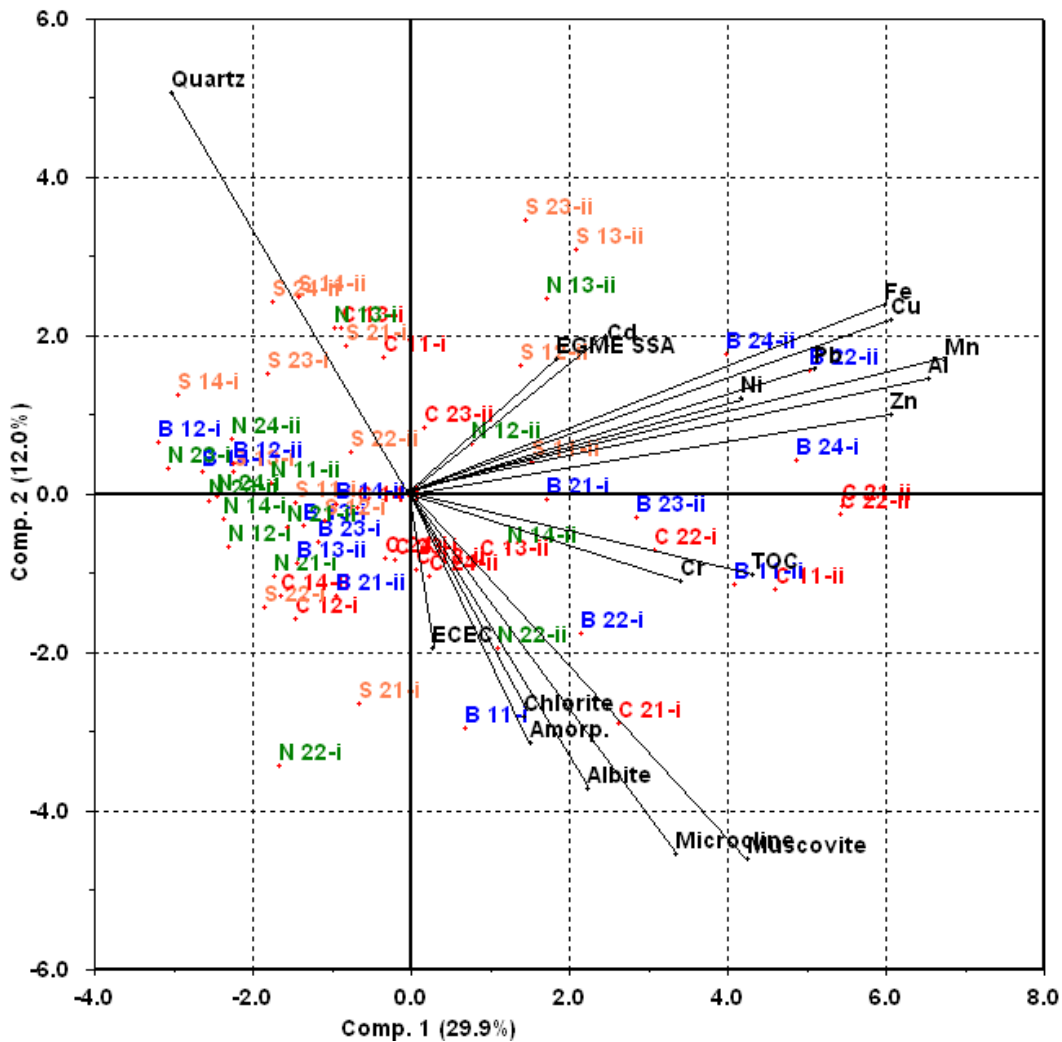


**Figure 6.3: PC 1 vs PC 2 biplot obtained from PCA for particle size range 150-425µm**

Note: C– Clearview Estate, N- Nerang, B- Benowa, S- Surfers Paradise, 1 and 2 - first and second sampling event

According to Figure 6.3, all of the variables, with the exception of quartz, are located on the positive PC 1 axis. All heavy metal elements (with the exception of Cr), EGME SSA and quartz are on the positive PC 2 axis. Furthermore, all clay forming minerals, amorphous content and TOC are on the negative PC 2 axis. Accordingly, it can be seen that PC 1 separates the heavy metal elements and the majority of the physical and chemical parameters. PC 2 distinguishes quartz from all of the other variables. All of the mineralogical components, other than quartz, are strongly correlated, and weakly correlated with heavy metal elements. Therefore, the contribution of mineralogical components to heavy metal adsorption would be



**Table 6.6: Correlation matrix for the particle size range 150-425µm**

	EGME SSA	TOC	Al	Cr	Mn	Fe	Ni	Cu	Zn	Cd	Pb	ECEC	Amorp.	Quartz	Albite	Microcline	Chlorite	Muscovite
EGME SSA	1																	
TOC	0.154	1																
Al	0.108	<b>0.429</b>	1															
Cr	0.104	<b>0.288</b>	0.243	1														
Mn	0.189	<b>0.314</b>	<b>0.861</b>	<b>0.34</b>	1													
Fe	0.088	<b>0.272</b>	<b>0.872</b>	0.022	<b>0.801</b>	1												
Ni	0.309	0.294	0.292	0.39	<b>0.417</b>	0.291	1											
Cu	0.185	0.300	<b>0.558</b>	0.284	<b>0.720</b>	<b>0.587</b>	0.398	1										
Zn	0.144	0.347	<b>0.615</b>	0.299	<b>0.676</b>	<b>0.548</b>	0.353	0.689	1									
Cd	0.190	0.089	0.304	0.072	0.256	<b>0.375</b>	0.235	0.223	0.032	1								
Pb	0.146	0.372	<b>0.432</b>	0.227	0.397	<b>0.459</b>	0.317	0.620	0.601	0.160	1							
ECEC	0.047	-0.001	0.02	<b>0.247</b>	0.042	-0.035	-0.063	-0.080	0.012	-0.035	-0.104	1						
Amorp.	-0.057	0.175	0.145	-0.069	0.047	0.120	-0.086	0.013	0.180	0.06	0.092	-0.039	1					
Quartz	0.046	-0.239	-0.247	-0.03	-0.183	-0.211	-0.017	-0.122	-0.258	-0.078	-0.126	-0.017	<b>-0.892</b>	1				
Albite	0.073	-0.045	0.109	0.093	0.219	0.168	0.231	0.171	0.075	-0.023	-0.069	0.074	-0.078	-0.322	1			
Microcline	-0.098	0.314	<b>0.224</b>	<b>0.419</b>	<b>0.278</b>	0.063	0.212	0.167	0.179	0.019	0.136	0.118	-0.090	-0.248	0.453	1		
Chlorite	-0.015	0.019	0.025	-0.035	0.067	0.02	0.062	0.075	0.216	-0.007	0.11	-0.006	0.050	-0.205	0.204	0.194	1	
Muscovite	0.105	<b>0.433</b>	<b>0.337</b>	<b>0.319</b>	<b>0.289</b>	<b>0.214</b>	0.154	0.228	0.247	0.069	0.313	0.188	0.108	-0.409	0.377	0.630	0.269	1

relatively low in this particle size range. Quartz shows no correlation to the majority of the heavy metal elements. This indicates that quartz, which is the most abundant mineral component in this particle size range, does not contribute to the adsorption of heavy metals in road deposited solids. As indicated by Filep (1999), quartz has an electrically neutral crystal lattice and it is highly resistant to physical and chemical changes to its structure. Hence, the increase in quartz content potentially reduces the heavy metal content in the sample. This could be the primary reason for the low heavy metal content in the coarse particle size range, as observed in Section 6.1.

As evident in Figure 6.3, Fe, Al and Mn are strongly correlated, and show strong correlation to other heavy metal elements. Similar to the finer particle size ranges, this indicates that a significant proportion of Fe, Al and Mn in solids samples would be present as oxides and influence metals adsorption. Fe, Al and Mn show weak correlation with TOC and clay forming minerals of microcline and muscovite. Relatively similar correlation coefficient values for Fe, Al and Mn with TOC, microcline and muscovite as given in Table 6.6, indicating the almost equal contribution of TOC and clay forming minerals to metal oxide retention on solids particles. This suggests that Fe, Al and Mn oxides would be present as coatings in both clay mineral surfaces and organic matter content (Farquhar et al. 1997). Low clay forming minerals and organic matter content in solids particles in this size range would have also influenced the distribution of metal oxides on the particle surfaces.

In Figure 6.3, Zn, Cu, Pb, Ni and Cd show strong correlation with Fe, Al and Mn. Thus, a significant proportion of these metals would be adsorbed to Fe, Al and Mn oxides. Due to the weak correlation of metal elements with ECEC, it can be postulated that the adsorption of Zn, Cu, Pb, Ni and Cd to metal oxides is limited through cation exchange mechanism.

Furthermore, TOC is strongly correlated to all the heavy metal elements. According to the correlation coefficients given in Table 6.6, Zn, Cu, Pb, Ni and Cd have relatively high values with TOC. Therefore, it can be concluded that, after metal oxides, Zn, Cu, Pb, Ni and Cd metal elements would preferentially adsorb with

organic matter content. EGME SSA also shows strong correlation with heavy metals. EGME SSA is an important indicator in the adsorption of heavy metals to solids particles. Although ECEC shows good correlation with TOC in Figure 6.3, according to the correlation matrix given in Table 6.6, ECEC has very weak correlation with TOC. Therefore, it is postulated that TOC would adsorb metal elements by a mechanism other than ion exchange. Similar to the finer particles, this leads to the conclusion that organic matter would adsorb metal elements by chemisorption.

As discussed in Section 5.3.2, organic matter content in this particle size range is relatively low compared to the finer particle sizes. However, metal elements have a strong preference for TOC over clay minerals in this particle size range. Similarly, the 75-150 $\mu\text{m}$  particle size range showed high influence of TOC on metal adsorption compared to the <75 $\mu\text{m}$  particle size range. Therefore, it can be concluded that this particle size range contains a predominant amount of decomposed organic matter compared to the finer particles.

While the majority of metal elements did not correlate closely with clay forming minerals in the 75-150 $\mu\text{m}$  particle size range, clay minerals show good correlation with all metal elements in this particle range (See Table 6.6). Fe, Al and Mn especially show strong correlation with muscovite and microcline minerals. However, these correlations cannot be clearly seen in Figure 6.3. This indicates that the clay forming minerals do not directly interact with heavy metal elements, and heavy metal adsorption to clay would occur through the metal oxides. Therefore, Fe, Al and Mn would be present as a coating on clay forming minerals and adsorb heavy metal elements. Thus, the majority of charge sites in clay minerals would be occupied by metal oxides.

According to Figure 6.3, Cr is different in its association with particles compared to the other metals. Cr is positively correlated with clay forming minerals, ECEC and TOC. Thus, Cr could adsorb to clay minerals and organic matter by cation exchange. Even though Cr shows weak correlation to the amorphous content in the PCA biplot

(See Figure 6.3), the correlation matrix shows a negative correlation with the amorphous content. Thus, Cr would not be available in the amorphous content in this particle size range.

Interestingly, amorphous content shows a positive correlation with all metal elements other than Ni and Cr (Table 6.6). Similar to the fine particle sizes, amorphous content has a negative correlation with ECEC. Therefore, it can be surmised that these metal elements would not be exchanged with the exchangeable cations in amorphous material, or exchanged with Zn in tyre particles. Zn, Cu, Pb, Cd, Al, Fe and Mn metal would be embedded in the traffic related particles such as tyre wear, brake lining material and corrosion products in amorphous material.

#### **6.4 ANALYSIS OF HEAVY METALS IN BULK BUILD-UP SAMPLES**

Adsorption characteristics for different particle size ranges of road deposited solids were discussed in Section 6.3. However, it is necessary to understand the characteristics of bulk build-up pollutants present on road surfaces to provide guidance for pollutant mitigation in stormwater runoff. Consequently, analysis was carried out for combined samples of solids.

The pre-treated data matrix, which combined all particle sizes, was subjected to PCA. The first three principal components were selected based on the Scree plot method (Appendix B/Figure B.5). The resulting PCA biplot of PC 1 vs PC 2 is shown in Figure 6.4, and the PC 1 vs PC 3 biplot is shown in Figure 6.5. As shown in Figure 6.4 and Figure 6.5, the first three PCs account for a total data variance of 55.8%. The relatively low data variance explained by the first three principal components suggested the necessity of another form of analysis to confirm the interpretations derived from PCA. For this purpose, a correlation matrix (Table 6.7), which substantiates the extent of correlations of the overall principal component analysis, was used (Farnham et al. 2003).

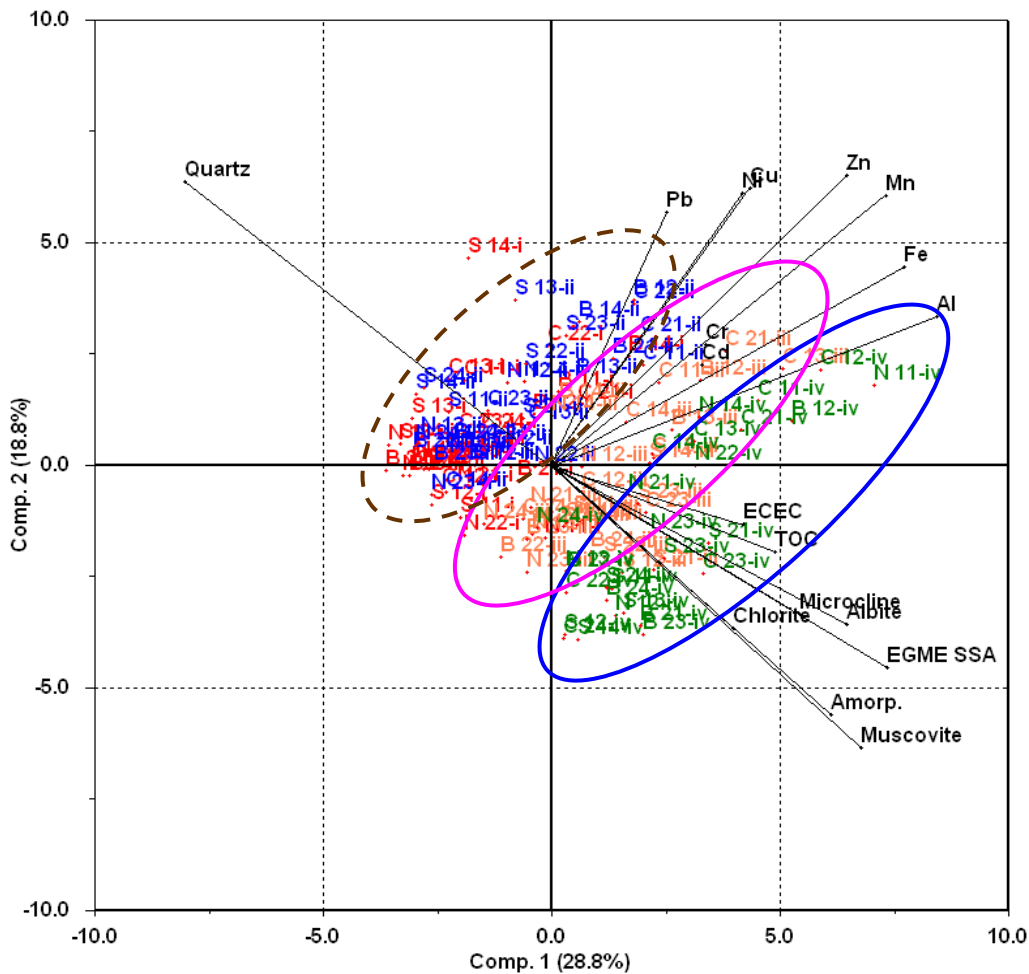


**Figure 6.4: PC 1 vs PC 2 biplot obtained from PCA on all the particle size ranges**

Note: C– Clearview Estate, N- Nerang, B- Benowa, S- Surfers Paradise, 1 and 2 - first and second sampling event

In Figure 6.4, all heavy metal elements and all of the physical and chemical parameters other than quartz are located along the positive PC 1 axis, while quartz is located along the negative PC 1 axis. All heavy metal elements and quartz are located along the positive PC 2 axis, while all physical and chemical parameters are located on the negative PC 2 axis. Figure 6.4 indicates that clay forming minerals, TOC, EGME SSA and ECEC do not exert a significant influence on heavy metal adsorption. However, in Figure 6.5, microcline, muscovite, albite, amorphous, Cr, Cu Ni and Pb metal elements are located on the positive PC 3 axis, indicating the influence of mineralogical components on Cr, Cu, Ni and Pb adsorption. Furthermore, chlorite, TOC, ECEC, Fe, Al and Mn are located in the direction of the

negative PC 3 axis. This confirms the role of chlorite and TOC in retaining metal oxides of Fe, Al and Mn.

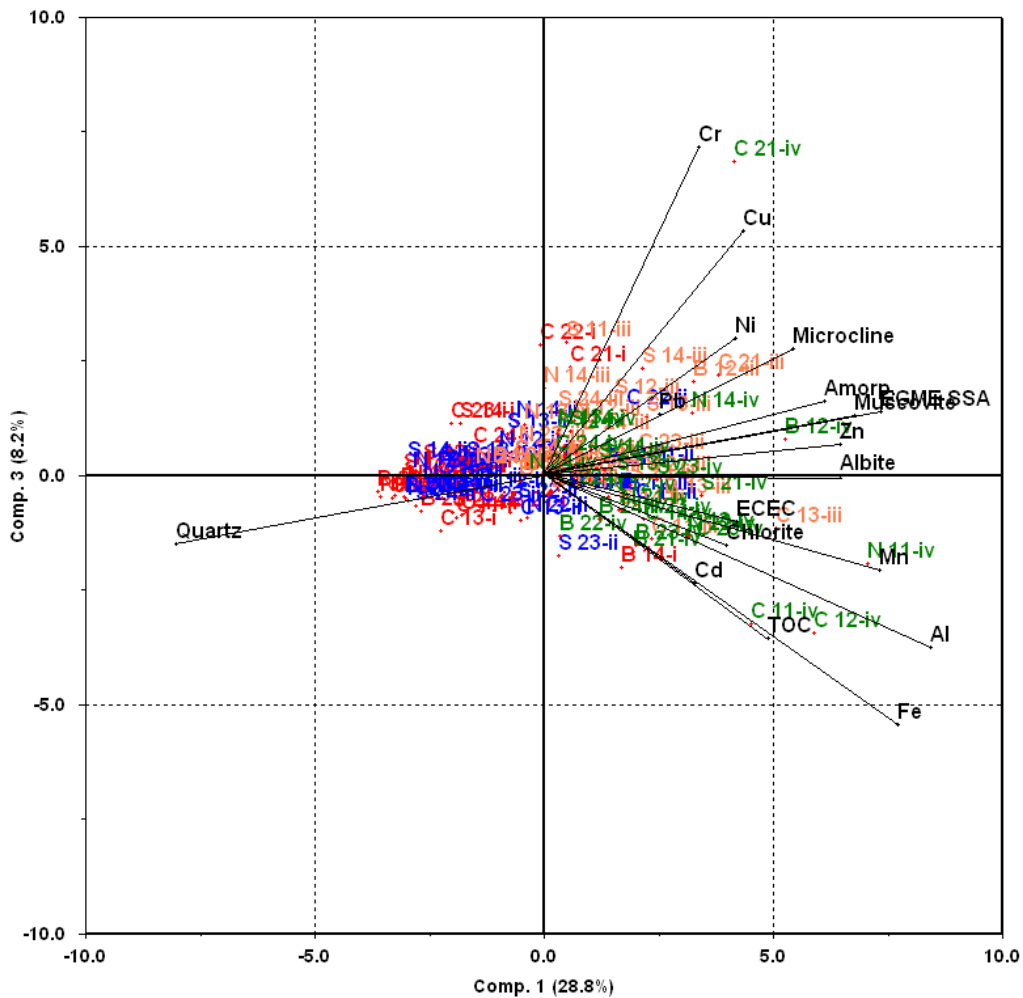


**Figure 6.5: PC 1 vs PC 3 biplot obtained from PCA on all the particle size ranges**

Note: C– Clearview Estate, N- Nerang, B- Benowa, S- Surfers Paradise, 1 and 2- first and second sampling event

**Table 6.7: Correlation matrix for the PCA analysis of all the particle size ranges**

	EGME SSA	TOC	Al	Cr	Mn	Fe	Ni	Cu	Zn	Cd	Pb	ECEC	Amorp.	Quartz	Albite	Microcline	Chlorite	Muscovite
EGME SSA	1																	
TOC	<b>0.35</b>	1																
Al	0.256	<b>0.529</b>	1															
Cr	0.149	0.233	<b>0.596</b>	1														
Mn	0.146	<b>0.34</b>	<b>0.872</b>	0.572	1													
Fe	0.188	<b>0.451</b>	<b>0.937</b>	<b>0.532</b>	<b>0.849</b>	1												
Ni	0.111	0.253	<b>0.696</b>	<b>0.626</b>	<b>0.751</b>	<b>0.74</b>	1											
Cu	0.118	0.214	0.487	<b>0.531</b>	<b>0.594</b>	0.453	<b>0.592</b>	1										
Zn	0.104	<b>0.354</b>	<b>0.808</b>	0.570	<b>0.855</b>	<b>0.815</b>	0.781	<b>0.687</b>	1									
Cd	0.126	0.064	0.288	0.090	0.287	0.345	0.237	0.264	0.308	1								
Pb	0.086	<b>0.439</b>	<b>0.669</b>	<b>0.541</b>	<b>0.606</b>	<b>0.738</b>	<b>0.692</b>	<b>0.503</b>	<b>0.703</b>	0.241	1							
ECEC	<b>0.338</b>	0.014	0.015	-0.037	0.047	0.023	-0.074	-0.068	0.001	0.125	-0.053	1						
Amorp.	<b>0.614</b>	0.372	<b>0.266</b>	<b>0.153</b>	0.097	0.142	-0.029	0.089	<b>0.127</b>	<b>0.109</b>	0.059	0.152	1					
Quartz	-0.705	-0.374	-0.381	-0.202	-0.238	-0.285	-0.107	-0.134	-0.238	-0.148	-0.111	-0.243	<b>-0.898</b>	1				
Albite	<b>0.454</b>	0.118	0.283	0.102	0.312	0.3	0.247	0.072	0.211	0.029	0.034	0.294	0.204	-0.569	1			
Microcline	0.271	0.057	0.208	0.142	0.172	0.133	0.128	0.167	0.149	0.002	0.026	0.236	0.208	-0.496	0.557	1		
Chlorite	0.267	0.154	<b>0.557</b>	<b>0.408</b>	<b>0.476</b>	<b>0.651</b>	<b>0.517</b>	0.220	0.551	0.265	<b>0.492</b>	0.03	0.168	-0.349	0.287	0.169	1	
Muscovite	<b>0.633</b>	<b>0.346</b>	0.203	0.069	0.085	0.128	0.028	0.023	0.096	0.107	0.041	0.206	<b>0.517</b>	-0.742	0.556	0.520	0.290	1

Figure 6.4 shows three clearly separated groups of objects. The three groups consist of objects with particle sizes  $<75\mu\text{m}$  (iv),  $75\text{-}150\mu\text{m}$  (iii) and  $150\text{-}425\mu\text{m}$  (i, ii) respectively. The finer particles of  $<75\mu\text{m}$  and  $75\text{-}150\mu\text{m}$  show separation, while  $150\text{-}300\mu\text{m}$  and  $300\text{-}425\mu\text{m}$  overlay. Objects of  $150\text{-}300\mu\text{m}$  and  $300\text{-}425\mu\text{m}$  are overlaid due to the similarity in their physical and chemical parameters, as discussed in Section 5.6. These objects groups are formed perpendicular to quartz and physico-chemical parameter vectors. As evident in the correlation matrix in Table 6.7, quartz has strong negative correlation with EGME SSA (-0.705) and amorphous material (-0.898). The negative correlations of quartz with amorphous and EGME SSA are also evident in Figure 6.5. Therefore, it can be surmised that three objects groups are formed perpendicular to the amorphous content, EGME SSA and quartz vectors. This suggests that the differences in the three particle sizes in relation to heavy metals adsorption would mainly arise from the quartz and amorphous content of the solids, and from differences in EGME SSA of the three particle size ranges.

Quartz shows strong negative correlation with all of the physical and chemical parameters of solids, especially the amorphous content (See Table 6.7). Similarly, quartz is not correlated with all of the heavy metals (See Figure B.6 and Table 6.7). The distribution of variables in Figure 6.4 is similar to the distribution observed for the particle size  $150\text{-}425\mu\text{m}$  in Figure 6.3. This suggests that the predominant amount of quartz content present in solids could affect their physico-chemical behaviour due to the electrically neutral crystal lattice of quartz. Therefore, it can be concluded that road deposited solids particles dominated by quartz would adsorb low concentrations of heavy metals.

Although Figure 6.4 shows very weak or no correlation of heavy metal elements with physical and chemical parameters, in Figure 6.5, mineralogical components show good affinity to metal elements. This can be clearly seen in the correlation matrix given in Table 6.7. Albite shows positive correlation with all metal elements. Among the metal elements, Fe, Al, Mn, Zn, Ni and Cr have high correlation coefficients with albite (Table 6.7). Albite also shows fairly good correlation with ECEC, which indicates that most of the metal elements associated with albite are



adsorbed by ion exchange (Figure 6.4). This agrees with the results described in Section 6.3, which discussed different particle size ranges of solids particles. As evident in the correlation matrix (Table 6.7), chlorite shows positive correlation to a majority of metal elements and ECEC. Chlorite is the lowest detected mineral component in solids (Section 5.3.3). Therefore, the proportion of metal content in chlorite would be relatively low compared to the other mineral components. However, the data analysis discussed in Section 6.3 indicated that cation exchange would be the dominant mechanism of metal adsorption by the mineralogical components of solids.

According to Figure 6.4 and Figure 6.5, TOC has a fairly good correlation with Al and Fe and Pb, Zn and Mn being the next most preferred metal elements. Pb would preferentially associate with TOC rather than Fe and Al (Table 6.7). This further confirms the preferential association of Pb with TOC noted in the individual particle sizes discussed in Section 6.3. Although TOC shows good correlation with ECEC in Figure 6.4, according to the correlation matrix, TOC has poor correlation with ECEC (0.014). This suggests that TOC predominantly adsorbs metals by mechanisms other than cation exchange. As discussed in Section 6.3, it can be concluded that Pb is adsorbed to organic matter by chemisorption.

EGME SSA is positively correlated with all of the heavy metal elements (Figure 6.4 and Figure 6.5), having a similar coefficient of correlation for all metal elements other than Pb (Table 6.7). As seen in Section 6.3, in the analysis of individual particle sizes, EGME SSA is consistently correlated with the predominant charge sites in each of the particle size ranges. For example, in the <75 $\mu$ m particle size range, EGME SSA is strongly correlated with the clay forming minerals of albite and chlorite which have a strong influence on metal adsorption. Similarly, in the 75-150 $\mu$ m particle size range, EGME SSA is strongly correlated with TOC. This suggests that heavy metals preferentially associate with materials with high SSA. Therefore, it can be concluded that heavy metal adsorption is always increased with high EGME SSA of the adsorbing surface.

Geochemically originating metal elements such as Al, Fe and Mn are closely correlated with physical and chemical parameters. This can be clearly seen in Figure 6.5 where Fe, Al and Mn are in the direction of the negative PC 1 axis, while all the other metal elements are in the direction of the positive PC 1 axis, indicating the differences in geochemically originated metal elements compared to the other metal elements. As identified in the analysis of individual particle size fractions, this indicates that a high percentage of Fe, Al and Mn present in solids are oxides. These metal elements show positive correlation with all of the clay forming minerals (Table 6.7). Preference of Fe, Al and Mn metal elements for clay forming minerals could vary. As seen in Figure 6.3 and the correlation matrix (Table 6.7), Fe is the preferred metal element for the clay forming minerals. The availability of Fe, Al and Mn in oxide form in clay forming minerals would follow the order of Fe, Al and Mn respectively. Similarly, Fe, Al and Mn metal elements also show positive correlation with organic matter (Figure 6.4 and Figure 6.5). Preference for organic matter is in the order of Al, Fe and Mn (Table 6.7). Therefore Fe, Al and Mn would be present as metal oxides on clay forming minerals and organic matter, and increase the adsorption of other heavy metal cations on solids particles (Filep 1999).

Zn, Ni and Cu show strong correlation to Fe, Al and Mn (Figure 5.6). Among Zn, Ni and Cu metal elements, Cu shows higher correlation coefficients with Fe, Al and Mn, and correlation with clay forming minerals and organic matter content are relatively low. This suggests that Cu would be predominantly adsorbed to metal oxides rather than to organic matter and clay forming minerals (Figure 5.6 and Table 6.7). Cu would be predominantly adsorbed to Mn oxides. Following Mn oxide, Cu would be preferentially adsorbed on Al and Fe oxides and organic matter content. Furthermore, Cu shows negative or no correlation (-0.068) to ECEC. Therefore, this suggests that Cu would be associated with solids particles by mechanism other than cation exchange. This conclusion is further confirmed by Milberg et al. (1978), who noted that Cu is bound to Mn oxide and organic matter by inner sphere complexation. Thus, Cu would be present in solids in non-exchangeable form with metal oxides. Mn shows the highest correlation coefficient with ECEC (Table 6.7 and Figure 6.5). This suggests that Mn adsorption to solids is enhanced by high

ECEC. However, as evident in Figure 6.4, Cu shows very weak correlation to clay minerals. This confirms that Cu adsorption to clay minerals would be low.

As evident in Figure 6.4, amorphous material shows very weak correlation with the majority of the metal elements other than Ni, Cu and Pb. This is also further confirmed by the correlation matrix which shows no correlation with Ni, Cu and Pb metal elements (Table 6.7). This suggests that a significant amount of metal elements could be present in amorphous material, embedded in traffic related particles. Cd and Zn would be the most common metal elements that would be present mostly in amorphous content, embedded to traffic related particles. This agrees with the analysis of individual particle sizes.

The percentage of heavy metals released mainly depends on the characteristics of the traffic related particles. For example, Smolders and Degryse (2000) found that Zn release from tyre wear particles depends on the particle matrix, whether it is a car tyre or a truck tyre. Both Cd and Zn primarily originate from tyre wear particles (McKenzie et al. 2009; Blok 2005), while brake lining is also a major source of Cd to road surface pollutant. Analysis revealed that, with the exception of Ni, all metal elements could be embedded in traffic related particles. This conclusion was derived as there is no correlation of Ni with amorphous content in any of the particle sizes of road deposited solids (See Figure 6.1, Figure 6.3 and Figure 6.4). This, in turn, explains why a major portion of Ni in tyre and brake lining wear would be readily released to the environment.

Although heavy metals bind preferentially to the strongest charge sites in solids (Benjamin and Leckie 1981), in the current study, a specific heavy metal showed preference for several different charge sites in solids. The preference for a variety of charge sites is attributed to the electro negativity (acid – base), valency, ionic radii, competing cations, limitation of preferred charge sites and metal speciation (See Section 2.5). A variety of heavy metal species can be present due to hydrolysis. For example, Cr can be extensively hydrolysed in mild acid conditions to species such as  $\text{Cr}(\text{OH})^{2+}$ ,  $\text{Cr}_2(\text{OH})_4^{2+}$ ,  $\text{CrOH}^{2+}$  or  $\text{Cr}^{3+}$  (hydrated free cation) (Bradl 2004;

Murakami et al. 2008). Heavy metal organic complexes and carbonates can also be present in minor portions, such as  $\text{CuHCO}_3^{3+}$  and  $\text{ZnHCO}_3^{3+}$  (Dijkstra et al. 2004; Murakami et al. 2008). However, Murakami et al. (2008) noted that the majority of the heavy metals on road surface pollutants would be present as free metal ions (hydrated), while different species could be present in minor fractions. Preferred charge sites for different species could vary from one site to another. This suggests that the presence of different species would also influence heavy metal elements being selectively adsorbed to different charge sites.

Analysis revealed the differences in organic matter in different particle sizes. The fine particle size range ( $<75\mu\text{m}$ ) contained high organic matter derived mainly from plant matter (Section 5.3.2). The majority of TOC in the fine particle size range ( $<150\mu\text{m}$ ) is present primarily in the form of organic residue. This suggests that, rather than the amount of organic matter present, its composition or nature would be the most important factor in relation to metal adsorption. Furthermore, it was found that coarse particles ( $>150\mu\text{m}$ ) contain more active organic matter than fine particles ( $<150\mu\text{m}$ ). Humic compounds are more effective in heavy metals adsorption rather than residual organic compounds (Section 2.4.1.). Organic matter in fine solids is easily decomposed and associates with the mineral phase (Kahle et al. 2003). However, the characteristics of organic matter associated with different soils particles (clay, silt and sand) could vary with the types of minerals present (Laird et al. 1994) or with the amorphous metal oxides content (crystalline minerals) (Kleber et al. 2004; Mikutta et al. 2005).

## 6.5 CONCLUSIONS

The chapter has discussed the outcomes of the data analysis which focused on understanding the role of physical and chemical characteristics of solids on heavy metals adsorption. Heavy metal concentrations in build-up solids collected from road surfaces were investigated in relation to their physical and chemical parameters, including total organic carbon (TOC), specific surface area (SSA), effective cation exchange capacity (ECEC) and solids mineralogy. The analysis was carried out with respect to particle size ranges to understand the mechanisms involved in heavy metal

adsorption to solids particles. The important conclusions from the analysis are listed below.

- Heavy metals load from industrial, commercial and residential land uses shows inherent variation due to site specific characteristics. The variation in traffic related activities in different land uses is the primary factor which influences the differences in heavy metal loads in build-up.
- Heavy metal concentrations in solids reduce with the increase in particle size. In the majority of the study sites, metal concentrations in the particle size range 150-300 $\mu\text{m}$  and 300-425 $\mu\text{m}$  are considerably similar. It was found that the high quartz content is the primary reason for the low heavy metal content in coarse particle sizes (>150 $\mu\text{m}$ ).
- Heavy metals that originate from geochemical sources (Fe, Al and Mn) show relatively higher concentration than those from traffic related sources. While mineralogical analysis did not detect the crystalline forms of Fe, Al and Mn in solids samples, it is highly likely that Fe, Al and Mn are present as oxides in the soil. Therefore, it can be argued that a higher fraction of geochemical origin metal elements in solids are present as oxides attached to clay minerals and organic matter content.
- Road deposited solids consist of distinct groups of charge sites that are inherent in mineralogical components, organic matter content, and Fe, Al and Mn oxides. The characteristics and the amount of charge sites in solids are different for different particle sizes due to the solids composition. Specific heavy metal ions can be adsorbed into any of the different charge sites; however, the adsorption mechanism and the strength of bond can be different. Heavy metal element selectivity for charge sites varies due to electro negativity (hard soft acid – base), valency, ionic radii and metal speciation. However, metal ions may not necessarily have the opportunity to form their preferred bond due to the lack of preferred charge sites and the ability to reach the preferred charge sites. Consequently, heavy metals may be adsorbed to secondary charge sites. Consequently, heavy metal adsorption is influenced by the physical and chemical characteristics of solids due to the heterogeneity of surface charge sites.

- Table 6.8 provides a summary of the preference and metal adsorption characteristics of different particle sizes.

**Table 6.8: Heavy metal adsorption characteristics of different particle sizes**

<b>&lt;75µm</b>	<b>75-150µm</b>	<b>150-425µm</b>
Fe, Al and Mn are present in oxide form in clay forming minerals, especially in albite	Fe, Al and Mn are present in oxide form in organic matter content	Fe, Al and Mn are present in oxide form in both clay forming minerals and organic matter content
Major portion of Zn, Cu, Pb, Ni and Cr is associated with metal oxides through chemisorption	Major portion of Zn, Cu, Pb, Ni and Cd is associated with metal oxides through chemisorption	Major portion of Zn, Cu, Pb, Ni and Cd is associated with metal oxides through chemisorption
Considerable amount of Zn, Cu, Pb and Ni is adsorbed to albite by cation exchange  High ECEC and EGME SSA associated with albite increases metal adsorption	Considerable amount of Zn, Cu, Pb and Cr is adsorbed to TOC by chemisorption  High EGME SSA associated with TOC increases metal adsorption	Considerable amount of Zn, Cu, Pb, Ni and Cd is adsorbed to TOC by chemisorption
Considerable amount of Pb chemisorbed to TOC	Clay forming minerals of albite and chlorite associated with ECEC, but very low contribution to heavy metal adsorption	Clay forming minerals do not directly interact with heavy metal elements
Cd embedded in traffic related particles of amorphous content	Significant amount of Cr, Zn, Cu, Pb and Al embedded in traffic related particles of amorphous content	Significant amount of Zn, Cu, Pb, Cd, Al, Fe and Mn embedded in traffic related particles of amorphous content

- The characteristics of the organic matter content are more important than its source or quantity for heavy metal adsorption to solids particle surfaces.

Coarse particles (>150 $\mu\text{m}$ ) contain more active organic matter than the fine particles (<150 $\mu\text{m}$ ).

- While amorphous material has high EGME SSA, the material does not act as an adsorbent for heavy metals. Therefore, metals present in traffic related particles are mainly embedded.
- Amorphous material in coarse particles contains higher metal concentrations than fine particles. This suggests that a relatively higher amount of metals in fine particles is leached out once the metals are exposed to the environment during the antecedent dry period. Thus, traffic related coarse particles may have a potentially greater environmental impact in the long term than fine particles.
- A combination of clay forming minerals, organic matter, EGME SSA and ECEC influence metal adsorption to road deposited solids.
- Metal adsorption to clay forming minerals primarily occurs by ion exchange, and the occurrence of chemisorption at edge sites of clay forming minerals is insignificant. The primary mechanism in heavy metal adsorption to organic matter is chemisorption, while cation exchange is the secondary mechanism. Fe, Al and Mn oxides may adsorb a significant fraction of metal elements to solids.
- Zn, Cu, Pb and Ni have similar adsorption characteristics. They have high affinity to metal oxides in the order of Mn, Fe and Al. Adsorption mostly occurs by chemisorption.
- Cd and Cr mostly prefer ion-exchangeable adsorption. Primarily, these metals are associated with amorphous content, mineralogical components and organic matter.
- Appreciable amount of Cr, Cd and Zn are available in the amorphous content, as a direct input of traffic related by-products.
- Pb is mostly found in association with organic matter content. Preferential association of Pb is found to be organic matter > metal oxide > mineralogical components. Association could be mostly a chemisorptions mechanism,

rather than a cation-exchange mechanism. Surface area is not an influential parameter for the Pb adsorption to solids.

- Cu has strong bonds which do not occur by cation exchange. The presence of Cu in amorphous material is insignificant. Cu adsorption affinity decreases in the order of metal oxide > clay.



# Chapter 7: Interaction of Heavy Metals with Solids

---

## 7.1 INTRODUCTION

Road deposited solids are heterogeneous and use several different mechanisms for heavy metal adsorption. Heavy metals in road deposited solids are adsorbed to the clay forming minerals, organic matter and metal oxides which are embedded in traffic related amorphous material. Among these, clay minerals, organic matter and metal oxides content are the most significant substances that influence heavy metal adsorption, since they increase the charge sites in solids particles. However, each of these substances exhibits different forms of influence on metal adsorption mechanisms.

Analysis in Chapter 6 provided important insights into heavy metal adsorption processes. However, further analysis is required to confirm the outcomes generated. In Chapter 6, adsorption processes were defined based on the analysis of heavy metals species that are available in road deposited sediments. In nature, only a part of the available adsorption sites in solids particles is occupied by heavy metals. By allowing for all of the adsorption sites to be occupied by metal species, adsorption behaviour at an extreme contamination level can be determined. By doing so, variations in adsorption behaviour due to the variations in heavy metal concentration can be understood.

For this purpose, batch adsorption/desorption experiments were undertaken, as detailed in Section 4.6. Adsorption experiments were undertaken to investigate the total capacity available in solid particles to adsorb heavy metals. Adsorption occurs due to a range of adsorption mechanisms, including cation exchange and chemisorption, and depends primarily on sample composition and characteristics of the heavy metal elements.

In the batch experiments, particular attention was paid to the cation exchangeable heavy metal adsorption process as it is considered to be the dominant mechanism of adsorption (Bond 1995). Furthermore, heavy metals that are adsorbed as exchangeable cations are potentially bio-available due to their easily reversible bonds (Polcaro et al. 2003). The cation exchangeable heavy metal content was measured by a desorption experiment (as detailed in Section 4.6) which extracted the exchangeable metal elements from the solids particles. The remaining metal elements in solids particles were considered to represent the strongly bound (chemisorbed) heavy metals. Consequently, the adsorption/desorption experiments enabled the identification of the primary heavy metals adsorption mechanisms of road deposited solids.

This chapter discusses the data analysis and outcomes generated from the batch adsorption/desorption experiments to confirm the metal adsorption mechanisms identified in Chapter 6. Initially, the theoretical background of the batch adsorption/desorption experiments and the characteristics of the adsorbate and adsorbent are described. The preliminary information collected from the pilot scale batch adsorption experiment (kinetic study) are then discussed. The adsorption process of the selected heavy metals was investigated based on a comparison of the desorbed metal concentrations with respect to the adsorbed heavy metals in the solids. Finally, the influential physical and chemical properties in relation to different metal adsorption process are discussed.

## **7.2 ADSORPTION/DESORPTION EXPERIMENTS**

### **7.2.1 SELECTION OF METAL ELEMENTS (ADSORBATE)**

Metal element selection for the batch adsorption/desorption experiments was carried out according to the criteria listed in Section 4.6, and based on the outcomes of the analysis discussed in Chapter 6. As noted in Section 6.2, the metal concentrations in solids is in the order of Fe>Al>Zn>Cu>Mn>Pb>Ni>Cr>Cd. From these metal elements, Zn, Cu, Pb and Cr were selected for the batch adsorption/desorption experiments, based on the different adsorption characteristics that they have shown. Among the nine heavy metals given above, Zn, Pb, Cu and Ni show similar

adsorption behaviour, as discussed in Chapter 6. From this cluster, Zn was selected as the representative adsorbate in the batch experiment, due to its abundance in road deposited solids. Pb and Cu were selected due to their strong affinity to organic matter and metal oxides, respectively. Both Cd and Cr demonstrated exceptional adsorption behaviour and are toxic to the environment in excess concentrations. Although Cd is very toxic, due to the considerably low concentration in build-up solids compared to Cr, a stronger environmental impact could be expected from Cr. Consequently, Cr was selected for the batch adsorption experiment. Fe, Al and Mn were eliminated as they are common metal elements in soils and present as metal oxides.

### **7.2.2 CHARACTERISTICS OF THE SELECTED SOLID SAMPLES (ADSORBENT)**

Only a selected set of pollutant build-up samples were subjected to batch adsorption/desorption experiments. The sample set was selected based on their particle size and physical and chemical properties. The experiments were undertaken for three particle size ranges, namely, <75 $\mu\text{m}$ , 75-150 $\mu\text{m}$  and 150-425 $\mu\text{m}$ . Due to the commonality of particle size 150-300 $\mu\text{m}$  and 300-425 $\mu\text{m}$  in terms of their physical and chemical properties (Section 5.6) and heavy metal adsorption characteristics (Section 6.3), the two particle sizes were selected and combined. Therefore, coarser particles from the same study sites were combined in equal proportions.

For each particle size, two samples were selected: one sample having physical and chemical properties highly (H) favorable for adsorption and the other having physical and chemical properties less (L) favorable for adsorption. These two samples were selected based on the PROMETHEE II ranking of each particle size, as described in Section 5.5.1 (See Table 5.8 and Appendix A/Table A.10, Table A.11, and Table A.13). The sample identification and their physical and chemical properties are given in Table 7.1. The selected sample set provides a good representation of the spread of physical and chemical properties and the solids composition, as presented in Appendix A/Table A.1.

Prior to carrying out the batch adsorption/desorption experiments, the time required for each metal element to reach equilibrium in its adsorption to solids particles was determined from a pilot study (kinetic study). Subsequently, four separate adsorption/desorption experiments were carried out to investigate the adsorption behaviour of each metal element.

**Table 7.1: Physical and chemical properties of the solids particles subject to batch adsorption/desorption experiments**

Sample ID	Original sample ID	EGME SSA (m <sup>2</sup> /g)	TOC (mg/g)	ECEC (meq/100g)	Amorp. (%)	Quartz (%)	Albite (%)	Microcline (%)	Chlorite (%)	Muscovite (%)
H iv	S iv	25.9	0.41	3.41	35.1	34.0	12.8	4.7	4.7	8.8
H iii	S iii	10.3	0.39	24.3	17.5	51.0	11.2	8.6	4.1	7.5
H i/ii	N i/ii	3.60	0.34	8.24	26.9	54.3	10.3	2.8	3.2	2.7
L iv	N iv	11.7	1.30	6.37	39.0	41.5	12.2	3.3	0.8	3.1
L iii	N iii	8.69	0.11	5.61	21.6	56.2	13.7	3.4	1.5	3.6
L i/ii	S i/ii	3.97	0.16	6.75	14.4	72.9	7.10	1.4	2.6	1.7

Note: H- highly favourable for adsorption; L- less favourable for adsorption; N- Nerang; S- Surfers Paradise: i/ii- particle size 150-425µm; iii- particle size 75-150µm; iv- particle size <75µm

### 7.2.3 DATA PROCESSING

The adsorbed heavy metal concentrations (mg/L) in solids was determined by calculating the difference between the initial metal concentration in the solution and the concentration remaining in the solution at the end of the equilibrium period. This concentration was then converted to metal ion concentration per unit weight of the solids ( $q_{0-i}$ , mmol/kg), using the equation given in Section 4.6. As the solids particles already contained an adsorbed metal content, the net metal concentration adsorbed ( $q_T$ , mmol/kg) by the solids particles (adsorption capacity) at the end of the batch experiment was calculated by taking the pre-existing metal concentration into account (See Section 4.6 for details). Desorbed metal concentrations (mg/L) were

measured after the desorption equilibrium was reached in order to determine the amounts of metals released from the sample. These concentrations were converted to metal per unit weight of solids ( $q_{ex}$ , mmol/kg), using the equation given in Section 4.6. The data analyses in relation to adsorption and desorption were carried out separately for each metal element.

#### 7.2.4 DETERMINATION OF EQUILIBRIUM TIME

As part of the batch experiment, a pilot study was carried out separately to determine the equilibrium time for adsorption and desorption of each metal element. From this study, the optimum level of metal concentration was also determined, as the adsorption/desorption experiments were carried out using a standard metal concentration (Section 4.6).

The pilot study was conducted over a 3-day period until the equilibrium state was reached, as described in Section 4.6. Figure 7.1 shows the variation in adsorbed metal concentrations (mmol/kg) with time.

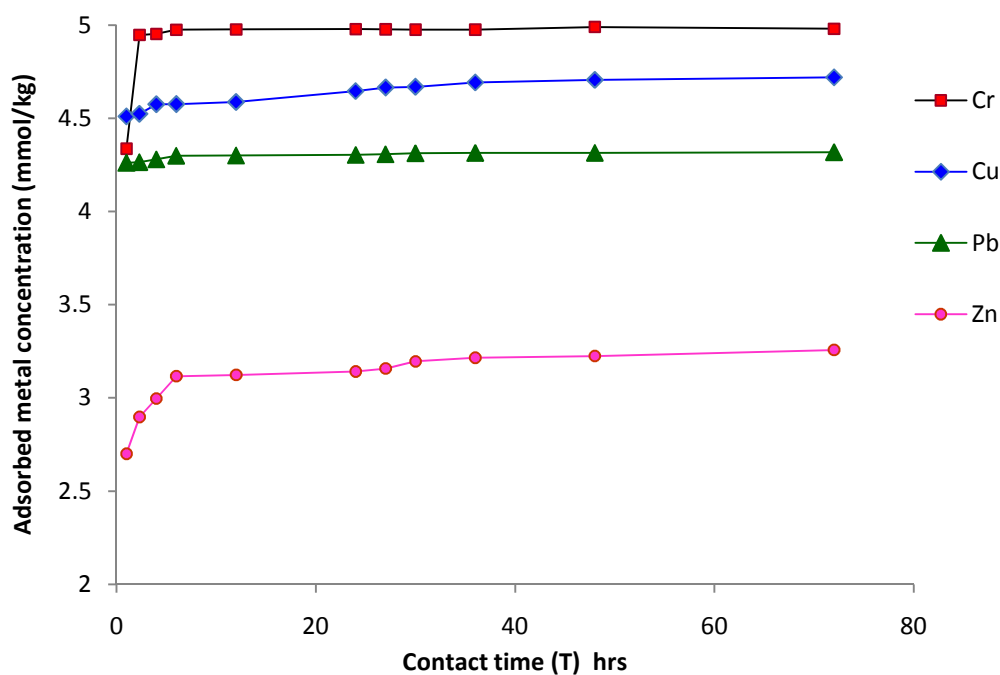


**Figure 7.1: Variation in metal solution concentrations with time**

As evident in Figure 7.1, for all metals, the rate of adsorption is relatively rapid at the beginning (within 2-4 hours) because of the high availability of adsorption sites in the solids particles. The maximum percentage adsorption was achieved within 24 hours, with all metal elements reaching an equilibrium state. This observation led to the decision to maintain a 24 hour period for the batch adsorption experiment, similar to previous research studies on metal adsorption to soils (Elliot et al. 1986; Polcaro et al. 2003; Veeresh et al. 2003). It was found that after a 24 hour period, more than 5% of the initial metal concentration ( $C_0$ ) remained in the supernatant. Consequently, this suggests that there was sufficient metal concentration to achieve equilibrium with 0.1mM (Cr - 0.21mg/g, Cu – 0.25mg/g, Zn – 0.26mg/g and Pb – 0.82 mg/g) of initial metal concentration.

### **7.3 ADSORPTION AND DESORPTION OF HEAVY METALS**

#### **7.3.1 ADSORPTION OF HEAVY METALS TO ROAD DEPOSITED SOLIDS**

Four separate experiments were carried out for each metal element to identify the adsorption characteristics of the solids particles. Since metal adsorption to solids depends on the metal ion and solids surface characteristics, variation in affinity of different metal ions can be expected. Therefore, in order to identify the adsorption of specific heavy metal elements to solids particles, the amount of heavy metals adsorbed to particles during the batch experiment ( $q_{0-i}$ ) was calculated. To compare the metal adsorption affinity, the percentage of adsorbed metal concentration ( $q_{0-i}$ ) with respect to total metal adsorbed ( $q_T$ ) was compared, as shown in Table 7.2. The adsorption of heavy metals (mmol/kg) to particulates, as determined by the batch adsorption experiment, is given in Table 7.2.

As evident in Table 7.2, higher metal concentrations were adsorbed to solid particles during the batch adsorption experiment compared to the pre-existing metal concentration. The pre-existing metal concentration is given in Appendix C/Table C.1. On average, the values in Table 7.2 indicate that 99% of the total Cr, 79% of the total Cu, 68% of the total Zn and 86% of the total Pb present have been adsorbed to solids particles during the adsorption experiment. This indicates that the road surface solids contain a significantly high amount of vacant charge sites.

**Table 7.2: Adsorbed Cr, Cu, Zn and Pb concentration ( $q_{0-i}$ ) and adsorbed metals as a percentage of total adsorbed metal concentration ( $(q_{0-i}/q_T)\%$ )**

Sample	Cr	Cu	Zn	Pb	Cr	Cu	Zn	Pb
	mmol/kg				%			
H iv	4.05	3.85	3.35	3.12	100	77.4	65.8	88.3
H iii	3.59	3.72	3.60	2.97	99.6	69.6	58.3	89.0
H i/ii	3.86	3.54	3.38	2.98	100	72.1	77.3	94.2
L iv	3.77	3.44	3.03	2.55	100	89.9	67.9	94.7
L iii	3.79	3.58	2.92	2.51	100	95.4	76.2	97.4
L i/ii	2.61	2.83	1.83	1.86	92.4	63.9	57.5	50.8

Note: H– Highly favourable for adsorption, L- Less favourable for adsorption, i/ii- particle size 150-425 $\mu$ m, iii- particle size 75-150 $\mu$ m, iv- particle size <75 $\mu$ m

Similar to Section 6.2, the adsorbed metal concentration with respect to particle size indicates that the adsorption decreases with the increase in particle size. This is attributed to the fact that fine particles offer relatively higher adsorption sites than the coarse particles. As can be seen in Table 7.1, compared to the coarse particles, fine solids particles exhibit high SSA and TOC. Similarly, with the exception of a few samples, the majority of fine particles exhibited high ECEC. However, the differences in adsorbed metal concentrations for the three particle size are comparatively low. This suggests that coarse particles have adsorbed high metal concentration, same as the fine particles. However, as documented in Section 6.2, the three particle sizes showed significant difference in heavy metal concentrations under field conditions. The lower differences in metal concentrations in the experiment could be attributed to the high metal concentrations present in the solution under experimental conditions, which would have led to the creation of weak bonds with amorphous material and quartz. As noted by Rowley et al. (1984) and Calisir et al. (2009), rubber and tyre particles present in the amorphous content of solids would have influenced the higher metal adsorption by ion-exchange (by displacement of zinc). Calisir et al. (2009) showed that rubber is a good adsorbent for Cu at pH 6.0, and Rowley et al. (1984) showed that tyre particles can adsorb Pb from aqueous solutions.

Cr is the highest adsorbed metal element in most samples and, in the majority of samples, metal adsorption affinity (order of selectivity) increased in the order of  $Zn < Cu < Pb < Cr$ . This supports the selectivity found in the equilibrium state batch results shown in Figure 7.1. A similar selectivity sequence was also observed by past researchers in relation to soil samples for bivalent and trivalent cations (Kinniburgh et al. 1976; Aualiitia and Pickering 1986; Elliott et al. 1986; Fontes and Gomes 2003). This indicates that Cr is the most preferred metal element associated with road deposited solids.  $Cr^{3+}$  is a trivalent cation which has relatively high electro negativity and high charge density. This could be the primary reason for its high affinity to solids. However, as observed in Section 6.2, in terms of load, Cr is the lowest adsorbed metal element in road deposited solids particles. This is attributed to the low availability of Cr in the urban road environment.

The adsorption capacity ( $q_T$ , or the net metal concentration) of the solids for the metal concentration used (0.1mM) was calculated by the summation of the pre-existing metal concentration and the adsorbed metal concentration during the experiment. The adsorption capacities for the four heavy metal elements are presented in Table 7.3. Values given in Table 7.3 are directly comparable with the findings from previous researchers. For example, the adsorption capacities are consistent with the study by Jain and Ram (1997), who studied the metal adsorption behaviour of 100-400 $\mu$ m particle sizes in river sediments. The capacities they observed ranged from 1.9-2.9mmol/kg (0.4-0.6mg/g) for Pb, and 2.66-3.3mmol/kg (0.17-0.22mg/g) for Zn. Similarly, the present values are consistent with the adsorption capacities reported by Markiewicz-Patkowska et al. (2005) for surface soil at a brownfield site, and are below an order of magnitude in adsorption capacities reported by Polcaro et al. (2003) for soils and by Abollino et al. (2003) for clay minerals.



**Table 7.3: The adsorption capacity ( $q_T$ ) of road deposited solids for 0.1mM concentration of Cr, Cu, Zn and Pb in three different particle sizes**

Sample	Cr	Cu	Zn	Pb
	mmol/kg			
H iv	4.05	4.97	5.09	3.54
H iii	3.6	5.34	6.17	3.34
H i/ii	3.86	4.91	4.37	3.16
L iv	3.77	3.82	4.47	2.7
L iii	3.79	3.75	3.83	2.58
L i/ii	2.83	4.43	3.19	3.66

Note: H- Highly favourable for adsorption, L- Less favourable for adsorption, i/ii- particle size 150-425 $\mu$ m, iii- particle size 75-150 $\mu$ m, iv- particle size <75 $\mu$ m

As seen in Table 7.3, Zn is the highest adsorbed metal ion–( $q_T(\text{Zn}) = 6.2\text{mmol/kg}$ )– to solids particles, whereas Cu, Cr and Pb are adsorbed to a lesser extent: ( $q_T(\text{Cu}) = 5.3\text{ mmol/kg}$ ;  $q_T(\text{Cr}) = 4.1\text{mmol/kg}$ , and  $q_T(\text{Pb}) = 3.7\text{mmol/kg}$ ). Accordingly, the metal adsorption capacity of solids increased in the order of  $\text{Pb} < \text{Cr} < \text{Cu} < \text{Zn}$ , although few differences were observed in a few particle size ranges. However, data in Table 7.2 show that Cr was the highest adsorbed metal element during the adsorption experiment. Although Zn was the lowest adsorbed metal element during the adsorption experiment (See Table 7.2), Zn has the highest adsorption capacity. This confirms that the adsorption capacities observed in this study would have been influenced by the pre-existing metal content in the solids samples.

### 7.3.2 DESORPTION OF HEAVY METALS FROM ROAD DEPOSITED SOLIDS

The concentrations of the total desorbed metals from solid particles are given in Table 7.4. To compare the metal desorption, the percentage of desorbed metal concentration ( $q_{\text{ex}}$ ) with respect to total metal adsorbed ( $q_T$ ) was compared, as shown in Table 7.4. Here again, metal concentrations were obtained from individual metal desorption experiments.

**Table 7.4: Desorbed Cr, Cu, Zn and Pb concentrations ( $q_{ex}$ ) and desorption as a percentage of total adsorbed metal concentration ( $(q_{ex}/q_T)\%$ )**

Sample	Cr D	Cu D	Zn D	Pb D	Cr D	Cu D	Zn D	Pb D
	mmol/kg				%			
H iv	0.004	0.000	0.83	0.012	0.10	0.00	16.4	0.34
H iii	0.005	0.001	1.35	0.038	0.14	0.01	21.9	1.15
H i/ii	0.000	0.002	1.33	0.581	0.01	0.03	30.4	18.4
L iv	0.001	0.001	1.62	0.024	0.03	0.01	36.3	0.87
L iii	0.001	0.076	3.29	0.100	0.01	2.03	86.0	3.90
L i/ii	0.008	0.114	2.03	0.854	0.28	2.57	63.7	23.3

Note: D- desorbed metal concentrations, H– Highly favourable for adsorption, L- Less favourable for adsorption, i/ii- particle size 150-425 $\mu$ m, iii- particle size 75-150 $\mu$ m, iv- particle size <75 $\mu$ m

The desorbed heavy metal concentrations given in Table 7.4 can be considered as the amount of exchangeable heavy metals or easily removable metal concentration in the solids particles. As evident in Table 7.4, the percentages of desorbed heavy metals with respect to adsorbed heavy metal content are significantly low. Particularly, desorbed Cr and Cu concentration from solids samples is negligible.

Among the metal elements, Zn desorption is predominant compared to Cr, Cu and Pb. On average, the percentages of total Zn desorbed from L and H samples as a percentage of total adsorption are approximately 62% and 23% respectively. This suggests that a higher percentage of Zn would be in exchangeable form in solids particles. Similar conclusions have been drawn by Biddappad et al. (1981) who noted that Zn is present in soils in predominantly water soluble or exchangeable form. As indicated by Liu et al. (2009), the weak bonding of Zn compared to Cr and Cu is attributed to the electron configuration of  $Zn^{2+}$  [ $3d^{10} 4s^0$ ] compared to  $Cr^{3+}$  [ $3d^3 4s^0$ ] and  $Cu^{2+}$  [ $3d^9 4s^0$ ]. Transition metals (Zn, Cr and Cu) with small ionic radii and empty orbitals easily form complexation with surface functional groups. The outer orbital of  $Zn^{2+}$  is full [ $3d^{10}$ ] and there is no empty orbital to form a strong bond with surface functional groups. Therefore, Zn forms weak bonds with charge sites compared to the other transition metal elements.

The presence of a high fraction of exchangeable Zn agrees with the findings in Section 6.2. It was concluded in Chapter 6 that the adsorption of Zn to clay forming minerals occurs by cation exchange mechanism, especially in fine particles. However, in coarser particles ( $>75\mu\text{m}$ ), Zn was found mostly associated with metal oxides and organic matter rather than clay minerals. The presence of Zn in exchangeable form increases its bio-availability and can cause significant damage to the receiving water environment.

In contrast, the desorption process only removed  $<10\%$  of adsorbed Pb. This suggests that Pb is associated with solids particles by much stronger bonding. This confirms the findings in Section 6.3 which found that Pb is adsorbed to organic matter or metal oxides by chemisorption. Hence, it can be concluded that the bio-availability of Pb would be relatively low under natural conditions. However, Pb precipitation could also occur since its hydroxide formation is common at pH 7 (Markiewicz-Patkowska et al. 2005). Since throughout the experiment the pH was maintained at pH 6.5, precipitated Pb would have also contributed to the portion that desorbed from solids.

Similar to the findings in Section 6.3, a predominant fraction of Cu is adsorbed to solids by chemisorption. This hypothesis is based on the very low desorption of Cu from solids, which is within 2.6% or less of the Cu concentration, as shown in Table 7.4. Nevertheless, desorbed Cr content is 0.3% or less for all samples. Cr is a trivalent cation, which has a high electro negativity (hard acid) compared to the other metal elements. Therefore, Cr can compete with other metal elements for complexation sites and mainly forms strong bonds of chemisorption with solids particles (Bradl 2004). This agrees with the findings in Section 6.3 where Cr in  $<75\mu\text{m}$  particles was found to be adsorbed to solids through chemisorption. Cr association with solids particles through cation exchange is expected to be very low. This agrees with the findings of Covelo et al. (2007) who noted near-zero concentration of extractable Cr in batch adsorption studies of soil samples. This further suggests that at natural pH levels in stormwater runoff, Cr and Cu mobility and bio-availability would be very low compared to that of the other metal elements.

However, further analysis is required to identify the influence of physical and chemical properties on the desorption process.

Furthermore, it was found that fine particles retain more heavy metals than coarse particles. For example, it can be seen that a high amount of Zn is desorbed from coarse particles ( $>75\mu\text{m}$ ) (Table 7.4). This trend is similar for Pb, which shows that a considerably higher amount of Pb is released by coarse particles than by fine particle sizes. This is attributed to the strong bonds in fine particles compared to the coarse particles. In  $<75\mu\text{m}$  particles, heavy metal cations can be adsorbed to the interlayer surfaces of clay minerals (illite/mica, smectite). The heavy metal ions are more strongly adsorbed to internal surfaces than the external surface area of the minerals. Consequently, it is more likely that heavy metals will be released more easily by the coarse particles rather than by the fine particles (Rybicka et al. 1995). However, it should be noted that the any changes in pH, ionic strength and dissolved organic components in receiving water could change the desorption processes observed for the metal elements investigated.

#### **7.4 HEAVY METAL ADSORPTION IN RELATION TO PHYSICAL AND CHEMICAL PROPERTIES OF SOLIDS**

The analysis undertaken in Section 7.3 focused on identifying the general trends in adsorption with respect to particle size. However, generalisation of adsorption processes according to particle size is misleading since a complex range of physical and chemical properties are involved. In order to understand the influence of physical and chemical characteristics on adsorption processes, the data set was analysed using multivariate analytical techniques. This was to avoid the difficulties which arise in interpreting processes involving multiple variables. The method of principal component analysis (PCA) was primarily selected for the analysis. However, because of the limitations which arise as a result of the limited number of samples, PROMETHEE and GAIA analyses were also used to establish the relationships among adsorption and desorption processes of solids. More details on PROMETHEE and GAIA can be found in Sections 3.3.4 and 5.5.

The analysis was carried out in two phases. Initially, adsorbed ( $q_T$  - Table 7.3) and desorbed ( $q_{ex}$  - Table 7.4) metal concentrations were analysed together with the mineral components, TOC, ECEC and EGME SSA to identify the influence exerted by these parameters. The six objects were classified into two groups of H and L in the analysis. Data tabulated in Table 7.1 were used in the analysis. Since the batch adsorption/desorption experiments were carried out singly for each metal element, data analysis was also carried out accordingly. Additionally, a separate PROMETHEE and GAIA analysis was carried out with the inclusion of Fe, Al and Mn to the data matrix to explore the influence of the oxides of these metals on the adsorption process. As discussed in Chapter 6, fractions of Fe, Al and Mn that may be present as metal oxides in the solids particles could act as adsorbing sites for other heavy metals in addition to the other common adsorption mechanisms.

As discussed in Sections 3.3.4 and 5.5, the selection of appropriate analytical parameters is critical in PROMETHEE II analysis. To obtain the preference ranking order, variables were set to maximum so that the most favourable objects for metal adsorption were ranked first in the PROMETHEE II ranking. All variables were given the same weighting so that no variable was favoured over another. The V-shaped preference function was selected so that a threshold value was required to be applied to each variable. The preference threshold P was set to the maximum concentration of each variable (Herngren et al. 2005; Ayoko et al. 2007). The interpretation of the GAIA biplot was carried out according to the guidelines given by Keller et al. (1991) (See Section 3.3.4). In the GAIA biplots given below, triangular shapes denote the objects in Groups H and L (actions) and the rectangular shapes represent the physical and chemical parameters (criteria).

#### **7.4.1 Cr ADSORPTION AND DESORPTION**

The resulting 6 x 11 data matrix was subject to PROMETHEE and GAIA analysis. Figure 7.2 (a) shows the resulting GAIA biplot obtained. A total data variance of 70.9% is explained in the GAIA biplot, indicating the incorporation of the majority of the variance. The resulting PROMETHEE II ranking is shown in Table 7.5.

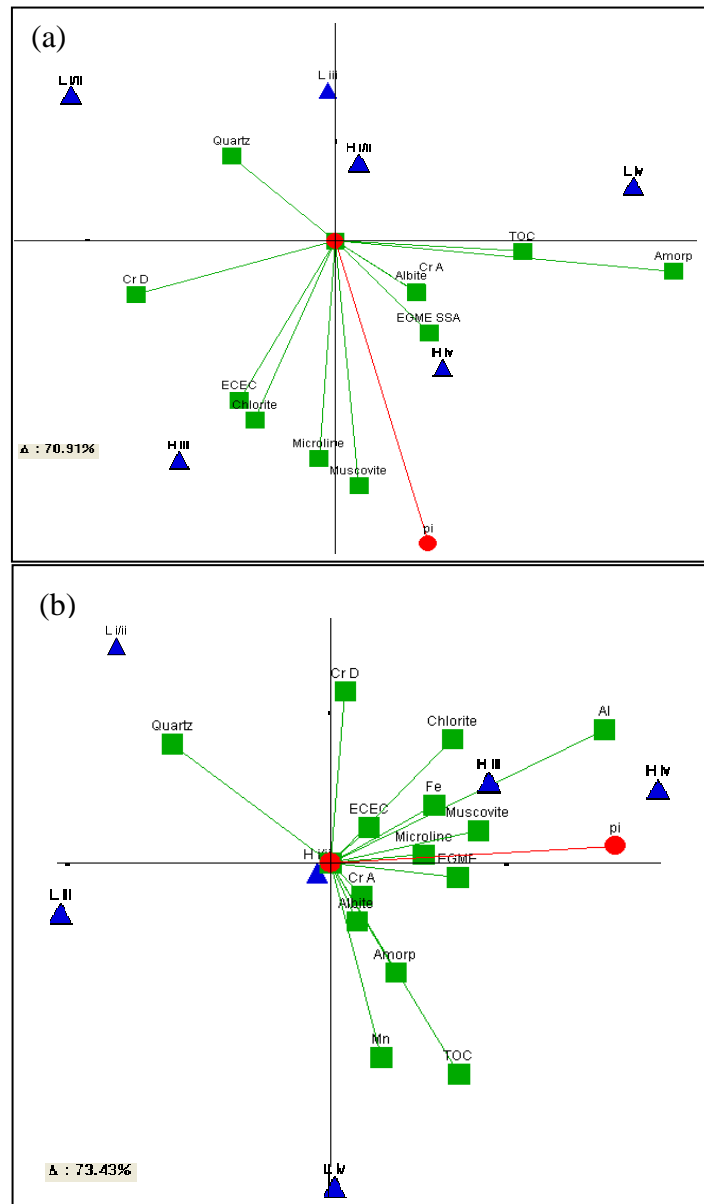


**Figure 7.2: GAIA biplot of Cr adsorption and desorption (a) with physical and chemical properties (b) with physical and chemical properties and Fe, Al and Mn**

Note: Cr A– Chromium adsorption, Cr D–Chromium desorption, i/ii– Particle size 150-425µm, iii– Particle size 75-150µm, iv– Particle size <75µm

**Table 7.5: PROMETHEE II ranking for Cr adsorption**

<b>Sample</b>	<b>Net <math>\Phi</math></b>	<b>Ranking order</b>
H iii	0.1913	1
H iv	0.1335	2
L iv	0.0645	3
H i/ii	-0.1078	4
L iii	-0.1117	5
L i/ii	-0.1699	6

In Figure 7.2, the decision axis  $\pi_i$  points towards the fine particles of Group H and in the same direction as the Cr A vector. This indicates the degree of significance of fine particles of Group H in Cr adsorption. The importance of the fine particles in Group H in Cr adsorption can also be confirmed by their higher ranking in Table 7.5. In Table 7.5, Group H objects are ranked above Group L objects. This suggests that the Group L objects have a lower preference for metal adsorption.

In Figure 7.2 (a), albite, amorphous, TOC, muscovite and EGME SSA vectors and the total adsorbed Cr (Cr A) vector are strongly correlated. This suggests that the majority of Cr adsorbed to solid particles is present in TOC, albite, amorphous content and muscovite. Cr adsorption to these substances would increase with the increase in surface area of the particles. Due to very weak correlation of albite and TOC with ECEC, adsorption of Cr as exchangeable cations is minimal. Therefore, it can be suggested that Cr adsorption to albite and TOC is due to chemisorption. Chemisorption can occur in the clay forming minerals at edge sites by donating electrons to heavy metals (McBride 1994). This confirms the conclusions derived in Section 6.3 where it was noted that Cr is preferentially adsorbed to metal oxides of Fe, Al and Mn through chemisorption in particles other than 75-150 $\mu$ m. Other forms of adsorption can exist in lower size fractions. A PROMETHEE and GAIA analysis with the inclusion of Fe, Al and Mn metal content as variables was undertaken to confirm this conclusion.

The resulting GAIA biplot with Fe, Al and Mn as variables is shown in Figure 7.2 (b), and accounts for 73.4% of the variance. The addition of Fe, Al and Mn caused the ECEC variable vector to be insignificant, and projected the EGME SSA variable vector away from the Cr A vector. Additionally, Mn was projected in the same direction as Cr A, suggesting a strong correlation with Cr A, while Fe and Al were projected orthogonal to Cr A. This suggests that a significant portion of Cr is adsorbed to Mn oxides. Adsorption to Fe and Al oxides are comparatively low. As further confirmation, it was noted in Section 6.3 that Mn oxides show preference for Cr adsorption, rather than Fe and Al oxides. This agrees with the findings of Bradl (2004), who noted that Cr specifically bonds to Mn oxides.

In Figure 7.2 (a), Cr D, ECEC, chlorite, muscovite, microcline and EGME SSA are correlated. This suggests that desorbed Cr had been attached to clay forming minerals of chlorite and muscovite (layer silicates). Since the experiment was designed only to desorb exchangeable cations, Cr bonding with clay forming minerals is evidently by cation exchange. Al and Fe oxide bound Cr would also be present in exchangeable form. This is hypothesised due to the strong correlation of Cr D and Al observed in Figure 7.2 (b), where Al is a significant variable projected in the direction of ECEC. This indicates that cation exchange sites in Al and Fe oxides would also involve the retention of an exchangeable form of Cr.

Other than the exchangeable fraction, a minor fraction of precipitated Cr would also influence the Cr D vector. It is reported that Cr hydroxide precipitation is common at pH 6.5 (Bradl 2004; Covelo et al. 2007b). However, in both Figure 7.2 (a) and Figure 7.2 (b), Cr D has strong correlation with ECEC. This suggests that the majority of the desorbed Cr would have been attached to particles through cation exchange, while the portion of Cr precipitation would be very low in these particles. Analysis in Section 7.3.2 indicated that 0.3% of the Cr desorbed while retaining about 99.7% of the Cr in the sample. Thus, the exchangeable form of Cr bound to clay forming minerals and metal oxide would be very low compared to the total adsorbed Cr concentration. Therefore, it can be concluded that Cr adsorption to albite, organic matter and Mn oxides by strong bonds such as chemisorption is



dominant compared to cation exchange with clay forming minerals, and Fe and Al oxides.

As reported in Section 6.4, unlike the adsorption characteristics shown by fine particles in road deposited solids, the Cr in coarse particle sizes is in cation-exchangeable form on mineral surfaces, or present in the residual fraction of traffic related materials. The adsorbed and desorbed Cr presented in Section 7.3.2 confirmed that Cr adsorption to solids mainly occurs in non-exchangeable form. Although Cr demonstrated cation exchangeable adsorption at low concentrations (Section 6.3), in the presence of high Cr content in solution, non-exchangeable form of adsorption with organic matter, albite and Mn oxide occurs. Furthermore, the analysis undertaken suggests that the environmental impact of Cr bio-availability at the pH level of natural stormwater runoff would be very low. However, the metal content in the particulate fraction would be very high as solids have high selectivity for Cr metal. Therefore, the removal of solids particles would mitigate Cr contamination of receiving waters.

#### **7.4.2 Zn ADSORPTION AND DESORPTION**

The data matrix of size 6 x 11 was used to determine the adsorption and desorption characteristics of Zn using PROMETHEE and GAIA analysis. The GAIA biplot obtained from analysis is shown in Figure 7.3 (a). A data variance of 78.46% is explained by the GAIA biplot and is considered adequate to provide comprehensive information on the data set. The preferential ranking obtained from the analysis is given in Table 7.6.

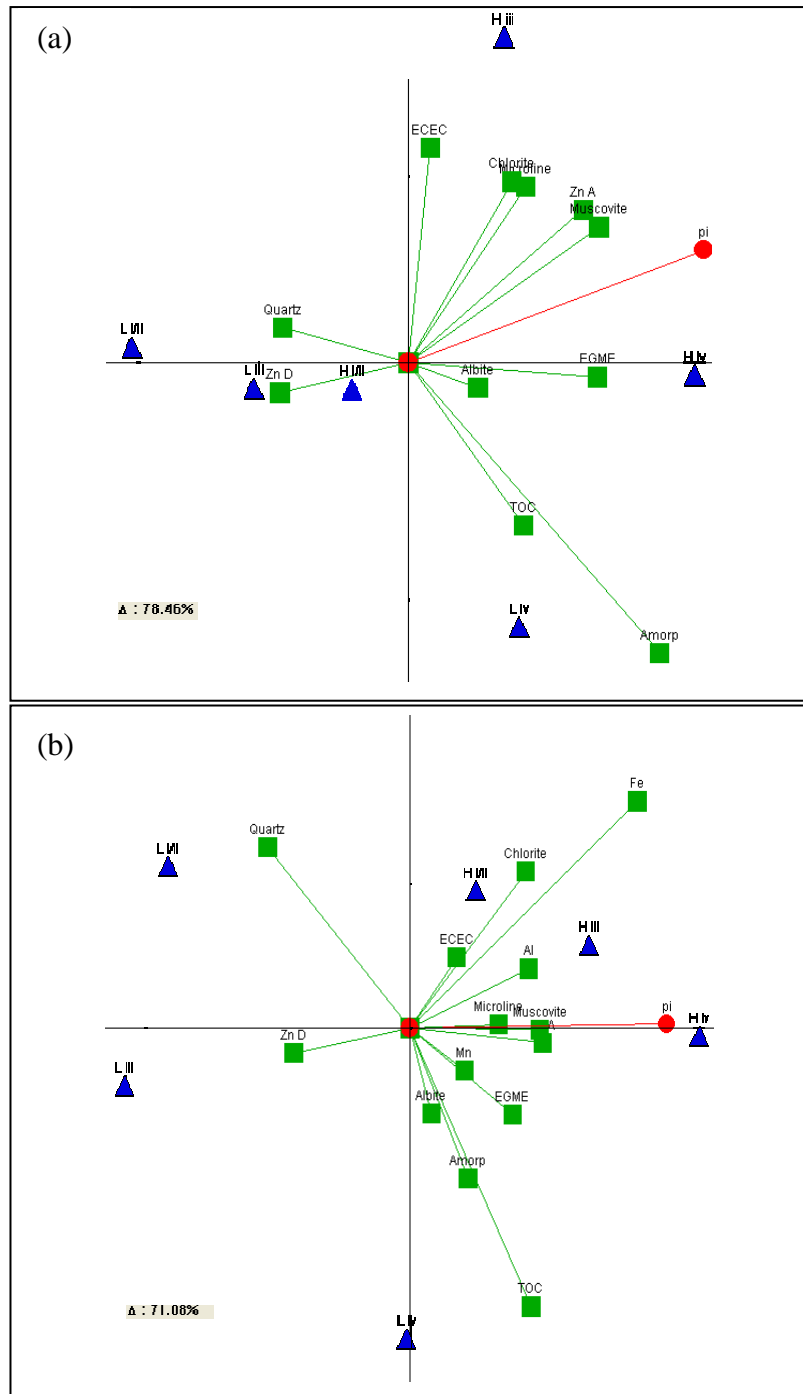


**Figure 7.3: GAIA biplot of Zn adsorption and desorption (a) with physical and chemical properties (b) with physical and chemical properties and Fe, Al and Mn**

Note: Zn A– Zinc adsorption, Zn D– Zinc desorption, i/ii– Particle size 150-425 $\mu$ m, iii– Particle size 75-150 $\mu$ m, iv– Particle size <75 $\mu$ m

**Table 7.6: PROMETHEE II ranking for Zn adsorption**

Sample	Net $\Phi$	Ranking order
H iii	0.1813	1
H iv	0.1703	2
L iv	0.0475	3
L iii	-0.0737	4
H i/ii	-0.0901	5
L i/ii	-0.2352	6

In Figure 7.3, most of the variable vectors such as ECEC, chlorite, muscovite and microcline that enhance metal adsorption are projected towards the Group H objects. This suggests that Group H objects have high affinity for metals due to favourable physical and chemical properties. Also, objects belonging to Group L form a cluster opposite the projection of the pi axis, indicating their weakness in relation to Zn adsorption. The resulting PROMETHEE II high ranking of the fine particles in Group H (given in Table 7.6) also confirms that they provide a favourable environment for Zn adsorption.

As evident in Figure 7.3, all of the clay forming minerals, Zn A, ECEC and EGME SSA vectors are projected in the direction of pi decision axis. This confirms the significance of these parameters in defining the adsorption characteristics of Zn. The correlation of clay forming minerals with ECEC indicates that a significant fraction of the permanent charge sites which are on offer supports cation exchangeable adsorption. Among clay forming minerals, the layer silicate minerals of muscovite and chlorite show greater correlation to Zn A than the framework silicates of albite (feldspar). At the same time, the correlation of EGME SSA and muscovite indicates that there is a strong influence of interlayer surface area of muscovite on adsorption. Thus, it can be concluded that Zn is preferentially adsorbed to the interlayer surfaces of the clay minerals through cation exchange mechanism (Reddy and Perkins 1976; Bradl 2004). This confirms the findings of Section 6.3 and Section 6.4, which

established that in the majority of particle sizes (particles other than 75-150 $\mu\text{m}$ ), Zn is preferentially adsorbed to clay minerals.

However, the analyses in Chapter 6 indicated that a predominant fraction of Zn is adsorbed to metal oxides, rather than to clay minerals. Therefore, a separate PROMETHEE and GAIA analysis was carried out with the inclusion of Fe, Al and Mn in the matrix mentioned above, which expanded to 6 x 14. A total data variance of 71% is explained in the GAIA biplot [Figure 7.3 (b)]. Inclusion of three metal elements leads only to minor changes in the vector orientation. However, Fe and Al are projected with strong correlation to Zn A in the GAIA biplot. This leads to the conclusion that after the clay forming minerals, Zn would preferentially adsorb to oxides of Fe and Al. Unlike Al, Fe oxides would provide significant sites for Zn adsorption. This was hypothesised due to the very long Fe vector that is projected in the same direction of the decision axis  $\pi_1$  and Zn A [Figure 7.3 (b)].

Furthermore, Fe and Al strongly correlate with ECEC. Therefore, it can be concluded that Zn adsorption to Fe and Al would be dominated by cation exchange mechanism. Although a similar preference was noted in Section 6.3, Zn adsorption to metal oxides occurred by chemisorption at low concentration. The difference in the adsorption mechanism could be attributed to the higher amount of Zn adsorption to solids particles during the batch adsorption study. At low concentrations, heavy metals are bound to the strongest adsorption sites and, at high concentrations, heavy metals will also bind to the weaker adsorption sites (Spadini et al. 1994). Since surface adsorption sites consist of several distinct charge sites [carboxyl (-COOH), carbonyl and phenolic groups in organic matter, Fe oxide, Al oxide and exchangeable sites], at high concentration, Zn would have formed weak cation exchangeable bonds (Benjamin and Leckie 1981; Aualiitia and Pickering 1986).

In both Figure 7.3 (a) and Figure 7.3 (b), Zn A shows a weak to no correlation with TOC indicating that the influence of TOC in Zn adsorption is minimal. However, as reported in Section 6.3, Zn shows high preference to TOC in >75 $\mu\text{m}$  particles, after the metal oxides. This suggests that the influence of TOC in Zn adsorption is limited

to when Zn is available in high concentration. This could be attributed to the low organic matter content in the road deposited solids.

In Figure 7.3, Zn D and quartz show strong correlation and have negative loadings on PC1, and Zn D shows negative correlation with ECEC. As seen in Table 7.4, on average, 62% of the Zn in L samples was removed in the desorption experiment. However, Zn D is negatively correlated to ECEC. This indicates that a high amount of Zn adsorption was by cation exchange, resulting in the strong correlation of ECEC with Zn A. However, researchers have also shown that a significant amount of Zn adsorbed to clay mineral surfaces is reversible, while the irreversible non-exchangeable form of Zn associated with edge sites is very low (Tiller and Hodgson 1962). The analysis further revealed that a high amount of Zn adsorbed to clay forming minerals and metal oxides in road deposited solids is subject to release due to weak bonds such as cation exchange.

#### **7.4.3 Cu ADSORPTION AND DESORPTION**

The data matrix of 6 x 11 was subjected to PROMETHEE and GAIA analysis. The resulting GAIA biplot from the analysis is shown in Figure 7.4 (a). A significant data variance of 78.7% explained by the GAIA biplot is considered adequate to provide comprehensive information on the data set. Preferential ranking obtained from the analysis is given in Table 7.7.



**Table 7.7: PROMETHEE II ranking for Cu adsorption**

Sample	Net $\Phi$	Ranking order
H iv	0.1611	1
H iii	0.1292	2
L iv	0.0007	3
L iii	-0.0763	4
H i/ii	-0.0915	5
L i/ii	-0.1231	6

In Figure 7.4 (a), the decision axis  $\pi_1$  is directed towards the fine particles and Cu A is in the same direction. Similar to the analysis of Zn, it can be concluded that Cu adsorption is favoured by the fine particles and the preference is always dominated by the Group H objects in comparison to Group L objects. This can be confirmed by the ranking given in Table 7.7, where Group H objects are ranked above the Group L objects.

As evident in Figure 7.4 (a), Cu A is strongly correlated with ECEC, clay forming minerals and EGME SSA. However, Cu A is negatively correlated with TOC. Thus, it can be concluded that Cu adsorption is dominated by the clay forming minerals. This observation agrees with the outcomes of the investigation of individual particle sizes undertaken in Section 6.3, where particle sizes  $<75\mu\text{m}$  and  $>150\mu\text{m}$  indicated high affinity to clay minerals. However, according to Section 6.3, Cu is preferentially adsorbed on metal oxides by all particle sizes rather than on the clay forming minerals. Therefore, PROMETHEE II analysis was carried out with the inclusion of Fe, Al and Mn to the data set. The resulting GAIA biplot [Figure 7.4 (b)] accounts for 75.6% variance, and the addition of the three metal elements (criteria) causes only minor movement of the vectors. The Fe, Al and Mn vectors are projected in the direction of the decision axis  $\pi_1$ , with moderate lengths. In Figure 7.4 (b), Cu A shows strong affinity to metal oxides in the decreasing order of Fe, Al and Mn. However, clay minerals still show strong correlation with Cu A. Thus, it can be concluded that Cu adsorption is dominated by metal oxides, followed by clay

forming minerals. With the exception of the order of preference of Fe, Al and Mn oxides, this confirms the conclusions derived in Section 6.5. The adsorption to metal oxides would occur by chemisorption. This hypothesis is based on the weak correlation of Fe, Al and Mn with ECEC.

Cu D is strongly correlated with quartz. Furthermore, the Cu D vector is directed towards the Group L object cluster. This suggests that the high amount of Cu associated with Group L objects (sandy matrix) is easily removed due to the low availability of clay forming minerals (See Table 7.1). Similarly, Figure 7.4 (a) shows vectors of clay forming minerals in opposite direction to the Group L objects. Due to the less favourable conditions offered by Group L solids for adsorption, Cu would have precipitated on the solids surfaces. Thus, it can be hypothesised that the majority of desorbed Cu is present as precipitate or with weak electrostatic attachment to charged surfaces. However, as observed in Table 7.4, Cu desorption is <2.6% of the total adsorbed Cu and, in most of the samples, desorption is less than 0.1%. This suggests that a high amount of Cu is retained on the particles and adsorption would be by chemisorption. Thus, the bio-availability of this metal will be very low.

#### **7.4.4 Pb ADSORPTION AND DESORPTION**

The data matrix of 6 x 11 was subject to PROMETHEE II analysis to identify the adsorption and desorption characteristics of Pb. The resulting GAIA biplot of the analysis is shown in Figure 7.5 (a). A large data variance explained by the GAIA biplot (77.5%) is considered adequate to provide comprehensive information in relation to the data set. The resulting PROMETHEE II ranking is shown in Table 7.8.



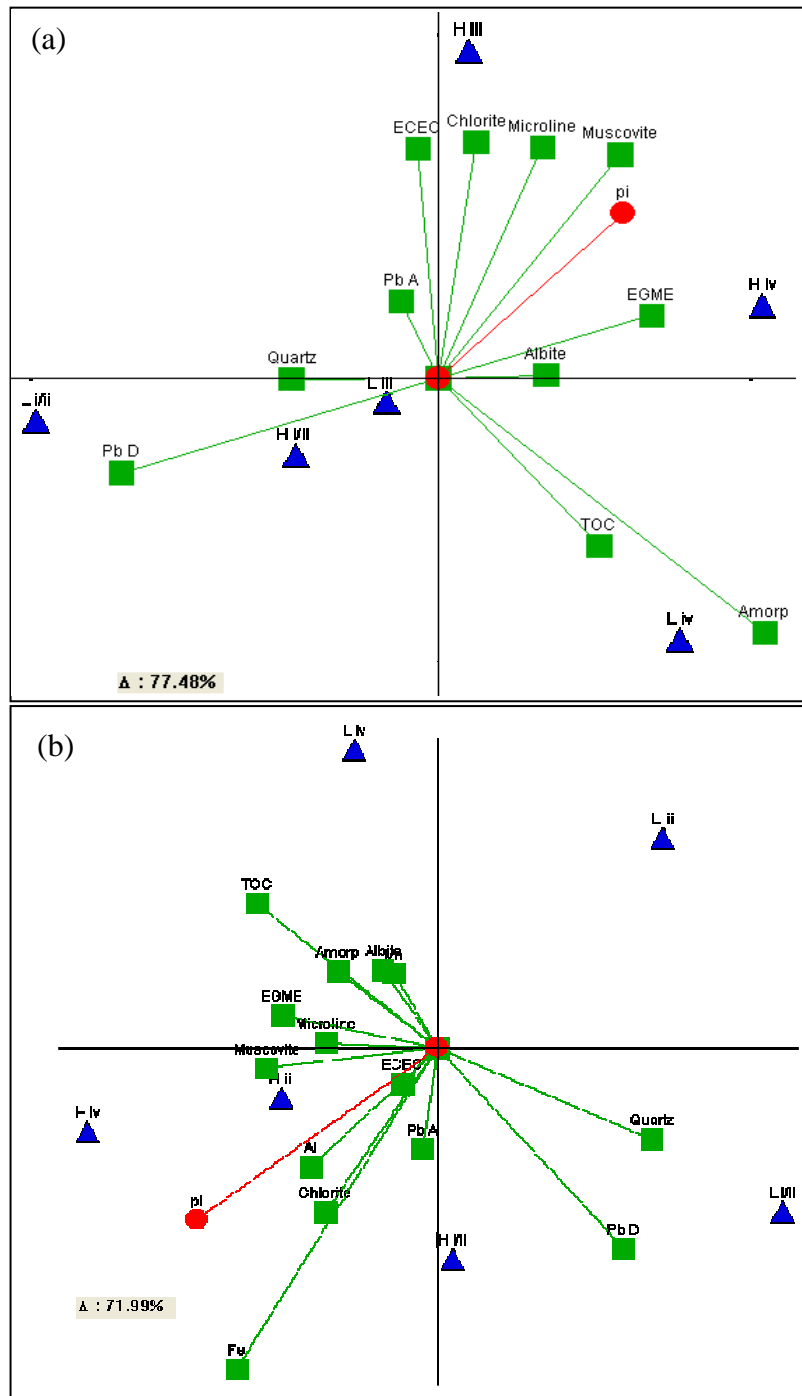


**Figure 7.5: GAIA biplot of Pb adsorption and desorption (a) with physical and chemical properties (b) with physical and chemical properties and Fe, Al and Mn**

Note: Pb A– Lead adsorption, Pb D– Lead desorption, i/ii– particle size 150-425 $\mu\text{m}$ , iii– particle size 75-150 $\mu\text{m}$ , iv– particle size <75 $\mu\text{m}$

**Table 7.8: PROMETHEE II ranking for Cu adsorption**

Sample	Net $\Phi$	Ranking order
H iv	0.1628	1
H iii	0.1145	2
L iv	0.0010	3
H i/ii	-0.0286	4
L i/ii	-0.1007	5
L iii	-0.1489	6

The PROMETHEE II ranking given in Table 7.8 shows that finer particles are favoured for metal adsorption over coarser particles. Group H objects are ranked first, similar to the other metals. Thus, it is clear that Pb adsorption is dominated by Group H objects over Group L objects, due to the favourable physical and chemical properties of the particles.

As evident in Figure 7.5, Pb A shows strong correlation to ECEC and clay forming minerals of chlorite, microcline and muscovite. Thus, Pb adsorption would be dominated by clay minerals. Correlations with ECEC indicate that the adsorption to clay minerals occurs by the cation exchange. However, it was identified in Section 6.5 that Pb is preferentially adsorbed to organic matter through chemisorption. In contrast, Pb A in Figure 7.5 (a) shows strong negative correlation to TOC. This can be attributed to the differences in Pb availability. In the case of Section 6.4, the analysis was based on Pb content present in the original samples, whereas the analysis undertaken in this chapter is based on additional Pb being added to the samples.

According to the analyses in Section 6.4, other than the adsorption to TOC, metal oxides show significant correlation with Pb. Therefore, PROMETHEE II analysis was carried out, with the inclusion of Fe, Al and Mn to the data matrix. The resulting GAIA biplot is shown in Figure 7.5 (b), which accounts for 72% of the data

variance. The addition of Fe, Al and Mn (variables) leads to some changes to the vectors in the GAIA biplot. Microcline and muscovite vectors project away from Pb A, pointing to a weak correlation with Pb A, and the ECEC vector is less significant without interference to its projection [Figure 7.5 (b)]. Figure 7.5 (b) indicates that Pb A is strongly correlated with both Fe and Al, while negatively correlated with Mn. Fe being a long vector in the direction of the decision axis  $\pi_1$ , it can be concluded that Fe has the dominant influence on Pb adsorption. Since the inclusion of Fe, Al and Mn reduced the projected ECEC vector length, it can be concluded that the adsorption to oxides would be dominated by a non-exchangeable form. As metal oxides predominately create complexations with heavy metal cations, the adsorption of Pb to metal oxides would occur by chemisorption.

While, at relatively low concentrations, Pb is preferentially bound to organic matter, at high concentrations, metal oxides became the preferred adsorbing site for Pb. This can be attributed to the limited organic matter content in the solids samples which would have been saturated by the excess Pb added during the batch adsorption experiment. Thus, it can be concluded that due to the lack of primary preferential adsorbing sites for Pb in the solids particles, Pb had adsorbed to secondary sites. Similar observations were reported by Zhuang and Yu (2002) based on a study of Pb adsorption to metal oxides. This is the primary reason for the low adsorption capacity of Pb when compared to the other metal elements, as noted in Section 7.3.1. Thus, it is reasonable to suggest that preferential adsorption of Pb (presence of low organic matter content in the sample) would follow the order of Fe oxide > Al oxide > clay forming minerals. This confirms the findings in Section 6.4 where, with the exception of organic matter, metal oxides provided the preferred adsorption sites for Pb.

In Figure 7.5, Pb D shows negative correlation with ECEC, TOC, clay forming minerals and EGME SSA. Figure 7.5 (b) shows that Pb D is weakly correlated with chlorite and Pb A. This confirms the above finding that clay bound Pb is present in exchangeable form. Additionally, Pb precipitation would have occurred during the adsorption process, since formation of Pb hydroxides is common at pH 6.5 (Aualiitia

and Pickering 1987; Fontes and Gomes 2003; Bradl 2004). Thus, it can be concluded that Pb precipitation would have been responsible for a fraction of the desorbed Pb content. As identified in Section 7.3.2, desorbed Pb is <10% of the total adsorbed metal concentration. This indicates that an amount of particulate Pb is present in a non-exchangeable form, and confirms the findings in Section 6.4. Therefore, it can be hypothesised that Pb adsorption to road deposited solids would occur with metal oxides and clay forming minerals in the presence of low organic matter content. At high metal concentrations, Pb precipitation can also occur. Therefore, the bio-availability of Pb would have a significant effect on road deposited solids. However, Pb retention would be very high compared to Zn.

## 7.5 CONCLUSIONS

An in-depth analysis of the adsorption processes of solids particles was carried out through adsorption/desorption experiments, using four common heavy metals (Zn, Cu, Pb and Cr) present as road surface pollutants. Preferred adsorption sites and adsorption mechanisms of the heavy metals were investigated by understanding the relationships between adsorbed and desorbed heavy metal concentrations with different physical and chemical parameters. Furthermore, the influence of metal oxides on heavy metal adsorption was also investigated.

The adsorption/desorption experiments confirmed the adsorption mechanisms identified in Chapter 6. However, for some of the heavy metals, the high metal concentrations affected the preferred adsorption sites or order of preference of adsorbing sites. The analyses provided an in-depth understanding of how heavy metals are attached to solids particles. This understanding of adsorption processes led to identifying the mobility of heavy metals in road deposited solids. Based on the data analysis, the following conclusions were derived:

- Heavy metal elements are rapidly adsorbed to road deposited solids particles once they interact with the solids surfaces.
- Road deposited solids have a higher amount of vacant charge sites available to adsorb high metal concentrations. The adsorption capacities are different

for different heavy metals. The heavy metal adsorption capacities of the solids samples increase in the order of  $Pb < Cr < Cu < Zn$  for all particle sizes. The desorbed heavy metal concentrations from solids follow the order of  $Cr < Cu < Pb < Zn$ .

- Cr is more rapidly adsorbed to solids particles than the other metals. At high concentrations, Cr is mostly adsorbed to organic matter by strong bonding, such as chemisorption. A small fraction of Cr is present in exchangeable form, attached to clay forming minerals and Mn, Fe and Al oxides. Comparatively, the amount of Cr adsorbed to Fe and Al oxides would be higher than the Cr adsorbed to Mn oxides. Bio-availability of Cr is very low compared to the other metal elements. However, changes in receiving water pH could release Cr once the particles enter the receiving waters. Therefore, removal of particles is important to avoid Cr contamination in receiving waters.
- Zn is preferentially adsorbed in the order of Fe oxide, Al oxide and clay forming minerals through cation exchange. The amount of Zn chemisorption to organic matter is very low compared to the amount of cation exchangeable form of Zn in metal oxides and clay forming minerals. Zn precipitation also occurs under the natural pH level of stormwater if high concentrations are available. Therefore, Zn is the metal most susceptible to bio-availability compared to the other three metals, and Zn retention by solids particles is low.
- Cu adsorption is dominated by the metal oxides, followed by the clay forming minerals. Cu forms strong bonds with particles which are in non-exchangeable form. Therefore, bio-availability of Cu is relatively low and a large fraction of Cu is present, adsorbed to solids particles.
- Pb adsorption is dominated by metal oxides and clay minerals when organic matter present in the sample is low. The adsorption to metal oxides occurs by the chemisorption mechanism, while adsorption to clay forming minerals occurs by cation exchange.
- Fine solids particles ( $<150\mu m$ ) have high metal adsorption capacity compared to coarse particles ( $>150\mu m$ ). Heavy metals are strongly adsorbed to fine solids, and desorption is low compared to the coarse particles.

Therefore, fine solids particles retain a relatively higher metal load and exert significant impact once they enter receiving waters.

- Although the adsorption capacity of coarse particles ( $>150\mu\text{m}$ ) is low compared to fine particles, there is high potential for the release of adsorbed heavy metals.

# Chapter 8: Conclusions and Recommendations for Further Research

---

## 8.1 CONCLUSIONS

The research study undertaken developed an in-depth understanding of the properties of build-up solids on road surfaces and the influence exerted by these properties on heavy metal adsorption to solids particles. Road surfaces accumulate a high content of solids which can adsorb large amounts of heavy metals. Therefore, understanding the fundamental processes governing the fate of heavy metals in road deposited solids is very important. A primary objective of this study was to understand the adsorption behaviour of heavy metal species with solids on urban road surfaces.

The road deposited solids characteristics were assessed using a suite of data collected from a series of field investigations and laboratory tests. The required data was obtained from pollutant build-up samples collected from sixteen road surfaces in four urbanised suburbs located in a major river catchment in the Gold Coast region. These roads represented the various soil mineralogical characteristics of the surrounding area and land uses. The build-up sampling was carried out using small plot areas to overcome the difficulties which arise in using non homogeneous areas.

Investigations using bulk solids are not adequate to understand the heavy metal adsorption processes of solids particles. This is due to the nature and amount of charge sites on the surface which are directly or indirectly controlled by the physical and chemical characteristics of solids. Due to the heterogeneous matrix and dynamic nature of solids accumulation on road deposited solids, it is hard to predict the physical and chemical characteristics of solids. Heavy metal adsorption is significantly influenced by the composition of solids.

### **8.1.1 IDENTIFICATION OF IMPORTANT PHYSICAL AND CHEMICAL PARAMETERS OF SOLIDS FOR HEAVY METAL ADSORPTION**

Detailed knowledge of solids properties was developed using the understanding derived from the physical and chemical parameters of different particle sizes of build-up solids. The analysis of build-up solids revealed that the total solids load in each road surface was different. This was primarily attributed to the different land use characteristics. However, the data analysis confirmed the predominance of the finer fraction, with 70% of the solids being finer than 150 $\mu$ m, independent of the land use. These particles possess physical and chemical parameter values which are favourable to heavy metals adsorption.

Road deposited solids mainly contain soil derived minerals such as quartz, albite, microcline, muscovite and chlorite minerals and amorphous material. Quartz and amorphous material are the predominant components in solids, irrespective of the geographical location. Fine solids particles (<150 $\mu$ m) consist of a clayey matrix and high amorphous content (in the region of 40%). Coarse particles (>150 $\mu$ m) consist of a sandy matrix, with about 60% quartz content at all study sites. Overall, build-up pollutants contained about 30% amorphous content, since road deposited solids are dominated by fine particles. Detailed analysis of road deposited solids and the roadside soils showed that the amorphous content is mainly derived from traffic related activities common to the urban environment. Amorphous material has high EGME SSA.

EGME SSA, TOC content, ECEC and the clay forming minerals content of solids decrease with the increase in particle size. Particles smaller than 150 $\mu$ m exhibited high EGME SSA, TOC, ECEC and clay forming minerals content. The EGME SSA, TOC and ECEC of the solids are not only influenced by the particle size but are also largely influenced by the sample mineralogical components and organic matter content. Although the EGME SSA, TOC, ECEC and clay forming minerals decreased with the increase in particle size, the extent of these physical and chemical characteristics differed in the various study sites. Similarly, significant differences in mineralogical compositions were noted in the various sites. This validates the strategy adopted for the study sites selection for this research. Therefore, traffic



density and site location (geological) were considered as the most significant site specific characteristics influencing the physical and chemical parameters of road deposited solids.

EGME SSA, TOC, ECEC and mineralogical components are correlated. Clay forming minerals primarily influence EGME SSA and ECEC in particles  $<150\mu\text{m}$ , whilst organic matter primarily influences EGME SSA and ECEC in particle  $>150\mu\text{m}$ . This suggests that the physical and chemical characteristics of solids are primarily influenced by the solids composition.

Data analysis indicated that the differences in physical and chemical characteristics of  $150\text{-}300\mu\text{m}$  and  $300\text{-}425\mu\text{m}$  solids particles are insignificant and are independent of the location of sample collection. Both particle sizes showed similar correlations among mineralogical components, and also variation in EGME SSA, TOC and ECEC indicated similar behaviour. This is primarily attributed to the high quartz content (approximately 60%) which is dominant in both  $150\text{-}300\mu\text{m}$  and  $300\text{-}425\mu\text{m}$  solids particles. As the particle size reduces below  $150\mu\text{m}$ , the amorphous material and clay forming minerals increase proportionately, thereby reducing the quartz content, and amorphous content becomes the dominant component in  $<75\mu\text{m}$  particles, irrespective of the land use. This results in significant differences in the physical and chemical characteristics of  $<75\mu\text{m}$  and  $75\text{-}150\mu\text{m}$  particle sizes. Thus, the consistency of the composition of mineralogical components and organic matter content in coarse particles ( $>150\mu\text{m}$ ) are the primary reasons for similar EGME SSA and ECEC in these particle sizes.

### **8.1.2 THE INFLUENCE OF PHYSICAL AND CHEMICAL CHARACTERISTICS ON HEAVY METAL ADSORPTION**

Two approaches were used to investigate the influence of physical and chemical characteristics of solids in heavy metal adsorption. Firstly, field samples collected from road surfaces were analysed. Secondly, batch experiments were undertaken to validate the conclusions derived from the field sample analyses. Only a part of the available adsorption sites in solids particles on road surfaces are occupied by heavy

metals. Thus, the batch experiments were used to provide important insight into the heavy metal adsorption processes, by allowing all charge sites to be occupied by heavy metal elements.

The analysis of heavy metal content in solids was carried out separately for different particle size ranges. Heavy metal concentrations in solids decreased with the increase in particle size, irrespective of land use. The heavy metal concentrations in the 150-300 $\mu\text{m}$  and 300-425 $\mu\text{m}$  sizes were similar. This is due to their similar mineralogical and organic matter composition. The high quartz content in these particles is the primary reason for the low heavy metal content. This confirms that the particle size and mineralogical composition are significant parameters that control the adsorption behaviour of solids. The particle size range <75 $\mu\text{m}$  had the highest heavy metal content, corresponding with its high clay forming minerals, high organic matter and low quartz content which increased EGME SSA and ECEC.

The research study revealed that road deposited solids consist of distinct groups of charge sites created by the mineral components, organic matter and oxides of Fe, Al and Mn. Due to the heterogeneous nature of the solids composition, the nature and the amount of the charge sites in different particle sizes vary. Therefore, a heavy metal cation can be adsorbed by any of the different charge sites on solids. Although heavy metal cations can have preference for charge sites based on their electro negativity (Hard Soft Acid Base), valency, ionic radii and metal speciation, they do not necessarily get the opportunity to form a preferred bond. The two main reasons are the lack of preferred binding sites and the inability to reach the preferred binding site due to competition between different heavy metal species. The adsorption mechanism and the bond strength between a heavy metal element and a charge site are different for different sites. This confirms that heavy metal adsorption is significantly influenced by the physical and chemical parameters of solids that lead to heterogeneity in surface charge sites.

Heavy metals show preference for association with clay forming minerals in fine solids particles (<150 $\mu\text{m}$ ), while in coarse particles (>150 $\mu\text{m}$ ) they preferentially

associate with organic matter. Therefore, the organic matter content in coarse particles ( $>150\mu\text{m}$ ) is more active in heavy metal adsorption than in the case of finer particles ( $<150\mu\text{m}$ ), despite the high organic matter content. Similarly, the influence of organic matter on ECEC in fine solids particles is low. Therefore, chemical composition is more important for heavy metal adsorption than the source or quantity of organic matter present in road deposited solids samples.

Traffic related material in amorphous content results in high heavy metal concentration in road deposited solids. Amorphous material in coarse particle sizes preferentially associates with heavy metals, whilst only some heavy metals preferentially associate with amorphous material in fine particle sizes.

The presence of materials with high SSA has a positive effect on ECEC and influences heavy metal adsorption. EGME SSA of particles is the primary parameter responsible for differences in adsorbed metal concentrations in different particle sizes. However, in a specific particle size, mineral composition, organic matter and amorphous content are the governing factors which can cause differences in adsorbed heavy metal concentrations. This is attributed to surface charge sites and surface functional groups that are dependent on the composition of solids and are vital for cation adsorption to solids surfaces.

Even though the solids may have low ECEC, heavy metal elements are mainly adsorbed to clay forming minerals through cation exchange. Heavy metal complexation with clay forming minerals at edge sites is low in road deposited solids. Heavy metal adsorption to organic matter is dominated by surface complexation or chemisorption. Additionally, a significant fraction of metal elements to solids particles can be adsorbed in the preferred order of Al oxide  $>$  Fe oxide  $>$  Mn oxide. Predominantly, metal oxides in solid particles are present in clay forming minerals and heavy metals are adsorbed through chemisorption. The preferential characteristics of different heavy metal elements on road surfaces solids are listed below.

- Zn, Cu, Pb and Ni show similar metal adsorption characteristics. These metal elements have high affinity to metal oxides of Mn, Fe and Al.
- Cd and Cr mostly show ion-exchangeable adsorption. These cations are associated with amorphous content, mineralogical components and organic matter. Appreciable amounts of Cr, Cd and Zn are available in the amorphous content as a result of traffic related by-products.
- Pb is mostly found in association with organic matter content. The preferential association of Pb is in the order of organic matter > metal oxide > mineralogical components. Association occurs by strong bonds rather than by cation exchange mechanism.

### 8.1.3 ADSORPTION AND DESORPTION OF HEAVY METALS IN SOLIDS

Important findings include:

- Road deposited solids particles have high concentrations of heavy metals which exceed the ANZECC (1992) guideline values for Assessment and Management of Contaminated Sites. Furthermore, the solids particles have a significant amount of vacant charge sites to further adsorb additional cations.
- Fine solids particles (<150µm) have high metal adsorption capacity compared to the coarse particles (>150µm). However, heavy metals create more stable bonds with fine solids than those adsorbed to the coarse solids particles and therefore desorption is relatively low compared to the coarse particles.
- At high metal concentrations, Cr, Cu and Pb are strongly bound to particles by chemisorption mechanisms. In contrast, Zn has a high likelihood of being released from the solids particles.
- Adsorption processes are generally independent of land use or geographical location. However, traffic characteristics and, by implication, land use can exert a significant influence on solids composition and heavy metal content in solids on road surfaces.

#### 8.1.4 PRACTICAL APPLICATION OF RESEARCH OUTCOMES

The knowledge resulting from this research study includes the following findings and their practical implications for stormwater mitigation strategies:

- Road deposited solids have a capacity (vacant charge sites) for the adsorption of heavy metals, over and above the already adsorbed heavy metals content. Therefore, during transport, solids could act as adsorbents of dissolved heavy metals in stormwater runoff and increase the heavy metal content in solids. *This highlights the importance of removing solids from stormwater which, in turn, will reduce the threat of polluted solids entering receiving water bodies.*
- Fine solids particles (<150µm) have a high metal adsorption capacity compared to the coarse particles (>150µm). Therefore, heavy metals adsorbed to solids can be easily transported and thereby pose a significant threat to receiving waters. *Therefore, in terms of heavy metal pollution of receiving waters, designing effective stormwater quality mitigation strategies to remove fine solids, rather than coarse particles, from stormwater runoff is very important.*
- Among the heavy metal elements considered in the present study, excluding those of geochemical origin, Zn was the predominant species that originates from traffic related activities. A significant portion of adsorbed Zn can be released from solids particles to stormwater runoff by small changes to the solute characteristics. *Therefore, in the removal of Zn, the removal of solids particles in a dry state should be considered. In this regard, effective source control of Zn is needed.*
- Heavy metals adsorbed to organic matter and metal oxides by chemisorption could potentially desorb due to microbial degradation of organic matter or chemical changes in water. *Consequently, a reduction in the long retention time of stormwater in retention/detention basins, and measures to control pH changes can be considered in an effort to reduce the potential risk posed by the bioavailability of heavy metals.*
- Road deposited solids are a heterogeneous mixture. The fate of heavy metals and the bioavailability of heavy metals are significantly influenced

by the mineralogical composition of solids (binding sites), rather than by the other parameters. *Therefore, determination of solids characteristics is very important for designing effective stormwater quality management strategies.*

- There is wide variability in solids' physical and chemical characteristics with particle size; this, in turn, plays a critical role in heavy metals adsorption. *Therefore, the investigation of different particle sizes is essential for implementing effective stormwater quality mitigation strategies.*

## **8.2 RECOMMENDATIONS FOR FURTHER RESEARCH**

As summarised above, the research work carried out in this project generated important fundamental knowledge relating to the physico-chemical behaviour of road deposited solids and the adsorption/desorption behaviour of heavy metals on solid surfaces. The research study also identified a number of issues that require further investigations to enhance the practical application of this knowledge to stormwater quality mitigation. Consequently, further research is recommended on the issues identified below.

- The higher amounts of amorphous material contained in solids particles are primarily derived from traffic related activities. It is recommended that further investigations are needed undertaken on the (amount and size range) and qualitative (surface and morphological) characterisation of traffic related particles on road surfaces to develop a greater understanding of urban stormwater runoff quality.
- Road surface pollutants include organic matter as decomposed compounds or in residual form. The study outcomes confirmed the importance of the characteristics of the organic matter in heavy metal adsorption, rather than (simply) the amount of organic matter. The degradation of organic matter can cause changes in solids characteristics and increase the bioavailability of heavy metals. Therefore, detailed investigations relating to the degradation of organic compounds is recommended.

- Competitive adsorption and desorption of heavy metal elements at different concentrations should be undertaken to enhance the understanding of adsorption and bioavailability of heavy metals in stormwater runoff.
- This study was limited to the investigation of heavy metal adsorption on build-up solids on road surfaces. It is also recommended that analysis of the adsorption process of stormwater runoff solids be undertaken to enhance the current knowledge base on heavy metal pollution. It is hypothesised that the bioavailability of adsorbed heavy metals can be affected by the physical and chemical mechanisms involved in solids re-suspension and settlement.





## Chapter 9: References

---

1. Abollino, O., Aceto, M., Malandrino, M., Sarzanini, C. and Mentasti, E. (2003). Adsorption of heavy metals on Na-montmorillonite. Effect of pH and organic substances, *Water Research*, Vol. 37 (No.7), pp. 1619-1627.
2. ABS. (2009). Australian Bureau of Statistics. Qld Stats. <http://www.abs.gov.au/AUSSTATS>.
3. Adachi, K. and Tainosho, Y. (2004). Characterization of heavy metal particles embedded in tire dust. *Environmental Engineering Science*, Vol.30, pp. 1009-1017.
4. Adachi, K. and Tainosho, Y. (2005). Single particle characterization of size-fractionated road sediments. *Applied Geochemistry*, Vol. 20, pp. 849–859.
5. Adams, M.J. (1995). *Chemometrics in analytical spectroscopy*. Cambridge [England], Royal Society of Chemistry.
6. Adriano, D.C. (2001). *Trace Elements in Terrestrial Environments*, Springer-Verlag, New York, Berlin, Heidelberg.
7. Al-Chalabi, A. S. and Hawker, D. (1996). Retention and exchange behavior of vehicular lead in street dusts from major roads. *Science of the Total Environment*, Vol. 187, pp. 105-119.
8. Allen, H.E. (1993). The significance of trace metal speciation for water, sediment and soil quality criteria and standards. *Science of The Total Environment*, Vol. 134, pp. 23-45.
9. Allen, T. (1990). *Particle size measurement*. Chapman and Hall, New York.
10. Allison, R.A., Chiew, F.H.S. and McMahon, T.A. (1998). Nutrient contribution of leaf litter in urban stormwater. *Journal of Environmental Management*, Vol. 54, pp. 269-272.
11. Alloway, B.J. (1995). *Heavy Metals in Soils*, 2<sup>nd</sup> (Edn), Blackie Academic and Professional, London.
12. Andral, M.C., Roger, S., Montréjaud-Vignoles, M. and Herremans, L. (1999). Particle size distribution and hydrodynamic characteristics of solid matter carried by runoff from motorways. *Water Environment Research*, Vol. 71 (No.4), pp. 398-407.

13. Angino, E.E., Magnuson, L.M. and Stewart, G.F. (1972). Effects of urbanisation on stormwater runoff quality: A limited experiment, Naismith Ditch, Lawrence, Kansas. *Water Resources Research*, Vol.8, pp. 135-140.
14. ANZECC (1992). Australian and New Zealand Guidelines for the Assessment and Management of Contaminated Sites. Australian and New Zealand Environment and Conservation Council and Agriculture and Resource Management Council, Australia, Canberra.
15. APHA. (2005). Standard methods for the examination of water and wastewater. American Public Health Association, American Water Works Association, Water Environment Federation, Washington.
16. Arnepalli, D.N., Shanthakumar, S., Hanumantha Rao, B. and Singh, D.N. (2008). Comparison of methods for determining specific-surface area of fine-grained soils. *Geotechnical and Geological Engineering*, Vol. 26, pp. 121-132.
17. Arnold, C.L. and Gibbons, C.J. (1996). Impervious surface coverage: the emergence of a key environmental indicator. *Journal of the American Planning Association*, Vol. 62 (No.2), pp. 243–258.
18. Arya, S.P. (1999). Air pollution meteorology and dispersion. Oxford University Press, New York.
19. AS/NZS 5667.1:1998. (1998). Water Quality- Sampling – Guidance on the Design of Sampling Programs, Sampling Techniques and the Preservation and Handling of Samples. Australia/New Zealand Standards.
20. ASTM. (2006). E965 – 96 Standard Test Method for Measuring Pavement Macrotexture Depth Using a Volumetric Technique. ASTM International, West Conshohocken, PA.
21. ATSDR, Agency for Toxic Substances and Disease Registry. (1995). Toxicological Profile for Polycyclic Aromatic Hydrocarbons. United States Department of Health and Human Services, Agency for Toxic Substances and Disease Registry, Public Health Service, Atlanta, G.A.
22. Aualiitia, T.U. and Pickering, W.F. (1986). Anodic stripping voltammetric study of the lability of Cd, PbCu ions sorbed on humic acid particles. *Water Research*, Vol. 20, pp. 1397-1406.
23. Aualiitia, T. U. and Pickering, W. F. (1987). Specific Sorption of trace amounts of Cu, Pb, and Cd by inorganic particulates. *Water, Air, and Soil Pollution*, Vol. 35 (No.1-2), pp. 171-185.

24. Ayoko, G.A., Morawska, L., Kokot, S. and Gilbert, D. (2004). Application of multicriteria decision making methods to air quality in the microenvironments of residential houses in Brisbane, Australia. *Environmental Science and Technology*, Vol. 38, pp. 2609-2616.
25. Ayoko, G.A., Singh, K., Balarea, S. and Kokot, S. (2007). Exploratory multivariate modeling and prediction of the physico-chemical properties of surface water and groundwater. *Journal of Hydrology*, Vol. 336 (No.1-2), pp. 115-124.
26. Azema, N., Pouet, M.F. Berho, C. and Thomas, O. (2002). Wastewater suspended solids study by optical methods. *Physicochemical and Engineering Aspects*, Vol. 204 (No.1), pp. 131-140.
27. Bachoc A. (1992). Location and general characteristics of sediment deposits into man-entry combined sewers. *Water Science and Technology*, Vol. 25, pp. 47-55.
28. Baker, D.E. and Eldershaw, V.J. (1993). Interpreting soil analysis for agricultural land use in Queensland, Division of Land Use and Fisheries, Report Series Q093014, Department of Primary Industries.
29. Baldock, J.A. and Skjemstad, J.O. (1999). Soil organic carbon, soil organic matter. Peverill, K.I., Sparrow, L.A. and Reuter, D.J. (Ed.) *Soil Analysis: an interpretation manual*. CSIRO Publication, Australia, pp. 159-170.
30. Ball, J.E., Jenks, R. and Aubourg, D. (1998). An assessment of the availability of pollutant constituents on road surfaces. *The Science of the Total Environment*, Vol. 209, pp. 243-254.
31. Banerjee, A.D.K. (2003). Heavy metal levels and solid phase speciation in street dusts of Delhi, India. *Environmental Pollution*, Vol. 123, pp. 95-105.
32. Bannerman, R.T., Owens, D.W., Dodds, R.B. and Hornewer, N.J. (1993). Sources of pollutants in Wisconsin stormwater. *Water Science and Technology*, Vol. 28 (No.3-5), pp. 241-259.
33. Barker, W.W., Welch, S.A., Chu, S. and Banfield, J.F. (1998). Experimental observations of the effects of bacteria on aluminosilicate weathering. *American Mineralogist*, Vol. 83, pp. 1551-1563.
34. Beckwith, P.R., Ellis, J.B. and Revitt, D.M. (1986). Heavy metal and magnetic relationships for urban source sediments. *Physics of the Earth and Planetary Interiors*, Vol. 42, pp. 67-75.

35. Bell, L.C. (1993). Basic properties of soils. *Environmental Soil Science: Invited Lectures : A Training Course for the Non-Soils Specialist*, Fergus, I.F., Coughlan, K.J., (Ed.), Australian Society of Soil Science Inc., Queensland, Brisbane, Australia, pp. 33-54.
36. Benjamin, M.M. and Leckie, J.O. (1981). Multiple-site adsorption of Cd, Cu, Zn, and Pb on amorphous iron oxyhydroxide. *Journal of Colloid and Interface Science*, Vol. 79 (No.1), pp 209-221.
37. Bernardin, F.E. (1985). Experimental Design and testing of adsorption and adsorbates. Slejeko F.L. (Ed.) *Adsorption Technology: A Step by Step Approach to Process Evaluation and Application*. Tall Oaks Publishing, Voorhees, New Jersey, pp. 37 -90.
38. Bian, B. and Zhu, W. (2008). Particle size distribution and pollutants in road-deposited sediments in different areas of Zhenjiang, China. *Environ Geochem Health*, Vol. 31 (No.4), pp. 511-520.
39. Biddappa, C.C., Chino, M. and Kumazawa, K. (1981). Adsorption, desorption, potential and selective distribution of heavy-metals in selected soils of Japan. *Journal of Environmental Science and Health Part B-Pesticides Food Contaminants and Agricultural Wastes*, Vol. 16, pp. 511-528.
40. Birch, G. F. and Scollen, A. (2003). Heavy metals in road dust, gully pots and parkland soils in a highly urbanised sub-catchment of Port Jackson, Australia *Australian Journal of Soil Research*, Vol. 41 (No.7), pp. 1317-1327.
41. Bish, D.L. and Post, J.E. (1989). *Modern Powder Diffraction*. Reviews in Mineralogy, Vol. 20. Mineralogical Society of America.
42. Bish, D.L. (1993). Rietveld refinement of the kaolinite structure at 1.5 K. *Clays and Clay Minerals*, Vol. 41, pp. 738-744.
43. Blakemore, L.C., Searle, P.L. and Daly, B.K. (1987). *Soil bureau laboratory methods: a method for chemical analysis of soils*. New Zealand: Soil Bureau Scientific Report 80.
44. Blok, J. (2005). Environmental exposure of road borders to zinc. *Science of the Total Environment*, Vol. 348, pp. 173–90.
45. Bolt, G.H., Bruggenwert, M.G.M. and Kamphorst, A. (1976). Adsorptions of cations by soils. Bolt, G.H. and Bruggenwert, M.G.M. (Ed.) *Soil Chemistry A Basic Elements*. Elsevier, North-Holland, New York.

46. Bond, W.J. (1995). On the Rothmund-Kornfeld description of cation exchange. *Soil Science Society of America Journal*, Vol. 59, pp. 436-443.
47. Bortoluzzi, E.C., Tessier, D., Rheinheimer, D.S. and Julien, J.L. (2006). The cation exchange capacity of a sandy soil in southern Brazil: an estimation of permanent and pH-dependent charges. *European Journal of Soil Science*, Vol. 57, pp. 356-364.
48. Brabec, E., Schulte, S. and Richards, P.L. (2002). Impervious Surfaces and water quality: A review of current literature and its implications for watershed planning. *Journal of Planning Literature*, Vol. 16 (No.4), 499-512.
49. Bradford, W.L. (1977). Urban stormwater pollutant loadings: A statistical summary through 1972. *Journal Water Pollution Control Federation*, Vol. 49, pp. 613-57.
50. Bradl, H.B. (2004). Adsorption of heavy metal ions on soils and soils constituents. *Journal of Colloid and Interface Science*, Vol. 277, pp. 1-18.
51. Brans, J.P., Vincke, P.H. and Mareschal, B. (1986). How to select and how to rank projects, the PROMETHEE method. *European Journal of Operational Research*, Vol. 24, pp. 228-238.
52. Brick, C. and Moore, J. (1996). Diel variation of trace metals in the upper Clark Fork River Montana. *Environmental Science and Technology*, Vol. 30 (No.6), pp. 1953-1960.
53. Brikeland, P. W. (1999). *Soils and Geomorphology*. Oxford University Press, New York, pp. 372.
54. Brindley, G.W. and Brown, G. (1984). X-ray Diffraction procedures for clay minerals identification: Brindley, G.W. and Brown, G. (Ed.) *Crystal Structures of Clay Minerals and Their X-Ray Identification*, Mineralogical Society, London.
55. Brinkmann, W.L.F. (1985). Urban Stormwater pollutants: Sources and loadings. *GeoJournal*, Vol. 11 (No.3), pp. 277-283.
56. Bris, F.J., Garnaud, S.G., Apperry, N., Gonzalez, A., Mouchel, J.M., Chebbo, G. and Thevenota, D.R. (1999). A street deposit sampling method for metal and hydrocarbon contamination assessment. *The Science of the Total Environment*, Vol. 235, pp. 211-220.
57. Brodie, I.M. and Porter, M.A. (2006). Stormwater particle characteristics of five different urban surfaces. In: *7th International Conference on Urban*

- Drainage Modelling and 4th International Conference on Water Sensitive Urban Design, Melbourne, Australia.
58. Brown, J. N. and Peake, B.M. (2006). Sources of heavy metals and polycyclic aromatic hydrocarbons in urban stormwater runoff. *Science of the Total Environment*, Vol. 359 (No.3), pp. 145-155.
  59. Brunauer, S, Emmett P.H. and Teller, E. (1938). Adsorption of gases in multi-molecular layers. *Journal of the American Chemical Society*, Vol. 60, pp.309–319.
  60. Buffle, J.F. and Stumm, W. (1994). General chemistry of aquatic systems. In: *Chemical and Biological Regulation of Aquatic Systems*, J. Buffle and R.R. DeVitre, (Eds.), CRC Press, Boca Raton, FL, pp. 1–42.
  61. Cadle, S.H. and Williams, R.L. (1978). Gas and particle emissions from automobile tires in laboratory and field studies. *Rubber Chemistry and Technology*, Vol. 52, pp. 146–158.
  62. Calisir, F.F., Roman, F.R., Alamo, L., Perales, O., Arocha, M.A. and Akman, S. (2009). Removal of Cu(II) from aqueous solutions by recycled tire rubber. *Desalination*, Vol. 249, pp. 515-518.
  63. Carmody, O., Kristof, J., Frost, R.L., Mako, E., Kloprogge, J.T. and Kokot, S. (2005). A spectroscopic study of mechanochemically activated kaolinite with the aid of chemometrics. *Journal of Colloid and Interface Science*, Vol. 287, pp. 43-56.
  64. Carmody, O., Frost, R.L., Kristof, J., Kokot, S., Kloprogge, J.T. and Mako, E. (2006). Modification of kaolinite surfaces through mechanochemical activation with quartz-a DRIFT and chemometrics study. *Applied Spectroscopy*, Vol. 60 (No.12), pp. 1414-1422.
  65. Carroll, S., Goonetilleke, A. and Dawes, L. (2004). Framework for Soil Suitability Evaluation for Sewage Effluent Renovation. *Environmental Geology*, Vol. 46 (No.2), pp. 195-208.
  66. Carroll, S.P. and Goonetilleke, A. (2005). Assessment of high density of onsite wastewater treatment systems on a shallow groundwater coastal aquifer using PCA. *Environmetrics*, Vol. 16 (No.3), pp. 257-274.
  67. Carter, D.L., Heliman, M.D. and Gonzalez, C.L. (1965). Ethylene Glycol Monoethyl Ether for determining surface area of silicate minerals. *Soil Science*, Vol. 100 (No.5), pp. 356-360.

68. Carter, D.L., Mortland, M.M. and Kemper, W.D. (1986). Specific Surface, Methods of Soil Analysis, Part 1. Physical and Mineralogical Methods, Chapter 16, Agronomy, No.9, 2<sup>nd</sup> (Edn), American Society of Agronomy, pp. 413-423.
69. Castaldi, P. and Santona, L., Enzo, S. and Melis P. (2008). Sorption processes and XRD analysis of a natural zeolite exchanged with Pb<sup>2+</sup>, Cd<sup>2+</sup> and Zn<sup>2+</sup> cations. *Journal of Hazardous Materials*, Vol. 156, pp. 428-434.
70. CCME, Canadian Council of Ministers of the Environment. (1995). Protocol for the Derivation of Canadian Sediment Quality Guidelines for the Protection of Aquatic Life. Report CCME EPC-98E. Prepared by the Technical Secretariat of the Water Quality Guidelines Task Group, Winnipeg, Manitoba.
71. Cerato, A.B. and Lutenegeger, A.J. (2002). Determination of surface area of fine-grained soils by the Ethylene Glycol Monoethyl Ether (EGME) Method. *Geotechnical Testing Journal*, Vol. 24 (No. 3), pp. 1-7.
72. Charbonneau, R. and Kondolf, G.M. (1993). Land use change in California, USA: Nonpoint source water quality impacts. *Environmental Management*, Vol. 17, pp. 453-460.
73. Charlesworth, S.M. and Lees, J.A. (1999). Particulate-associated heavy metals in the urban environment: Their transport from source to deposit, Coventry, UK. *Chemosphere*, Vol. 39 (No.5), pp. 833-848.
74. Charlesworth, S., Everett, M., McCarthy, R., Ordonez, A. and Miguel, E. (2003). Comparative study of heavy metal concentration and distribution in deposited street dust in a large and a small urban areas: Birmingham and Coventry, West Midlands, United Kingdom. *Environment International*, Vol. 29, pp. 563-573.
75. Christophi, C.A. and Axe, L. (2000). Competition of Cd, Cu and Pb adsorption on goeeteite. *Journal of Environmental Engineering - ASCE*, Vol. 126 (No.1), pp. 66 – 74.
76. Cordery, I. (1977). Quality characteristics of urban storm- runoff water in Sydney, Australia. *Water Resources Research*, Vol.13 (No. 1), pp. 197-202.
77. Cornell, R.M. and Schwertmann, U., (1996). The iron oxides. Structure, Properties, Reactions, Occurrences and Uses. Wiley VCH, Weinheim, Germany.

78. Covelo, E.F., Andrade, C.M.L. and Vega, F.A. (2004). Competitive adsorption and desorption of cadmium, chromium, copper, nickel, lead, and zinc by Humic Umbrisols. *Communications in Soil Science and Plant Analysis*, Vol. 35, pp. 2709 — 2729.
79. Covelo, E.F., Vega, F.A. and Andrade, M.L. (2007a). Competitive sorption and desorption of heavy metals by individual soil components. *Journal of Hazardous Materials*, Vol. 140, pp. 308-315.
80. Covelo, E.F., Vega, F.A. and Andrade, M.L. (2007b). Heavy metal sorption and desorption capacity of soils containing endogenous contaminants. *Journal of Hazardous Materials*, Vol. 143 (No.1-2), pp. 419-430.
81. Covelo, E.F., Vega, F.A. and Andrade, M.L. (2008). Sorption and desorption of Cd, Cr, Cu, Ni, Pb and Zn by a Fibric Histosol and its organo-mineral fraction. *Journal of Hazardous Materials*, Vol. 159, pp. 342-347.
82. Cullity, B.D. (1978). *Elements of X-Ray Diffraction*, 2<sup>nd</sup> Edition. Addison-Wesley Publishing Co. Menlo Park, CA.
83. Dahl, A., Gharibi, A., Swietlicki, E., Gudmundsson, A., Bohgard, M., Ljungman, A., Blomqvist, G. and Gustafsson, M. (2006). Traffic generated emissions of ultrafine particles from pavement–tire interface. *Atmospheric Environment*, Vol. 40 (No.7), pp. 1314–1323.
84. Dannis, M.L. (1974). Rubber dust from the normal wear of tires. *Rubber Chemistry Technology*, Vol. 47, pp. 1011–1037.
85. Davis, A.P. and Upadhyaya, M. (1996). Desorption Of Cadmium from Goethite (~-FeOOH). *Water Research*, Vol. 30 (No.8), pp. 1894-1904.
86. Davis, A.P. Shokouhian, M. and Ni, S. (2001). Loading estimates of Lead, Copper, Cadmium, and Zink in urban runoff from specific sources. *Chemosphere*, Vol.44, pp. 997-1009.
87. Dawes, L. and Goonetilleke, A. (2003). Using soil properties to predict long-term effluent treatment potential. In Patterson, R. and Malcolm, J. (Eds.) *Onsite 03 Conference: Future Directions for On-Site systems: Best Management Practice*, 28-30 September 2003, Armidale.
88. Dawes, L. and Goonetilleke, A. (2005). Using multivariate analysis to predict the behaviour of soils under effluent irrigation. *Water, Air and Soil Pollution*, Vol.172 (No.1-4), pp. 109-127.



89. Dawes, L. (2006). Role of soil physical and chemical characteristics and landscape factors in defining soil behaviour under long term wastewater disposal. PhD Thesis, Queensland University of Technology.
90. Dawes, L. A. and Goonetilleke, A. (2006). Using undisturbed columns to predict long term behaviour of effluent irrigated soils under field conditions. *Australian Journal of Soil Research*, Vol. 44 (No. 7), pp. 661-676.
91. Dawes, L., Goonetilleke, A. and Cox, M. (2006). Assessment of physical and chemical attributes of sub-tropical soil to predict long term effluent treatment potential. *Soil and sediment contamination: Soil and Sediment Contamination*, Vol. 14, pp. 211-230.
92. De Bartolomeo, A., Poletti, L., Sanchini, G., Sebastiani, B. and Morozzi, G. (2004). Relationship among parameters of lake polluted sediments evaluated by multivariate statistical analysis. *Chemosphere*, Vol. 55, pp. 1323-1329.
93. De Miguel, E., Llamas, J.F., Chaco'n, E., Berg, T., Larssen, S. and Røyset, O. (1997). Origin and patterns of distribution of trace elements in street dust: unleaded petrol and urban lead. *Atmos Environ*, Vol. 31, pp. 2733– 40.
94. Dean, C.M., Sansalone, J.J., Cartledge, F.K. and Pardue, J.H. (2005). Influence of hydrology on rainfall-runoff metal element speciation. *Journal of Environmental Engineering*, Vol. 13 (No.4), pp. 632-642.
95. Deletic, A. and Maksimovic C.T. (1998). Evaluation of water quality factors in storm runoff from paved areas. *Journal of Environmental Engineering*, Vol. 124, pp. 869-879.
96. Deletic, A. and Orr, D.W. (2005). Pollution buildup on road surfaces. *Journal of Environment Engineering*, Vol. 131 (No. 1), 49-59.
97. Delmas, C., Larpin, L., Legret, M. and Astruc, M. (2002). Mobility and Adsorption Capacity of Pb and Zn in a Polluted Soil from a Road Environment: Laboratory Batch Experiments. *Environ. Technol*, Vol.23, pp. 381–390.
98. Department of Transport and regional Services, Australia (2007). Estimating urban traffic and congestion cost trends for Australian cities, Working Paper 71. Bureau of Transport and Regional Economics, Department of Transport and Regional Services, Canberra, Australia.

99. Dijkstra, J.J., Meeussen, J.C.L. and R.N.J. Comans. (2004). Leaching of heavy metals from contaminated soils: an experimental and modeling study. *Environmental Science and Technology*, Vol. 38, pp. 4390–4395.
100. Dong, A., Chesters, G. and Simsiman, G.V. (1984). Metal composition of soil, sediments, and urban dust and dirt samples from the Menominee River Watershed, Wisconsin, USA. *Water, Air, and Soil Pollution*, Vol. 22, pp. 257-275.
101. Dong, D., Nelson, Y. M., Lion, L. W., Shuler, M. L. and W. C. Ghiorse (2000). Adsorption of Pb and Cd onto metal oxides and organic material in natural surface coatings as determined by selective extractions: new evidence for the importance of Mn and Fe oxides. *Water Research*, Vol. 34 (No.2), pp. 427-436.
102. Drapper, D., Tomlinson, R. and Williams, P. (2000). pollutant concentrations in road runoff Southeast Queensland case study. *Journal of Environmental Engineering*, Vol. 126, pp. 313-320.
103. Duncan, H.P. (1995). A review of urban stormwater quality processes. Report No. 95/9, Cooperative Research Centre for Catchment Hydrology.
104. Egodawatta, P. and Goonetilleke, A. (2006). Characteristics of pollutants built-up on residential road surfaces. *Proceedings of the 7th International Conference on HydroScience and Engineering*. Philadelphia, USA: Drexel University.
105. Egodawatta, P., Goonetilleke, A., Ayoko, G.A. and Thomas, E. (2006). Understanding the interrelationship between stormwater quality and rainfall and runoff factors in residential catchments. *Proceedings of the Seventh International Conference on Urban Drainage Modeling and the Fourth International Conference on Water Sensitive Urban Design*, Melbourne, Australia, pp. 43-50.
106. Egodawatta, P. (2007). Translation of small plot pollution mobilisation and transport measurements from impermeable urban surfaces to urban catchment scale. PhD Thesis, Queensland University of Technology, Brisbane Australia.
107. Egodawatta, P.E., Thomas, E. and Goonetilleke, A. (2007). Mathematical interpretation of pollutant wash-off from urban road surfaces using simulated rainfall. *Water Research*, Vol. 41 (No.13), pp. 3025-3031.

108. Egodawatta, P. and Goonetilleke, A. (2008). Understanding road surface pollutant wash-off and underlying physical processes using simulated rainfall. *Water science and technology*, Vol. 57 (No.8), pp. 1241-1246.
109. Einax, J.W., Truckenbrodt, D. and Kampe, O. (1998). River pollution data interpreted by means of chemometric methods. *Microchemical Journal*, Vol. 58, pp. 315-324.
110. Eisma, D. (1981). Suspended matter as a carrier for pollutants in estuaries and sea. Geyer, R. A. (Ed.), *Marine Environmental Pollution, 2. Mining and Dumping*. Elsevier, Amsterdam, pp. 281-95.
111. Elliott, H.A., Liberati, M.R. and Huang, C.P. (1986). Competitive sorption of heavy metals by soils. *J. Environmental Quality*, Vol. 15 (No.3), pp. 214-218.
112. Ellis, J.B. (1976). Sediments and water quality of urban stormwater. *Water Services*, pp.730-734.
113. Ellis, J.B. and Revitt, D.M. (1982). Incidence of heavy metals in street surface sediments-solubility and grain size studies. *Water, Air and Soil Pollution*, Vol. 17, pp. 87–100.
114. Ellis, J.B., Revitt, D.M. and Llewellyn, N. (1997). Transport and the Environment: Effects of organic pollutants on water quality. *Water and Environment Journal*, Vol. 11 (No.3), pp. 170-77.
115. Ellis, K.V. (1989). Types and sources of contamination. *Surface water pollution and its control*, Basingstoke, Macmillan, London, pp. 99-109.
116. Espey, W.H., Winslow, D.E. and Moore, W.L. (1969). Urban effects on the unit hydrograph. *Proceedings of the Second Water Resources Symposium, Effects of Watershed Changes on Stream Flow*, pp. 215-228.
117. Espinasse, B., Picolet, G. and Chouraqui, E. (1997). Negotiation support systems: A multi-criteria and multi-agent approach. *European Journal of Operational Research*, Vol. 103, pp. 389-409.
118. Evan, C.M. and Scott, B.J. (2007). Surface soil acidity and fertility in the central-western wheatbelt of New South Wales. *Australian Journal of Experimental Agriculture*, Vol. 47, pp. 184–197.
119. Evans, J.J. (1997). Rubber tire leachates in the aquatic environment. *Reviews of Environmental Contamination and Toxicology*, Vol. 151, pp. 67–115.

120. Facchinelli, A., Sacchi, E. and Mallen, L. (2001). Multivariate statistical and GIS-based approach to identify heavy metal sources in soils. *Environmental Pollution*, Vol. 114 (No.3), pp. 313-324.
121. Farahmand, T., Fleming, S.W. and Quilty E.J. (2007). Detection and visualization of storm hydrograph changes under urbanization: An impulse response approach. *Journal of Environmental Management*, Vol. 95, pp. 93-100.
122. Farnham, I.M., Johannesson, K.H., Singh, A.K., Hodge, V.F. and Stetzenbach, K.J. (2003). Factor analytical approaches for evaluating groundwater trace element chemistry data. *Analytica Chimica Acta*, Vol. 490, pp. 123-138.
123. Farquhar, M.L., Vaughan, D.J., Hughes, C.R., Charnock, J.M. and England, K.E.R. (1997). Experimental studies of the interaction of aqueous metal cations with mineral substrates: Lead, cadmium, and copper with perthitic feldspar, muscovite, and biotite. *Geochimica et Cosmochimica Acta*, Vol. 61, pp. 3051-3064.
124. Fauser, P., Tjell, J.C., Mosbaek, H. and Pilegaard, K. (1999). Quantification of tire-tread particles using extractable organic zinc as a tracer. *Rubber Chemistry and Technology*, Vol. 72, pp. 969-977.
125. Fenton, G., Helyar, K., Abbott, T. and Orchard, P. (1996). Soil acidity and liming. *Agfact AC. 19. 2<sup>nd</sup> (Edn)*, NSW Agriculture: Orange, NSW.
126. Fergusson, J.E. and Ryan, D. (1984). The elemental composition of street dust from large and small urban areas related to city type, source and particle size. *Science of the Total Environment*, Vol. 34, pp.101-116.
127. Fergusson, J.E. and Kim, N. (1991). Trace elements in street and house dusts: source and speciation. *The Science of the Total Environment*, Vol. 100, pp. 125–150.
128. FHWA. (2005). Federal Highway Administration Technical Advisory Report T5040.36. US Department of Transportation.
129. Filep, G. (1999). *Soil Chemistry: Processes and Constituents*, Akademiai Kiado, Budapest, Hungary.
130. Fitzpatrick, R.W., McKenzie, N.J. and Maschmedt D. (1999). Soil morphological indicators and their importance to soil fertility. In: Peverell, K., Sparrow, L.A. and Reuter, D.J. (Ed.), *Soil Analysis: an Interpretation Manual*. Melbourne, Australia, CSIRO Publishing, pp. 55–69.

131. Fontes, M.P.F. and Gomes, P.C. (2003). Simultaneous competitive adsorption of heavy metals by the matrix of tropical soils. *Applied Geochemistry* Vol.18, pp. 795–804.
132. Frost, R., Carmody, O., Xi. Y. and Kokot, S. (2007). Adsorption of hydrocarbons on organo-clays -implications for oil spill remediation. *Journal of Colloid and Interface Science*, Vol.305, pp. 17-24.
133. Fulcher, G.A. (1994). Urban Stormwater quality from a residential catchment. *The Science of the total Environment*, Vol. 146, pp. 535-542.
134. GCCC (2004). Gold Coast City Council, Our Living City Report - Chapter 2. [http://www.goldcoast.qld.gov.au/attachment/publications/our\\_living\\_city0405\\_chp2.pdf](http://www.goldcoast.qld.gov.au/attachment/publications/our_living_city0405_chp2.pdf)
135. GCCC-Web (2009). Gold Coast City Council's web page- [http://www.goldcoast.qld.gov.au/gcplanningscheme\\_0110/maps.html](http://www.goldcoast.qld.gov.au/gcplanningscheme_0110/maps.html).
136. Gillman, G. and Bell, L. (1976). Surface charge characteristics of six weathered soils from tropical north Queensland. *Australian Journal of Soil Research*, Vol. 14 (No.3), pp. 351-360.
137. Gillman, G. and Bell, L. (1978). Soil solution studies on weathered soils from tropical north Queensland. *Australian Journal of Soil Research*, Vol. 16 (No.1), pp. 67-77.
138. Gillman, G.P. and Sumpter, E.A. (1986). Modification to the compulsive exchange method for measuring exchange characteristics of soils. *Australian Journal of Soil Research*, Vol. 24, pp. 61–66.
139. Gnecco, I., Berretta, C., Lanza, L.G. and La Barbera, P. (2005). Stormwater pollution in the urban environment of Genoa, Italy. *Atmospheric Research*, Vol. 77, pp. 60– 73.
140. Gobel, P., Dierkes, C. and Coldewey, W.G. (2006). Stormwater runoff concentration matrix for urban areas. *Journal of Contaminant Hydrology*, Vol. 52 (No.2), pp.213-221.
141. Gomes, P.C., Fontes, M.P.F., Silva, A.G., de Mendonça, S.E. and Netto, A.R. (2001). Selectivity sequence and competitive adsorption of heavy metals by Brazilian soils. *American Journal of Soil Science Society*, Vol. 65 (No.4), pp. 1115–1121.
142. Goonetilleke, A. and Thomas, E. (2003). Water quality impacts of urbanisation: Evaluation of current research. Technical Report, Centre for Built

- Environment and Engineering Research, Queensland University of Technology, Australia.
143. Goonetilleke, A., Thomas, E., Ginn, S. and Gilbert, D. (2005). Understanding the role of land use in urban stormwater quality management. *Journal of Environmental Management*, Vol. 74, pp. 31-42.
  144. Goonetilleke, A., Egodawatta, P. and Kitchen, B. (2009). Evaluation of pollutant build-up and wash-off from selected land uses at the Port of Brisbane, Australia. *Marine Pollution Bulletin*, Vol. 58 (No.2), pp. 213-221.
  145. Greenland, D.J. and Hayes, M.H.B. (1981). *The Chemistry of Soil Processes*. Wiley, Chichester, UK.
  146. Gregg, S.J. and Sing K.S.W. (1967) *Adsorption, surface area and porosity*, Academic Press, London and New York.
  147. Gromaire-Mertz, M. C., Garnaud, S., Gonzalez, A. and Chebbo, G. (1999). Characterisation of urban runoff pollution in Paris. *Water Science and Technology*, Vol. 39 (No.2), pp. 1-8.
  148. Gualtieri, M.M., Andrioletti, M., Vismara, C. Milani, M. and Camatini, M. (2005). Toxicity of tire debris leachates. *Environment International*, Vol. 31, pp. 723-730.
  149. Guo, H.T., Wang, T. and Louie, P.K.K. (2004). Source apportionment of ambient non-methane hydrocarbons in Hong Kong: Application of a principal component analysis/absolute principal component scores (PCA/APCS) receptor model. *Environmental Pollution*, Vol. 129, pp. 489-498.
  150. Gupta, K. and Saul, A.J. (1996). Specific relationships for the first flush load in combined sewer flows. *Water. Research*, Vol. 30 (No.5), pp. 1244-1252
  151. Haiping, Z. and Yamada, K. (1998). Simulation of nonpoint source pollutant loadings from urban area during rainfall: an Application of a Physically-Based Distributed Model. *Water Science and Technology*, Vol. 38 (No.10), pp. 199-206.
  152. Hall, M.J. and Ellis, J.B. (1985). Water quality problems of urban areas, *GeoJournal*, Vol. 11 (No.3), pp. 265-275.
  153. Hamilton, R.S., Revitt, D.M. and Warren, R.S. (1984). Levels and physico-chemical associations of Cd, Cu, Pb and Zn in road sediments. *The Science of the Total Environment*, Vol. 33, pp. 59-74.

154. Hancock, R.D. and Martell, A.E. (1989). Ligand design for selective complexation of metal ions in aqueous solution. *Chemical Reviews*, Vol. 89 (No.8), pp.1875-1914.
155. Harrison, R.M., Laxen, D.P.H. and Wilson, S.J. (1981). Chemical Associations of Lead, Cadmium, Copper, and Zinc in Street Dusts and Roadside Soils. *Environmental Science and Technology*, Vol. 15 (No.11), pp. 1378-1383.
156. Hart, B.T. (1982). Uptake of trace metals by sediments and suspended particulates: a review. *Hydrobiologia*, Vol. 91, pp. 299-313.
157. Harter, R.D. (1992). Competitive sorption of cobalt, copper, and nickel ions by a calcium-saturated soil. *Soil Science Society of America Journal*, Vol. 56 (No.2), pp. 444-449.
158. Hartmann, A., Gräsle, W. and Horn, R. (1998). Cation exchange processes in structured soils at various hydraulic properties. *Soil and Tillage Research*, Vol. 47, pp. 67-72.
159. Head, K.H. (1980). *Manual of soil Laboratory Testing: Soil Classification and Compaction Tests*. Halsted Press, New York, Vol. 1, pp. 249-250.
160. Helling, C.S., Chesters, G. and Corey, C. (1964). Contribution of organic matter and clay to soil cation-exchange capacity as affected by the pH of the saturating solution. *Soil Science Society of America. Proc.* 28, pp. 517-520.
161. Hergren, L. (2005). Build-up and wash-off process kinetics of PAHs and heavy metals on paved surfaces using simulated rainfall. PhD Thesis, Queensland University of Technology, Brisbane, Australia.
162. Hergren L., Goonetilleke A. and Ayoko G.A. (2005). Understanding heavy metal and suspended solids relationships in urban stormwater using simulated rainfall. *Journal of Environmental Management*, Vol. 76, pp. 149-58.
163. Hergren, L., Goonetilleke, A. and Ayoko, G.A. (2006). Analysis of heavy metals in road-deposited sediments. *Analytica Chimica Acta*, Vol. 571, pp. 270-278.
164. Hildemann, L.M., Cass, G.R. and Markowski, G.R. (1989). A dilution stack sampler for collection of organic aerosol emissions: design, characterization and field tests. *Aerosol Science and Technology*, Vol. 10, pp. 193-204.
165. Hoffman, E.J., Mills, G.L., Latimer, J.S. and Quinn, J.G. (1984). Urban runoff as a source of polycyclic aromatic hydrocarbons to coastal waters. *Environmental Science and Technology*, Vol.18, pp. 580-587.

166. Hoffman, E.J., Latimer, J.S., Hunt, C.D., Mills, G.L. and Quinn, J.G. (1985). Stormwater runoff from highways. *Water, Air and Soil Pollution*, Vol. 25, pp. 349-364.
167. Hofstede, H. (1994). Use of bauxite refining residue to reduce the mobility of heavy metals in municipal solid waste compost. PhD Thesis, Environmental Science, Murdoch University, Australia.
168. Hollis, J.M. (1991). The classification of soils in urban areas, Bullock P. and Gregory P. J. (Ed.), *Soils in the Urban Environment*, Blackwell Scientific Publications, Oxford, pp. 1-4.
169. Hopke, P.K., Lamb, R.E. and Natusch, D.F.S. (1980). Multielemental characterization of urban roadway dust. *Environmental Science and Technology*, Vol. 14, pp. 164-172.
170. Horowitz, A.J. (1991). *A Primer to Sediment-Trace Element Chemistry*. Lewis Publishers.
171. Hseu, Z., Chen, Z., Tsai, C., Tsui, C., Cheng, S., Liu, C. and Lin, H. (2002). Digestion Methods for total heavy metals in sediments and soils. *Water, Air and Soil Pollution*, Vol. 141 (No.1-4), pp. 189-205.
172. Hseu, Z.Y. (2004). Evaluating heavy metal contents in nine composts using four digestion methods. *Bioresource Technology*, Vol. 95, pp. 53-59.
173. Huang, J., Du, P., Ao, C., Lei, M., Zhao, D., Ho, M. and Wang, Z. (2007). 'Characterization of surface runoff from a subtropics urban catchment', *Journal of Environmental Sciences*, Vol. 19 (No.2), pp. 148-152.
174. Hunter, K.A. and Liss, P.S. (1982). Organic matter and the surface charge of suspended particles in estuarine waters *Limnol. Oceanogr*, Vol. 27 (No.2), pp. 322-335.
175. Hwang, H.M. and Foster, G.D. (2006). Characterization of polycyclic aromatic hydrocarbons in urban stormwater runoff flowing into the tidal Anacostia River, Washington, DC, USA. *Environmental Pollution*, Vol. 140, pp. 416-426.
176. Inglezakis, V.J. and Grigoropoulou, H. (2004). Effects of operating conditions on the removal of heavy metals by zeolite in fixed bed reactors. *Journal of Hazardous Materials*, Vol. 112 (No.1-2), pp. 37-43.
177. Isbell, R.F. (1996). *The Australian Soil Classification*. CSIRO Publishing, Australia.



178. Isbell, R.F., McDonald, W.S. and Ashton, L.J. (1997). Concepts and Rationale of the Australian Soil Classification. CSIRO Land and Water, Australia.
179. Israelachvili, J.N. (1985). Intermolecular and Surface Forces. Academic Press, London.
180. Jackson, J.E. (1991). A User's Guide to Principal Components. John Wiley and Sons, New York, p. 592.
181. Jain, C.K. and Ram, D. (1997). Adsorption of metal ions on bed sediments', Hydrological Sciences Journal, Vol. 42(No.5), pp. 713-723.
182. James, W. and Shivalingaiah, B. (1985). Storm water pollution modelling: buildup of dust and dirt on surfaces subject to runoff. Canadian Journal of Civil Engineering, Vol. 12, pp. 906-915.
183. Jartun, M., Ottesen, R.T., Steinnes, E. and Volden, T. (2008). Runoff of particle bound pollutants from urban impervious surfaces studied by analysis of sediments from stormwater traps. Science of the Total Environment, Vol. 396 (No.3), pp. 147-163.
184. Joffe, J. and Kunin, R., (1943). Mechanical separates and their fractions in the soil profile. II. The cation exchange properties and pedogenic implications. Proceedings of Soil Science Society of America, Vol. 8, pp. 384-387.
185. Johnston, C.T. (1996). Sorption of organic compounds on clay minerals: A surface functional group approach. Sawhney, B.L. (Ed.) Organic pollutants in the environment, CMS workshop lectures. Vol. 8, Clay Minerals Society, Boulder, pp. 1-44.
186. Jullien, A. and D. François (2006). Soil indicators used in road environmental impact assessments. Resources, Conservation and Recycling, Vol. 48, pp. 101-124.
187. Kahle, M., Kleber, M., Torn, M.S. and Jahn, R. (2003). Carbon storage in coarse and fine clay fractions of illitic soils. Soil Science Society of America Journal, Vol. 67, pp. 1732-1739.
188. Kang, J., Li, Y., Lau, S., Kayhanian, M. and Stenstrom, M.K. (2007). Particle Destabilization in Highway Runoff to Optimize Pollutant Removal. Journal of Environmental Engineering, Vol. 133 (No.4), pp. 353-461.
189. Kaoser, S., Barrington, S., Elektorowicz, M. and Wang, L. (2005). Effect of Pb and Cd on Cu adsorption by sand-bentonite liners. Canadian Journal of Civil Engineering, Vol. 32, pp. 241-249.

190. Karim, A. and Islam, A. (1956). A study of ion-exchange properties of silt. *Soil Sci.* Vol. 82, pp. 433-436.
191. Keller, H.R., Massart, D.L. and Brans, J.P. (1991). Multicriteria decision making: a case study. *Chemometrics and Intelligent laboratory systems*, Vol. 11, pp. 175-189.
192. Khalil, W.A.S., Goonetilleke, A., Kokot, S. and Carroll, S. (2004). Use of chemometrics methods and multicriteria decision-making for site selection for sustainable on-site sewage effluent disposal. *Analytica Chimica Acta*, Vol. 506, pp. 41–56.
193. Khalil, W. (2005). Integrated land capability for ecological sustainability of on-site sewage treatment systems. PhD Thesis, Queensland University of Technology.
194. Kim, L., Zoh, K., Jeong, S., Kayhanian, M. and Stenstrom, M.K. (2006). Estimating pollutant mass accumulation on highways during dry periods. *Journal of Environmental Engineering*, Vol. 132 (No.9), pp. 985-993.
195. Kinniburgh, D. G., Jackson, M. L. and Syers, J. K. (1976). Adsorption of alkaline earth, transition and heavy metal cations by hydrous oxide gels of iron and aluminium. *Proceedings - Soil Science Society of America*, Vol. 40, pp. 796-799.
196. Kleber, M., Mertz, C., Zikeli, S., Knicker, H. and Jahn, R. (2004). Changes in surface reactivity and organic matter composition of clay subfractions with duration of fertilizer deprivation. *European Journal of Soil Science*, Vol. 55, pp. 381–391
197. Kokot, S. and Yang, P. (1995). Comparison of thermogravimetric and differential scanning calorimetric results for cellulosic fabrics by chemometrics. *Analytica Chimica Acta*, Vol. 304, pp. 297-305.
198. Kokot, S., Grigg, M., Panayiotou, H. and Phuong, T.D. (1998). Data interpretation by some common chemometrics methods. *Electroanalysis*, Vol. 10 (No.16), pp.1-8.
199. Kokot, S., Leonard, G., O'Shea, M. and Purcell, D. (2005). A chemometrics investigation of sugarcane plant properties based on the molecular composition of Epicuticular Wax. *Chemometrics and Intelligent Laboratory Systems*, Vol. 76 (No.2), pp. 135-147.

200. Kraepiel, A. M., Keller, K. and Morel, F. M. M. (1999). A model for metal adsorption on montmorillonite. *Journal of Colloid and Interface Science*, Vol. 210, pp. 43-54.
201. Kreider, M.L., Panko, J.M., McAtee, B.L., Sweet, L.I. and Finley, B.L. (2010). Physical and chemical characterization of tire-related particles: Comparison of particles generated using different methodologies. *Science of the Total Environment*. Vol.408, pp. 652-659.
202. Lahdelma, R., Miettinen, K. and Salminen. P. (2003). Ordinal criteria in stochastic multicriteria acceptability analysis (SMAA). *European Journal of Operational Research*, Vol. 147, pp. 117-127.
203. Laird, D.A., Yen, P.Y., Koskinen, W.C., Steinhelmer, T.R. and Dowdy, R.H. (1994). Sorption of atrazine on soil clay components. *Environmental Science and Technology*, Vol. 28, pp. 1054–1061.
204. Latimer, J.S., Hoffman, E.J., Hoffman, G., Fasching, J.L. and Quinn, J.G. (2004). Sources of petroleum hydrocarbons in urban runoff. *Water, Air and Soil Pollution*, Vol. 52, pp. 1-21.
205. Lau, S. and Stenstrom, M.K. (2005). Metals and PAHs adsorbed to street particles. *Water Research*, Vol. 39 (No.17), pp. 4083-4092.
206. Lee, J.H., Bang, K.W., Ketchum, L.H., Choe, J.S. and Yu, M.J. (2002). First flush analysis of urban storm runoff. *The Science of the Total Environment*, Vol. 293, pp. 163-175.
207. Li, Y., Lau, S., Kayhanian, M. and Stenstrom, M.K. (2005). Particle size distribution in highway runoff. *J. Environmental Engineering*, Vol. 131 (No.9), pp. 1267-1276.
208. Li, Y., Lau, S., Kayhanian, M. and Stenstrom, M.K. (2006). Dynamic characteristics of particle size distribution in highway runoff: implications for settling tank design. *J. Environmental Engineering*, Vol. 132 (No.8), pp. 852-861
209. Li, Y., Xiang, L., Liu, J., Tian, P., Song, K., Shi, J. and Yang, Z. (2008). Characteristics of particles on urban impervious surfaces: heavy metals, TOC and specific surface area. In: *Proceedings of the 12th International Conference on Integrated Diffuse Pollution Management (IWA DIPCON 2008)*, Khon Kaen University, Thailand.

210. Librando, V., Magazzu, G. and Puglisi, A. (1995). Multivariate micropollutants analysis in marine waters. *Water Science Technology*, Vol. 32 (No.9-10), pp. 341-348.
211. Liebens, J. (2001). Heavy metal contamination of sediments in stormwater management systems: the effect of land use, particle size and age. *Environmental Geology*, Vol. 41, pp. 341-351.
212. Lin, C.F. and Benjamin, M.M. (1992). The effects of strongly complexing ligands on the adsorptive partitioning of metal ions. *Water Research*, Vol. 26, pp. 397-407.
213. Lin, J.G. and Chen, S.Y. (1998). The relationship between adsorption of heavy metal and organic matter in river sediments. *Environment International*, Vol. 24, pp. 345-352.
214. Lisiewicz, M.R., Heimbürger, R. and Golimowski, J. (2000). Granulometry and the content of toxic and potentially toxic elements in vacuum-cleaner collected, indoor dusts of the city of Warsaw. *The Science of the Total Environment*, Vol. 263, pp. 69-78.
215. Liu, A. and Gonzalez, R.D. (1999). Adsorption/Desorption in a system consisting of humic acid, heavy metals, and clay minerals. *Journal of Colloid and Interface Science*, Vol. 218, pp.225-232.
216. Liu, C.C., Wang, M., Chiou, C., Li, Y., Yang, C. and Lin, Y. (2009). Biosorption of chromium, copper and zinc by wine-processing waste sludge: Single and multi-component system study. *Journal of Hazardous Materials*, Vol. 171, pp. 386-392.
217. Mahbub, S.M.P., Goonetilleke, A. and Egodawatta, P. (2009). Experimental methodology for determining heavy metals and total petroleum hydrocarbons in pollutant build-up and wash-off due to urban traffic and climate change. *Proceedings of the Second Infrastructure Theme Postgraduate Conference*, Queensland University, Brisbane, Australia, pp. 355-63.
218. Malvern Instrument Ltd. (1997). *Sample Dispersion and Refractive Index Guide*, MAN 0079, U.K.
219. Markiewicz-Patkowska, J.A., Hursthouse, A. and Przybyla-Kij, H. (2005). The interaction of heavy metals with urban soils: sorption behaviour of Cd, Cu, Cr, Pb and Zn with a typical mixed brownfield deposit. *Environment International*, Vol. 31, pp. 513-521.

220. Martin, C., Ruperd, Y. and Legret, M. (2007). Urban stormwater drainage management: The development of a multicriteria decision aid approach for best management practices. *European Journal of Operational Research*, Vol. 181, pp. 338-349.
221. Massart, D.L., Vandeginste, B.G.M., Deming, S.M., Michotte, Y. and Kaufman, L. (1988). *Chemometrics—A Text Book*, Elsevier, Amsterdam.
222. Massart, D.L., Vandeginste, B.G.M., Buydens, L.M.C., De Jong, S., Lewi, P.J. and Smeyers-Verbeke, J. (1997). *Handbook of chemometrics and qualimetrics. Part A*. Elsevier, Amsterdam, Oxford.
223. McBride, M. (1989). Reactions controlling heavy metal solubility in soils. *Advances in Soil Sciences*, Vol.10, pp. 1–56.
224. McBride, M.B. (1994). *Environmental chemistry of soil*, Oxford University Press, New York.
225. McGrath, P.S. (1998). Assessment of the Bioavailability of metals in soils amended with sewage sludge using chemical speciation techniques and a LUX-based biosensor. *Environmental Toxicology and Chemistry*, Vol. 18 (No.4), pp. 659-663.
226. McGrath, S.P. and Smith, S. (1990). Chromium and nickel. Alloway, B.J. (Ed.), *Heavy Metals in Soils*. John Wiley & Sons, Inc, New York, pp. 125–150.
227. McKenzie, E.R., Money, J. E., Green, P.G. and Young, T.M. (2009). Metals associated with stormwater-relevant brake and tire samples. *Science of the Total Environment*, Vol. 407 (No.22), pp. 5855-5860.
228. Miguntanna, N.P. (2009a). Nutrients build-up and wash-off processes in urban land uses. PhD Thesis, Queensland University of Technology, Brisbane Australia.
229. Miguntanna, N.S. (2009b). Determination of set of surrogate parameters to evaluate urban stormwater quality. MSc Thesis, Queensland University of Technology, Brisbane Australia.
230. Mikutta, R., Kleber, M. and Jahn, R. (2005). Poorly crystalline minerals protect organic carbon in clay subfractions from acid subsoil horizons. *Geoderma*, Vol. 128, pp. 106-115.
231. Mikutta, R., Kleber, M., Kaiser, K. and Jahn, R. (2005). Review: removal of organic matter from soils using hydrogen peroxide, sodium hypochlorite and

- disodium peroxodisulfate. *Soil Science Society America Journal*, Vol. 69, pp.120-135.
232. Milani, M., Pucillo, F.P., Ballerini, M., Camatini, M., Gualtieri, M. and Martino, S. (2004). First evidence of tyre debris characterization at the nanoscale by focused ion beam. *Materials Characterization*, Vol. 52, pp. 283-288.
233. Milberg, R. P., Brower, D. L. and Lagerwerff, J. V. (1978). Exchange sorption of trace quantities of cadmium in soils treated with calcium and sodium: a reappraisal. *Soil Science Society America Journal, Colloid Surface Area*, Vol. 42, pp. 892-894.
234. Ming, D. W. and Dixon, J.B. (1987). Quantitative determination of clinoptilolite in soils by a cation-exchange capacity method. *Clays and Clay Minerals*, Vol. 35 (No.6), pp. 463-468.
235. Morera M.T., Echeverria J.C. and Garrido J.J. (2001). Mobility of heavy metals in soils amended with sewage sludge. *Canadian Journal of Soil Science*, Vol. 81, pp. 405-413.
236. Morras, H.J.M. (1995). Mineralogy and cation exchange capacity of the fine silt fraction in two soils from the southern Chaco Region (Argentina). *Geoderma*, Vol. 64, pp. 281-295.
237. Morrison, G.M., Revitt, D.M. and Ellis, B. (1988). Transport mechanisms and processes for metal species in a gullypot system. *Water Research*, Vol. 22 (No.11), pp. 1417-1427.
238. Mozgawa, W and Bajda, W. (2005). Spectroscopic study of heavy metals sorption on clinoptilolite. *Physics and Chemistry of Minerals* Vol. (31), pp. 706–713.
239. Mulla, D.J., Low, P.F. and Roth, C.B. (1985). Measurement of the Specific Surface Areas of Clays by Internal Reflectance Spectroscopy. *Clays and Clay Minerals*, Vol. 33 (No.5), pp. 391-396.
240. Murakami, M., Nakajima, F. and Furumai, H. (2008). The sorption of heavy metal species by sediments in soakaways receiving urban road runoff. *Chemosphere*, Vol. 70, pp. 2099-2109.
241. Muschack W. (1990). Pollution of street runoff by traffic and local conditions. *Science of the Total Environment*, Vol.93, pp. 419– 31.

242. Namdeo, A.K., Colls, J.J. and Baker, C.J. (1999). Dispersion and re-suspension of fine and coarse particulates in an urban street canyon. *The Science of the Total Environment*, Vol. 235 (No.1-3), pp. 3-13.
243. Neff, J.M. (1990). Composition and fate of petroleum and spill-treating agents in the marine environment. In: *Sea Mammals and Oil: Confronting the Risks*, J.R. Geraci and D.J. St.Aubin (Eds.), Academic Press, San Diego, CA, pp. 1-34.
244. Nesbitt, H.W. (1992). Diagenesis and metasomatism of weathering profiles, with emphasis on Precambrian paleosols. Martini, I.P. and Chesworth, W. (Eds.) *Weathering, Soils and Paleosols*. Elsevier, Amsterdam, New York.
245. Ni, Y., Liu, Y. and Kokot, S. (2010). Two-dimensional fingerprinting approach for comparison of complex substances analysed by HPLC-UV and fluorescence detection. *The Analyst*, Vol. 136 (3), pp. 550-559.
246. Noble, K.E. (1996). Resource Information. Noble K.E. (Eds.) *Understanding and managing soils in the Moreton region*. Department of Primary Industries Training Series QE96003, Brisbane.
247. Novotny, V. and Chesters, B. (1981). *Handbook on nonpoint pollution: Sources and management*. Van Nostrand and Reinhold Company, New York.
248. Novotny, V., Sung, H.M., Bannerman, R. and Baum, K. (1985). Estimating nonpoint pollution from small urban watersheds. *Journal - Water Pollution Control Federation*, Vol. 57, pp. 339-348.
249. NRC (National Research Council). (1983). *Polycyclic Aromatic Hydrocarbons: Evaluation of Sources and Effects*. National Research Council, National Academy Press, Washington, D.C.
250. Olphen, H.V. (1963). *Clay Colloid Chemistry: for Clay Technologists, Geologists, and Soil Scientists*, 2<sup>nd</sup> (Edn), Wile- Interscience publication, John Wiley and Sons, Inc, New York, United States of America.
251. Olson, K.W. and Skogerboe, R.K. (1975). Identification of soil lead compounds from automotive sources. *Environmental Science and Technology*, Vol. 9, pp. 227-230.
252. Ongley, E.D., Bynoe, M.C. and Percival, J.B. (1982). Physical and geochemical characteristics of suspended solids, Wilton Creek, Ontario. *Hydrobiologica*, Vol. 91, pp. 41-57.

253. Parks, S.J. and Baker, L.A. (1997). Sources and transport of organic carbon in an Arizona river-reservoir system. *Water Research*, Vol. 31, pp. 1751-1759.
254. Patra, A., Colvile R., Arnold, S., Bowen, E., Shallcross, D., Martin, D., Price, C., Tate, J., ApSimon, H. and Robins, A. (2008). On street observations of particulate matter movement and dispersion due to traffic on an urban road. *Atmospheric Environment*. Vol. 42, pp. 3911-3926.
255. Persaud, D., Jaagumagi, R. and Hayton, A. (1990). Guidelines for the protection and management of aquatic sediment quality in Ontario. Ontario Ministry of Environment and Energy, Toronto, Ont.
256. Petersen, W., Bertino, L., Callies, U. And Zorita, E. (2001). Process identification by principal component analysis of river water-quality data. *Ecological Modelling*, Vol. 138, pp. 193-213.
257. Pierson, W. R. and Brachaczek W. W. (1983). Particulate matter associated with vehicles on the road, II. *Aerosol Science and Technology*, Vol.4, pp.1-40.
258. Pinheiro, J.P., Mota, A.M. and Benedetti, M.F. (1999). Lead and calcium binding to fulvic acids: Salt effect and competition. *J. Environ. Sci. Technol.*, Vol. 33, pp. 3398-3440.
259. Pitcher, S.K., Slade, R.C.T. and Ward, N.I. (2004). Heavy metal removal from motorway stormwater using zeolites. *Science of the Total Environment*. 334-335, pp. 161-166.
260. Pitt, R. (1979). Demonstration of nonpoint pollution abatement through improved street cleaning practices. U.S. Environmental Protection Agency, Report No. EPA/600/2-79-161.
261. Pitt, R., Bannerman, R., Clark, S. and Williamson, D. (2004). Sources of Pollutants in Urban Areas (Part 2) – Recent Sheetflow Monitoring. James, W., Irvine, K.N., McBean, E.A. and Pitt, R.E. (Eds.) *Effective Modeling of Urban Water Systems*. Monograph 13, pp. 485-506.
262. Pitt, R., Field, R., Lalor, M. and Brown, M. (1995). Urban stormwater toxic pollutants: assessment, sources and treatability. *Water Environment Research*, Vol. 67 (No.3), pp. 260-275
263. Plassard, F.T., Winiarski, T. and Petit-Ramel, M. (2000). Retention and distribution of three heavy metals in a carbonated soil: comparison between batch and unsaturated column studies. *Journal of Contaminant Hydrology*, Vol. 42 (No.2-4), pp. 99-111.



264. Polcaro, A. M., Mascia, M., Palmas, S., Vacca, A. and Tola, G. (2003). Competitive sorption of heavy metal ions by soils. *Environmental Engineering Science*, Vol. 20 (No.6), pp. 607-616.
265. Post, J. and Buseck, P.R. (1985). Quantitative energy dispersive analysis of lead halide particles from the Phoenix urban aerosol. *Environment Science and Technol.* Vol. 19 (No.8), pp. 682-685.
266. Prakash, A. (2005). Impact of urbanization in watersheds on stream stability and flooding. *Proceedings of Watershed Management Conference*, Williamsburg, Virginia.
267. Purcell, D.E., Leonard, G.J., O'Shea, M.G. and Kokot, S. (2005). A chemometrics investigation of sugarcane plant properties based on the molecular composition of epicuticular wax. *Chemometrics and Intelligent Laboratory Systems*, Vol. 76, pp. 135-147.
268. Purcell, D.E., O'Shea, M.G. and Kokot, S. (2007). Role of chemometrics for at-field application of NIR spectroscopy to predict sugarcane clonal performance. *Chemometrics and Intelligent Laboratory Systems*, Vol. 85 (No.1), pp. 113-124.
269. Qu, W. and Kelderman, P. (2001). Heavy metal contents in the Delft canal sediments and suspended solids of the river Rhine: Multivariate analysis for source tracing. *Chemosphere*, Vol. 45, pp. 919-925.
270. Quirk, J.P. and Murray, R.S. (1999). Appraisal of the Ethylene Glycol Monoethyl Ether Method for Measuring Hydratable Surface Area of Clays and Soils. *Soil Science Society of America Journal*, Vol. 63, pp. 839-849.
271. Rabb, S. A. and Olesik, J. W. (2008). Assessment of high precision, high accuracy Inductively Coupled Plasma-Optical Emission Spectroscopy to obtain concentration uncertainties less than 0.2% with variable matrix concentrations. *Spectrochimica Acta Part B: Atomic Spectroscopy*, Vol. 63, pp. 244-256.
272. Ratuszny, T., Gong, Z. and Wilke, B.M. (2009). Total concentrations and speciation of heavy metals in soils of the Shenyang Zhangshi Irrigation Area, China. *Environ. Monit. Assess.*, Vol. 156, pp. 171-180.
273. Rayment, G.E. and Higginson, F.R. (1992). *Australian Laboratory Handbook of Soil and Water Chemical Methods*. Melbourne, Australia: Inkata Press.
274. Reddy, M.R. and Perkins, H.F. (1976). Fixation of manganese by clay minerals. *Soil Science* Vol. 121, pp. 21-24.

275. Rengasamy, P. and Churchman, G.J. (1999). Cation exchange capacity, exchangeable cations and sodicity. Peverill, K.I., Sparrow, L.A., Reuter, D.J. (Eds.) *Soil Analysis: an Interpretation Manual*. CSIRO publication, Australia, pp.149-158.
276. Robertson, D.J., Taylor, K. G. and Hoon, S.R. (2003). Geochemical and mineral magnetic characterisation of urban sediment particulates, Manchester, UK. *Applied Geochemistry*, Vol. 18, pp. 269-282.
277. Roger, S., Montrejaud-Vignoles, M., Andral, M.C., Herremans, L. and Fortune, J.P. (1998). Mineral, physical and chemical analysis of the solid matter carried by motorway runoff water. *Water Research*, Vol. 32, pp. 1119-1125.
278. Rogge, W.F., Hildemann, L.M., Mazurek, M.A. and Cass, G.R. (1993). Sources of Fine organic aerosol. 3. Road dust, tire debris, and organometallic brake lining dust: Roads as sources and sinks. *Environmental Science and Technology*, Vol. 27, pp. 1982-1994.
279. Ross, S.M. (1993). Organic matter in tropical soils: current conditions, concerns and prospects for conservation. *Progress in Physical Geography*, Vol. 17, pp. 265-305.
280. Rowley, A.G., Husband, F.M. and Cunningham, A.B. (1984). Mechanisms of metal adsorption from aqueous solutions by waste tyre rubber. *Water Research*, Vol. 18, pp. 981-984.
281. Ruellan, A. and Delétang, J. (1967). Les phénomènes d'échange de cations et d'anions dans les sols. In: *Initiations Documentations Techniques*, ORSTOM, Paris.
282. Rybicka, E.H., Calmano, W. and Breeger, A. (1995). Heavy metals sorption/desorption on competing clay minerals; an experimental study. *Applied Clay Science*, Vol. 9 (No.5), pp. 369-381.
283. Sabina, L.D., Lim, J.H., Venezia, M.T., Winer, A.M, Schiff, K.C. and Stolzenbach, K.D. (2006). Dry deposition and resuspension of particle-associated metals near a freeway in Los Angeles. *Atmospheric Environment*, Vol. 40, pp.7528–7538.
284. Sakurai, K., Teshima, A. and Kyuma, K. (1990). Changes in zero point of charge (ZPC), specific surface area (SSA), and cation exchange capacity (CEC) of kaolinite and montmorillonite, and strongly weathered soils caused by Fe and Al coatings. *Soil Science Plant Nutrient*, Vol. 36 (No.1), pp. 73–81.

285. Salminen, P., Hokkanen, J. and Lahdelma, R. (1998). Comparing multicriteria methods in the context of environmental problems. *European Journal of Operational Research*, Vol. 104, pp. 485-496.
286. Sanchez, A.G., Ayuso, E.A. and Blas, O.J.D. (1999). Sorption of heavy metals from industrial waste water by low-cost mineral silicates. *Clay Minerals*, Vol. 34 (No.3), pp. 469-469.
287. Sanders, P.G., Xu, N., Dalka, T.M. and Maricq, M.M. (2003). Airborne brake wear debris: size distributions, composition, and a comparison of dynamometer and vehicle tests, *Environmental Science and Technology*, Vol. 37 (No.18), pp. 4060–4069.
288. Sansalone, J.J., Buchberger, S.G. and Al-Abed, S.R. (1996). Fractionation of heavy metals in pavement runoff. *Science of the Total Environment*, Vol. 189/190, pp. 371-378.
289. Sansalone, J.J., Buchberger, S.G., Koran, J.M. and Smithson, J.A. (1997). Relationship between particle size distribution and specific surface area of urban roadway stormwater solids transportation research record: *Journal of the Transportation Research Board*. Report No.1601, pp. 95-108.
290. Sansalone, J.J., Koran, J.M., Smithson, J.A. and Buchberger, S.G. (1998). Physical Characteristics of Urban Roadway Solids Transported during Rain Events. *Journal of Environmental Engineering*, Vol. 124, pp. 427-440.
291. Sansalone, J.J. and Buchberger, S.G. (1997). Partitioning and first flush of metals in urban roadway storm water. *Journal of Environmental Engineering ASCE*, Vol. 123 (No.2), pp. 132-43.
292. Sansalone J. and Kim J.Y. (2008). Transport of Particulate Matter Fractions in Urban Source Area Pavement Surface Runoff. *Journal of Environmental Quality*, Vol. 37 (No.5), 1883-1893.
293. Sansalone, J.J. and Kim, J. (2008). Suspended particle destabilization in retained urban stormwater as a function of coagulant dosage and redox conditions. *Water Research*, Vol. 42 (No.4-5), pp. 909-922.
294. Santamarina, J.C. and Klein, K.A. (2002). Specific surface: Determination and relevance. *Canadian Geotechnical Journal*, Vol. 39 (No.1), pp. 233-241.
295. Santamarina, J.C., Klein, K.A., Wang, Y.H. and Prencke, E. (2002). Specific Surface: determination and relevance. *Canadian Geotechnical Journal*, Vol. 39, pp. 233-241.

296. Sartor, J.D. and Boyd, B.G. (1972). Water pollution aspects of street surface contaminants. U.S. Environmental Protection Agency, Washington, DC, USA, Report No. EPA- R2-72/081.
297. Sartor, J.D., Boyd, B.G. and Agardy, F.J. (1974). Water pollution aspects of street surface contaminants. U.S. Environmental Protection Agency, Washington, DC, USA, Report No.EPA- R2-72/081.
298. Sawyer, C.N., McCarty, P.L. and Parkin, G.F. (1994). Chemistry for Environmental Engineering, 4<sup>th</sup> (Edn), McGraw-Hill, New York.
299. Schnitzer, M. and Khan, S.U. (1989). Soil Organic Matter. Elsevier Scientific, New York.
300. Schoonover, J.E., Lockaby, B.G. and Helms, B. S. (2006). Impacts of land cover on stream hydrology in the West Georgia Piedmont, USA. *Journal of Environmental Quality*, Vol. 35, pp. 2123-2131.
301. Settacharnwit, S., Buckney, R.T. and Lim, R.P. (2003). The nutrient status of Nong Han, a shallow tropical lake in north-eastern Thailand: spatial and temporal variations. *Lakes and Reservoirs: Research and Management*, Vol. 8, pp. 189–200.
302. Settle, S., Goonetilleke, A. and Ayoko, G.A. (2007). Determination of surrogate indicators for phosphorus and solids in urban stormwater: Application of multivariate data analysis techniques. *Water, Air and Soil Pollution*, Vol. 182 (No.1-4), pp. 149-161.
303. Shaheen, D.O. (1975). Contributions of urban roadway usage to water pollution. Municipal Pollution Control Division, Office of Research and Development, U.S. Environmental Protection Agency, Washington, DC, USA, Report No. EPA-600/ 2-75/004.
304. Shaw D.J. (1992). *Colloid and Surface Chemistry*, 4<sup>th</sup> (Edn), Butterworth-Heinemann, Boston.
305. Shilton, V.F., Booth, C.A., Smith, J.P., Giess, P., Mitchell, D.J. and Williams, C. D. (2005). Magnetic properties of urban street dust and their relationship with organic matter content in the West Midlands, UK. *Atmospheric Environment*, Vol. 39, pp. 3651-3659.
306. Sillen, L.G. (1971). *Stability Constant of Metal-Ion Complexes Supplement No.1, Special Publication No.25*. The Chemical Society, London.

307. Smolders, E. and Degryse, F. (2002). Fate and effect of zinc from tire debris in soil. *Environmental Science and Technology*, Vol. 36 (No.17), pp. 3706–3710.
308. Sorption of pentachlorophenol on surficial sediments: The roles of metal oxides and organic materials with co-existed copper present
309. Spadini, L., Manceau, A., Schindler, P.W. and Charlet, L. (1994). Structure and stability of  $\text{Cd}^{2+}$  surface complexes on ferric oxides, Results from EXAFS spectroscopy. *Journal of Colloid and Interface Science*, Vol. 168, pp.73-86.
310. Sparks, D.L. (1996). *Methods of Soil Analysis. Part 3, Chemical Methods*. American Society of Agronomy, Madison, Wisconsin.
311. Sparks, D.L. (2003). *Environmental Soil Chemistry*, 2<sup>nd</sup> (Edn), Academic Press, San Diego.
312. Spassov S., Egli R., Heller F., Nourgaliev D.K. and Hannam J. (2004). Magnetic quantification of urban pollution sources in atmospheric particulate matter. *Geophys. J. Int.*, Vol. 159, pp.555–564.
313. Sposito, G. (1984). *The Surface Chemistry of Soils*. Oxford Univ. Press, New York.
314. Sposito, G., (2000). Ion exchange phenomena. Sumner, M.E. (Eds.) *Handbook of Soil Science*. CRC Press, Boca Raton, FL, pp. B-241–B-264.
315. Stanford, M. K. and Jain, V. K. (2001). Friction and wear characteristics of hard coatings. *Wear*, Vol. 250 (No.1-12), pp. 990-996.
316. Stevenson, F.J. (1965). Amino acid. In: Black C.A. et al. (Eds.), *Methods of Soil Analysis, Part 2: Chemical and Microbial Properties*. American Society of Agronomy, Madison, USA, pp. 1409-1421.
317. Stevenson, F.J. (1976). Stability constanta of  $\text{Cu}^{2+}$ ,  $\text{Pb}^{2+}$  and  $\text{Cd}^{2+}$  complexes with humic acids. *Soil Science Society of American Journal*, Vol. 40, pp. 665-672.
318. Stone, R.B., Coston, L.C., Hoss, D.E. and Cross, F.A. (1975). Experiments on some possible effects of tire reefs on pinfish (*Lagodon rhomboides*) and black sea bass (*Centropristis striata*), *Marine Fisheries Review*, Vol. 37, pp. 18–20.
319. Strawn, D. G., Scheidegger, A.M. and Sparks, D.L. (1998). Kinetics and mechanisms of Pb(II) sorption and desorption at the aluminum oxide–water interface. *Environmental Science and Technology*, Vol. 32, pp 2596–2601.

320. Stumm, W. (1992). Chemistry of the solid-water interface: processes at the mineral-water and particle-water interface in natural systems. Wiley-Interscience.
321. Sutherland, R.A., Tack, F.M.G., Ziegler, A.D. and Bussen, J.O. (2004). Metal extraction from road-deposited sediments using nine partial decomposition procedures. *Applied Geochemistry*, Vol. 19, pp. 947-955.
322. Tai, Y.L. (1991). Physical and chemical characterisation of street dust and dirt from urban areas, MSc Thesis, Pennsylvania State University.
323. Taylor, R. M., McKenzie, R. M., Fordham, A. W. and Gillman, G. P. (1983). Oxide minerals. In *Soils: An Australian Viewpoint*. Division of Soils, CSIRO. CSIRO: Melbourne/ Academic Press: London, pp. 309-334.
324. Ter Haar, G.L. and Bayard, M.A. (1971), Composition of airborne lead particles. *Nature (London)*, Vol. 232, pp. 553-554.
325. Tessier, A, Campbell, P. G. C. and Blsson, M. (1979). Sequential extraction procedure for the speciation of particulate trace metals, *Analytical Chemistry*, Vol. 51 (No.7), pp. 844–851.
326. Tiller, K. G. and Hodgson, J. F. (1962). The specific sorption of Co (II) and Zn (II) by layer silicates. *Clays Clay Mineral*, Vol. 9, pp. 393-403.
327. Tiller, K. G. and Smith, L. H. (1990). Limitations of EGME retention to estimate the surface area of soils. *Australian Journal of Soil Research*, Vol. 26, pp. 1-26.
328. Tipping, E. (1986). Some aspects of the interactions between particulate oxides and aquatic humic substances. *Marine Chemistry*, Vol. 18, pp. 161-169.
329. TriStar 3000, Operator's Manual. (2001). Micromeritics Instrument Corporation, Norcross, USA.
330. Tucker, B. M. (1983). Basic exchangeable cations. In *Soils: an Australian Viewpoint*. Division of Soils, CSIRO. CSIRO: Melbourne/Academic Press: London, pp. 401-16.
331. Tuul, J. and Innes, W.B. (1962). Inorganic oxide air adsorption at room temperature and correlation with surface area. *Analytical Chemistry*, Vol. 36 (No.7), pp. 818–820.
332. Tyler, B.J., Rayala, G. and Castner, D.G. (2007). Multivariate analysis strategies for processing ToF-SIMS images of biomaterials. *Biomaterials*, Vol. 28, pp. 2412–2423.

333. US EPA. (1993). Natural wetlands and urban stormwater: Potential impacts and management. U.S. Environmental Protection Agency.
334. US EPA. (1994). Method 200.7, Trace elements in waters and wastes by inductively coupled plasma- mass spectrometry. Creed, J.T., Brockhoff, C.A. and Martin, T.D., Revision 5.4. U.S. Environmental Protection Agency, Ohio.
335. US EPA. (1994). Method 200.8: Trace elements in waters and wastes by inductively coupled plasma- mass spectrometry. U.S. Environmental Protection Agency, Ohio.
336. US EPA, (1999). Particles contributing to turbidity. Guidance Manual Turbidity Provisions. U.S. Environmental Protection Agency, Ohio.
337. US EPA. (2005). National management measures to control nonpoint source pollution from urban areas. U.S. Environmental Protection Agency, Report No. EPA /841/B-05/004.
338. Van Meter, P.C., Mahler, B.J. and Furlong, E.T. (2000). Urban Sprawl Leaves its PAH signature. *Environmental Science and Technology*, Vol. 34 (No.19), pp. 4064-4070.
339. Vaze, J., Chiew, F.H.S., Suryadi, L. and Khanal, K. (2000). Pollutant accumulation on an urban road surface. *Urban Water*, Vol.4, pp. 265- 270.
340. Vaze, J. and Chiew, F.H.S. (2002). Experimental study of pollutant accumulation on an urban road surface. *Urban Water*, Vol. 4, pp. 379-389.
341. Vaze, J. and Chiew, F.H.S. (2004). Nutrient loads associated with different sediment sizes in urban stormwater and surface pollutants. *Journal of Environmental Engineering*, Vol. 130, (No.4), pp.391-396.
342. Vdovic, N., Biscan, J. and Juracic, M. (1991). Relationship between specific surface area and some chemical and physical properties of particulates: study in the northern Adriatic. *Marine Chemistry*, Vol. 36, pp. 317-328.
343. Veeresh, H., Tripathy, S., Chaudhuri, D., Hart, B. R. and Powell, M. A. (2003). Competitive adsorption behavior of selected heavy metals in three soil types of India amended with fly ash and sewage sludge. *Environmental Geology*, Vol. 44, pp. 363-370.
344. Vega, M., Pardo, R. Barrado, E. and Deban, L. (1998). Assessment of seasonal and polluting effects on the quality of river water by exploratory data analysis. *Water Research*, Vol. 32, pp. 3581-3592.

345. Vignoles M. and Herremens L. (1995). Metal contamination in motorway surface runoff water. Proceedings of the Water Environment Federation 68th Annual Conference and Exposition (WEFTEC95), Miami, Volume IV. pp. 85–93.
346. Viklander, M. (1998). Particle size distribution and metal content in street sediments. *Journal of Environmental Engineering*, Vol. 124 (No.8), pp. 761-66.
347. Visual Decision Inc. (2000). *Decision Lab 2000 – Getting Started Guide*, Montreal, Canada.
348. Walker, T.A. and Wong, T. H. F. (1999). Effectiveness of street sweeping for stormwater pollution control, Technical report, Report 99/8, Cooperative Research Centre for Catchment Hydrology.
349. Walker, W.J., McNutt, R.P. and Maslanka, C.K. (1999). The potential contribution of urban runoff to surface sediments of the Passaic River: Sources and chemical characteristics. *Chemosphere*, Vol. 38 (No.2), pp. 363-377.
350. Wang, J., Huang, C. P., Allen, H. E., Cha, D. K. and Kim, D. (1998). Adsorption characteristics of dye onto sludge particulates. *Colloid and Interface Science*, Vol. 208, pp. 518–528.
351. Wang, X., Li, Y. and Dong, D. (2008). Sorption of pentachlorophenol on surficial sediments: The roles of metal oxides and organic materials with co-existed copper present. *Chemosphere*, Vol. 73 (No.1), pp.1-6.
352. Wanielista M. and Yousel Y. (1993) *Stormwater Management*. John Wiley and Sons, Inc., New York, NY, USA, pp. 579.
353. Warren, L.A. and Zimmermann, A.R. (1994). Suspended particulate grain size dynamics and their implications for trace metal sorption in the Don River. *Aquatic Sciences*, Vol. 56.
354. Warren, N., Allan, I. J., Carter, J. E., House, W. A. and Parker, A. (2003). Pesticides and other micro-organic contaminants in freshwater sedimentary environments- A review. *Applied Geochemistry*, Vol. 18 (No.2), pp. 159-194.
355. Weber, W.J. and Smith, E.H. (1988). Simulation and design models for adsorption processes. *Environmental Science and Technology*, Vol. 21, pp. 1040–1050.
356. Weber, W.J., McGinley, P.M. and Katz, L.E. (1991). Sorption phenomena in subsurface systems: Concepts, models and effects on contaminant fate and transport. *Water Research* Vol. 25 (No.5), pp. 499-528.



357. Weber, W.J., McGinley, P.M. and Katz, L.E., (1992). A distributed reactivity model for sorption by soils and sediments. 1. Conceptual basis and equilibrium assessments. *Environmental Science and Technology*, Vol. 26, pp. 1955-1962.
358. Weltens, R., Goossens, R. and Puymbroeck, S.V. (2000). Ecotoxicity of contaminated suspended solids for filter feeders. *Archives of Environmental Contamination and Technology*, Vol. 39, pp. 315-23.
359. Westerlund, K.G. (2001). Metal emissions from Stockholm traffic - wear of brake linings, The Stockholm Environment and Health Protection Administration, Stockholm, Sweden.
360. White, R.E. (2006). *Principles and Practice of Soil Science*. 4<sup>th</sup> Revised Edition. Blackwell Publication, Malden, USA.
361. Wik, A. and Dave, G. (2009). Occurrence and effects of tire wear particles in the environment - A critical review and an initial risk assessment. *Environmental Pollution*, Vol. 157 (No.1), pp. 1-11.
362. Wik, A., Nilsson, E., Källqvist, T., Tobiesen, A. and Dave, G. (2009). Toxicity assessment of sequential leachates of tire powder using a battery of toxicity tests and toxicity identification evaluations. *Chemosphere*, Vol. 77, pp. 922-927.
363. Wu, M.L. and Wang, Y.S. (2007). Using chemometrics to evaluate anthropogenic effects in Daya Bay, China. *Estuarine, Coastal and Shelf Science*. Vol. 72, pp. 732-742.
364. Wulfsberg, G. (1991). *Principles of Descriptive Organic Chemistry*. University Science Books, Sausalito, CA.
365. Xie, S. Dearing, J.A., Bloemendal, J. And Boyle, J.F. (1999). Association between the organic matter content and magnetic properties in street dust, Liverpool, UK. *Science of the Total Environment* Vol. 241, pp. 205-214.
366. Xie, S., Dearing, J.A. and Bloemendal, J. (2000). The organic matter content of street dust in Liverpool, UK, and its association with dust magnetic properties. *Atmospheric Environment*, Vol. 34 (No.2), pp. 269-275.
367. Yamada, K., Umehara, T. and Ichiki, A. (1993). Study on statistical characteristics of nonpoint pollutants deposited in urban areas. *Water Science and Technology*, Vol. 28 (No.3-5), pp. 283-290.
368. Yang, Y. and Baumann, W. (1995). Seasonal and areal variations of polycyclic aromatic hydrocarbon concentrations in street dust determined by supercritical

- fluid extraction and gas chromatography-mass spectrometry. *Analyst*, Vol. 1220, pp. 243-248.
369. Yaziz M I, Gunting H, Sapari N and Ghazali, A.W. (1989). Variations in rainwater quality from roof catchments. *Journal of Water Research*, Vol. 23 (No.6), pp. 761-765.
370. Yong, R.N., Mohamed, A.M.O. and Warkentin, B.P. (1992). *Principles of Contaminant Transport in Soils*. Elsevier, New York.
371. Young, T. C., DePinto, J.V. and Kipp, T.W. (1987). Adsorption and desorption of Zn, Cu, and Cr by sediments from the Raisin River (Michigan). *Journal of Great Lakes Research*, Vol. 13 (No.3), pp. 1353-1366.
372. Yukselen, Y. and Kaya, A. (2006). Comparison of methods for determining specific surface area of soils. *Journal of Geotechnical and Geoenvironmental Engineering*, Vol. 132 (No.7), pp. 931-936.
373. Zerwer, A. and Santamarina, J.C. (1994). Double layer in pyrometa-morphosed bentonite: index properties and complex permittivity. *Applied Clay Science*, Vol. 9, pp. 283-291.
374. Zhao, H., Li, X., Wang, X. and Tian, D. (2010). Grain size distribution of road-deposited sediment and its contribution to heavy metal pollution in urban runoff in Beijing, China. *J Hazard Mater*, Vol. 183, pp. 203-210.
375. Zhuang, J. and Yu, G. (2002). Effects of surface coatings on electrochemical properties and contaminant sorption of clay minerals. *Chemosphere*, Vol. 49 (No.6), pp. 619-628.
376. Zoppou, C., (2001). Review of urban stormwater models. *Environmental Modelling and Software*, Vol.16 (No.3), pp. 195-231.

# **APPENDIX A**

## **Analysis of physical and chemical parameters of solids**



**Table A.1: Physical and chemical properties of build-up pollutants****Particle size range 300-425µm**

Identification	TOC (mg/g)	EGME SSA (m <sup>2</sup> /g)	BET SSA (m <sup>2</sup> /g)	Amorphous (%)	Quartz (%)	Albite (%)	Microcline (%)	Chlorite (%)	Muscovite (%)
C 11-i	0.53	2.05	0.90	4.30	78.6	7.10	2.8	0.7	1.5
C 12-i	0.35	5.16	0.44	9.30	68.9	10.2	3.4	1.7	3.1
C 13-i	0.13	0.70	0.93	3.20	84.4	6.20	1.9	0.9	1.4
C 14-i	0.23	2.77	0.57	24.3	64.2	5.18	2.9	1.6	1.8
C 21-i	1.27	2.26	0.37	21.5	61.8	6.70	4.3	1.8	3.9
C 22-i	0.86	5.61	0.78	11.9	69.1	8.60	5.6	2.1	2.6
C 23-i	0.36	3.50	0.75	15.3	71.2	4.30	3.6	1.4	4.1
C 24-i	0.36	3.66	0.50	18.2	66.3	7.70	4.4	2.6	0.9
N 11-i	0.05	5.35	0.51	18.4	50.3	15.8	8.0	3.5	4.1
N 12-i	0.10	0.98	0.39	18.6	68.9	7.00	1.7	1.9	1.9
N 13-i	0.27	1.43	0.58	13.4	78.6	4.90	0.6	1.6	0.8
N 14-i	0.01	0.27	0.85	12.4	73.5	8.40	1.4	2.4	1.9
N 21-i	0.14	3.16	0.63	41.7	49.9	5.00	0.9	1.1	1.5
N 22-i	0.38	1.38	0.26	35.2	48.0	9.30	2.7	2.8	2.0
N 23-i	0.09	4.04	0.11	14.6	75.2	6.10	1.1	1.9	1.2
N 24-i	0.07	1.84	0.44	15.2	73.0	6.30	2.3	1.6	1.6
B 11-i	0.42	1.87	0.19	17.0	61.3	7.60	4.4	6.0	3.7
B 12-i	0.26	3.46	0.37	14.2	76.6	4.80	1.1	1.9	1.5
B 13-i	0.82	2.88	0.44	5.2	78.9	6.80	3.6	3.2	2.4
B 14-i	0.29	3.95	0.39	22.8	68.3	4.70	1.0	1.7	1.4
B 21-i	0.51	4.30	0.22	31.6	56.5	5.22	1.4	4.3	1.0
B 22-i	1.62	0.75	0.24	24.4	59.3	6.20	4.2	1.8	4.1
B 23-i	0.54	4.66	0.22	23.8	64.2	6.07	2.3	1.8	1.9
B 24-i	1.19	3.80	0.24	29.6	55.5	6.20	3.3	1.7	3.6
S 11-i	0.40	3.50	0.16	17.4	70.7	5.90	1.9	2.2	2
S 12-i	0.28	1.27	0.26	21.4	66.0	6.80	2.6	1.8	1.4
S 13-i	0.06	1.91	0.26	32.3	60.9	3.60	0.7	1.4	1.0
S 14-i	0.52	2.04	0.17	15.7	78.4	2.10	2.2	1.5	0.1
S 21-i	1.96	3.30	0.16	31.0	55.3	4.80	3.9	1.5	3.5
S 22-i	0.07	4.81	0.20	25.2	61.3	5.50	3.8	1.5	2.7
S 23-i	0.03	2.62	0.22	11.1	79.0	5.00	0.9	2.1	1.8
S 24-i	0.02	2.13	0.21	10.2	85.3	2.90	0.0	1.6	0.0

Notes:

1. C – Clearview Estate, N- Nerang, B- Benowa and S- Surfers Paradise
2. 1 and 2 - sampling event
3. i, ii, iii and iv - particle size ranges 300-425µm, 150-300µm, 75-150µm and <75µm

**Table A.1: Physical and chemical properties of build-up pollutants (continued from previous page)**

**Particle size range 300-425µm**

Identification	TSS (mg/g)	pH	EC (µS/cm)	Ca (meq (+)/100 g)	Al (meq (+)/100 g)	Mg (meq (+)/100 g)	Na (meq (+)/100 g)	K (meq (+)/100 g)	EC/EC (meq (+)/100 g)
C 11-i	15.33	7.8	26.2	2.29	0.01	0.18	0.22	0.01	2.70
C 12-i	17.96	6.8	164.8	2.90	0.01	0.48	0.57	0.12	4.09
C 13-i	108.2	7.1	90.2	5.52	0.09	0.48	0.10	0.13	6.31
C 14-i	55.56	7.2	64.9	2.58	0.06	0.17	0.16	0.00	2.97
C 21-i	54.14	8.7	73.6	8.10	0.63	4.12	4.01	7.46	24.3
C 22-i	45.14	8.6	49.6	0.17	0.01	0.01	0.33	0.04	0.56
C 23-i	251.6	8.4	38.0	3.57	0.40	0.65	0.34	0.02	4.98
C 24-i	65.88	8.1	53.5	3.56	0.40	0.64	0.35	0.02	4.98
N 11-i	25.09	6.4	171	7.97	0.01	0.11	0.05	0.07	8.21
N 12-i	126.9	5.7	105.1	4.80	0.00	0.31	0.28	0.13	5.53
N 13-i	165.9	6.1	39.9	2.11	0.00	0.12	0.99	0.03	3.25
N 14-i	42.48	6.1	46.8	0.02	0.00	0.00	1.87	0.09	1.98
N 21-i	198.4	7.0	97.5	4.57	0.01	0.18	0.22	0.13	5.09
N 22-i	18.52	7.8	50.4	7.55	0.01	0.18	0.36	0.11	8.21
N 23-i	26.43	7.2	58.7	8.38	0.00	0.23	0.35	0.09	9.05
N 24-i	137.6	6.9	100	2.36	0.00	0.13	0.21	0.08	2.78
B 11-i	42.63	6.4	73.9	2.58	0.01	0.00	0.35	0.02	2.97
B 12-i	66.72	6.4	62.7	0.45	0.01	0.00	0.36	0.03	0.86
B 13-i	66.16	6.4	38.6	0.36	0.01	0.00	0.36	0.04	0.77
B 14-i	78.98	7.4	49.1	1.49	0.01	0.00	0.36	0.03	1.89
B 21-i	58.85	7.6	109	4.87	0.01	0.38	1.31	0.13	6.70
B 22-i	203.8	7.3	72.6	1.37	0.01	0.13	1.56	0.08	3.14
B 23-i	53.34	7.0	73.1	3.21	0.01	0.36	0.99	0.10	4.66
B 24-i	47.12	6.2	120	2.37	0.01	0.35	0.56	0.19	3.48
S 11-i	419.0	8.8	97.7	4.45	0.00	1.02	0.07	0.15	5.70
S 12-i	11.51	8.6	46.4	4.14	0.01	0.15	0.22	0.06	4.58
S 13-i	356.2	8.3	46.6	3.10	0.01	0.17	0.31	0.01	3.60
S 14-i	331.5	7.5	123	9.53	0.00	0.59	0.19	0.11	10.4
S 21-i	42.16	8.7	54.0	1.74	0.03	0.32	0.06	0.04	2.18
S 22-i	21.58	8.3	78.7	0.01	0.00	0.01	1.92	0.07	2.01
S 23-i	332.7	7.9	74.1	0.01	0.00	0.01	1.93	0.11	2.05
S 24-i	330.7	7.4	183	4.04	0.39	0.70	0.04	0.05	5.23

Notes:

1. C – Clearview Estate, N- Nerang, B- Benowa and S- Surfers Paradise
2. 1 and 2 - sampling event
3. i, ii, iii and iv - particle size ranges 300-425µm, 150-300µm, 75-150µm and <75µm

**Table A.1: Physical and chemical properties of build-up pollutants (continued from previous page)**

**Particle size range 150-300µm**

Identification	TOC (mg/g)	EGME SSA (m <sup>2</sup> /g)	BET SSA (m <sup>2</sup> /g)	Amorphous (%)	Quartz (%)	Albite (%)	Microcline (%)	Chlorite (%)	Muscovite (%)
C 11-ii	0.52	3.00	1.47	26.5	46.5	12.7	3.2	1.9	3.0
C 12-ii	0.54	6.34	0.38	13.4	65.6	10.3	3.8	1.1	2.4
C 13-ii	0.32	6.24	1.02	4.00	78.5	7.50	4.5	1.8	3.7
C 14-ii	0.52	0.80	0.49	35.3	53.2	6.90	2.2	1.5	0.9
C 21-ii	1.42	6.94	0.44	17.7	65.0	7.30	4.0	2.2	3.7
C 22-ii	0.86	3.19	0.56	20.2	62.2	7.40	5.3	2.0	2.9
C 23-ii	0.79	3.78	0.65	14.8	73.9	5.20	2.3	2	1.7
C 24-ii	0.80	3.49	0.43	15.6	67.5	8.10	4.4	2.2	2.3
N 11-ii	0.09	4.74	0.47	13.2	74.3	6.80	1.8	2.5	1.4
N 12-ii	0.10	5.13	0.36	13.2	72.4	7.70	2.9	2.0	1.8
N 13-ii	0.31	6.85	0.39	9.40	79.3	6.10	2.1	1.7	1.4
N 14-ii	0.05	3.85	0.70	16.1	65.3	10.1	3.7	2.1	2.7
N 21-ii	0.24	2.57	0.52	20.3	67.3	6.80	2.7	1.8	1.1
N 22-ii	0.29	5.82	0.26	18.6	60.5	11.3	2.8	3.5	3.3
N 23-ii	0.13	9.15	0.12	24.3	65.8	5.80	1.2	1.7	1.2
N 24-ii	0.10	3.72	0.45	7.10	80.2	7.20	2.3	1.9	1.3
B 11-ii	0.80	2.25	0.18	31.7	51.7	5.90	3.2	4.0	3.5
B 12-ii	0.46	2.08	0.30	11.3	77.9	4.90	2.7	1.7	1.5
B 13-ii	0.47	1.38	0.38	11.9	73.2	5.80	3.5	3.1	2.5
B 14-ii	0.35	4.27	0.70	22.2	66.2	5.30	2.0	1.7	2.5
B 21-ii	0.34	2.31	0.21	21.0	66.2	4.38	2.1	3.1	3.2
B 22-ii	1.35	8.34	0.32	21.7	65.0	5.87	2.0	2.8	2.6
B 23-ii	0.84	2.76	0.23	36.2	51.6	6.28	2.0	1.3	2.6
B 24-ii	1.51	4.75	0.18	21.6	66.8	5.40	1.9	1.6	2.6
S 11-ii	1.44	13.0	0.18	18.3	69.2	5.50	1.9	1.9	3.1
S 12-ii	0.68	1.73	0.24	26.9	64.3	4.80	1.7	1.5	0.7
S 13-ii	0.19	7.99	0.25	20.8	70.1	4.50	1.3	1.6	1.7
S 14-ii	0.88	1.76	0.18	10.4	83.5	2.20	2.1	1.5	0.2
S 21-ii	1.67	8.88	0.16	11.2	79.1	6.30	0.3	2.0	1.1
S 22-ii	0.05	14.2	0.27	24.7	63.6	6.10	1.8	2.0	1.8
S 23-ii	0.02	5.92	0.27	9.30	80.4	6.00	1.0	2.2	1.1
S 24-ii	0.02	2.90	0.16	12.4	81.2	2.70	1.3	1.5	1.0

Notes:

1. C – Clearview Estate, N- Nerang, B- Benowa and S- Surfers Paradise
2. 1 and 2 - sampling event
3. i, ii, iii and iv - particle size ranges 300-425µm, 150-300µm, 75-150µm and <75µm

**Table A.1: Physical and chemical properties of build-up pollutants (continued from previous page)**

**Particle size range 150-300µm**

Identification	TSS (mg/g)	pH	EC (µS/cm)	Ca (meq (+)/100 g)	Al (meq (+)/100 g)	Mg (meq (+)/100 g)	Na (meq (+)/100 g)	K (meq (+)/100 g)	EC/EC (meq (+)/100 g)
C 11-ii	78.28	7.8	26.2	6.74	0.01	0.63	0.23	0.11	7.72
C 12-ii	181.5	6.8	165	4.38	0.00	1.08	0.18	0.26	5.90
C 13-ii	159.5	7.1	90.2	20.9	0.28	2.85	0.32	1.11	25.5
C 14-ii	190.5	7.2	64.9	2.33	0.04	0.17	0.05	0.01	2.58
C 21-ii	141.1	8.7	73.6	3.36	0.00	0.26	0.01	0.06	3.69
C 22-ii	172.6	8.6	49.6	0.06	0.01	0.01	0.34	0.03	0.44
C 23-ii	190.4	8.4	38.0	3.57	0.39	0.64	0.35	0.03	4.97
C 24-ii	290.1	8.1	53.5	3.61	0.40	0.65	0.35	0.03	5.02
N 11-ii	114.3	6.4	171	9.85	0.01	0.15	0.14	0.07	10.2
N 12-ii	269.0	5.7	105	4.49	0.01	0.28	0.44	0.11	5.32
N 13-ii	226.1	6.1	39.9	0.88	0.00	0.04	1.61	0.10	2.63
N 14-ii	269.7	6.1	46.8	1.43	0.02	0.14	0.04	0.01	1.65
N 21-ii	69.00	7.0	97.5	6.48	0.01	0.25	0.30	0.14	7.18
N 22-ii	159.8	7.8	50.4	7.72	0.01	0.22	0.22	0.11	8.27
N 23-ii	208.5	7.2	58.7	8.57	0.00	0.28	0.35	0.12	9.33
N 24-ii	427.7	6.9	100	2.97	0.01	0.20	0.28	0.09	3.54
B 11-ii	297.4	6.4	73.9	2.14	0.01	0.00	0.36	0.02	2.53
B 12-ii	292.3	6.4	62.7	3.66	0.40	0.65	0.36	0.01	5.08
B 13-ii	369.4	6.4	38.6	0.30	0.01	0.00	0.36	0.03	0.70
B 14-ii	208.3	7.4	49.1	0.37	0.01	0.00	0.36	0.02	0.76
B 21-ii	56.06	7.6	109	10.9	0.00	1.21	0.16	0.32	12.6
B 22-ii	219.8	7.3	72.6	4.21	0.01	0.59	0.96	0.18	5.93
B 23-ii	196.1	7.0	73.1	3.32	0.00	0.38	1.12	0.20	5.02
B 24-ii	129.2	6.2	120	1.66	0.00	0.25	0.92	0.11	2.95
S 11-ii	132.2	8.8	97.7	5.06	0.00	1.51	0.15	0.24	6.95
S 12-ii	8.096	8.6	46.4	3.73	0.01	0.19	0.43	0.07	4.44
S 13-ii	206.6	8.3	46.6	3.92	0.00	0.23	0.27	0.00	4.42
S 14-ii	355.6	7.5	123	3.23	0.01	0.23	0.29	0.00	3.77
S 21-ii	262.4	8.7	54.0	0.01	0.01	0.01	1.92	0.08	2.01
S 22-ii	101.3	8.3	78.7	0.01	0.00	0.01	1.92	0.07	2.01
S 23-ii	261.9	7.9	74.1	0.01	0.02	0.01	1.92	0.09	2.05
S 24-ii	341.5	7.4	183	3.66	0.40	0.66	0.04	0.03	4.78

Notes:

1. C – Clearview Estate, N- Nerang, B- Benowa and S- Surfers Paradise
2. 1 and 2 - sampling event
3. i, ii, iii and iv - particle size ranges 300-425µm, 150-300µm, 75-150µm and <75µm



**Table A.1: Physical and chemical properties of build-up pollutants (continued from previous page)**

**Particle size range 75-150µm**

Identification	TOC (mg/g)	EGME SSA (m <sup>2</sup> /g)	BET SSA (m <sup>2</sup> /g)	Amorphous (%)	Quartz (%)	Albite (%)	Microcline (%)	Chlorite (%)	Muscovite (%)
C 11-iii	0.41	9.29	1.91	28.3	42.6	13.6	2.4	1.9	2.0
C 12-iii	0.52	8.70	0.62	22.0	44.3	18.8	5.4	1.2	3.6
C 13-iii	0.67	9.85	3.59	38.1	35.6	12.1	5.2	2.3	6.5
C 14-iii	0.63	1.10	0.90	14.5	55.8	12.4	10.5	2.9	3.9
C 21-iii	1.18	14.4	0.76	33.4	44.1	8.40	7.2	2.2	4.7
C 22-iii	2.16	5.41	0.74	27.1	43.4	13.8	8.4	2.6	4.6
C 23-iii	2.15	13.4	0.74	50.0	27.9	9.00	6.1	1.8	5.3
C 24-iii	0.86	8.48	0.65	23.5	52.0	13.0	6.1	2.8	2.6
N 11-iii	0.12	7.37	0.88	17.8	50.4	15.8	8.0	3.5	4.5
N 12-iii	0.04	7.19	0.56	39.4	39.4	10.8	5.2	1.8	3.4
N 13-iii	0.09	8.49	0.60	29.8	44.2	11.7	6.4	2.4	5.5
N 14-iii	0.02	5.33	1.10	18.7	55.7	15.8	4.6	0.3	4.9
N 21-iii	0.22	4.98	0.79	40.4	41.6	10.2	4.3	1.6	1.8
N 22-iii	0.25	13.7	0.33	23.0	50.2	13.8	5.2	3.6	4.1
N 23-iii	0.25	4.31	0.33	33.9	41.1	8.70	6.6	1.6	8.0
N 24-iii	0.11	8.69	0.46	21.6	56.2	13.7	3.4	1.5	3.6
B 11-iii	0.94	6.19	0.42	29.9	35.2	11.7	3.6	9.9	9.7
B 12-iii	0.42	1.09	0.51	26.3	47.4	11.4	4.0	3.9	7.0
B 13-iii	0.75	2.94	0.97	25.7	49.1	12.4	5.0	3.2	4.6
B 14-iii	0.38	13.8	0.85	45.5	30.0	8.70	6.5	2.4	7.0
B 21-iii	0.94	1.31	0.48	31.9	42.2	11.0	5.0	7.4	2.5
B 22-iii	0.28	18.5	0.69	28.3	45.5	12.8	4.9	3.8	4.7
B 23-iii	1.25	9.53	0.41	32.7	43.4	9.20	4.0	1.6	9.0
B 24-iii	1.37	5.78	0.21	18.5	63.4	7.90	3.9	2.2	4.1
S 11-iii	2.92	24.8	0.46	30.3	40.5	11.0	4.0	3.8	10.4
S 12-iii	0.80	7.00	0.56	27.2	39.4	13.7	5.9	4.1	9.6
S 13-iii	0.39	10.3	0.51	17.5	51.0	11.2	8.6	4.1	7.5
S 14-iii	0.84	4.60	0.50	28.9	43.0	6.90	14.5	1.7	5.1
S 21-iii	0.18	12.5	0.41	28.6	41.4	15.9	6.5	0.3	6.5
S 22-iii	0.04	17.7	0.71	35.8	32.2	12.0	6.9	2.8	10.3
S 23-iii	0.02	21.5	0.52	32.4	40.6	12.4	6.6	3.1	5.0
S 24-iii	0.02	10.3	0.38	29.8	39.4	9.70	14.3	2.6	4.3

Notes:

1. C – Clearview Estate, N- Nerang, B- Benowa and S- Surfers Paradise
2. 1 and 2 - sampling event
3. i, ii, iii and iv - particle size ranges 300-425µm, 150-300µm, 75-150µm and <75µm

**Table A.1: Physical and chemical properties of build-up pollutants (continued from previous page)**

**Particle size range 75-150µm**

Identification	TSS (mg/g)	pH	EC (µS/cm)	Ca (meq (+)/100 g)	Al (meq (+)/100 g)	Mg (meq (+)/100 g)	Na (meq (+)/100 g)	K (meq (+)/100 g)	ECEC (meq (+)/100 g)
C 11-iii	173.1	7.8	26.2	9.15	0.01	0.82	0.31	0.14	10.4
C 12-iii	173.2	6.8	165	6.28	0.01	1.73	0.20	0.33	8.54
C 13-iii	484.2	7.1	90.2	10.9	0.17	1.30	0.14	0.46	13.0
C 14-iii	267.2	7.2	64.9	4.71	0.00	0.23	0.76	0.01	5.71
C 21-iii	143.3	8.7	73.6	3.70	0.39	0.67	0.13	0.07	4.96
C 22-iii	503.3	8.6	49.6	0.20	0.01	0.03	0.32	0.00	0.56
C 23-iii	141.6	8.4	38.0	3.59	0.40	0.65	0.34	0.02	5.01
C 24-iii	166.8	8.1	53.5	3.70	0.39	0.66	0.33	0.04	5.12
N 11-iii	277.8	6.4	171	15.4	0.01	0.28	0.22	0.14	16.1
N 12-iii	192.5	5.7	105	6.84	0.01	0.52	0.48	0.18	8.02
N 13-iii	287.7	6.1	39.9	0.89	0.00	0.07	1.73	0.06	2.75
N 14-iii	311.7	6.1	46.8	2.44	0.05	0.27	0.11	0.03	2.90
N 21-iii	605.8	7.0	97.5	12.2	0.01	0.51	0.46	0.16	13.4
N 22-iii	199.5	7.8	50.4	10.3	0.00	0.35	0.40	0.15	11.2
N 23-iii	455.6	7.2	58.7	12.8	0.00	0.50	0.34	0.14	13.8
N 24-iii	228.1	6.9	100	4.98	0.01	0.32	0.20	0.11	5.61
B 11-iii	190.5	6.4	73.9	2.90	0.01	0.00	0.36	0.04	3.30
B 12-iii	131.0	6.4	62.7	0.40	0.01	0.00	0.36	0.03	0.80
B 13-iii	119.3	6.4	38.6	13.7	0.01	0.00	0.21	0.03	13.9
B 14-iii	289.7	7.4	49.1	1.37	0.01	0.00	0.36	0.02	1.77
B 21-iii	258.9	7.6	109	1.99	0.00	0.17	1.46	0.07	3.69
B 22-iii	110.8	7.3	72.6	10.7	0.00	2.12	0.00	0.85	13.6
B 23-iii	216.7	7.0	73.1	6.29	0.01	1.00	0.18	0.34	7.81
B 24-iii	157.6	6.2	120	2.33	0.01	0.33	0.95	0.16	3.78
S 11-iii	415.7	8.8	97.7	1.93	0.04	0.41	0.64	0.04	3.06
S 12-iii	323.5	8.6	46.4	6.66	0.00	0.38	0.99	0.01	8.04
S 13-iii	155.1	8.3	46.6	21.0	0.00	2.09	0.64	0.50	24.3
S 14-iii	178.4	7.5	123	7.16	0.01	0.52	0.62	0.03	8.34
S 21-iii	138.0	8.7	54.0	0.00	0.00	0.01	1.92	0.07	2.00
S 22-iii	304.6	8.3	78.7	0.00	0.00	0.01	1.93	0.10	2.03
S 23-iii	71.38	7.9	74.1	0.01	0.00	0.01	1.92	0.09	2.03
S 24-iii	85.40	7.4	183	10.6	0.39	1.62	0.06	0.70	13.3

Notes:

1. C – Clearview Estate, N- Nerang, B- Benowa and S- Surfers Paradise
2. 1 and 2 - sampling event
3. i, ii, iii and iv - particle size ranges 300-425µm, 150-300µm, 75-150µm and <75µm

**Table A.1: Physical and chemical properties of build-up pollutants (continued from previous page)**

**Particle size range <75µm**

Identification	TOC (mg/g)	EGME SSA (m <sup>2</sup> /g)	BET SSA (m <sup>2</sup> /g)	Amorphous (%)	Quartz (%)	Albite (%)	Microcline (%)	Chlorite (%)	Muscovite (%)
C 11-iv	2.57	10.2	3.98	31.6	44.8	8.30	6.5	3.3	5.4
C 12-iv	3.20	14.2	1.13	33.6	32.9	17.8	3.6	2.0	4.1
C 13-iv	1.60	12.9	5.77	33.9	38.9	10.3	4.8	2.8	6.1
C 14-iv	1.21	1.73	1.63	21.5	47.9	15.1	8.0	3.2	4.3
C 21-iv	0.38	19.6	2.69	70.7	12.4	5.00	3.9	2.2	5.8
C 22-iv	2.68	13.7	1.86	55.3	28.2	5.10	3.9	1.5	6.1
C 23-iv	1.47	22.6	1.49	38.2	29.3	13.5	9.7	2.3	6.9
C 24-iv	0.82	19.8	3.29	51.0	25.2	9.90	3.3	4.6	6.0
N 11-iv	3.84	21.6	2.89	40.5	31.8	16.0	3.6	3.4	4.7
N 12-iv	2.65	11.3	1.28	23.1	40.1	16.9	6.1	3.8	10.0
N 13-iv	3.29	9.4	1.22	27.2	41.1	12.9	6.4	2.9	9.5
N 14-iv	0.49	17.8	1.45	26.7	43.5	15.1	6.5	3.1	5.0
N 21-iv	0.38	13.7	2.73	31.7	44.1	13.7	4.5	2.4	3.8
N 22-iv	0.71	15.9	1.15	31.7	41.3	13.3	4.5	4.2	4.9
N 23-iv	4.35	26.5	0.74	34.5	44.2	11.2	3.8	2.3	4.0
N 24-iv	1.30	11.7	1.28	39.0	41.5	12.2	3.3	0.8	3.1
B 11-iv	0.46	18.8	0.99	57.3	19.1	6.90	2.2	10.5	4.0
B 12-iv	5.43	5.71	1.32	38.8	40.0	7.40	4.5	2.9	6.3
B 13-iv	7.06	10.4	2.55	43.4	26.9	11.0	5.1	3.3	10.3
B 14-iv	4.50	20.7	1.18	34.4	40.7	10.1	3.4	2.9	8.5
B 21-iv	4.28	15.3	1.29	22.3	35.2	15.1	6.0	17.4	4.0
B 22-iv	2.78	30.8	1.36	28.8	43.4	12.7	4.7	4.2	6.2
B 23-iv	13.7	20.7	1.23	49.3	27.7	10.0	2.7	2.7	7.6
B 24-iv	17.6	18.4	1.06	61.0	17.9	7.60	4.2	2.9	6.4
S 11-iv	2.07	20.3	0.85	57.4	19.0	10.6	3.5	2.3	7.3
S 12-iv	3.47	28.9	2.39	34.7	24.4	15.8	7.1	4.6	13.5
S 13-iv	0.41	25.9	1.33	35.1	34.0	12.8	4.7	4.7	8.8
S 14-iv	1.48	18.9	1.43	30.9	40.5	11.3	5.0	3.1	9.4
S 21-iv	0.34	18.9	0.93	47.0	26.1	11.3	5.2	3.6	6.9
S 22-iv	-0.15	19.6	1.89	55.5	19.8	11.3	3.9	2.7	6.8
S 23-iv	0.03	23.5	1.49	60.3	19.2	7.00	3.7	3.3	6.5
S 24-iv	0.04	22.5	1.15	52.0	24.8	9.60	6.4	2.0	5.3

Notes:

1. C – Clearview Estate, N- Nerang, B- Benowa and S- Surfers Paradise
2. 1 and 2 - sampling event
3. i, ii, iii and iv - particle size ranges 300-425µm, 150-300µm, 75-150µm and <75µm

**Table A.1: Physical and chemical properties of build-up pollutants (continued from previous page)**

**Particle size range <75µm**

Identification	TSS (mg/g)	pH	EC (µS/cm)	Ca (meq (+)/100 g)	Al (meq (+)/100 g)	Mg (meq (+)/100 g)	Na (meq (+)/100 g)	K (meq (+)/100 g)	ECCEC (meq (+)/100 g)
C 11-iv	733.3	7.8	26.2	9.43	0.00	1.03	0.27	0.25	11.0
C 12-iv	627.3	6.8	165	8.48	0.00	2.22	0.08	0.59	11.4
C 13-iv	248.1	7.1	90.2	4.85	0.00	0.60	0.39	0.16	6.01
C 14-iv	486.7	7.2	64.9	3.97	0.01	0.27	0.43	0.04	4.71
C 21-iv	661.5	8.7	73.6	3.57	0.39	0.64	0.31	0.01	4.93
C 22-iv	279.0	8.6	49.6	0.78	0.55	0.51	0.15	0.33	2.32
C 23-iv	416.4	8.4	38.0	3.61	0.39	0.66	0.34	0.03	5.03
C 24-iv	477.2	8.1	53.5	3.66	0.39	0.65	0.34	0.01	5.05
N 11-iv	582.9	6.4	171	21.6	0.00	0.75	0.00	0.26	22.6
N 12-iv	411.6	5.7	105	9.17	0.00	0.87	0.42	0.36	10.8
N 13-iv	320.4	6.1	39.9	0.38	0.00	0.06	1.78	0.08	2.31
N 14-iv	376.2	6.1	46.8	4.71	0.08	5.56	0.05	0.18	10.6
N 21-iv	126.8	7.0	97.5	20.8	0.00	1.04	0.54	0.25	22.7
N 22-iv	622.2	7.8	50.4	14.1	0.01	0.67	0.37	0.24	15.3
N 23-iv	309.5	7.2	58.7	17.6	0.01	0.85	0.34	0.29	19.1
N 24-iv	206.5	6.9	100	5.61	0.02	0.37	0.22	0.17	6.37
B 11-iv	469.5	6.4	73.9	3.73	0.01	0.00	0.36	0.04	4.14
B 12-iv	510.0	6.4	62.7	1.42	0.01	0.00	0.36	0.03	1.82
B 13-iv	445.1	6.4	38.6	0.59	0.01	0.00	0.36	0.04	1.01
B 14-iv	423.0	7.4	49.1	8.13	0.01	0.01	0.31	0.03	8.49
B 21-iv	626.1	7.6	109	2.08	0.01	0.19	1.46	0.11	3.85
B 22-iv	465.6	7.3	72.6	9.76	0.00	2.22	0.03	0.77	12.8
B 23-iv	533.9	7.0	73.1	2.37	0.00	0.35	0.56	0.19	3.48
B 24-iv	666.1	6.2	120	4.28	0.00	1.16	0.23	0.51	6.19
S 11-iv	33.08	8.8	97.7	9.68	0.00	3.33	0.25	0.83	14.1
S 12-iv	656.9	8.6	46.4	14.1	0.02	2.39	0.46	0.93	17.9
S 13-iv	282.0	8.3	46.6	2.86	0.01	0.17	0.36	0.02	3.41
S 14-iv	134.4	7.5	123	13.1	0.01	2.58	0.35	0.53	16.6
S 21-iv	557.4	8.7	54.0	0.00	0.00	0.01	1.92	0.07	2.00
S 22-iv	572.5	8.3	78.7	0.00	0.00	0.01	1.92	0.07	2.00
S 23-iv	334.1	7.9	74.1	16.0	0.41	2.74	0.87	0.75	20.7
S 24-iv	242.5	7.4	183	15.6	0.39	3.58	0.43	3.33	23.3

Notes:

1. C – Clearview Estate, N- Nerang, B- Benowa and S- Surfers Paradise
2. 1 and 2 - sampling event
3. i, ii, iii and iv - particle size ranges 300-425µm, 150-300µm, 75-150µm and <75µm

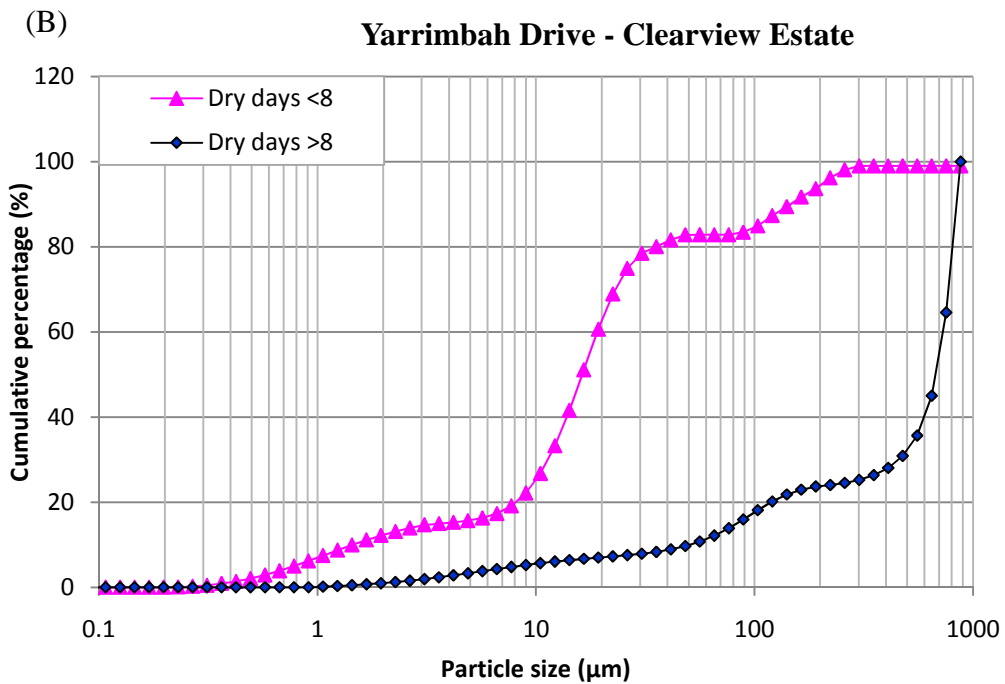
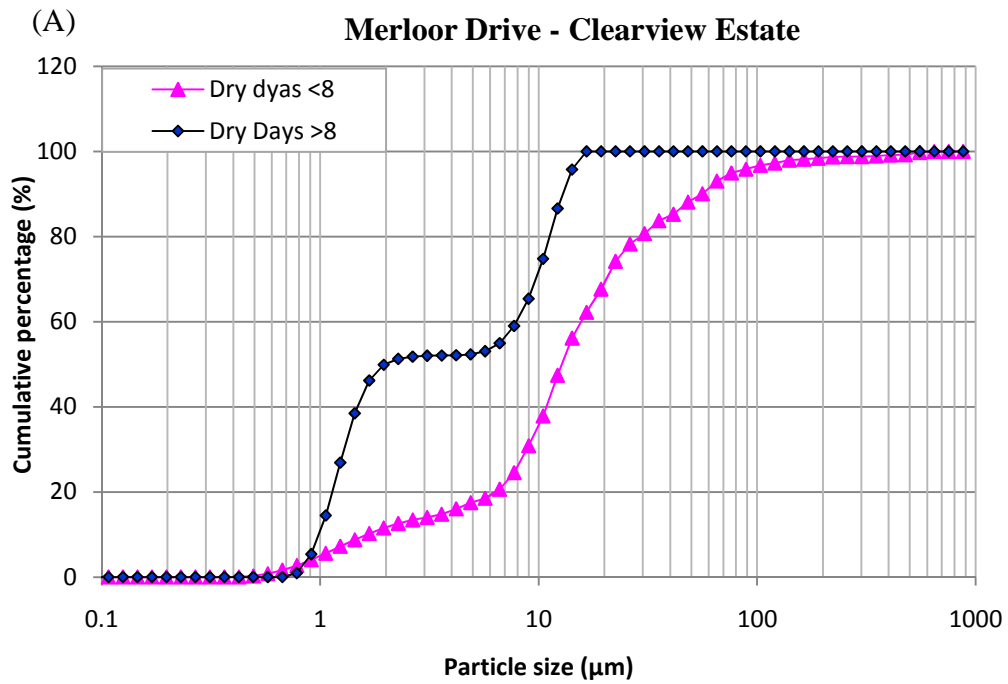


**Figure A.1: Variation of particle size distribution of build-up samples with antecedent dry days**

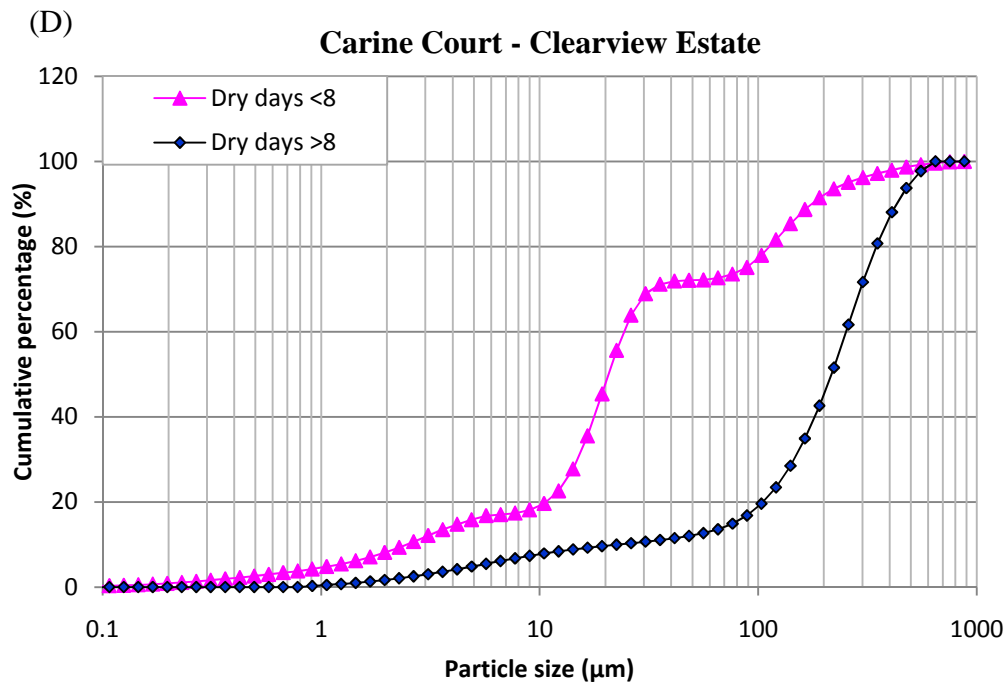
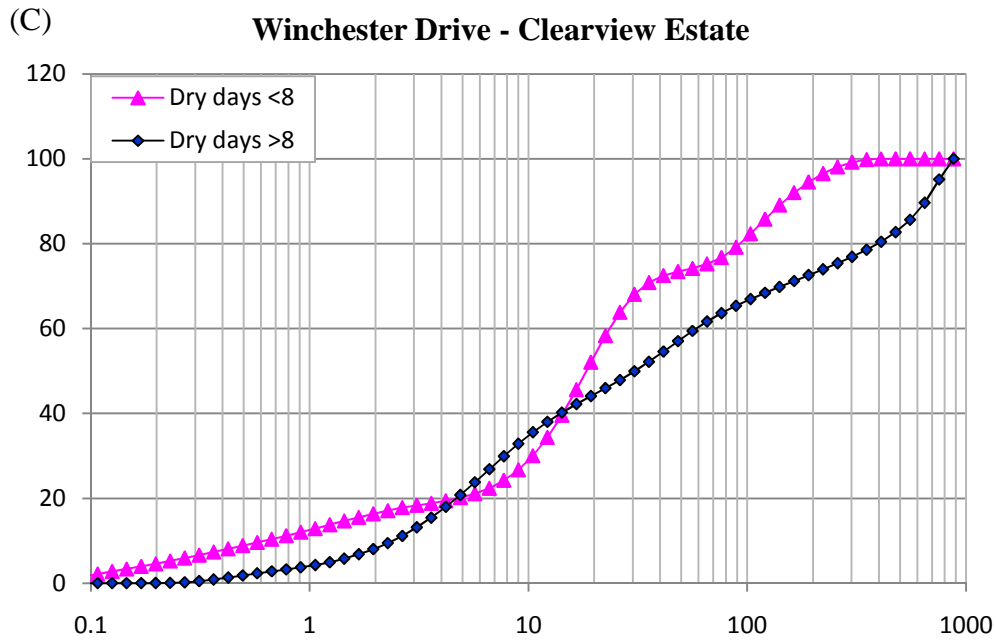


**Figure A.1: Variation of particle size distribution of build-up samples with antecedent dry days**

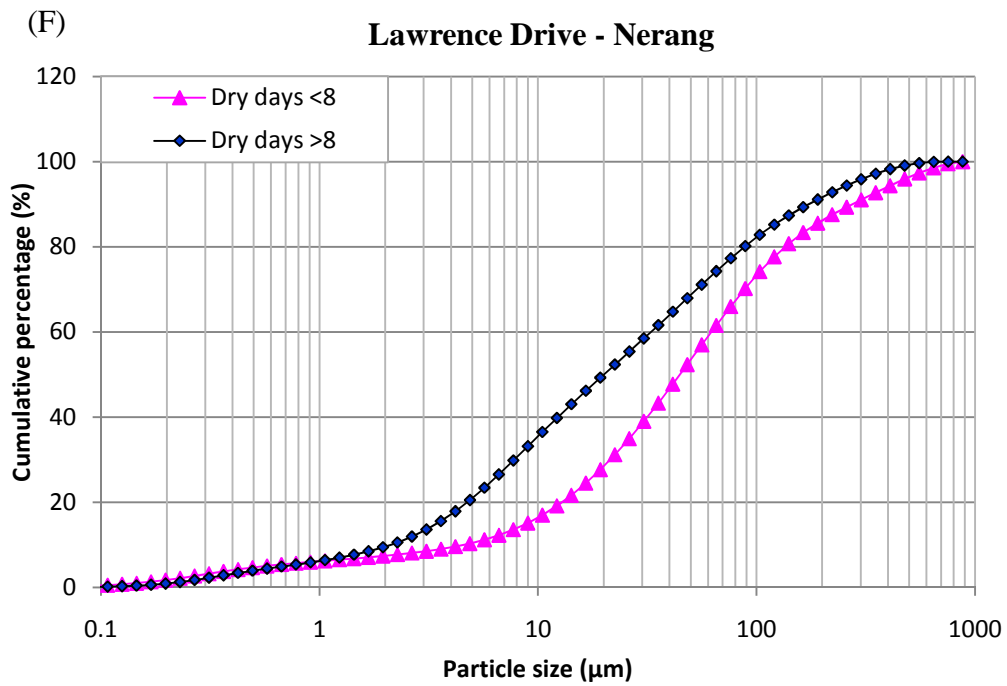
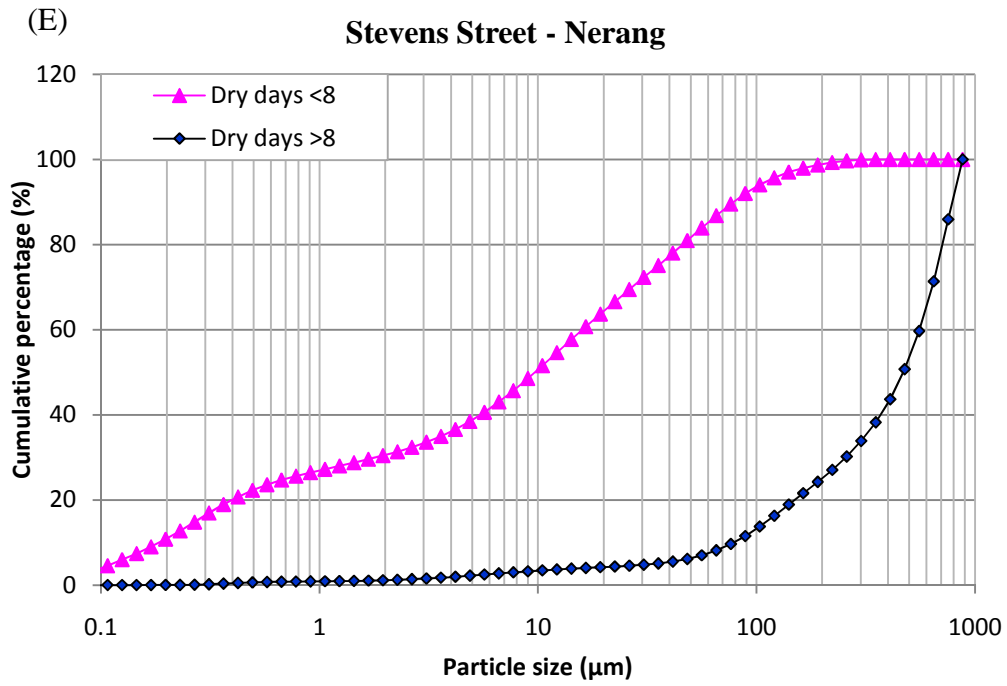


**Figure A.1: Variation of particle size distribution of build-up samples with antecedent dry days**

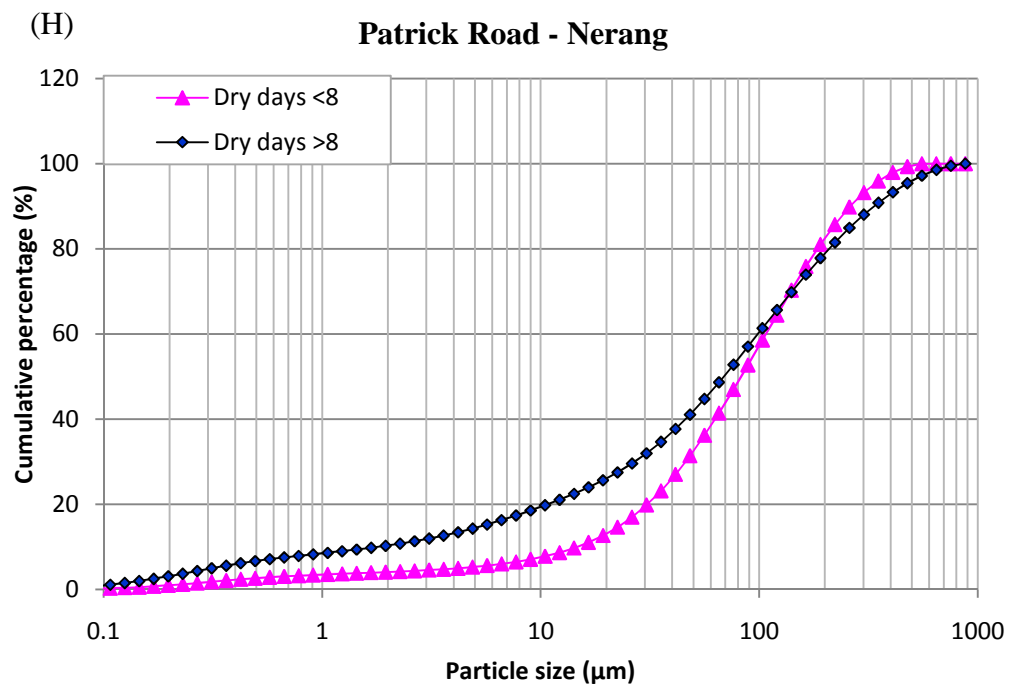
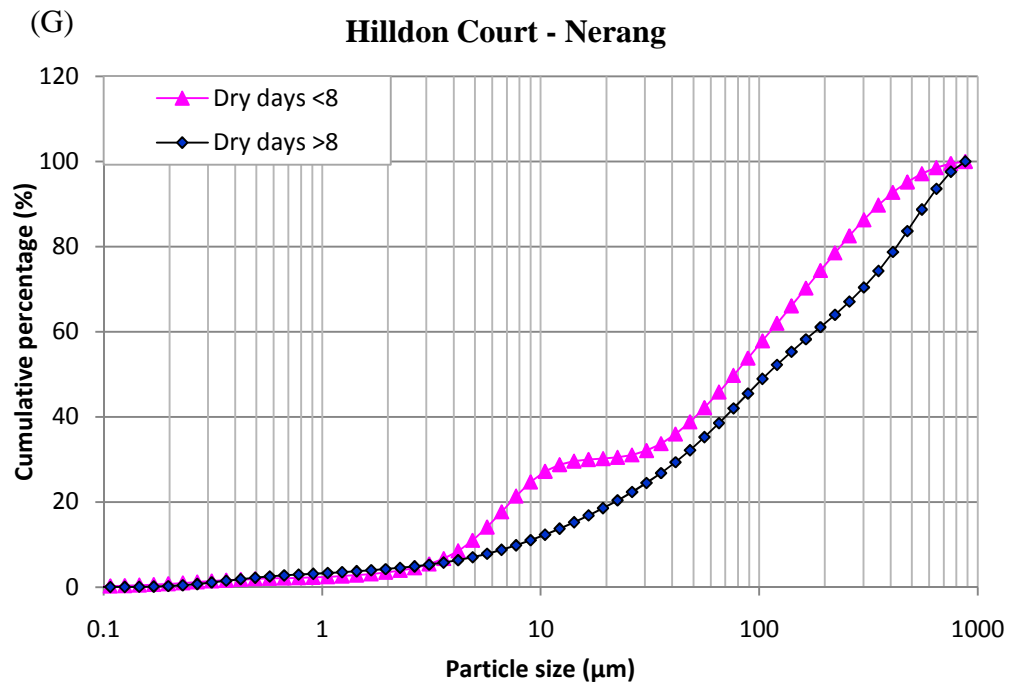


**Figure A.1: Variation of particle size distribution of build-up samples with antecedent dry days**



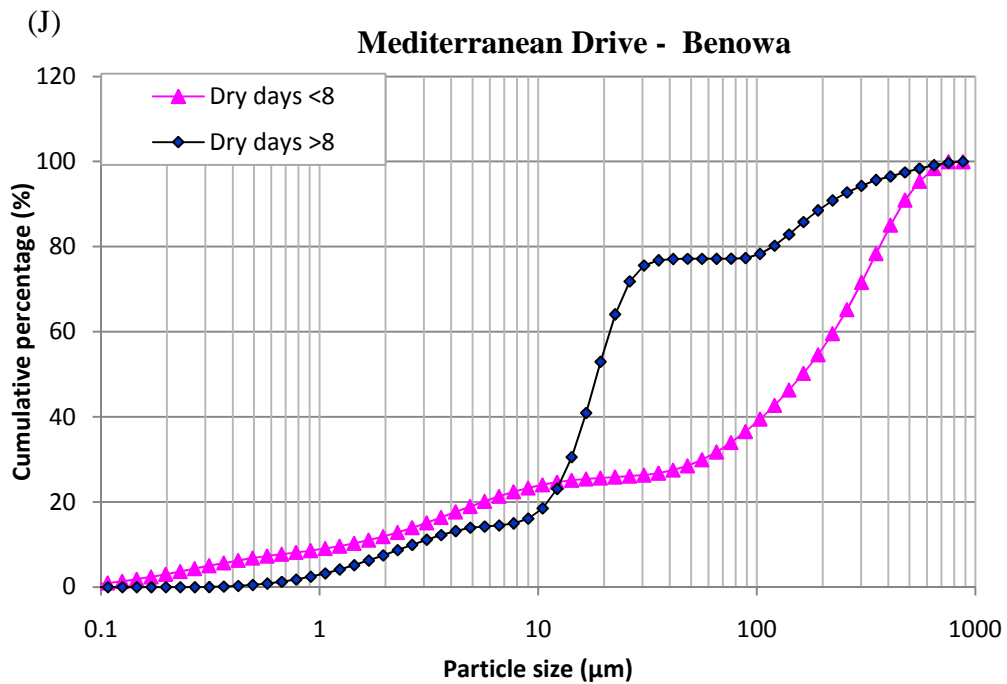
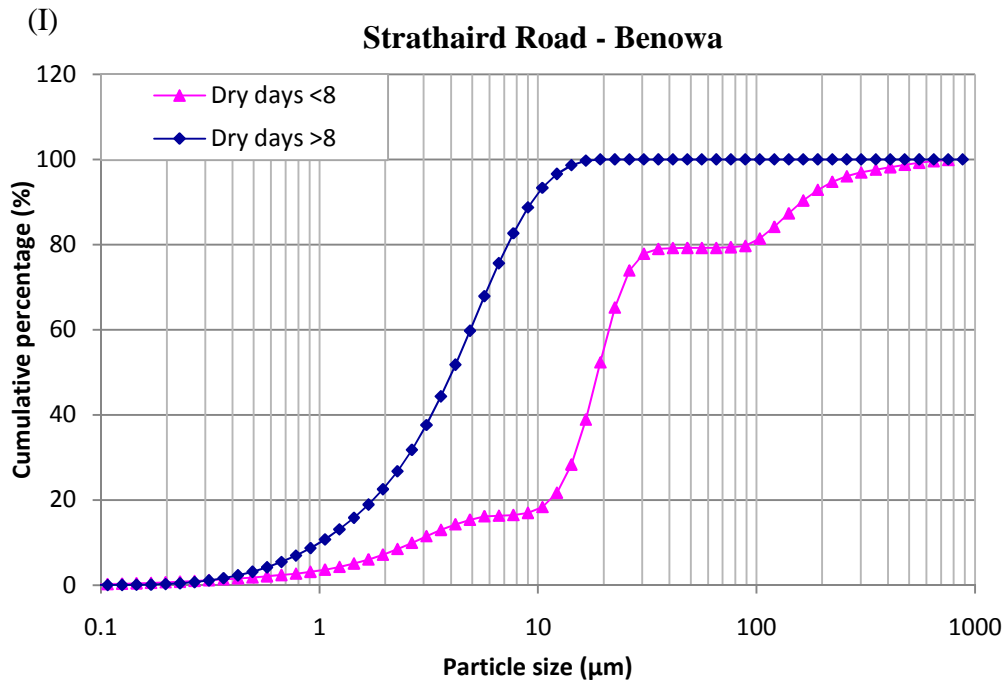


**Figure A.1: Variation of particle size distribution of build-up samples with antecedent dry days**

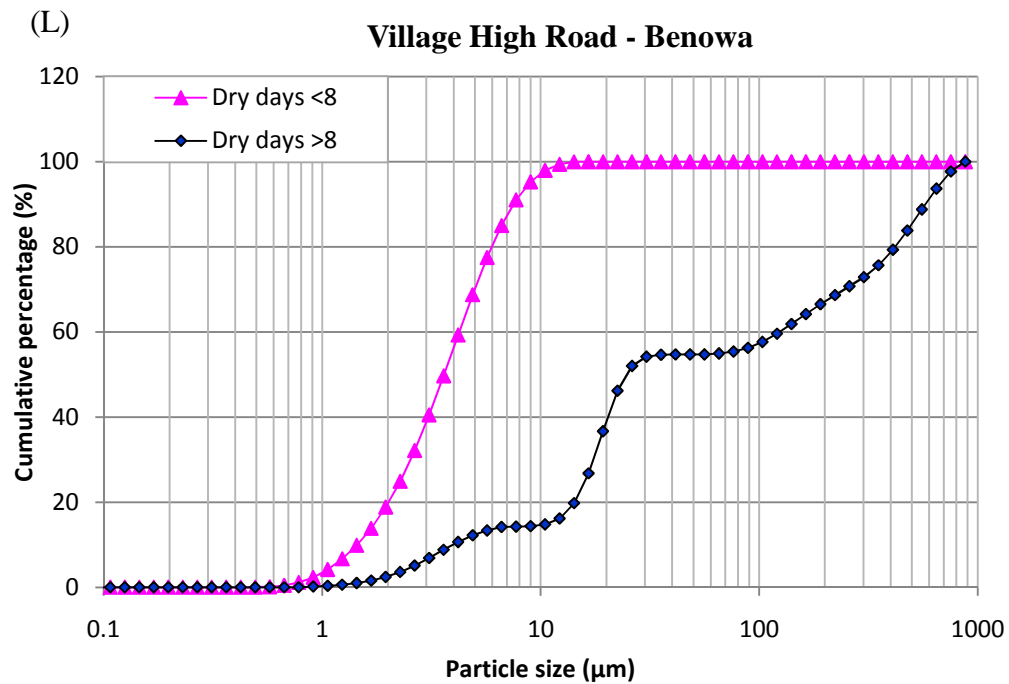
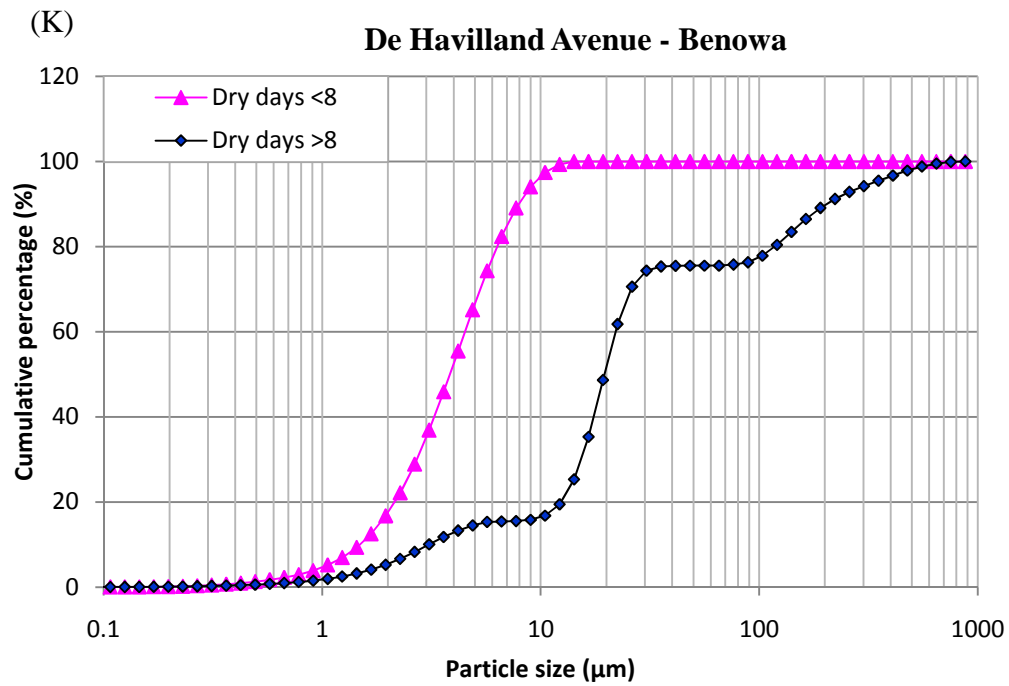


**Figure A.1: Variation of particle size distribution of build-up samples with antecedent dry days**

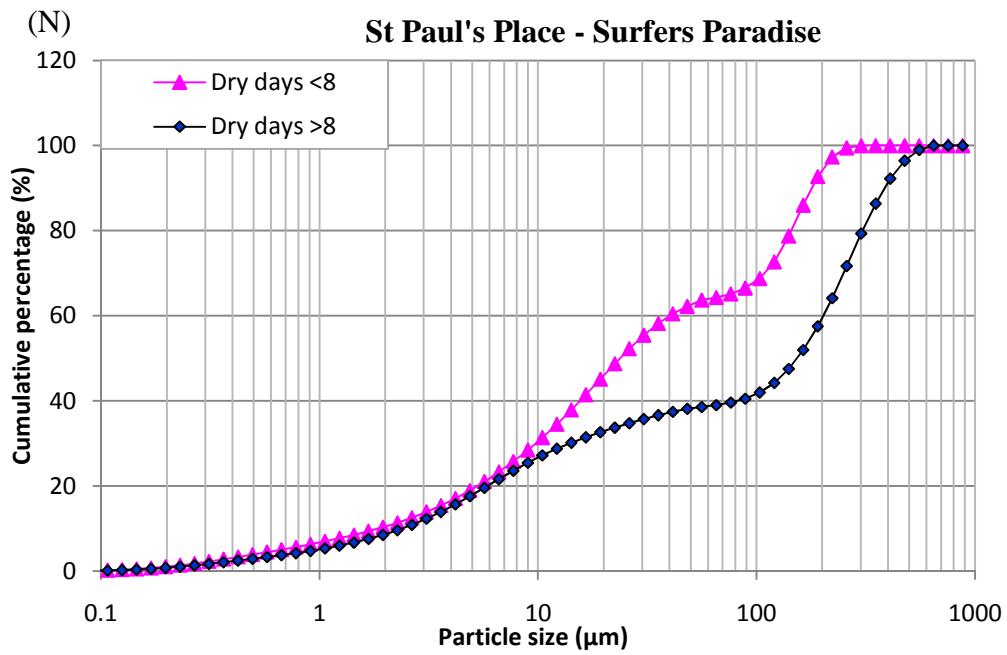
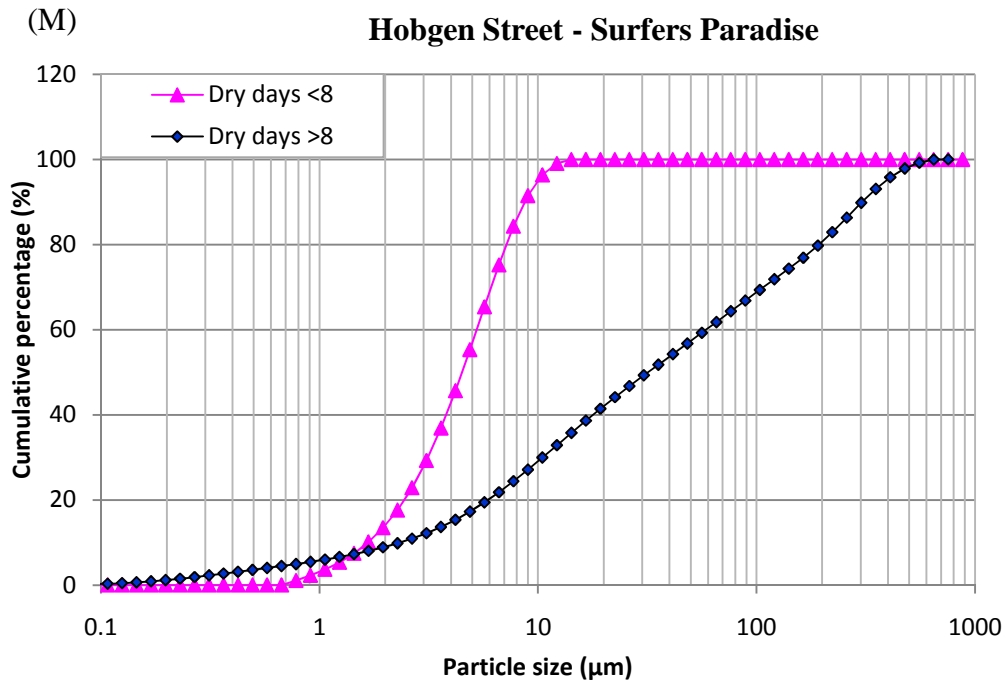


**Figure A.1: Variation of particle size distribution of build-up samples with antecedent dry days**

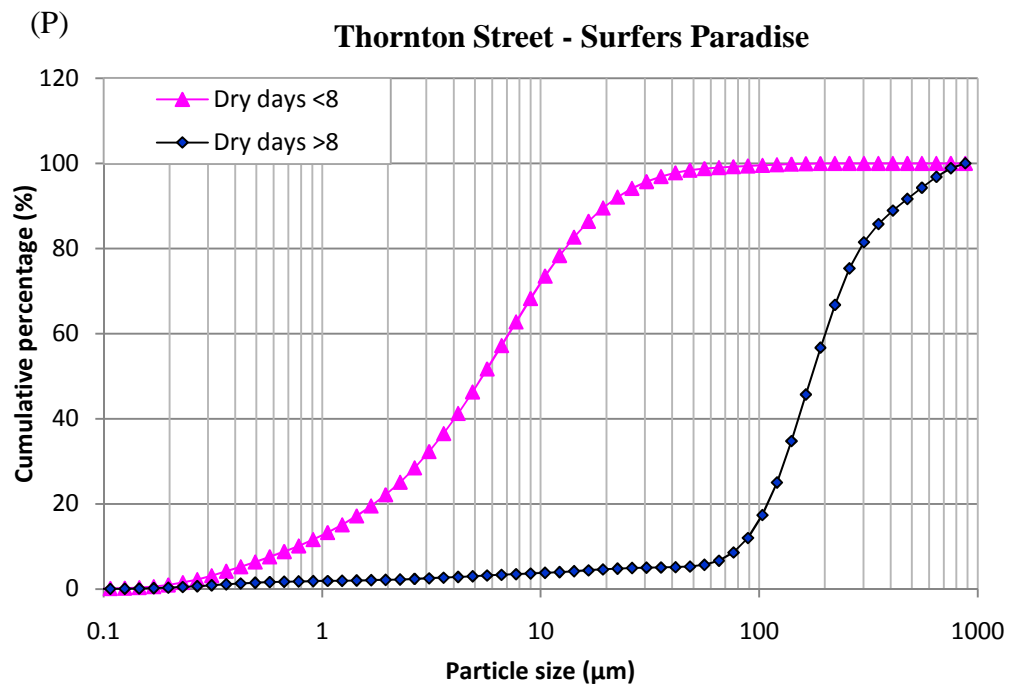
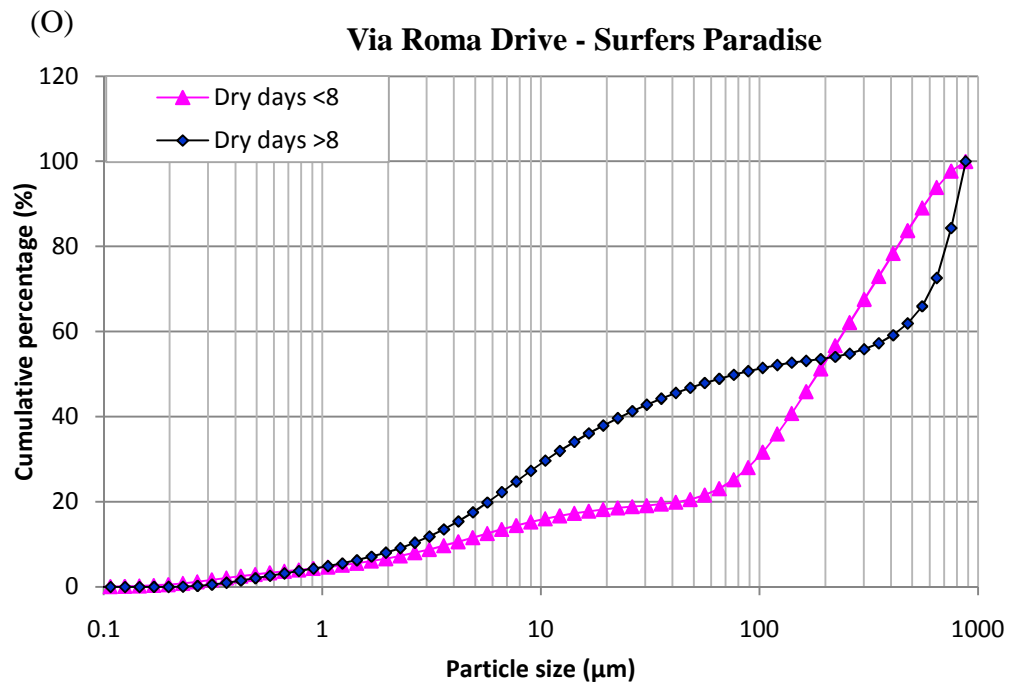


**Figure A.1: Variation of particle size distribution of build-up samples with antecedent dry days**

**Table A.2: Clay minerals detected by thin film clay analysis of build-up samples**

Suburb	Sample	Clay minerals				
Clearview Estate	C 1	chlorite	illite-mica	kaolinite		
	C 2	chlorite	illite-mica	kaolinite		sepolite
	C 3	chlorite	illite-mica	kaolinite		
	C 4	chlorite	illite-mica	kaolinite		sepolite
Nerang	N 1	chlorite	illite-mica	kaolinite	smectite	
	N 2	chlorite	illite-mica	kaolinite	smectite	sepiolite
	N 3	chlorite	illite-mica	kaolinite	smectite	sepiolite
	N 4	chlorite	illite-mica	sepiolite		
Benowa	B 1	chlorite	illite-mica	amphibole		
	B 2	chlorite	illite-mica	kaolinite	illite-smectite	sepiolite
	B 3	chlorite	illite-mica	kaolinite	smectite	
	B 4	chlorite	illite-mica	kaolinite	smectite	sepeolite
Surfers Paradise	S 1	chlorite	illite-mica	kaolinite	sepolite	
	S 2	chlorite	illite-mica	kaolinite	sepolite	
	S 3	chlorite	Illite-mica	sepolite		
	S 4	chlorite	illite-mica	kaolinite	palygorsite	sepolite

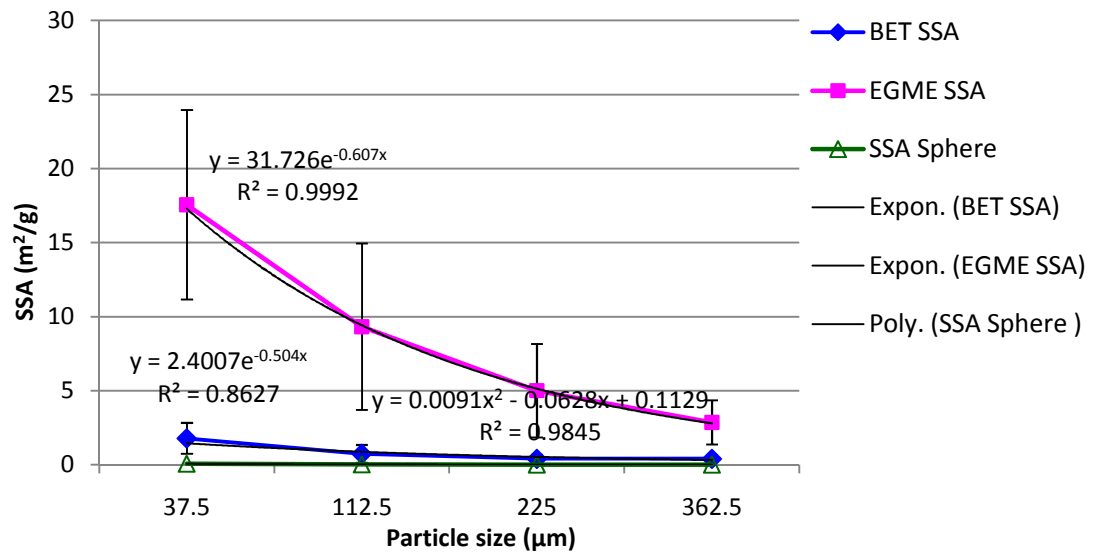


**Figure A.2: Variation in specific surface area with particle size**

**Table A.3: pH of build-up samples**

Suburb	pH	
	Average	Max/ Min
Clearview Estate	7.8	8.6/6.8
Nerang	6.6	7.8/5.7
Benowa	6.8	7.6/6.2
Surfers Paradise	8.2	8.8/7.3

**Table A.4: Percentage composition of minerals and organic matter in soil samples**

Suburb	Amorphous (%)	Quartz (%)	Albite (%)	Microcline (%)	Chlorite (%)	Muscovite (%)	Organic matter (%)
Clearview Estate	10.8	60.8	11.3	4.7	1.8	9.1	5.73
Nerang	12.8	51.2	16.4	4.9	1.9	10.7	6.12
Benowa	10.7	81.4	4.30	0.0	2.1	1.50	4.40
Surfers Paradise	4.40	81.3	3.50	3.4	0.9	5.00	2.61

**Table A.5: Clay minerals detected by thin film clay analysis of soil samples**

Suburb	Clay minerals			
Clearview Estate	Chlorite	Illite-mica	Kaolinite	Smectite
Nerang	Chlorite	Illite-mica	Kaolinite	Smectite
Benowa	Chlorite	Illite	Kaolinite	Illite-smectite
Surfers Paradise	Chlorite	Illite-mica	Kaolinite	

**Table A.6: Notations for soil samples**

<b>Suburb</b>	<b>Notation</b>
Clearview Estate	SO C
Nerang	SO N
Benowa	SO B
Surfers Paradise	SO S

**Table A.7: Solids sampling sites and notations for each site**

<b>Suburb</b>	<b>Site</b>	<b>Notation</b>	
		First field investigations (Dry days <8)	Second field investigations (Dry days >8)
Clearview Estate (C)	Merloo Drive	C 11	C 21
	Yarrimbah Drive	C 12	C 22
	Winchester Drive	C 13	C 23
	Carine Court	C 14	C 24
Nerang (N)	Stevens Street	N 11	N 21
	Lawrence Drive	N 12	N 22
	Hilldon Court	N 13	N 23
	Patrick Road	N 14	N 24
Benowa (B)	Strathaird Road	B 11	B 21
	Mediterranean Drive	B 12	B 22
	De Havilland Avenue	B 13	B 23
	Village High Road	B 14	B 24
Surfers Paradise (S)	Hobgen Street	S 11	S 21
	St Paul's Place	S 12	S 22
	Via Roma Drive	S 13	S 23
	Thornton Street	S 14	S 24

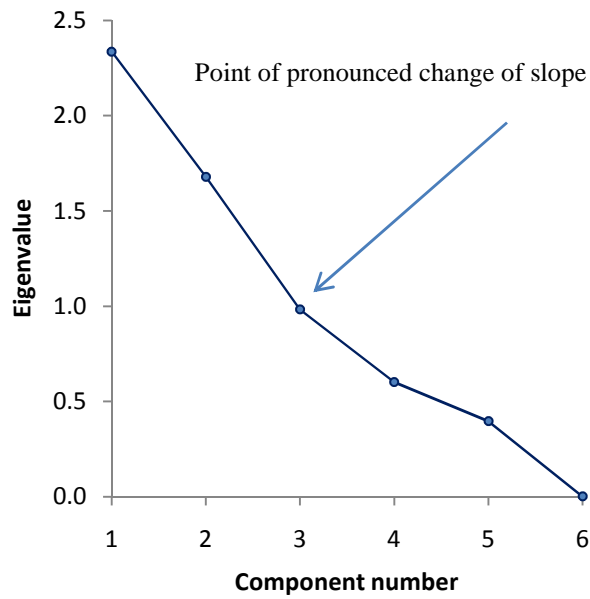


Figure A.3: Scree plot for soil and total build-up solids analysis

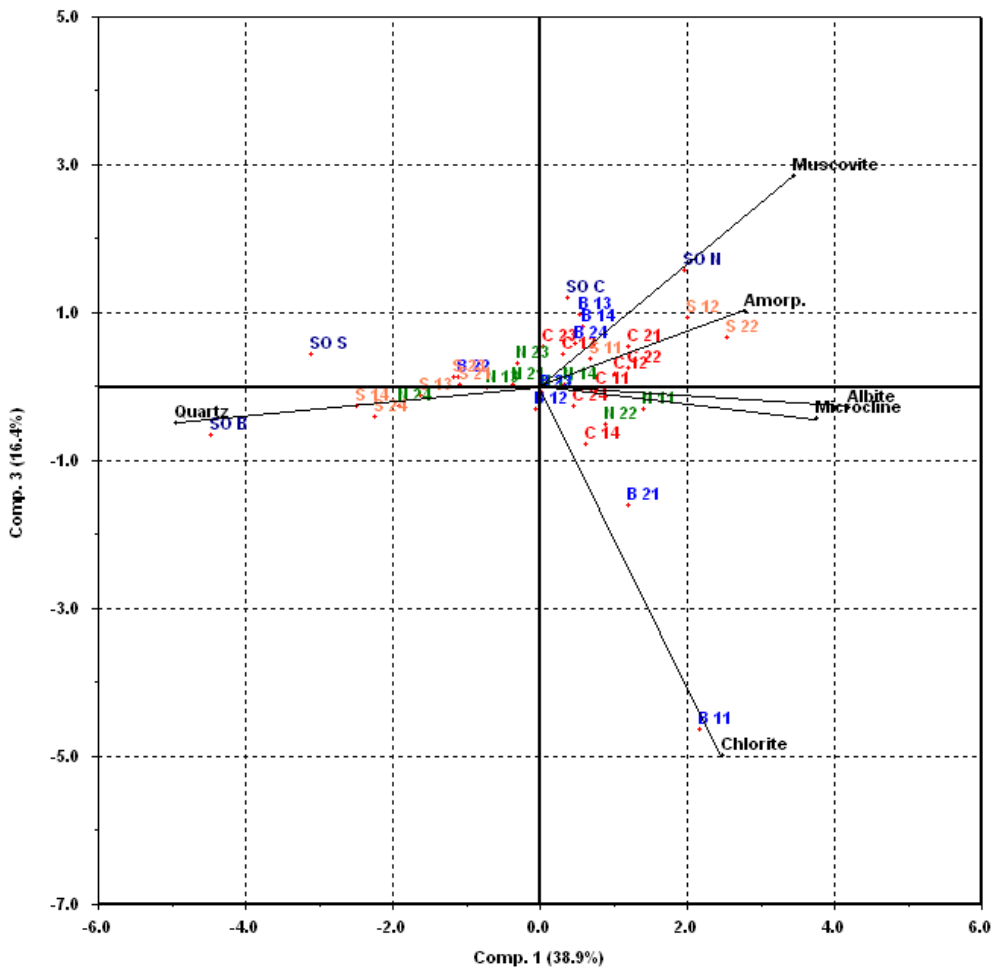
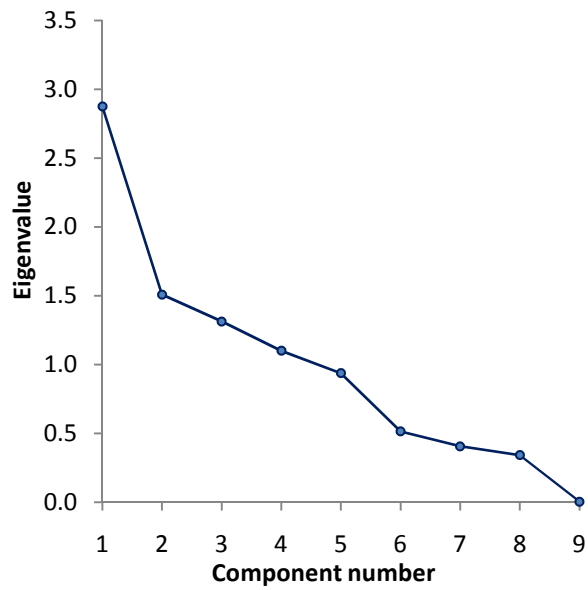


Figure A.4: PC 1 vs PC3 biplot obtained from PCA analysis for soil and total build-up total solids (weighted average)





**Figure A.5: Scree plot for the particle size <75µm**

**Table A.8: PROMETHEE II ranking for particle size <75µm for Surfers Paradise and Clearview Estate samples**

Sample	Net $\Phi$	Ranking order
S 22-iv	0.238	1
S 13-iv	0.116	2
S 14-iv	0.105	3
S 21-iv	0.102	4
C 21-iv	0.051	5
C 23-iv	0.049	6
S 12-iv	0.023	7
C 24-iv	-0.010	8
S 11-iv	-0.011	9
S 23-iv	-0.025	10
S 24-iv	-0.035	11
C 12-iv	-0.046	12
C 22-iv	-0.093	13
C 13-iv	-0.139	14
C 11-iv	-0.140	15
C 14-iv	-0.186	16

Note: C– Clearview Estate, N- Nerang, B- Benowa, S- Surfers Paradise

**Table A.9: PROMETHEE II ranking for particle size <75µm for Surfers Paradise and Clearview Estate samples basic set**

Sample	Net $\Phi$	Ranking order
S 22-iv	0.252	1
S 13-iv	0.124	2
S 22-iv	0.116	3
S 21-iv	0.110	4
S 12-iv	0.030	5
S 11-iv	-0.001	6
S 23-iv	-0.017	7
S 24-iv	-0.029	8
C 12-iv	-0.039	9
C 22-iv	-0.085	10
C 13-iv	-0.134	11
C 11-iv	-0.139	12
C 14-iv	-0.187	13

Note: C– Clearview Estate, N- Nerang, B- Benowa, S- Surfers Paradise

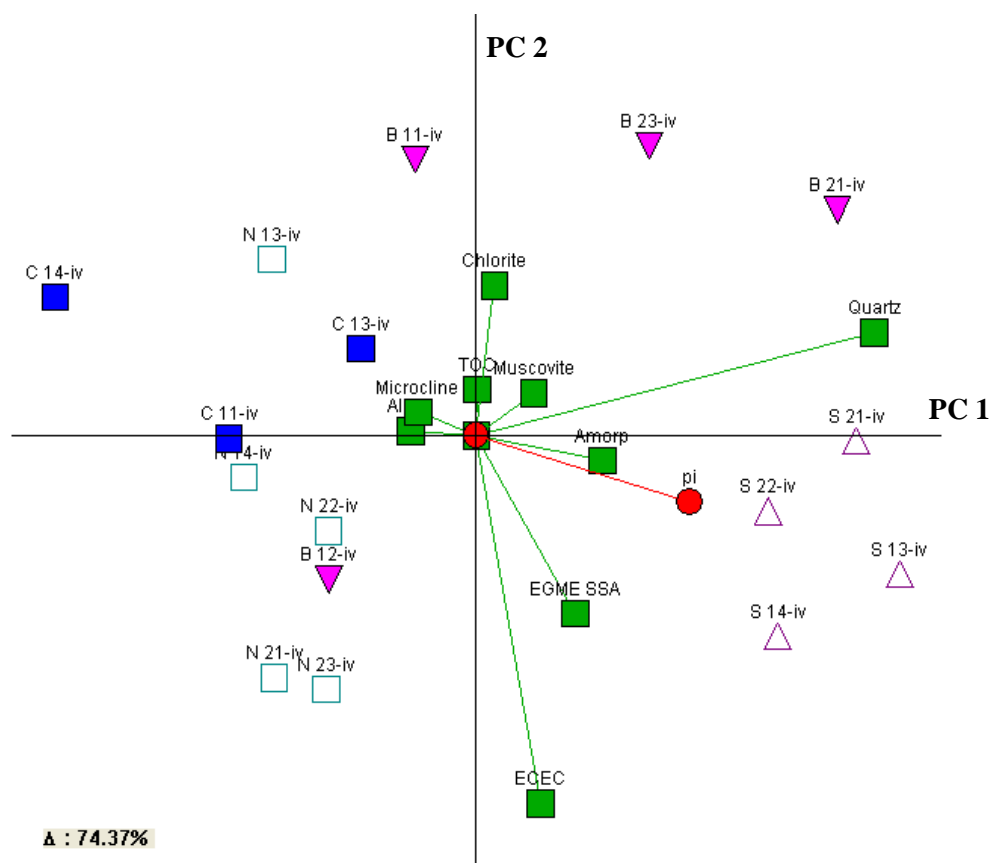


**Figure A.6: GAIA biplot for particle size <75µm for basic data set objects**

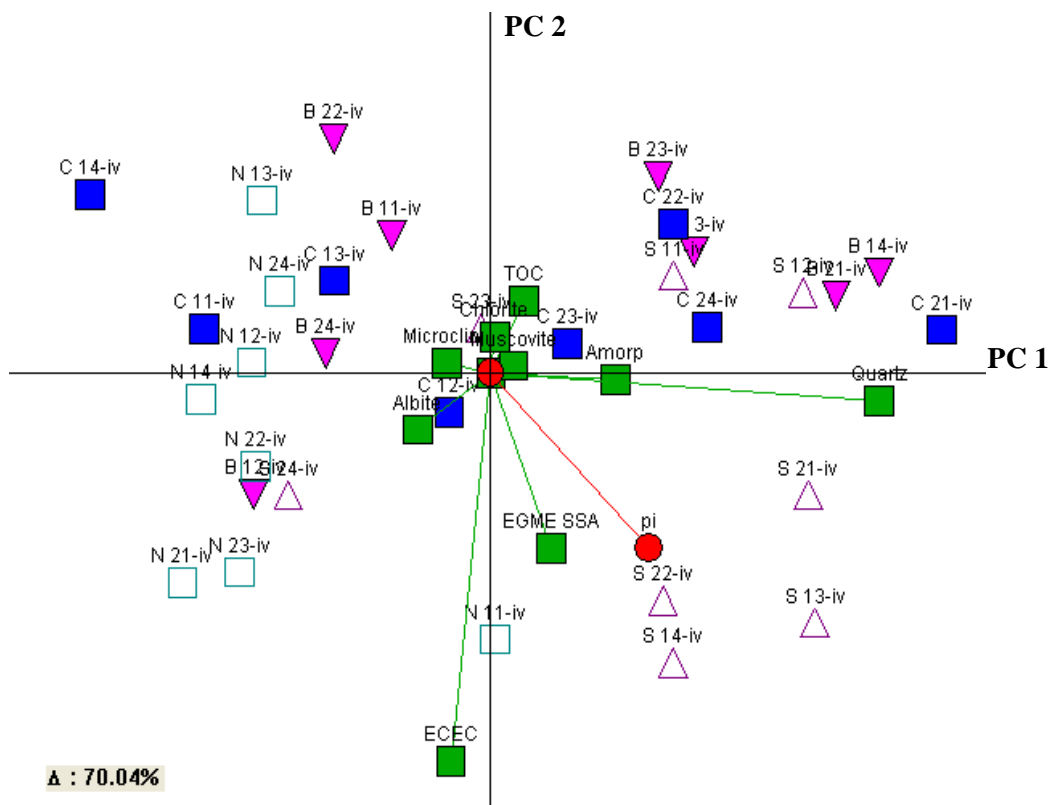


Figure A.7: GAIA biplot for particle size <75µm for all objects

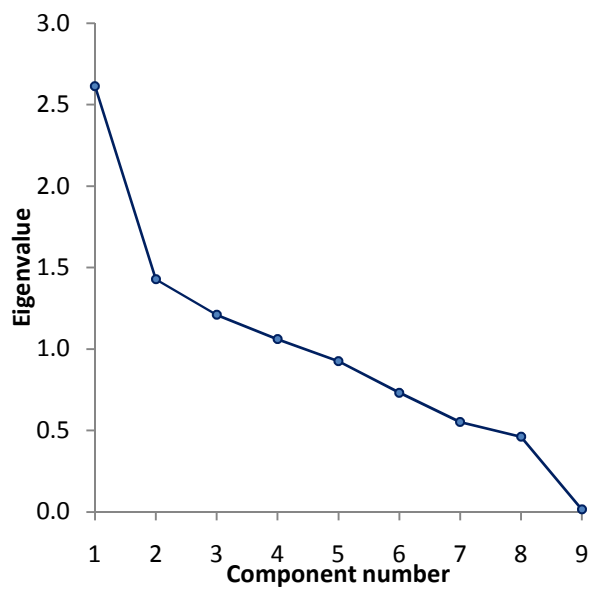
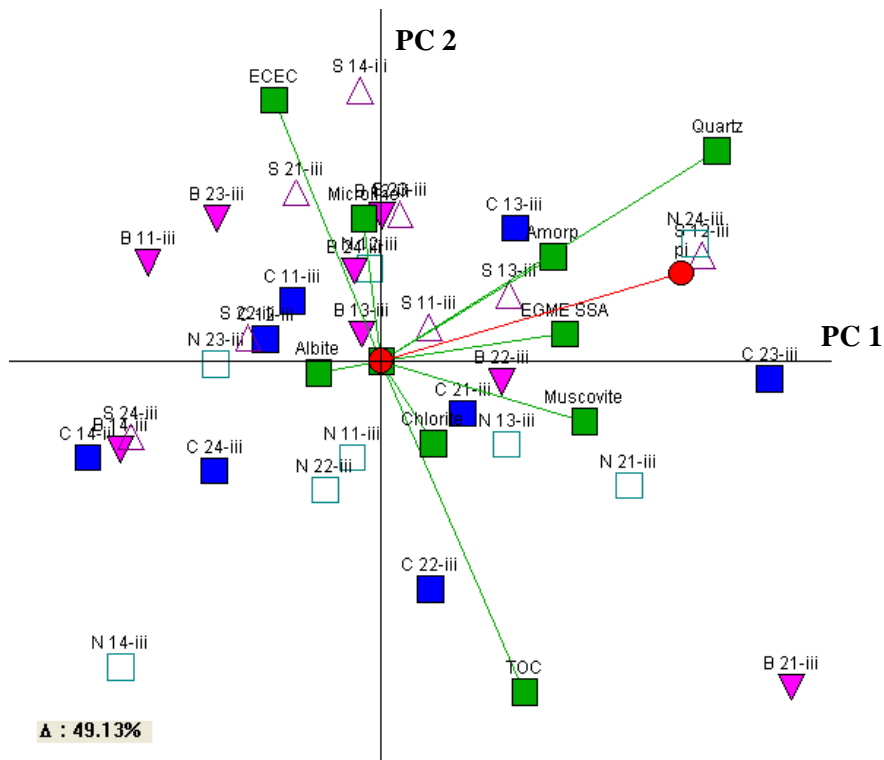


Figure A.8: Scree plot for the particle size 75-150µm

**Table A.10: PROMETHEE II ranking for particle size 75-150µm for all objects**

Sample	Net Φ	Ranking order	Sample	Net Φ	Ranking order
S 21-iii	0.199	1	S 11-iii	-0.012	17
C 23-iii	0.146	2	N 22-iii	-0.021	18
B 21-iii	0.121	3	C 12-iii	-0.025	19
S 12-iii	0.111	4	B 11-iii	-0.026	20
C 13-iii	0.082	5	B 23-iii	-0.037	21
S 22-iii	0.080	6	N 12-iii	-0.039	22
B 24-iii	0.071	7	N 13-iii	-0.053	23
S 14-iii	0.062	8	N 21-iii	-0.054	24
B 12-iii	0.046	9	C 11-iii	-0.061	25
S 13-iii	0.030	10	C 24-iii	-0.079	26
B 13-iii	0.027	11	B 22-iii	-0.091	27
C 22-iii	0.022	12	C 14-iii	-0.110	28
C 21-iii	0.012	13	S 24-iii	-0.148	29
S 23-iii	0.010	14	N 24-iii	-0.148	30
N 23-iii	0.010	15	N 14-iii	-0.162	31
N 11-iii	-0.007	16	B 14-iii	-0.173	32

Note: C– Clearview Estate, N- Nerang, B- Benowa, S- Surfers Paradise



**Figure A.9: GAIA biplot for particle size 75-150µm for all objects**

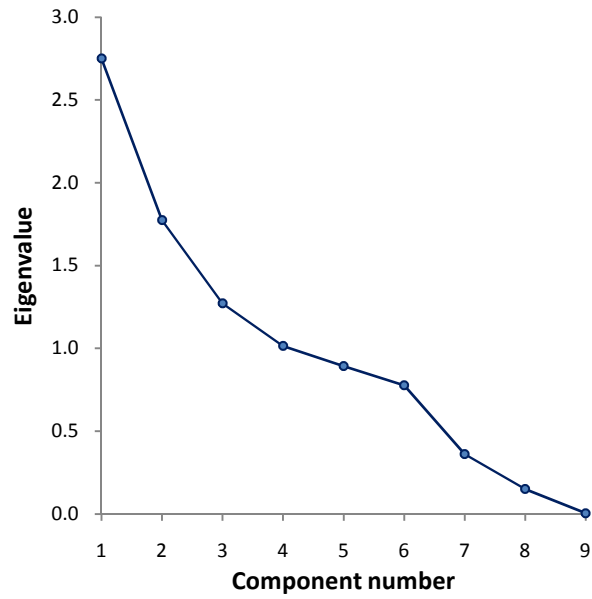


**Figure A.10: Scree plot for the particle size 150-300µm**

**Table A.11: PROMETHEE II ranking for particle size 150-300µm for all objects**

Sample	Net $\Phi$	Ranking order	Sample	Net $\Phi$	Ranking order
B 21-ii	0.175	1	N 23-ii	-0.024	17
C 21-ii	0.168	2	B 23-ii	-0.030	18
C 11-ii	0.168	3	S 11-ii	-0.037	19
N 22-ii	0.152	4	B 24-ii	-0.041	20
S 21-ii	0.136	5	N 12-ii	-0.047	21
B 12-ii	0.125	6	C 23-ii	-0.049	22
C 13-ii	0.110	7	N 21-ii	-0.054	23
C 22-ii	0.098	8	N 11-ii	-0.064	24
B 13-ii	0.080	9	S 23-ii	-0.070	25
C 24-ii	0.063	10	S 22-ii	-0.076	26
C 12-ii	0.049	11	B 22-ii	-0.115	27
B 14-ii	0.048	12	N 13-ii	-0.129	28
B 11-ii	0.047	13	N 24-ii	-0.141	29
S 12-ii	0.028	14	S 13-ii	-0.166	30
N 14-ii	0.019	15	S 24-ii	-0.195	31
C 14-ii	-0.012	16	S 14-ii	-0.216	32

Note: C– Clearview Estate, N- Nerang, B- Benowa, S- Surfers Paradise

**Table A.12: PROMETHEE II ranking for particle size 150-300µm for basic data set objects**

Sample	Net $\Phi$	Ranking order	Sample	Net $\Phi$	Ranking order
C 21-ii	0.224	1	B 24-ii	0.081	10
C 11-ii	0.238	2	N 12-ii	0.072	11
C 13-ii	0.220	3	N 21-ii	0.074	12
C 22-ii	0.178	4	N 11-ii	0.076	13
C 24-ii	0.139	5	N 13-ii	0.041	14
C 12-ii	0.142	6	N 24-ii	0.032	15
B 14-ii	0.149	7	S 13-ii	0.035	16
B 11-ii	0.152	8	S 24-ii	0.042	17
B 23-ii	0.099	9	S 14-ii	0.015	18

Note: C– Clearview Estate, N- Nerang, B- Benowa, S- Surfers Paradise

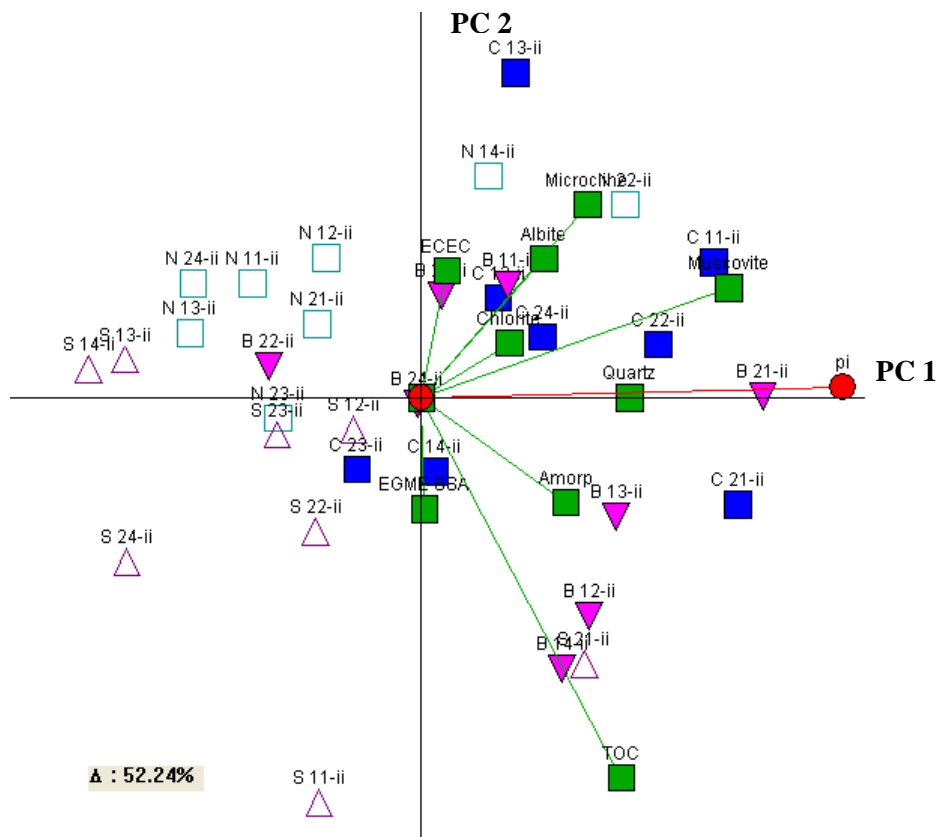


**Figure A.11: GAIA biplot for particle size 150-300µm for basic data set objects**

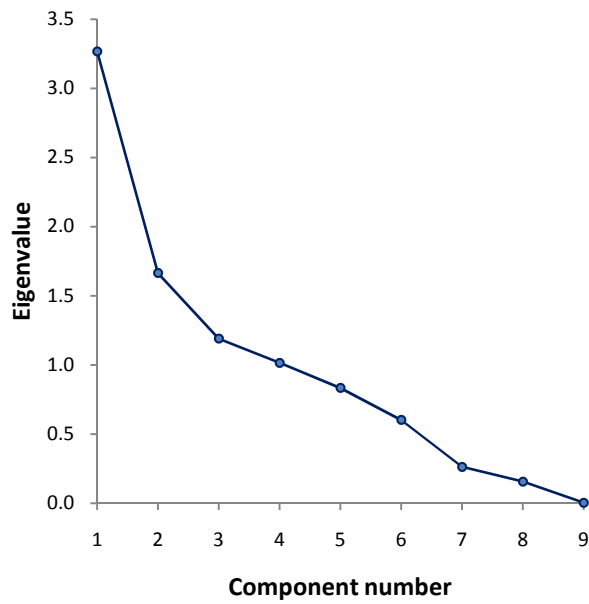


**Figure A.12: Scree plot for the particle size 300-425µm**

**Table A.13: PROMETHEE II ranking for particle size 300-425µm for all objects**

Sample	Net $\Phi$	Ranking order
N 11-i	0.313	1
C 21-i	0.221	2
S 11-i	0.184	3
B 14-i	0.159	4
B 21-i	0.134	5
B 12-i	0.126	6
C 22-i	0.112	7
N 22-i	0.108	8
B 11-i	0.09	9
C 12-i	0.069	10
S 12-i	0.054	11
B 13-i	0.046	12
C 23-i	0.033	13
C 24-i	0.025	14
N 21-i	0.025	15
S 21-i	-0.011	16
B 23-i	-0.014	17
C 14-i	-0.022	18
B 24-i	-0.053	19
S 22-i	-0.054	20
N 23-i	-0.059	21
N 12-i	-0.077	22
S 23-i	-0.086	23
N 24-i	-0.103	24
B 22-i	-0.104	25
C 11-i	-0.123	26
S 24-i	-0.124	27
N 14-i	-0.126	28
S 13-i	-0.133	29
N 13-i	-0.185	30
C 13-i	-0.192	31
S 14-i	-0.234	32

Note: C– Clearview Estate, N- Nerang, B- Benowa, S- Surfers Paradise

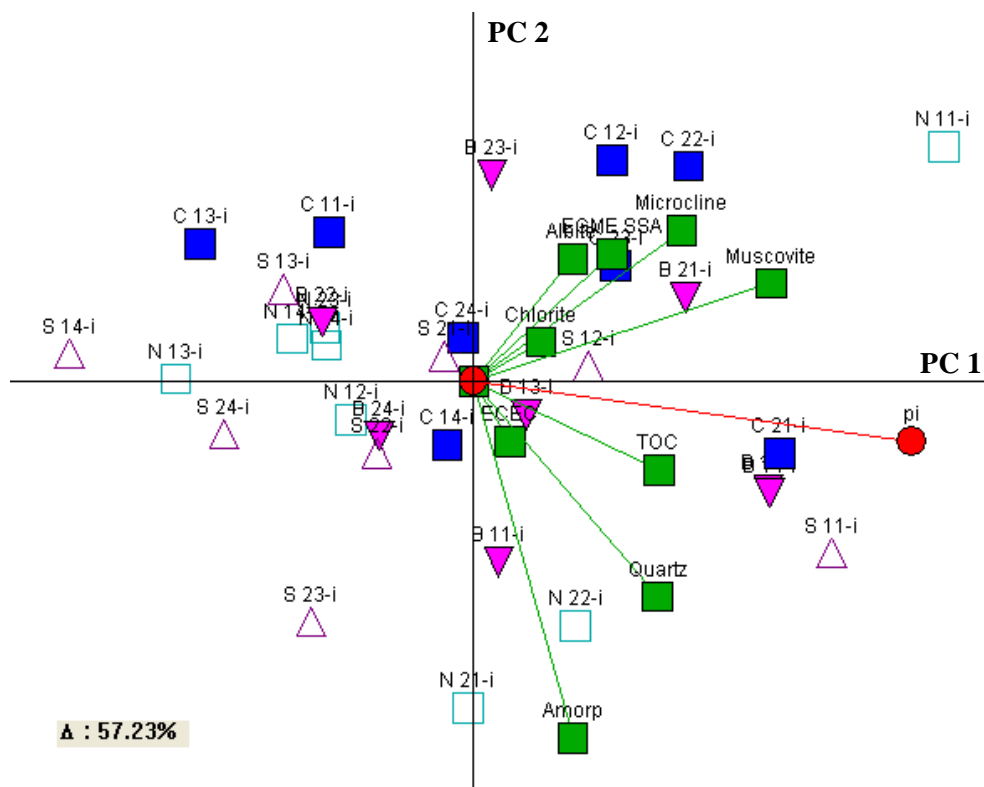


Figure A.13: GAIA biplot for particle size 300-425µm for basic data set objects



# **APPENDIX B**

## **Analysis of heavy metals in solids**



**Table B.1: Heavy metal concentrations of build-up pollutants****Dissolved fraction**

Identification	Al	Cr	Mn	Fe	Ni	Cu	Zn	Cd	Pb
	mg/L								
C 11	0.31	0.015	0.04	0.64	0.003	0.02	0.23	0.001	0.01
C 12	0.38	0.001	0.05	0.63	0.004	0.10	0.42	0.001	0.02
C 13	1.54	0.001	0.13	2.54	0.006	0.20	0.84	0.001	0.07
C 14	1.59	0.002	0.15	1.99	0.009	0.08	0.35	0.001	0.03
N 11	3.83	0.006	0.62	2.95	0.021	0.18	1.21	0.002	0.01
N 12	3.57	0.009	0.34	4.77	0.014	0.26	0.78	0.001	0.07
N 13	0.22	<0.001	0.02	0.15	<0.001	0.01	<0.001	<0.001	<0.001
N 14	0.05	<0.001	0.00	<0.001	<0.001	0.01	<0.001	<0.001	<0.001
B 11	0.71	0.020	0.45	7.07	0.009	0.07	0.41	0.002	0.04
B 12	5.24	<0.001	0.45	3.43	0.002	0.15	0.11	0.001	0.05
B 13	2.58	<0.001	0.17	4.50	0.001	0.01	0.06	<0.001	0.01
B 14	3.37	<0.001	0.20	4.50	0.002	0.03	0.23	0.001	0.10
S 11	0.03	0.007	0.15	1.16	0.007	0.01	0.11	<0.001	0.01
S 12	0.07	0.017	0.03	<0.001	0.007	0.01	0.16	<0.001	<0.001
S 13	0.08	0.003	0.10	<0.001	0.004	0.01	0.23	<0.001	<0.001
S 14	0.02	0.001	0.12	0.71	0.007	0.03	0.33	<0.001	0.03
C 21	2.23	0.054	0.22	3.22	0.010	0.11	0.84	<0.001	0.02
C 22	1.57	0.025	0.45	6.08	0.005	0.04	0.13	0.001	0.04
C 23	5.91	0.002	0.42	4.51	0.003	0.03	0.07	<0.001	0.04
C 24	1.97	0.001	0.27	3.03	0.006	0.06	0.16	<0.001	0.04
N 21	0.17	<0.001	0.03	0.42	0.001	0.01	0.02	<0.001	0.01
N 22	0.29	<0.001	0.02	0.60	0.002	0.01	0.09	0.001	<0.001
N 23	0.30	<0.001	0.02	0.59	0.001	0.01	0.08	0.001	<0.001
N 24	0.02	<0.001	0.12	0.18	0.001	0.01	0.14	0.001	0.01
B 21	0.01	0.030	0.01	0.04	0.001	0.01	0.10	0.001	0.01
B 22	0.04	0.001	0.03	0.11	0.001	0.01	0.11	<0.001	0.01
B 23	0.07	0.003	0.01	0.06	0.001	0.01	0.09	<0.001	0.01
B 24	0.64	<0.001	0.17	0.90	0.003	0.01	0.28	<0.001	0.03
S 21	1.45	0.005	0.07	1.51	0.009	0.03	0.04	<0.001	0.02
S 22	0.24	0.016	0.23	1.62	0.013	0.03	0.06	<0.001	0.01
S 23	1.81	0.083	1.09	6.71	0.042	1.20	0.36	0.001	0.17

Notes:

1. C – Clearview Estate, N- Nerang, B- Benowa and S- Surfers Paradise
2. 1 and 2 - sampling event

**Table B.1: Heavy metal concentrations of build-up pollutants (continued from previous page)**

**Particle size range 300-425µm**

Identification	Al	Cr	Mn	Fe	Ni	Cu	Zn	Cd	Pb
	(mg/g)								
C 11-i	2.09	0.001	0.06	5.20	0.006	0.10	0.12	0.002	0.02
C 12-i	0.45	0.001	0.03	0.94	0.001	0.04	0.05	0.001	0.01
C 13-i	2.56	0.001	0.12	6.05	0.009	0.02	0.09	0.001	0.01
C 14-i	2.55	0.001	0.08	5.42	0.002	0.03	0.05	0.001	0.01
C 21-i	1.49	0.051	0.08	1.80	0.012	0.14	0.26	0.001	0.03
C 22-i	1.31	0.036	0.08	1.72	0.018	0.19	0.22	0.001	0.13
C 23-i	1.11	0.016	0.03	0.86	0.001	0.09	0.11	0.001	0.08
C 24-i	0.91	0.006	0.05	0.84	0.009	0.06	0.30	0.001	0.02
N 11-i	1.15	0.006	0.05	2.49	0.003	0.02	0.05	0.001	0.01
N 12-i	0.33	0.005	0.03	0.88	0.001	0.05	0.05	0.001	0.01
N 13-i	2.33	0.009	0.07	6.45	0.003	0.04	0.23	0.001	0.01
N 14-i	0.31	0.003	0.03	1.88	0.002	0.04	0.02	0.001	0.01
N 21-i	1.03	0.001	0.03	1.31	0.001	0.01	0.17	0.001	0.01
N 22-i	0.05	0.001	0.00	0.78	0.001	0.04	0.00	0.001	0.01
N 23-i	0.19	0.001	0.01	0.97	0.001	0.02	0.02	0.001	0.01
N 24-i	1.21	0.001	0.03	1.67	0.001	0.00	0.03	0.001	0.01
B 11-i	1.78	0.001	0.06	3.82	0.004	0.05	0.12	0.001	0.03
B 12-i	0.25	0.001	0.01	0.48	0.001	0.01	0.01	0.001	0.01
B 13-i	1.03	0.001	0.03	2.69	0.001	0.02	0.01	0.001	0.01
B 14-i	0.59	0.001	0.02	1.12	0.001	0.01	0.03	0.001	0.01
B 21-i	2.78	0.004	0.10	4.70	0.007	0.10	0.52	0.001	0.07
B 22-i	1.47	0.001	0.08	4.32	0.004	0.13	0.36	0.001	0.08
B 23-i	0.87	0.001	0.03	1.67	0.002	0.04	0.18	0.001	0.02
B 24-i	6.31	0.001	0.16	12.4	0.007	0.16	0.13	0.003	0.08
S 11-i	1.18	0.002	0.05	2.63	0.002	0.03	0.04	0.001	0.02
S 12-i	1.44	0.001	0.08	4.67	0.002	0.03	0.08	0.001	0.01
S 13-i	1.13	0.001	0.05	2.76	0.002	0.01	0.04	0.001	0.01
S 14-i	0.43	0.002	0.03	0.98	0.001	0.02	0.05	0.001	0.01
S 21-i	0.36	0.001	0.02	0.45	0.002	0.04	0.00	0.001	0.01
S 22-i	0.30	0.001	0.01	0.95	0.001	0.02	0.00	0.001	0.01
S 23-i	0.48	0.001	0.03	1.31	0.003	0.07	0.08	0.001	0.07
S 24-i	1.81	0.023	0.06	5.03	0.016	0.03	0.03	0.001	0.34

Notes:

4. C – Clearview Estate, N- Nerang, B- Benowa and S- Surfers Paradise
5. 1 and 2 - sampling event
6. i, ii, iii and iv - particle size ranges 300-425µm, 150-300µm, 75-150µm and <75µm

**Table B.1: Heavy metal concentrations of build-up pollutants (continued from previous page)**

**Particle size range 150-300µm**

Identification	Al	Cr	Mn	Fe	Ni	Cu	Zn	Cd	Pb
	(mg/g)								
C 11-ii	4.40	0.001	0.18	9.52	0.006	0.29	0.39	0.002	0.04
C 12-ii	1.57	0.001	0.08	3.98	0.002	0.06	0.16	0.001	0.02
C 13-ii	3.03	0.001	0.13	4.31	0.005	0.06	0.19	0.001	0.02
C 14-ii	0.77	0.001	0.04	1.37	0.001	0.03	0.05	0.001	0.01
C 21-ii	6.58	0.028	0.22	7.54	0.007	0.20	0.54	0.001	0.01
C 22-ii	4.92	0.027	0.30	5.27	0.015	0.27	0.52	0.001	0.02
C 23-ii	3.71	0.010	0.10	3.79	0.006	0.05	0.07	0.001	0.01
C 24-ii	1.39	0.001	0.07	2.23	0.007	0.13	0.09	0.001	0.02
N 11-ii	0.79	0.003	0.07	1.62	0.002	0.03	0.09	0.001	0.01
N 12-ii	1.72	0.009	0.13	3.77	0.006	0.19	0.24	0.001	0.03
N 13-ii	2.02	0.012	0.10	5.53	0.006	0.21	0.60	0.001	0.07
N 14-ii	0.93	0.005	0.08	4.43	0.033	0.09	0.12	0.001	0.03
N 21-ii	1.08	0.001	0.05	2.30	0.001	0.01	0.16	0.001	0.01
N 22-ii	1.93	0.001	0.13	5.91	0.001	0.10	0.08	0.001	0.02
N 23-ii	0.26	0.001	0.01	0.92	0.001	0.01	0.05	0.001	0.01
N 24-ii	0.68	0.001	0.04	2.24	0.002	0.01	0.08	0.001	0.01
B 11-ii	2.81	0.001	0.14	5.43	0.009	0.23	0.66	0.001	0.09
B 12-ii	0.96	0.001	0.03	1.71	0.001	0.02	0.06	0.001	0.01
B 13-ii	1.00	0.001	0.03	1.84	0.001	0.02	0.12	0.001	0.02
B 14-ii	1.01	0.001	0.04	1.46	0.002	0.05	0.26	0.001	0.03
B 21-ii	0.98	0.001	0.04	1.82	0.003	0.05	0.19	0.001	0.03
B 22-ii	4.23	0.001	0.17	9.27	0.013	0.25	0.70	0.001	0.10
B 23-ii	3.84	0.002	0.12	7.09	0.006	0.11	0.47	0.001	0.08
B 24-ii	5.05	0.000	0.13	7.71	0.007	0.27	0.33	0.001	0.13
S 11-ii	1.53	0.013	0.12	3.25	0.007	0.09	0.15	0.001	0.07
S 12-ii	2.83	0.001	0.16	8.12	0.005	0.22	0.21	0.001	0.04
S 13-ii	3.18	0.009	0.15	7.87	0.012	0.09	0.13	0.006	0.04
S 14-ii	1.44	0.001	0.07	3.29	0.003	0.08	0.13	0.001	0.04
S 21-ii	0.70	0.001	0.03	0.93	0.024	0.07	0.08	0.001	0.01
S 22-ii	0.88	0.001	0.06	2.51	0.010	0.06	0.06	0.001	0.01
S 23-ii	1.22	0.001	0.13	5.19	0.007	0.46	0.32	0.001	0.06
S 24-ii	0.66	0.001	0.05	1.51	0.002	0.17	0.14	0.001	0.04

Notes:

1. C – Clearview Estate, N- Nerang, B- Benowa and S- Surfers Paradise
2. 1 and 2 - sampling event
3. i, ii, iii and iv - particle size ranges 300-425µm, 150-300µm, 75-150µm and <75µm

**Table B.1: Heavy metal concentrations of build-up pollutants (continued from previous page)**

**Particle size range 75-150µm**

Identification	Al	Cr	Mn	Fe	Ni	Cu	Zn	Cd	Pb
	(mg/g)								
C 11-iii	4.65	0.001	0.18	9.24	0.006	0.17	0.46	0.003	0.03
C 12-iii	2.21	0.001	0.09	4.33	0.004	0.06	0.23	0.001	0.02
C 13-iii	9.82	0.009	0.38	9.66	0.014	0.10	0.54	0.001	0.05
C 14-iii	4.98	0.002	0.19	8.90	0.009	0.09	0.24	0.001	0.03
C 21-iii	5.74	0.032	0.19	6.07	0.022	0.23	0.69	0.001	0.04
C 22-iii	11.7	0.029	0.58	11.4	0.034	0.45	1.01	0.001	0.06
C 23-iii	3.84	0.008	0.12	4.26	0.005	0.11	0.21	0.001	0.03
C 24-iii	0.88	0.001	0.05	1.51	0.002	0.08	0.08	0.001	0.02
N 11-iii	1.28	0.005	0.08	2.56	0.003	0.05	0.17	0.001	0.01
N 12-iii	1.58	0.008	0.11	3.09	0.005	0.16	0.24	0.001	0.05
N 13-iii	2.08	0.013	0.11	4.60	0.008	0.31	0.55	0.001	0.10
N 14-iii	0.67	0.006	0.08	2.95	0.025	0.16	0.13	0.001	0.05
N 21-iii	1.28	0.001	0.07	2.64	0.002	0.02	0.16	0.001	0.02
N 22-iii	1.02	0.001	0.06	4.12	0.001	0.11	0.09	0.001	0.02
N 23-iii	0.37	0.001	0.02	1.04	0.001	0.02	0.07	0.001	0.01
N 24-iii	0.42	0.001	0.03	1.26	0.001	0.01	0.06	0.001	0.01
B 11-iii	7.71	0.001	0.31	15.7	0.029	0.27	1.24	0.004	0.17
B 12-iii	0.52	0.001	0.02	0.86	0.001	0.02	0.06	0.001	0.01
B 13-iii	1.00	0.001	0.03	1.81	0.001	0.03	0.09	0.001	0.02
B 14-iii	1.57	0.001	0.04	2.50	0.003	0.05	0.26	0.001	0.04
B 21-iii	12.9	0.054	0.39	26.0	0.037	0.20	1.08	0.001	0.21
B 22-iii	2.74	0.001	0.14	5.58	0.028	0.39	0.40	0.001	0.07
B 23-iii	5.05	0.001	0.14	9.58	0.008	0.11	0.42	0.001	0.08
B 24-iii	3.75	0.001	0.09	6.12	0.007	0.14	0.19	0.001	0.10
S 11-iii	2.29	0.007	0.11	3.89	0.003	0.06	0.19	0.001	0.01
S 12-iii	1.45	0.001	0.07	3.53	0.005	0.05	0.15	0.001	0.02
S 13-iii	1.53	0.001	0.10	3.91	0.006	0.10	0.17	0.003	0.04
S 14-iii	0.90	0.001	0.06	2.20	0.002	0.12	0.13	0.001	0.05
S 21-iii	0.98	0.033	0.03	1.19	0.011	0.08	0.13	0.001	0.01
S 22-iii	1.49	0.016	0.06	3.79	0.004	0.06	0.12	0.001	0.03
S 23-iii	1.79	0.001	0.13	4.54	0.007	0.26	0.34	0.001	0.07
S 24-iii	1.56	0.003	0.09	3.08	0.005	0.30	0.38	0.001	0.08

Notes:

1. C – Clearview Estate, N- Nerang, B- Benowa and S- Surfers Paradise
2. 1 and 2 - sampling event,
3. i, ii, iii and iv - particle size ranges 300-425µm, 150-300µm, 75-150µm and <75µm

**Table B.1: Heavy metal concentrations of build-up pollutants (continued from previous page)**

**Particle size range <75µm**

Identification	Al	Cr	Mn	Fe	Ni	Cu	Zn	Cd	Pb
	(mg/g)								
C 11-iv	10.5	0.001	0.20	15.6	0.007	0.07	0.41	0.002	0.04
C 12-iv	9.03	0.002	0.45	16.6	0.011	0.03	0.43	0.001	0.07
C 13-iv	5.79	0.004	0.42	5.83	0.007	0.05	0.25	0.001	0.03
C 14-iv	7.05	0.018	0.15	11.1	0.005	0.04	0.13	0.001	0.02
C 21-iv	4.99	0.096	0.17	0.36	0.004	0.50	0.28	0.001	0.03
C 22-iv	4.95	0.001	0.01	1.12	0.001	0.01	0.01	0.001	0.01
C 23-iv	9.94	0.001	0.04	9.92	0.001	0.01	0.01	0.001	0.02
C 24-iv	0.49	0.001	0.01	0.67	0.001	0.00	0.01	0.001	0.01
N 11-iv	8.68	0.018	0.35	14.6	0.015	0.12	0.62	0.001	0.06
N 12-iv	2.38	0.008	0.00	4.54	0.001	0.00	0.01	0.001	0.01
N 13-iv	2.71	0.024	0.11	4.64	0.009	0.17	0.51	0.001	0.09
N 14-iv	2.92	0.012	0.17	7.29	0.029	0.17	0.24	0.001	0.06
N 21-iv	3.66	0.001	0.13	6.01	0.004	0.04	0.23	0.001	0.03
N 22-iv	5.05	0.001	0.22	9.42	0.004	0.10	0.31	0.001	0.04
N 23-iv	1.96	0.001	0.09	4.74	0.002	0.07	0.23	0.001	0.04
N 24-iv	1.10	0.001	0.05	2.64	0.003	0.02	0.09	0.001	0.02
B 11-iv	3.64	0.001	0.01	8.12	0.001	0.01	0.01	0.001	0.01
B 12-iv	2.73	0.001	0.02	3.50	0.001	0.01	0.01	0.001	0.02
B 13-iv	3.26	0.001	0.01	4.26	0.001	0.01	0.01	0.001	0.02
B 14-iv	2.19	0.001	0.01	3.17	0.001	0.01	0.01	0.001	0.04
B 21-iv	25.9	0.107	0.82	48.3	0.070	0.37	1.77	0.001	0.42
B 22-iv	6.47	0.028	0.17	9.53	0.020	0.23	0.41	0.001	0.05
B 23-iv	11.2	0.025	0.35	18.3	0.019	0.21	0.77	0.001	0.17
B 24-iv	14.5	0.029	0.28	20.0	0.023	0.35	0.84	0.001	0.29
S 11-iv	4.68	0.002	0.11	7.04	0.002	0.11	0.30	0.001	0.03
S 12-iv	1.79	0.001	0.05	3.38	0.001	0.06	0.07	0.001	0.02
S 13-iv	2.35	0.001	0.08	4.58	0.005	0.07	0.11	0.002	0.04
S 14-iv	1.31	0.001	0.03	2.35	0.001	0.06	0.07	0.001	0.04
S 21-iv	2.51	0.001	0.06	4.44	0.007	0.03	0.01	0.001	0.01
S 22-iv	0.95	0.001	0.01	1.14	0.001	0.01	0.01	0.001	0.01
S 23-iv	0.75	0.001	0.01	2.12	0.001	0.01	0.01	0.003	0.03
S 24-iv	0.47	0.001	0.01	0.01	0.001	0.01	0.01	0.001	0.01

Notes:

1. C – Clearview Estate, N- Nerang, B- Benowa and S- Surfers Paradise
2. 1 and 2 - sampling event
3. i, ii, iii and iv - particle size ranges 300-425µm, 150-300µm, 75-150µm and <75µm

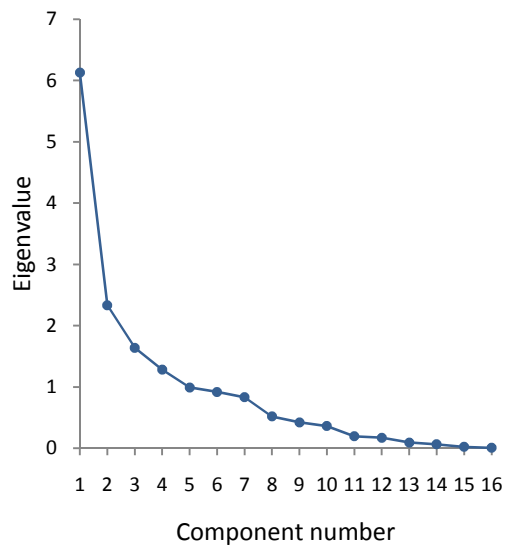


**Figure B.1: Scree plot for particle size <75µm**

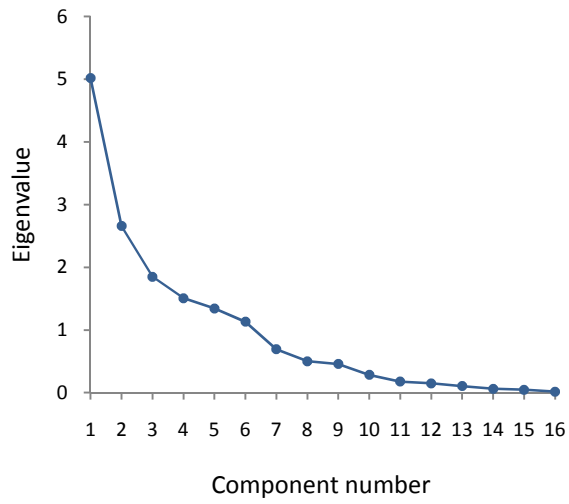


**Figure B.2: Scree plot for particle size 75-150µm**



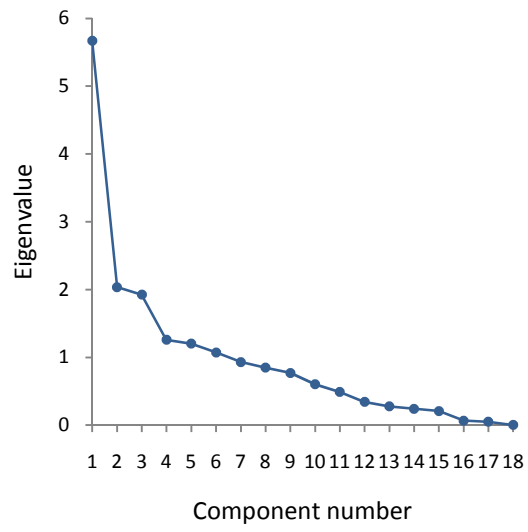


**Figure B.3: Scree plot for particle size 150-425µm**

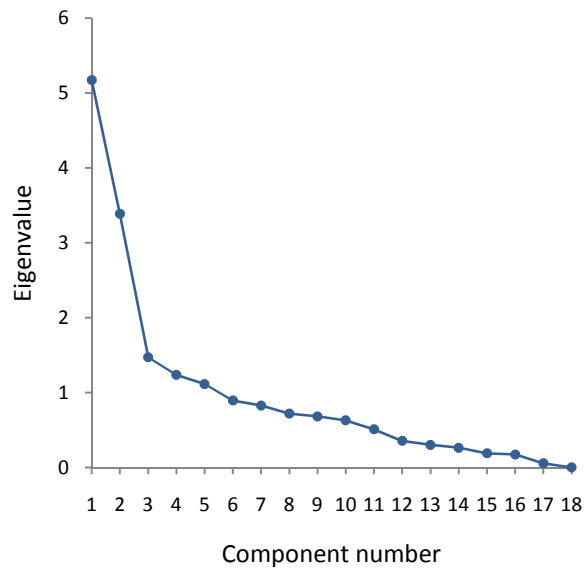


**Figure B.4: Scree plot for entire data set**



# **APPENDIX C**

## **Interaction of heavy metals with solids**



**Table C.1: Pre-existing heavy metal concentration in road deposited solids samples selected for adsorption/desorption experiments**

Sample	Al	Cr	Mn	Fe	Ni	Cu	Zn	Cd	Pb
	mmol/kg								
H iv	87.15	0.000	1.51	81.72	0.09	1.12	1.74	0.02	0.42
H iii	56.53	0.020	1.81	69.75	0.11	1.62	2.57	0.02	0.37
H i/ii	53.78	0.000	1.80	82.26	0.02	1.30	0.88	0.002	0.16
L iv	40.68	0.001	2.00	47.13	0.05	0.39	1.44	0.002	0.14
L iii	15.42	0.000	1.43	22.45	0.02	0.17	0.91	0.001	0.07
L i/ii	45.27	0.220	1.03	57.68	0.15	1.61	1.33	0.000	1.77